

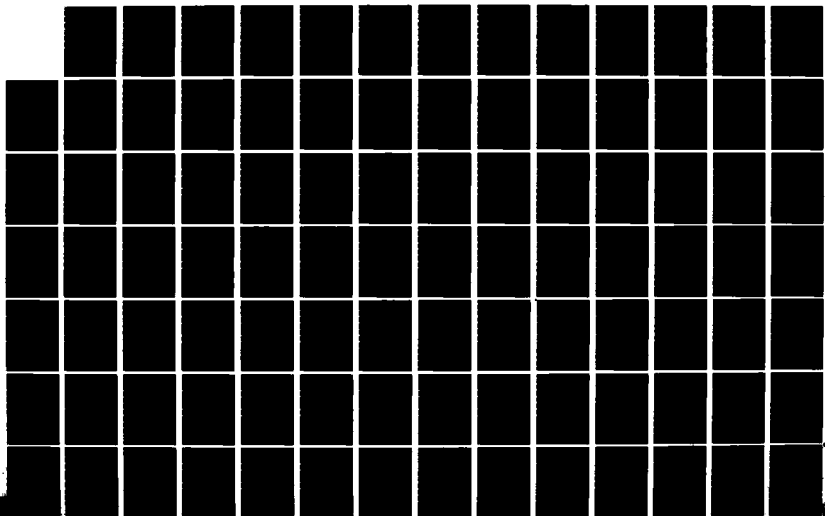
AD-A135 739

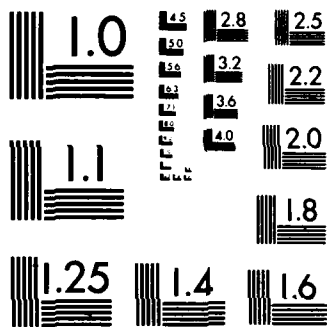
A COMPARATIVE THERMODYNAMIC ANALYSIS OF IMPURITY  
INCORPORATION IN VAPOR P. (U) FLORIDA UNIV GAINESVILLE  
DEPT OF CHEMICAL ENGINEERING T J ANDERSON ET AL

1/4

UNCLASSIFIED

31 OCT 83 AFOSR-TR-83-1108 AFOSR-81-0164 F/G 20/12 NL





MICROCOPY RESOLUTION TEST CHART  
NATIONAL BUREAU OF STANDARDS-1963-A

AFOSR-TR- 83 - 1 108



Report AFOSR-81-0164

AD-A135739

A COMPARATIVE THERMODYNAMIC ANALYSIS OF IMPURITY  
INCORPORATION IN VAPOR PHASE EPITAXIAL InP AND GaAs.

Timothy J. Anderson and Doug Meyer

Department of Chemical Engineering  
University of Florida  
Gainesville, Florida 32611

31 October 1983

Final Scientific Report for 15 March 1981 - 14 August 1982

Prepared for

Department of the Air Force  
AFOSR/PK  
Bolling AFB, D.C. 20332

DIC  
ELECTRONIC  
S DEC 1 1983 D  
D

Approved for unlimited  
distribution unlimited.

DIC FILE COPY

83 12 13 132

UNCLASSIFIED

SECURITY CLASSIFICATION OF THIS PAGE (When Data Entered)

REPORT DOCUMENTATION PAGE		READ INSTRUCTIONS BEFORE COMPLETING FORM	
1. REPORT NUMBER <b>AFOSR-TR-83-1108</b>	2. GOVT ACCESSION NO. <i>AD A135737</i>	3. REPORT'S CATALOG NUMBER	
4. TITLE and Subtitle A Comparative Thermodynamic Analysis of Impurity Incorporation in Vapor Phase Epitaxial InP and GaAs.		5. TYPE OF REPORT & PERIOD COVERED Final 15 March 1981-14 Aug. 1982	
7. AUTHOR(s) Timothy J. Anderson and Doug Meyer		6. PERFORMING ORG. REPORT NUMBER	
9. PERFORMING ORGANIZATION NAME AND ADDRESS Department of Chemical Engineering University of Florida Gainesville, FL 32611		8. CONTRACT OR GRANT NUMBER(s) AFCSR-81-0164-0	
11. CONTROLLING OFFICE NAME AND ADDRESS Department of the Air Force AFOSR/PK Bolling AFB, D.C. 20332		10. PROGRAM ELEMENT, PROJECT, TASK AREA & WORK UNIT NUMBERS <i>61102F</i> 2306/D9	
14. MONITORING AGENCY NAME & ADDRESS (if different from Controlling Office)		12. REPORT DATE 31 October 1983	
		13. NUMBER OF PAGES 312	
		15. SECURITY CLASS. (of this report) Unclassified	
16. DISTRIBUTION STATEMENT (of this Report) Approved for Public Release. Distribution unlimited.		15a. DECLASSIFICATION DOWNGRADING SCHEDULE	
17. DISTRIBUTION STATEMENT (of the abstract entered in Block 20, if different from Report)			
18. SUPPLEMENTARY NOTES "Complex Chemical Equilibrium in the In-P-H-C <sub>1</sub> -Si-O System as Applied to CVD". Presented at National AIChE Conference, Orlando, Fl., March 1982. "Unintentional Doping in GaAs Deposited by Hydride and Chloride CVD". Presented at Am. Vac. Sci. Conference, Anaheim, Ca., April 1983. To be submitted for publication.			
19. KEY WORDS (Continue on reverse side if necessary and identify by block number) Vapor Phase Epitaxy, GaAs, InP, Chemical Equilibrium, Si Impurity in GaAs and InP, Chloride and Hydride VPE of GaAs and InP.			
20. ABSTRACT (Continue on reverse side if necessary and identify by block number) The maximum extent of unintentional Si incorporation has been defined for deposition of GaAs and InP by both the chloride and hydride processes. The extents were determined on the basis of constrained chemical equilibrium being achieved in the CVD reactor. The input species consisted of the input gas components and excess condense phases of the group III source material and quartz reactor wall. The work performed included incorporation of a novel pseudo-steady state			

UNCLASSIFIED

20.

constraint for the liquid source, identifying vapor species not included before, and establishing the vapor composition relation to the point defect structure. The results indicate that Si incorporation levels can be significant. In general, the activity of Si was less in the hydride system and with the compound source in the chloride system. Furthermore, the activity of Si decreased significantly with temperature, small additions of H<sub>2</sub>O, HCl or VCl<sub>3</sub> to the mixing zone, and replacing the H<sub>2</sub> carrier gas by an inert in the chloride system. However, the activity of Si displayed a maximum with system pressure and was somewhat insensitive to input composition. Reviews of the literature are included for the thermochemical properties employed and unintentional doping in experimental GaAs and InP VPE films. Algorithms for computing complex chemical equilibrium using both stoichiometric and non-stoichiometric approaches were generated.

Accession For	
NTIS GRA&I	<input checked="" type="checkbox"/>
DTIC TAB	<input type="checkbox"/>
Unannounced	<input type="checkbox"/>
Justification	
By	
Distribution/	
Availability Codes	
Dist	Special
A/1	



## Table of Contents

		<u>Page</u>
1.	INTRODUCTION .....	1
	1.1 Importance of III-V Materials .....	1
	1.2 Epitaxy of III-V Materials .....	4
2.	REVIEW OF THE LITERATURE .....	10
	2.1 Impurities in GaAs and InP Epitaxial Films Grown by the Chloride Process .....	10
	2.2 Impurities in GaAs and InP Epitaxial Films Grown by the Hydride Process .....	15
3.	METHOD OF CALCULATION FOR COMPLEX CHEMICAL EQUILIBRIUM .....	19
4.	THERMODYNAMIC MODELS OF CVD .....	23
	4.1 Models for the CVD Source and Pre-source Zones .....	23
	4.2 Models for the CVD Mixing and Deposition Zones .....	25
	4.3 Solid State Defect Chemistry .....	31
5.	THERMOCHEMICAL PROPERTIES .....	38
	5.1 Introduction .....	38
	5.2 Pseudo-Steady State Constraint for Liquid Source Boat .....	39
	5.3 The Ga-As-Cl-H System .....	45
	5.4 The In-P-Cl-H System .....	48
	5.5 The Si-Cl-H System .....	51
	References: Thermochemical Properties .....	55
6.	RESULTS AND DISCUSSION .....	59
	6.1 Introduction .....	59
	6.2 The GaAs Chloride System .....	59
	6.3 The GaAs Hydride System .....	79
	6.4 The InP Chloride System .....	91
	6.5 The InP Hydride System .....	97
7.	CONCLUSIONS .....	101
8.	REFERENCES .....	103
9.	Appendix A. MCMPEC.RAND: A Computer Code for Calculating Chemi- cal Equilibria Using a Nonstoichiometric Algorithm .....	A1
10.	Appendix B. MCMPEC.STORC: A Computer Code for Calculating Chemi- cal Equilibria Using a Stoichiometric Algorithm .....	B1

MATTHEW J. ...  
Chief, Technical Information Division

## List of Illustrations

<u>Figure</u>	<u>Description</u>	<u>Page</u>
1.1	Lattice parameter of III-V compounds and solid solutions versus bandgap energy .....	2
1.2	Schematic of the chloride process .....	6
1.3	Schematic of the hydride process .....	8
6.1	Effect of temperature in the GaAs chloride system source zone (liquid source) .....	60
6.2	Effect of temperature in the GaAs chloride system source zone (liquid source) .....	61
6.3	Effect of temperature in the GaAs chloride system source zone (solid source) .....	62
6.4	Effect of temperature in the GaAs chloride system source zone .....	63
6.5	Effect of temperature on the GaAs chloride system presource zone .....	67
6.6	Effect of pressure on the GaAs chloride system source zone (liquid source) .....	71
6.7	Effect of pressure on the GaAs chloride system source zone (solid source) .....	72
6.8	Effect of pressure on the GaAs chloride system deposition zone .....	75
6.9	Effect of pressure on the GaAs chloride system deposition zone .....	76
6.10	Effect of adding HCl on the GaAs chloride system deposition zone .....	78
6.11	Effect of adding $H_2O$ on the GaAs chloride system deposition zone .....	80
6.12	Effect of replacing $H_2$ with inerts on the GaAs chloride system deposition zone .....	81
6.13	Effect of temperature on the Group V source zone of the GaAs hydride system .....	83
6.14	Effect of temperature on the Group III source zone of the GaAs hydride system .....	84
6.15	Effect of temperature on the Group III presource zone of the GaAs hydride system .....	85
6.16	Effect of temperature on the mixing zone of the GaAs hydride system .....	86
6.17	Effect of adding HCl on the GaAs hydride system deposition zone .....	89

**List of Illustrations (Cont'd)**

<u>Figure</u>	<u>Description</u>	<u>Page</u>
6.18	Effect of replacing $H_2$ with inerts on the GaAs hydride system deposition zone .....	90
6.19	Effect of temperature on the InP chloride system deposition zone .....	92
6.20	Effect of temperature on the InP chloride system deposition zone .....	93
6.21	Effect of temperature on the InP chloride system source zone (solid source) .....	95
6.22	Effect of temperature on the InP chloride system source zone (solid source) .....	96
6.23	Effect of temperature on the InP hydride system deposition zone .....	99
6.24	Effect of temperature on the InP hydride system deposition zone .....	100

## List of Tables

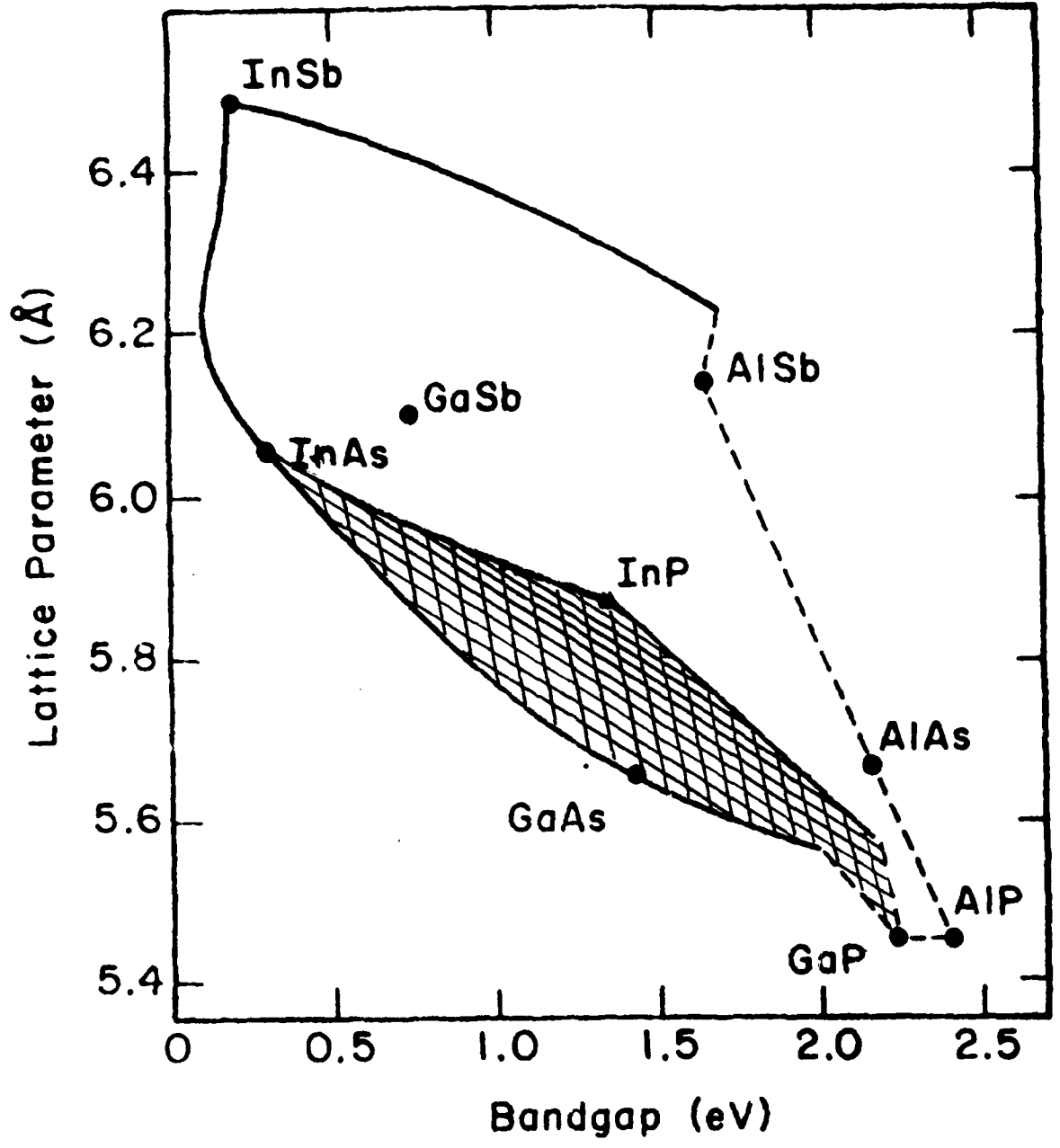
<u>Table</u>	<u>Description</u>	<u>Page</u>
1.1	Some properties of Si and III-V binary semiconductors at 300K .....	4
4.1	Some typical operating parameters for the GaAs and InP chloride systems .....	29
4.2	Some typical operating parameters for the GaAs and InP hydride systems .....	30
5.1	Selected thermochemical values .....	40
5.2	The molar Gibbs energy of formation of various species .....	42
5.3a	Thermochemical properties of GaAs and InP required for calculating $\Delta G_f^\circ$ .....	45
5.3b	Thermochemical properties of the elements Ga, In, As and P required for calculating $\Delta G_f^\circ$ .....	45
5.4	The reported standard enthalpy of formation of $\text{InF}_3$ ( $\Delta H_f^\circ$ ) .....	50
6.1	Enthalpies of formation and Gibbs energies of reaction for some silicon vapor species .....	68

## 1. INTRODUCTION

### 1.1 Importance of III-V Materials

The development of the solid-state electronics industry has principally centered around the semiconductor material Si, mainly as a result of its ease of preparation, available high purity, existence of an excellent native oxide and good electrical properties. The explosive growth in semiconductor technology has nurtured a multitude of ingenious solid-state device structures and functions that place an ever increasing demand upon the physical and electrical properties of the best semiconductor material. Although the material Si has satisfied a large number of the requirements for solid-state device applications, there exists no degree of freedom in the inherent electrical properties of this material. Because of this inflexibility, a considerable amount of the current research has focused on the development of alternative semiconductor materials to meet the demands of tomorrow's devices.

In particular, Group III-V compounds and solid solutions are presently receiving intense investigation. The motivation for the research resides in two principal advantages offered by III-V materials: the existence of three degrees of freedom in the properties of the material and improved inherent electrical properties. The first degree of freedom is found in the choice of the base binary system (nine possible compounds with the Group III elements Al, Ga and In and the Group V elements P, As and Sb). **While the second and third degrees of freedom are realized as a result of the ability to often form completely miscible substitutional solid solutions on both the Group III and the Group V sublattices independently.** Thus, for example, it would be possible to specify a lattice parameter, bandgap energy and thermal conductivity (within a certain range of values) to satisfy the constraints for a given device structure. This point is illustrated in Figure 1.1 which plots the lattice parameter of III-V binary compounds versus the observed room temperature bandgap energy. The solid dots represent binary compounds and the lines connecting each dot represent ternary solid solutions



Lattice parameter of III-V compounds and solid solutions versus bandgap energy;

Figure 1.1

of the two binary limits. Solid lines signify direct bandgap materials while broken lines indicate indirect materials. Essentially, the entire area enclosed in Figure 1.1 is accessible to the designer when employing ternary and quaternary III-V solid solutions. Such flexibility as encountered with III-V materials is extremely useful for optimal design of new solid-state electronic devices. Of interest here is the quaternary system  $In_x Ga_{1-x} As_y P_{1-y}$ . The available range of lattice parameter and bandgap energy for this system is given by the cross hatched surface shown in Figure 1.1. Thus the lattice parameter and bandgap energy may be specified independently with the composition of the quaternary solution chosen to meet these specifications. The application of one degree of freedom to the lattice parameter is extremely important since currently only GaAs, GaSb, GaP, InP and InSb are available in bulk crystal form for use as substrate materials. A disparity of greater than 0.1% between the lattice parameter of the substrate and epitaxial layer induces the formation of interface defects in the crystal structure which can degrade the device performance. One important application of the quaternary  $In_x Ga_{1-x} As_y P_{1-y}$  is in the development of heterojunction lasers for use as transmitters in optical fiber communication systems (11). Currently available optical fibers exhibit minima in attenuation and dispersion characteristics for radiation of approximately 1 eV (11). Choosing the values of  $x=0.8$  and  $y=0.35$  yields an emission energy of  $\sim 1.11$  eV (12) with a lattice parameter which closely matches that of the InP substrate.

The second advantage III-V materials offer is a general improvement in electrical properties. As examples, Table 1.1 illustrates some measured room temperature electron mobilities, bandgap energies and lattice parameters observed for III-V compounds and for Si (10). This summary indicates that as much as two orders of magnitude improvement can be encountered with the use of III-V compounds over Si and this improvement is extremely important in high speed or high frequency device applications. Thus, in the future, III-V materials are expected to play an increasing role as the host material for semiconductor devices. However, the widespread use of these

materials is currently limited, mainly as a result of technological problems.

**Table 1.1**

**Some Properties of Si and III-V Binary Semiconductors at 300K**

	Bandgap		Electron Mobility ( $cm^2/V \cdot S$ )	Lattice Constant ( $\text{\AA}$ )
	Type	Energy (eV)		
Si	indirect	1.12	1350	5.43
InSb	direct	0.17	50000	6.48
InAs	direct	0.36	23000	6.06
GaSb	direct	0.72	5000	6.10
InP	direct	1.35	4000	5.87
GaAs	direct	1.42	8500	5.65
GaP	indirect	2.26	300	5.45

### 1.2 Epitaxy of III-V Materials

There exist three primary methods for growing epitaxial III-V films: liquid phase epitaxy (LPE), molecular beam epitaxy (MBE) and chemical vapor deposition (CVD). LPE is the growth of thin single crystal layers from a liquid solution. The driving force (lowering the Gibbs energy of the solid surface below that of the contacting melt) can be provided by a variety of sources such as Peltier cooling and electromigration (electroepitaxy), initial supersaturation (isothermal LPE) and, most commonly, by decreasing the temperature. The advantages of LPE include:

- 1) The method is capable of growing multicomponent layers with a high reactivity disparity among the elements.
- 2) The equipment is relatively simple and inexpensive.
- 3) A large selection of dopants is available.
- 4) The process is near equilibrium at the surface thus allowing reproducibility.
- 5) The growth occurs below the film melting temperature.
- 6) The growth rate can be high.
- 7) The impurity distribution coefficients are generally favorable ( $K < 1$ ).

There are, however, several drawbacks with LPE. Often there exists the presence of surface defects such as incomplete melt removal, terraces, pinholes, and miniscus

lines. The thickness uniformity can be poor and, for solid solution films, inherent composition gradients are present. Furthermore, LPE is a small scale, batch operation and heteroepitaxy can be difficult.

Molecular beam epitaxy is a method for growing epitaxial thin films of semiconductors by impinging one or more thermal energy beams of atoms or molecules onto a heated substrate under ultra-high vacuum conditions. The distinguishing characteristic of MBE is the slow growth rate ( $0.1-2 \mu\text{m} / \text{hr}$ ) that permits precise control of layer thickness, composition and doping profiles. Furthermore, it is possible to achieve spatial resolution not offered by other techniques. As with LPE, the growth temperatures are reduced. In addition, in situ analysis of the surface structure and reaction conditions during growth is possible. However, the equipment is very expensive and the throughput is low.

Commercially the most successful technique for depositing epitaxial semiconductor films is *chemical vapor deposition*. Three source chemistries dominate the CVD process for III-V materials: Group III and/or Group V metalorganic (MOCVD), Group V hydride and Group V halide sources. The MOCVD technique involves an irreversible pyrolysis reaction in which a Group III metalorganic gaseous specie is fed to a cold-wall reactor along with a Group V specie (usually a hydride). These species then contact a heated (inductive or radiative) substrate, decompose, and deposit an epitaxial layer onto the substrate.

The focus of this work is with the halide (specifically the chloride) and hydride CVD processes. A schematic representation of the chloride CVD system is shown in Figure 1.2. The reactor consists of source, mixing and deposition zones which are usually operated at 100 kPa pressure. Due to the exothermic nature of the overall deposition reaction, the reactor is hot-wall in design and the temperature of the mixing zone is greater than or equal to that of the source zone while the deposition zone temperature is normally less than that of the source zone. Typically, hydrogen is used as the

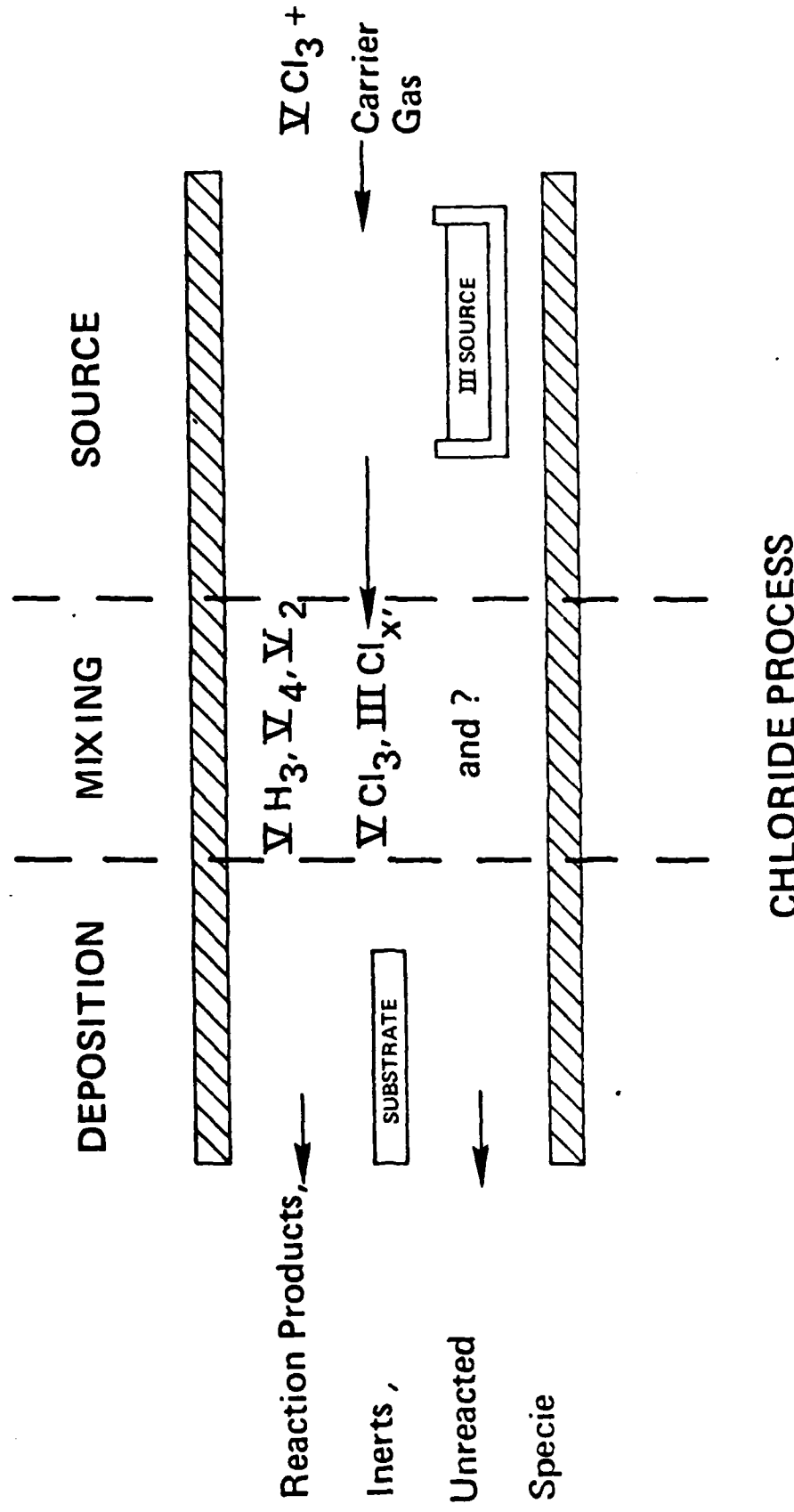


Figure 1.2

carrier gas with the concentration of the Group V chloride in the inlet being on the order of 1 volume percent. The Group III source is either the III-V stoichiometric compound (avoids initial source transient) or the Group III liquid metal saturated with the Group V element (generally available in higher purity). Upon entering the reactor the Group V chloride decomposes (either homogeneously or heterogeneously) to form primarily  $V_2$ ,  $V_4$  and HCl vapor species. The HCl then reacts with the Group III source to form III-Cl and other higher chlorides. The mixing zone allows the species in the vapor to equilibrate while transporting to the lower temperature deposition zone where the Group III and V vapor species react at the substrate surface to deposit an epitaxial layer. When a liquid Group III source is used the ratio of Group III to Group V atoms in the vapor is fixed at approximately 3 since essentially all of the chlorine atoms on the Group V chlorides react to predominantly form III-Cl. The use of a III-V stoichiometric compound as the Group III source limits the III/V ratio to a maximum value of 1 since one Group V atom is released from the solid for each Group III atom that reacts to form III-Cl.

The hydride CVD process is shown schematically in Figure 1.3. The source zone of the hydride system consists of two mass transfer isolated inputs: one for the Group V specie and one for the Group III specie. The Group V hydride, at a typical inlet composition of 1%, is introduced into the source zone where it decomposes to form primarily  $V_2$ ,  $V_4$  and  $H_2$ . As in the chloride process, the Group III element is transported principally as the mono-chloride by the reaction of HCl (typical HCl inlet concentration is 1%) with the liquid Group III metal. One major advantage the hydride system provides over the chloride system is the ability to vary, in a continuous fashion, the vapor III/V ratio by simply adjusting the input compositions or flowrates of  $VH_3$  and HCl. Typically the source and mixing zones in the hydride system are operated at higher temperatures than those of the chloride system in order to increase the rate of  $VH_3$  thermal decomposition (the decomposition kinetics of  $VH_3$  are much slower than  $VCl_3$ ). Again, hydrogen is usually used as the carrier gas and the mixing and deposition zones

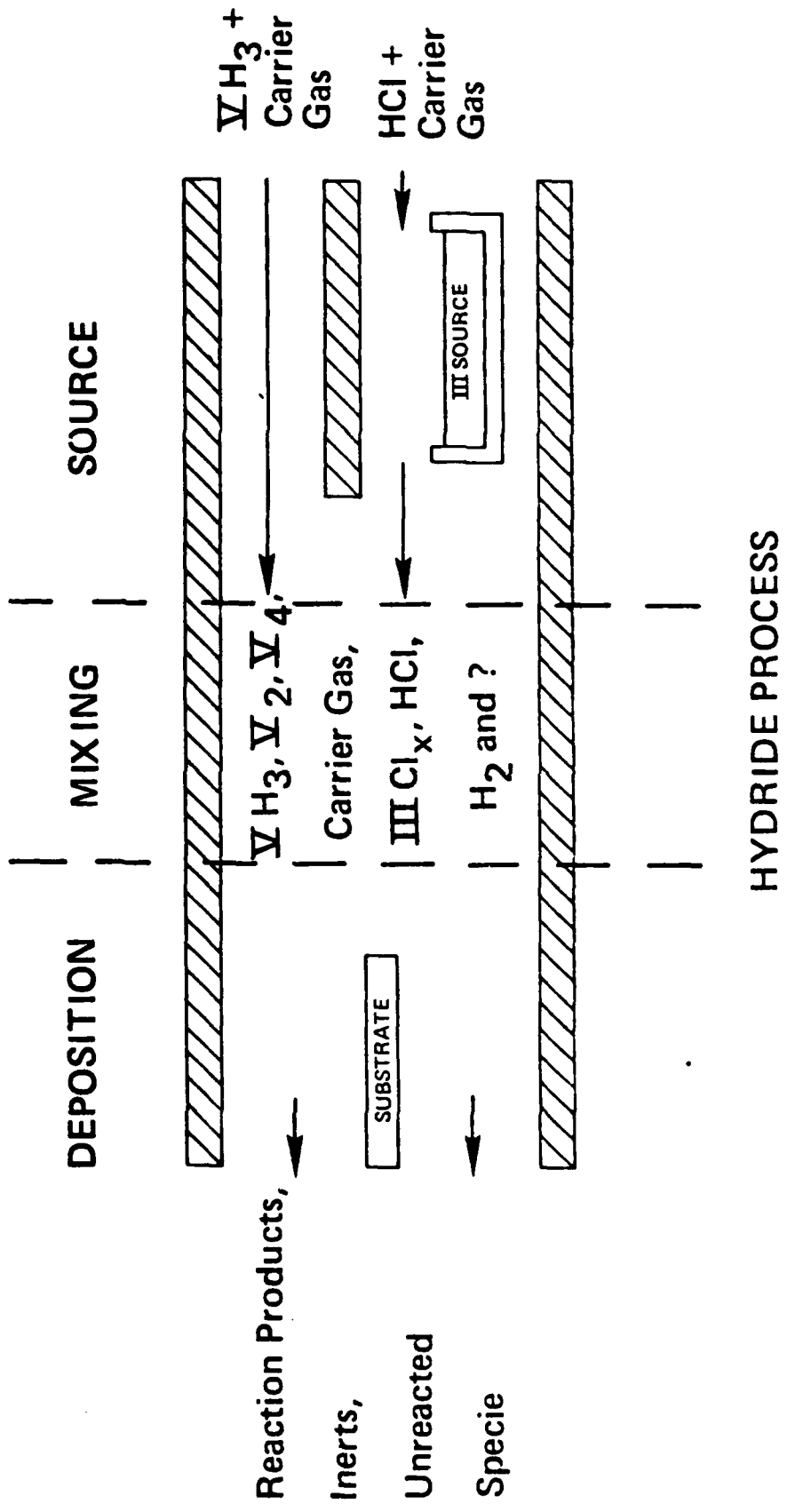


Figure 1.3

provide functions equivalent to those in the chloride system. Indeed, the equilibrium chemistry of the two systems are identical after the source zone.

Both the chloride and hydride systems are hot-wall designs (heating from the outside of the reactor tube by conduction). Therefore, interactions between the vapor phase and the reactor wall (usually quartz) can be thermodynamically favorable and not kinetically limited for the introduction of impurities into the vapor. The gas flowrates through these reactors are generally small ( $Re \sim 10$ ) such that the flow is decidedly laminar.

An understanding of the chemistry involved in the chloride and hydride CVD processes is essential in order to advance these technologies. The complex chemical equilibrium analysis of these systems developed in this study identifies the principal vapor phase species which must be accounted for in order to understand these CVD systems. The influence these species exert on the point defect structure of the epitaxial layers is discussed and the importance of these defects as undesired dopants is evaluated. This analysis also provides information regarding the degrees of supersaturation expected in the deposition zones and suggests methods for reducing the unintentional incorporation of silicon in III-V epitaxial layers. Both the chloride and hydride processes were investigated for the deposition of homoepitaxial GaAs and InP and thus allow direct comparisons to be made.

## 2. REVIEW OF THE LITERATURE

### 2.1 Impurities in GaAs and InP Epitaxial Films Grown by the Chloride Process

The feasibility of applying the chloride system CVD technique to the epitaxial growth of high purity GaAs was first demonstrated by Knight et al. [16] and Effer [17]. Initially, the commercially available  $AsCl_3$  contained sufficient impurities to cause significant contamination of the epitaxial layers and therefore the purity of the feed materials was believed to be the controlling factor for this system [19]. As better quality  $AsCl_3$  became available Cairns and Fairman [20,21] and DiLorenzo et al. [22] found that an increase in the  $AsCl_3$  mole fraction in the inlet gas stream resulted in a decrease in unintentional impurity incorporation in the epitaxial layer.

For materials grown in their laboratory, DiLorenzo and Moore [23] identified the primary unintentional dopant as being silicon, through the use of photoluminescence spectra. Further, they proposed a thermodynamic model for the generation of vapor phase chlorosilanes as a result of the interaction of HCl with the quartz ( $SiO_2$ ) reactor wall and presented an expression for the activity of solid silicon (i.e. as an impurity) as a function of the partial pressures of the chlorosilanes. Their model showed that increasing the vapor HCl concentration (e.g. as a result of  $AsCl_3$  decomposition) decreased the condensed phase silicon activity by further stabilizing the silicon species in the vapor phase in the form of chlorosilanes. Additionally, their model predicted that the generation of vapor phase silicon species could be suppressed by the introduction of  $H_2O$  in the vapor.

Rai-Choudhury [27] performed a thermodynamic analysis on the incorporation of silicon into GaAs epitaxial layers. His results reflected those of DiLorenzo and Moore [23] when considering the effects of  $H_2O$  and HCl but he also showed that higher temperatures increase the amount of vapor phase silicon species.

The work of Ashen et al. [26] further supported the conclusion that silicon was an impurity in GaAs. A BN lined reactor was used to grow epitaxial layers from liquid Ga

sources which were doped with Si. Comparing the electrical characteristics of these epi-layers to layers grown from pure Ga sources provided qualitative evidence for the presence of Si in GaAs. The effect of  $AsCl_3$  concentration on the amount of Si incorporated into the epi-layer was also verified by their experiments. Additionally, they provided evidence which indicated that Si was much more likely to reside on a Ga site than an As site and therefore behaves as a donor. This conclusion was also supported by Beiden et al. [29].

Wolfe, Stillman and Korn [24] have identified, through intentional doping and determination of ionization energies, three unintentional impurities, Si, C and one unknown (possibly Te), in GaAs grown by the chloride CVD system. Also, due to concerns over oxygen possibly being a shallow donor in GaAs [25], they attempted to dope the epitaxial layer with oxygen by adding  $Ga_2O_3$  to the liquid gallium source. The oxygen, however, was not incorporated into the epitaxial layer but the presence of oxygen in the system did reduce the amount of unintentional silicon which was incorporated into the epitaxial layer. This reduction in background doping due to the presence of oxygen was also investigated by Palm et al. [28] by injecting a hydrogen-oxygen mixture into the mixing zone of a chloride system CVD reactor. Using silane as an intentional dopant the presence of oxygen was found to reduce the incorporation of silicon in the epitaxial layers by as much as four orders of magnitude.

Seki et al. [33] performed a thermodynamic analysis of the GaAs chloride process in order to identify the effects of inerts, HCl and substrate temperature on the activity of silicon in the epitaxial layers. They found, in agreement with others, that increasing the HCl content or decreasing the substrate temperature lowered the silicon activity. They also found that replacing the hydrogen carrier gas with an inert caused a very large reduction in the silicon activity.

The effect of replacing the hydrogen carrier gas with an inert was investigated by Ozeki et al. [34]. They found, through far infrared photoconductivity measurements,

that sulfur was the dominant residual donor present in epitaxial GaAs when  $N_2$  was used in place of  $H_2$  as the carrier gas. They also found that the dominant residual donor when  $H_2$  was used as the carrier gas was sometimes Si and sometimes S. A possible source of S in the system was not discussed (although it was presumably in the feed gases) and elaboration on the growth conditions which caused Si or S to be dominant was not provided.

A thermodynamic analysis of the chloride CVD system performed by Boucher and Hollan [30] assumed solid GaAs as the Group III source material. They concluded, by comparison with experiment, that the dominant Group III and Group V species present in the vapor were GaCl and  $As_4$ . They further found that the deposition process was kinetically controlled with an activation energy of  $\sim 40$  kcal mol<sup>-1</sup>, and that reproducible growth conditions could only be assumed if 10% or less of the thermodynamically available GaAs was deposited in the vapor phase.

Gentner, Bernard and Cadoret [31] also studied the chloride process thermodynamically and experimentally but over a greater range of temperature, pressure and inlet  $AsCl_3$  composition than did previous investigators. They found that  $As_2$  became the dominant Group V specie below 10 kPa pressure and that GaCl was always the dominant Group III specie. At large  $AsCl_3$  inlet compositions the higher gallium chlorides became more pronounced but never competed with the monochloride as the dominant specie. They concluded, based on Cadoret's [32] kinetic model, a mass transfer model and experimental results, that the deposition of GaAs was kinetically rather than mass transfer controlled.

Shaw [7] studied the transport kinetics of the GaAs chloride system in the source and deposition zones. He found an activation energy of 49.1 kcal mol<sup>-1</sup>, in reasonable agreement with that of Boucher and Hollan [30], for a surface reaction associated with the deposition process.

The epitaxial growth of homoepitaxial InP using a chloride CVD system was first

demonstrated by Joyce et al. [40] and later by Hales et al. [41]. Both groups of investigators reported limitations on the purity of their epitaxial layers due to unintentional dopants. Joyce and Williams [42] tentatively identified the impurities as being Si and/or Zn acceptors. They also found evidence of a donor which was thought to be amphoteric Si.

The dependence of unintentional doping on  $PCl_3$  mole fraction in the InP chloride system was first reported by Clarke [43]. The similarity between the GaAs and InP chloride system reactors combined with the analogous dependences on the Group V hydride mole fraction supported the belief that Si was an impurity in InP epitaxial layers. Clarke [44] later studied the effect of III/V ratio in the vapor phase on the unintentional doping of InP epi-layers and found p-type conductivity for III/V < 3 and n-type for III/V > 3, with a minimum in the free carrier concentration at III/V  $\approx$  3. No explanation was offered for these observations.

Easton [45] investigated the unintentional doping of InP epitaxial layers grown by the chloride system and concluded that sulfur (acting as a donor) was the major impurity and that the origin of the sulfur was the  $PCl_3$  liquid source. Using mass spectrometric analysis Easton found Si, S and Zn present in the  $PCl_3$  source at levels between 1 ppm and 10 ppm (atomic) and Fe, Cu, Cd and Sn at  $\sim$  0.7 ppm. These same elements were found in the unused bulk In liquid at levels below 0.1 ppm. Analysis of the used In source liquid revealed impurity levels approximately 10 times larger than those in the unused liquid.

These results support the work of Weiner [9] who proposed models for the contamination of a Ga liquid source by Si in the GaAs and GaP systems. Weiner's results showed that the liquid Group III metal impurity level increased as the exposure to the CVD environment increased. He also found the level of Si contamination to be inversely related to the partial pressure of  $H_2O$  in the system.

Fairhurst et al. [46] studied the InP halide system using both  $PCl_3$  and  $PBr_3$ . They

found that oxyhalide salts were present in both phosphorous liquids at approximately the 100 ppm level. The presence of oxygen was expected to decrease the level of impurity incorporation in the epitaxial layers. This effect was not observed however, presumably due to this level of oxygen contamination being too low to be significant. Equilibrium calculations were performed which showed  $\text{InCl}$  and  $P_4$  to be the dominant Group III and V species in the vapor over a temperature range of 850 K to 1150 K and an inlet  $\text{PCl}_3$  mole fraction range of 0.1% to 6%. These results agreed with those of Boucher and Hollan [30] for the analogous GaAs system.

Hales and Knight [47] investigated the effect of introducing oxygen into the system in order to reduce the level of impurities in InP. They observed a monotonic decrease in free electron density for additions of  $O_2$  up to 24 ppm. The electron mobility (measured at 77 K) however reached a very broad maximum at approximately 16 ppm of added oxygen, which suggests that oxygen was becoming incorporated into the epitaxial layer and that there is a limit to the degree of benefit which may be obtained through oxygen addition. They also observed  $\text{POCl}_3$  to be an impurity in the liquid  $\text{PCl}_3$  used in the chloride system.

Investigations of the dependence of impurity incorporation on  $\text{PCl}_3$  inlet composition, total flowrate and deposition zone temperature were carried out by Chevrier, Huber and Linh [48]. They observed a decrease in free carrier concentration with increasing  $\text{PCl}_3$  concentration, as did other investigators, but also found that the impurity concentration increased with increasing total flowrate. This velocity effect had not been reported before and suggests the presence of a mass transfer resistance at the Group III source (if impurities are picked up from the liquid metal) and/or at the substrate in the deposition zone. They also studied the intentional doping of InP as a function of deposition zone temperature using  $\text{SnCl}_4$ . Lower free electron concentrations and higher electron mobilities were observed when the deposition zone temperature was decreased from 950 K to 910 K. Thus, the uptake of Group IV impurities (Sn, Si, etc.) was apparently reduced by lowering the deposition zone temperature.

Cardwell et al. [49] found kinetic limitations in both the source and deposition zones. The previously reported effect of  $PCl_3$  mole fraction on impurity levels in the epitaxial layers was observed. Intentional doping of InP using Sn followed the same behavior as that of unintentional dopants and therefore supports the use of Sn for studies regarding the reduction of unintentional impurities. In contrast to Chevrier et al. [48] no dependence of impurity uptake on total flowrate was found.

A thermodynamic analysis comparing the GaAs and InP chloride systems using the stoichiometric III-V solid as the Group III source material was reported by Shaw [50]. His results also confirmed GaCl,  $As_4$ , InCl and  $P_4$  to be the dominant Group III and V vapor species in these systems. Further, the degree of supersaturation in the deposition zone was calculated to be less for InP than for GaAs under analogous conditions. Since solid III-V source materials were employed etching conditions were predicted whenever the deposition zone temperature was greater than that of the source zone.

## 2.2 Impurities in GaAs and InP Epitaxial Films Grown by the Hydride Process

The feasibility of the hydride CVD system for the growth of high purity GaAs was demonstrated by Enstrom and Peterson [18]. Since the hydride system consists of a hot-wall quartz reactor with the elements H, Cl, Ga and As present in the vapor one would expect it to show an unintentional impurity incorporation problem similar to that of the chloride system. Pogge and Kemlage [35] investigated the effects of HCl,  $AsH_3$  and  $PH_3$  on the unintentional doping of GaAs and GaP grown by the hydride system. They found that the free carrier concentration decreased with increasing HCl,  $AsH_3$  or  $PH_3$  composition. The effect of HCl was less than that of the Group V hydrides and changes in  $PH_3$  showed larger effects than did  $AsH_3$ . They concluded that the HCl effect on the vapor phase composition was similar to that of the chloride system. Further, they concluded that  $As_4$  and  $P_4$  caused blocking of the available surface sites on the substrate surface due to the large size of these molecules. The unintentional dopant was assumed to be Si generated from reactions with the quartz wall.

Kennedy, Potter and Davies [36] investigated the effect of HCl inlet composition and additions of HCl downstream of the source zone on the unintentional doping of GaAs grown in a hydride CVD reactor. They found that increasing the HCl inlet composition (by decreasing the  $H_2$  carrier gas flowrate) greatly reduced the free carrier density in the epitaxial layer. In contrast to this result, however, when HCl was added downstream of the source zone the free carrier density was found to increase. This led to the conclusion that the equilibrium model as proposed by DiLorenzo and Moore [23] for the chloride system was not applicable to the hydride system. However, the HCl which was injected may not have been as pure as that which was generated from the decomposition of  $AsCl_3$  in the chloride system and therefore may have introduced additional impurities into the epi-layer.

The problem of obtaining sufficiently pure HCl for use in the hydride system was addressed by Enstrom and Appert [37]. When the HCl tank was cooled in dry ice and the "light" impurities were bled out of the tank, the purity of epitaxial GaAs layers grown with this HCl was found to increase significantly. Using photoluminescence measurements they found C, Be, Zn or O, Si, Mn and Cu in epitaxial GaAs grown with HCl before the HCl cylinder was cooled and bled. Epitaxial GaAs layers grown after the cooling and bleeding procedure displayed essentially unchanged Zn and Si concentrations but the other previously found impurities were undetectable.

The work of Skromme et al. [38] identified some of the unintentional donors and acceptors present in GaAs and InP prepared by the hydride CVD system. They found C, Zn, Cu and Mn as acceptors and Si, S and Ge as donors in GaAs. Epitaxial InP was found to contain Zn, C or Mg and an unidentifiable acceptor along with Si and S as donors. Additionally, in one of the laboratories (Honeywell) where the epi-layers were grown an increase in the impurity concentration in epitaxial GaAs was noted as the HCl gas cylinders "aged". This effect, however, was not observed at the other (Hanscom AFB) laboratory.

The effect of pressure was studied experimentally by Putz et al. [39] from 1 kPa to 100 kPa. They found that the unintentional doping of GaAs was reduced at pressures below 100 kPa.

Growth of InP epitaxial layers using the hydride system has been demonstrated by Olsen [51] and Hyder [52] among others. Both of these investigators observed unintentional impurity incorporation similar to that occurring in the GaAs system. Hyder also found that for the ternary  $In_xGa_{1-x}As$  ( $x=0.53$ ) a maximum in electron mobility occurred when the III/V ratio in the vapor phase was approximately 2 but the effect of III/V ratio on free carrier concentration was not discussed. Zinkiewicz et al. [53] also studied the growth of InP and the ternary  $In_xGa_{1-x}As$  in the hydride system. They found Zn, Cu and Hg to be present as unintentional donors.

Anderson [54] studied the hydride system for InP growth in order to determine the effect of HCl mole fraction,  $H_2$  flowrate and mixing zone temperature on unintentional impurity incorporation. He found that these parameters caused only minor changes in the electrical characteristics of the InP epitaxial layers. This suggests that the InP hydride system may perform somewhat differently than the GaAs hydride system.

Jones [55] performed a thermodynamic analysis of the InP hydride system in order to understand the effect of process parameters on unintentional silicon incorporation. The calculations predicted that decreasing temperatures lowered the silicon activity in the epitaxial layer. Additionally, the silicon activity was decreased by increasing the  $PH_3$  and/or HCl inlet composition. Very little effect was noted when HCl was added downstream of the source zone. His analysis used liquid In as the Group III source material and showed InCl and  $P_4$  to be the dominant Group III and V vapor species.

Bans and Ettenberg [56] coupled a mass spectrometer to a hydride system reactor used for the growth of  $In_xGa_{1-x}P$ . They compared measured vapor species to those predicted by a thermodynamic model and concluded that the model yielded an acceptable representation of the system. The major shortcomings of the model were

an overprediction of the amount of InCl generated from the heterogeneous reaction of HCl and In liquid, and a predicted greater degree of dissociation for  $PH_3$  than was measured. Due to the known slow decomposition kinetics of  $PH_3$  and the potential mass transfer and kinetic limitations associated with heterogeneous reactions these discrepancies were not surprising. Their mass spectrometric measurements identified the major vapor phase species as being InCl, GaCl, HCl,  $PH_3$ ,  $P_2$ ,  $P_4$  and  $H_2$ .

Usui and Watanabe [57] investigated the effects of temperature and oxygen additions on the unintentional doping of hydride grown InP. Additions of  $O_2$  in the 1 ppm to 10 ppm range decreased the free carrier concentration about one order of magnitude but further additions caused the free carrier concentration to increase, presumably due to uptake of oxygen by the epitaxial layer. The liquid In source that was used in these experiments was found to have a gettering effect on impurities in the inlet gases. Unused In showed less than 1 ppm levels of Si, S, Sn, Te, Zn, Fe and Cu while In exposed to the CVD environment contained increased levels ( $\sim 2$  ppm) of Fe, Cu and Sn. Increasing the source zone temperature caused a decrease in the free carrier concentrations in InP epi-layers due to an increased ability of the In liquid to getter impurities at high temperature. Thus, the purity of source gases still appears to be a major problem in the hydride system.

### 3. METHOD OF CALCULATION FOR COMPLEX CHEMICAL EQUILIBRIUM

The calculation of complex chemical equilibrium in multicomponent, multiphase systems has been reviewed most completely by Smith [1]. Essentially, there are two statements of the solution to this problem. Nonstoichiometric methods, such as the popular Rand algorithm [2], directly minimize the Gibbs energy of the total system in order to obtain a solution without recourse to a specific set of formation reaction equations. Stoichiometric methods [3] require that an independent set of chemical reactions be in equilibrium. Generally a formation reaction is written for each specie present in the system and the corresponding equilibrium constant for each reaction is generated from the Gibbs energy change of the reaction.

An extension of the Rand algorithm to include not only a gas phase with an inert specie, but also a multicomponent solution and pure condensed phases is presented in Appendix A. This extension, which was suggested in the original research proposal [4], was initially applied to the hydride and chloride CVD systems but was susceptible to finding local minima. In particular, component mole fractions were sought as low as  $10^{-10}$ . The contribution to the system Gibbs energy for these components is then quite small and the resulting component mole changes were not capable of releasing the Gibbs energy of the system from the local minima.

A stoichiometric algorithm, presented in Appendix B, was therefore developed which was superior to the extended Rand algorithm since a linearized Gibbs energy function was not required and dilute components were required to satisfy equilibrium reaction constraints. The stoichiometric algorithm performed well for all of the systems studied (comparison to standard literature calculations and independence with respect to initial guesses) and yielded results which were in agreement with those of the extended Rand algorithm, when successfully applied ( $\sim 95\%$  of the cases examined). Also, the amount of computer memory required for the stoichiometric algorithm was found to be much less than that required by the extended Rand algorithm in order to

solve identical systems.

The input data which was required in order to perform the calculations consisted of the standard enthalpy and entropy of formation and heat capacity for each specie along with the constraints of system temperature, pressure and inlet composition.

Aside from numerical difficulties, there are two major factors which must be considered in determining the overall accuracy of the calculated equilibrium compositions: 1) the choice of species postulated to be present in the system and 2) the accuracy of the thermodynamic data chosen for each specie. Choosing an appropriate set of species which accurately represent the system at equilibrium is an inherent difficulty in the calculation of multicomponent equilibrium. A true calculation of equilibrium in a given system would require the inclusion of any chemical specie which may be formed from any combination of the elements present in the system. The compilation of such a complete thermodynamic data base can represent a nearly impossible task, even for systems consisting of only a few elements.

It is important to realize that anytime a possible specie is not included in the data set a constrained equilibrium calculation will result. This is most easily understood if the calculation of chemical equilibrium is considered from the viewpoint of the Rand algorithm. In the Rand algorithm multicomponent equilibrium represents the optimal distribution of a given quantity of elements among a set of chemical species. The optimizing function for a constant pressure system is the minimization of the total Gibbs energy. Therefore, as the number of available chemical species is decreased the elements are constrained to reside in a smaller selection of molecules. This causes a shift in the calculated compositions in order to satisfy the atom balance while keeping the Gibbs energy of the system as low as possible. In general, the exclusion of a specie will impact the equilibrium composition of the remaining species containing similar atoms that are in the vicinity or below the equilibrium composition of the excluded specie.

The procedure for developing a specie list first excludes those species not expected to be present because of severe kinetic limitations. In practice this specie set is developed by including only those species which have been experimentally observed in the system or for dilute systems, in constrained subsystems. For example, mass spectroscopic work in the CVD of GaAs has indicated approximately 10 species but observations in the subsystem Si-H-Cl indicates approximately 15 additional species. The next step consists of generating an initial thermodynamic data base for all species. In practice this includes the sources: thermodynamic compilations, data bases of other investigators for similar systems and crude estimates for the remaining species. An initial equilibrium calculation is then performed at the extreme conditions and those species whose composition is more than  $\sim$  three orders of magnitude in mole fraction below the range of interest are excluded. Finally, the initial thermodynamic data base is fully developed by reference to the literature and the performance of internal consistency tests.

The sensitivity of the results to errors in the thermodynamic data was investigated by Smith [5] in terms of a Jacobian which relates the changes in the calculated results to changes in the input parameters. The first order approximation to the result was

$$|\delta n_i| < \sum_{j=1}^N \left| \frac{\partial n_i}{\partial \mu_j^0} \right| |\delta \mu_j^0| \quad (3.1)$$

Here,  $n_i$  is the number of moles of specie  $i$  present,  $\mu_j^0$  is the standard chemical potential of specie  $j$  and  $N$  is the total number of components. This expression, while simple in form, is extremely difficult to evaluate due to the complicated and implicit nature of the function  $n_i(\mu_j^0)$  for all values of  $i$ . If problems seem apparent for some species this function can be numerically evaluated. The work of Sirtl and Hunt [3] and similar calculations performed here (Section 5) showed by means of a calculated example the effects of changes in the enthalpy of formation of  $\text{SiHCl}_3$  on the predicted equilibrium ratio of  $\text{SiCl}_4/\text{SiHCl}_3$ . This ratio was found to change by approximately two orders of

magnitude for a 10% change in enthalpy of formation. The shape of the curve relating this ratio to temperature was also found to change markedly. Therefore, it is extremely important to critically review the thermodynamic data set in order to perform meaningful equilibrium calculations. The absolute composition of the calculated solution can be no better than the data set employed. Extreme care must also be used when comparing equilibrium compositions to experimental process compositions as the latter include possible kinetic limitations. However, these calculations are of great value in predicting directions of composition change or function process constraints, particularly at the high temperatures and low pressures encountered in this study.

#### 4. THERMODYNAMIC MODELS OF CVD

##### 4.1 Models for the CVD Source and Pre-Source Zones

The CVD system is naturally segmented on the basis of temperature or composition into four equilibrium zones: the pre-source, source, mixing and deposition regions. The pre-source zone was investigated as a source of Si by considering the equilibrium gas phase Si-content in the system:  $SiO_2(c)$  in excess, carrier gas ( $H_2$  or inert) and vapor reactant ( $VH_3$ ,  $VCl_3$  or  $HCl$ ). As the activity of  $Si(c)$  monotonically increased with increasing temperature, an uniform temperature equal to the source zone was used for a "worst" case calculation.

For the chloride process two different Group III source materials are generally employed ( $III_V(c)$  and  $III(l)$ ) and thus required two separate formulations of a model. In the pre-source zone, there is no "sink" (i.e. condensed phase) for the elements in vapor input compounds and  $SiO_2(c)$  is in excess while the source zone in both situations also had  $SiO_2(c)$  in excess. Thus, the equilibrium activity of Si is independent of the pre-source results. For the  $III-V(c)$  chloride source zone the model considered the inputs  $SiO_2(c)$  in excess,  $III-V(c)$  in excess, carrier gas ( $H_2$  or inert) and  $VCl_3(g)$  as a function of temperature, pressure and input vapor composition.

For the chloride process using Group  $III(l)$  as the Group III source material the situation is somewhat more complicated. Shaw [7] has studied this source zone and found that, following an initial transient, a constant rate of mass loss of material occurred. An overall mass balance on the source boat yields the following expression:

$$\frac{d}{dt} \left[ \frac{1}{2} n^c (M_{III} + M_V) + n^l (x M_{III} + (1-x) M_V) \right] = \bar{n}^V (y M_{III} + (1-y) M_V) = \text{constant} \quad (4.1.1)$$

while a Group III component mass balance on the source boat produces the constraint:

$$\frac{d}{dt} \left[ \frac{1}{2} n^c M_{III} + n^l x M_{III} \right] = \bar{n}^V y M_{III} \quad (4.1.2)$$

In these expressions:  $n^c$  and  $n^l$  are the moles of the solid source GaAs crust and of the liquid III-V mixture, respectively,  $M_{III}$  and  $M_V$  are the molecular weights of the Group III and V elements,  $x$  and  $y$  are the mole fractions of the Group III element in the liquid and vapor phase, respectively, and  $\dot{n}^V$  is the molar rate at which vapor species are formed on an atomic basis. If it is assumed that the solid and liquid phases are in equilibrium the liquid phase mole fraction is a function of temperature only and therefore constant for a given process condition. Furthermore if the actual kinetic processes produce a steady state value of the crust thickness the first term on the left side of both equations is zero. With these assumptions, equations (4.1.1) and (4.1.2) can be solved to show that  $\dot{n}^V = \frac{dn^l}{dt}$  and  $x=y$ . That is, the rate at which Group III and V atoms are introduced into the vapor phase is equal to the rate of loss for the melt and the vapor composition is the same as that in the melt. Another way of viewing the situation is to consider the three phase equilibrium problem. The activity of the Group III and V elements in the solid compound can vary to a large degree though the stoichiometry ( $\sim 1:1$ ) can be very small and therefore the sum of these two activities is nearly constant. The large amount of melt in equilibrium with the solid will, however, fix the activity of each element in the solid, with the Group III activity being considerably higher than the Group V one, which in turn fixes the vapor phase fugacity. In the event that the assumption of constant crust thickness is not valid the  $dn^S/dt$  terms in equations (4.1.1) and (4.1.2) must be retained and solution results in

$$\dot{n}^V = \text{constant} = \frac{(2x-1)}{2(x-y)} \frac{dn^c}{dt} = \frac{(2x-1)}{2y-1} \frac{dn^l}{dt} \quad (4.1.3)$$

The limit that  $\frac{dn^l}{dt} = 0$  implies that  $y = 1/2$  and the source can be considered to be pure solid compound. This limit is simply the first case examined (solid compound source). Thus an investigation of the two source zones described here should establish the limits of operation for the liquid source in the chloride process. In practice, the conditions of operation may lie somewhere in between with the observed III/V

ratio providing an indicator of the relative rates. However, if  $x$  is a constant as determined by the condition of solid-liquid equilibrium and  $y$  is also a constant as witnessed by a constant growth rate, it follows that both  $\frac{dn^l}{dt}$  and  $\frac{dn^c}{dt}$  are constant. If  $dn^l/dt$  is dependent upon the crust thickness,  $n^c$ , (i.e. a diffusion limited process) then it is impossible for  $dn^l/dt$  to be constant for a finite value of  $dn^c/dt$ , which implies operation at one of the limits.

The above considerations motivated a model for the liquid Group III source zone to consist of an ideal vapor phase in equilibrium with excess  $SiO_2(c)$  and  $III_x V_{1-x}(l)$ . The gas input stream contained  $VCl_3$  and carrier gas ( $H_2$  or inert). The development of a thermodynamic data set for the hypothetical specie  $III_x V_{1-x}(l)$  is presented in Section 5.2. Thus, with this formulation, the compound crust does not contribute elements to the system.

Two source zones, one for the thermal decomposition of the Group V hydride and one for volatilization of the Group III liquid, are found in the hydride CVD process. The Group V source zone was modeled as an ideal vapor phase in equilibrium with excess  $SiO_2(c)$ . The input gas reactants were the hydride ( $VH_3$ ) and carrier gas ( $H_2$  or inert) at a constant temperature and pressure. The Group III source zone included excess pure Group III liquid in equilibrium with excess  $SiO_2(c)$  and an ideal vapor phase (HCl plus carrier gas).

#### 4.2 Models for the CVD Mixing and Deposition Zones

Since the only differences between the chloride and hydride systems exist in the source regions the mixing and deposition zone models were identical in both systems. An ideal vapor phase in equilibrium with excess  $SiO_2(c)$  was used for the mixing zone model. Formation of solid III-V compound was postulated to be kinetically hindered and thus assumed not to exist in the mixing zone. As a result it was possible for this region to be supersaturated. The model also allowed the addition of various species (i.e. HCl,  $H_2O$ ,  $VCl_3$ ,  $VH_3$ ) in order to study their effects on silicon activity. The gas

reactant input for the mixing zone was identical to that calculated from the equilibrium source zone(s). Consistent with the source and mixing zone models, the vapor phase of the deposition zone was assumed to behave ideally. Due to the large volumetric flowrate of gases and the relatively small deposition rates in these CVD processes, the depletion of Group III, Group V and silicon species in the vapor phase as a result of film deposition or wall interaction was neglected. The equilibrium mixing zone gas mixture serves as the input to the deposition zone. Essentially, the above assumption fixes the gas phase atom numbers and the new equilibrium composition is produced as a result of a temperature change only. This model therefore provides an upper bound for the computed value of the Si activity. A lower temperature would shift the wall interactions towards  $SiO_2(c)$  formation while including the compound deposition with Si incorporation would remove Si from the gas phase. In addition, this would be enhanced by chlorine atom production. This model, therefore, assumes that the epi-film grows from a supersaturated vapor mixture of pseudo-steady state properties. Furthermore this procedure avoided having knowledge of the silicon activity coefficient. In order to implement this model the III-V solid phase was not included in the deposition zone, thus allowing calculation of the degree of supersaturation in this zone.

The effect of not accounting for depletion of the Group III and V atoms from the vapor phase can be tested by the following simple analysis. The molar growth rate of an epitaxial layer is just

$$g_m = g_l \rho_m A \quad (4.1.4)$$

where:

- $g_m$  = molar growth rate (moles/time)
- $g_l$  = linear growth rate (length/time)
- $\rho$  = compound molar density (moles/length<sup>3</sup>)
- A = substrate area (length<sup>2</sup>)

A typical set of operating parameters for a hydride CVD process would specify a total volumetric flowrate of 500 SCCM through each source zone having an inlet composition of 1% HCl to the Group III source zone and 1%  $\text{VH}_3$  composition to the Group V source zone. Assuming that all of the HCl reacts to form III-Cl results in  $3.7 \mu\text{-moles/s}$  of Group III atoms transported. The molar flowrate of Group V atoms would also be  $3.7 \mu\text{-moles/s}$ . Choosing as typical deposition parameters a 2.54 cm diameter circular substrate, a linear growth rate of  $1 \mu\text{m/min}$  and the molar density of GaAs as  $0.0367 \text{ moles/cm}^3$  [8] the resulting molar growth rate is  $0.31 \mu\text{-moles/s}$ . Thus, in the worst case less than 10% of the III and V atoms are depleted. The smaller the growth rate and substrate surface area or the larger the volumetric flowrate the better the approximation becomes. If reaction depletion were indeed important, highly non-uniform film thickness would be generated. However, this is not experimentally observed. Similar analyses applied to the GaAs chloride system and the analogous InP systems yield equivalent results.

The activity of silicon in the epi-layer was further studied in the presence and absence of the  $\text{SiO}_2$  reactor wall. Since the deposition zone is typically operated at a lower temperature than the source and mixing zones, inclusion of the reactor wall would be expected to decrease the silicon activity as some of the silicon in the vapor phase is redeposited on the reactor wall via reactions with  $\text{H}_2\text{O}$ . Neglecting interactions with the reactor wall in the deposition zone, therefore, provides an additional method of bounding the maximum value of the silicon activity in the epitaxial layer. Justification for neglecting the reactor wall lies in the heterogeneous nature of the gas-wall reaction. Due to the lower temperature of the deposition zone ( $\sim 873\text{K}$ ) it is expected that this heterogeneous reaction does not equilibrate as rapidly as it should in the source and mixing zones ( $\sim 973\text{K}$ ). This expectation arises from the fact that adsorption reaction rates decrease strongly, and to a lesser extent molecular diffusivities, with decreasing temperature. Additionally, the mean residence time is typically much smaller in the deposition zone. Thus the reactor wall in the deposition

zone should not interact with the vapor phase as strongly as it does in the source and mixing zones.

In order to carry out parametric analyses of the two processes "base cases" were chosen for each system around which each parameter could be varied. The base cases were chosen from commonly used operating parameters reported in the literature, shown in Tables 4.1 and 4.2, thus providing results which may be compared to experimental results. The chloride system base case parameters were:

Source Zone Temperature = Mixing Zone Temperature : 973K  
Deposition Zone Temperature : 873K  
Inlet  $VCl_3$  Composition : 1%  
Carrier Gas :  $H_2$   
System Pressure : 100 kPa

For the hydride system the following base case was chosen:

Source Zone Temperature = Mixing Zone Temperature : 973K  
Deposition Zone Temperature : 873K  
Inlet HCl Concentration = Inlet  $VH_3$  Concentration : 1%  
Carrier Gas :  $H_2$   
Pressure : 100 kPa

Typically the source zone of the hydride system is operated at a higher temperature than that of the chloride system in order to augment the decomposition of  $VH_3$ . Due to the strong influence of temperature on the species present the same temperatures were used in both systems in order to provide direct comparisons between the chloride and hydride CVD systems.

Table 4.1  
Some Typical Operating Parameters for the GaAs and InP Chloride Systems

System	Group III Source Material	% VCl <sub>3</sub> in Feed	Total Flowrate (SOCM)	Zone Temperatures (K)			Pressure (kPa)	Reference
				Source	Mixing	Deposition		
GaAs	liquid	0.1-0.7	250-800	1123	1123	983-1043	100	58
GaAs	solid	0.05-10.0	80	1100	1100	850-1050	0.5-100	31
GaAs	liquid	0.06-0.6	180-800	1123	1123	1000-1100	100	7
GaAs	liquid	0.6-1.2	> 100	1073	1073	1023	100	59
GaAs	solid	0.6-1.2	> 100	1073	1073	1023	100	59
GaAs	liquid	0.15-1.0	600	1123	1123	1023	100	28
GaAs	liquid	0.1-0.8	130	1123	1123	1023	100	23
GaAs	liquid	0.05-0.9	650	1073	1073	973	100	60
GaAs	liquid	0.08-0.35	600	1073	1073	943-993	100	61
GaAs	liquid	?	50	1073	1073	1023	100	17
GaAs	liquid	?	50	1073	1073	1023	100	16
InP	liquid	0.23-0.75	100-800	1023	1023	873-1023	100	62
InP	solid	0.23-0.75	100-800	1023	1023	873-1023	100	62
InP	liquid	?	?	973-1123	973-1123	873-1023	100	40
InP	liquid	0.2-2.0	?	1023	1023	923	100	43
InP	liquid	0.2-4.0	150-250	1023	1023	923	100	63
InP	liquid	0.1-2.9	250	973	973	923	100	44
InP	liquid	1.2	100	1023	1023	923	100	45
InP	solid	?	?	973	973	873	100	64
InP	liquid	0.9-4.6	56	873-1100	873-1100	848-973	100	46
InP	solid	4.6	66	1012-1113	1012-1113	887-991	100	46
InP	liquid	2.0-10.0	200	923-1023	923-1023	823-993	100	49
InP	liquid	0.9-4.5	100-200	1023	1023	933-953	100	48

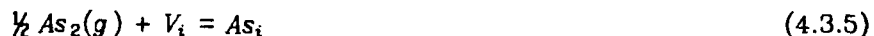
Table 4.2  
Some Typical Operating Parameters for the GaAs and InP Hydride Systems

System	% HCl in Feed	% VH <sub>3</sub> in Feed	Total Flowrate (SCCM)	Zone Temperatures (K)			Pressure (kPa)	Reference
				Source	Mixing	Deposition		
GaAs	0.2-1.0	0.3-1.4	560-2475	1048	1138	973	100	36
GaAs	0.3-3.0	0.3-6.0	30	1023	1073	1023	1-100	39
GaAs	5.0-25	0.2-1.6	1410-2650	1123	1123	1023	100	35
GaAs	0.3-2.4	0.7-1.4	420-980	?	?	973-1023	100	38
GaAs	0.2-2.0	0.05-2.0	?	1023	1023	1023	100	65
InP	2.0-2.6	2.0-2.6	177-1510	?	?	923	100	38
InP	0.65	1.2	500-900	1053-1123	1053-1123	923	100	53
InP	?	?	400-2400	?	973-1223	?	100	54
InP	0.11	0.11	5200	1043-1193	1043-1193	943	100	57
InP	0.3-0.9	0.3-1.9	1690-2400	1173	943-1250	923	100	66

### 4.3 Solid State Defect Chemistry

The model developed for the deposition zone specifies that reactant depletion is not important. That is the growing compound film is exposed to a vapor phase that is invariant with respect to composition. Therefore the vapor phase fugacity of Si is constant and the compound with impurity that is in equilibrium with this vapor phase also has a constant value of Si activity. The problem thus reduces to finding the Si concentration as a function of the fixed vapor composition and temperature. Necessary for this analysis is a description of the solid state composition dependence of the Si activity. Presented below is a point defect model which relates the Si concentration, [Si], to the temperature and gas phase composition.

Hurle (67-70) has recently proposed a model for native defects in GaAs and for Te, Sn and Ge doped GaAs. Strong evidence is presented to support this model and a similar model is developed here to include Si doped III-V compounds. The general model includes the presence of Frenkel disorder on the V sub-lattice and Schottky disorder in the compound. The Si can reside either on a III sub-lattice site (donor) or V sub-lattice site (acceptor). Furthermore, Si substituted on a III site is postulated to complex with both a Group III vacancy and Si substituted on a V site. For convenience of symbol usage, the model described here will specify the compound GaAs. An independent set of native defect reactions is postulated to consist of:



Reaction 4.3.1 represents Frenkel disorder on the As sub-lattice with As on a normal lattice site,  $As_{As}$ , moving to a vacant interstitial site,  $V_i$ , to produce an arsenic intersti-

tial,  $As_i$ , and a vacant arsenic site,  $V_{As}$ . Reaction 4.3.2 displays an electron,  $e^-$ , hole,  $h^+$ , generation step while reactions 4.3.3, 4.3.4 and 4.3.6 describes ionization of  $As_i$ ,  $V_{As}$  and a gallium vacancy,  $V_{Ga}$ . Interaction with gas phase is allowed for through reaction 4.3.5 while 4.3.7 entails Schottky disorder. An independent set of incorporation reactions considered here is:



The amphoteric nature of Si in GaAs is illustrated in reactions 4.3.8 and 4.3.9 while the last two reactions show the formation of the two complexes mentioned earlier. Assuming that Boltzmann statistics are applicable, the defects are sufficiently dilute so that their activities are equal to their concentrations, and the concentrations of  $As_{As}$ ,  $V_i$  and 0 are constant and normalized to unity, the following equilibrium relations can be written:

$$K_1 = [As_i][V_{As}] \quad (4.3.12)$$

$$K_2 = np \quad (4.3.13)$$

$$K_3 = [As_i^+]n / [As_i] \quad (4.3.14)$$

$$K_4 = [V_{As}^+]n / [V_{As}] \quad (4.3.15)$$

$$K_5 = [As_i] / P_{As_2} \quad (4.3.16)$$

$$K_6 = [V_{Ga}^-]p / [V_{Ga}] \quad (4.3.17)$$

$$K_7 = [V_{Ga}][V_{As}] \quad (4.3.18)$$

$$K_8 = [Si_{Ga}^+]n / [V_{Ga}]a_{Si} \quad (4.3.19)$$

$$K_9 = [Si_{As}^-]p / [V_{As}]n_{Si} \quad (4.3.20)$$

$$K_{10} = [Si_{Ga} V_{Ga}^-]p / [V_{Ga}][Si_{Ga}^+] \quad (4.3.21)$$

$$K_{11} = [Si_{Ga} Si_{As}] / [Si_{As}^-][Si_{Ga}^+] \quad (4.3.22)$$

In addition the condition of charge neutrality requires that:

$$p + [Si_{Ga}^+] + [As_i^+] + [V_{As}^+] = n + [V_{Ga}^-] + [Si_{As}^-] + [Si_{Ga} V_{Ga}^-] \quad (4.3.23)$$

In these equations  $K_1$  through  $K_{11}$  are equilibrium constants and a function of temperature only. It is seen that equations 4.3.12 through 4.3.25 contain 15 variables. The problem considered here is to determine the 12 defect concentrations from the 11 equilibrium relationships and the electroneutrality condition given the external parameters  $T$ ,  $P_{As_2}$  and  $a_{Si}$ . An analytical solution to these equations is possible with the results summarized below.

$$[As_i] = K_5 P_{As_2}^{1/2} \quad (4.3.24)$$

$$[V_{As}] = (K_1 / K_5) P_{As_2}^{1/2} \quad (4.3.25)$$

$$[V_{Ga}] = (K_7 K_5 / K_1) P_{As_2}^{1/2} \quad (4.3.26)$$

$$[As_i^+] = K_3 K_5 P_{As_2}^{1/2} n^{-1} \quad (4.3.27)$$

$$[V_{As}^+] = (K_1 K_4 / K_5) P_{As_2}^{-1/2} n^{-1} \quad (4.3.28)$$

$$[V_{Ga}^-] = (K_5 K_8 K_7 / K_1 K_2) P_{As_2}^{1/2} n \quad (4.3.29)$$

$$P = K_2 n^{-1} \quad (4.3.30)$$

$$[Si_{Ga}^+] = (K_5 K_7 K_8 / K_1) P_{As_2}^{1/2} a_{Si} n^{-1} \quad (4.3.31)$$

$$[Si_{As}^-] = (K_1 K_9 / K_2 K_5) P_{As_2}^{-1/2} a_{Si} n \quad (4.3.32)$$

$$[Si_{Ga} V_{Ga}^-] = (K_5^2 K_8 K_7^2 K_8 K_{10} / K_1^2 K_2^2) P_{As_2} a_{Si} n \quad (4.3.33)$$

$$[Si_{Ga} Si_{As}^-] = (K_7 K_8 K_9 K_{11} / K_2) a_{Si}^2 \quad (4.3.34)$$

and the concentration of electrons by

$$n = \left[ \frac{K_2 + K_3 K_5 P_{As_2}^{1/2} + (K_1 K_4 / K_5) P_{As_2}^{-1/2} + (K_5 K_7 K_8 / K_1) P_{As_2}^{1/2} a_{Si}}{1 + (K_5 K_8 K_7 / K_1 K_2) P_{As_2}^{1/2} + (K_1 K_9 / K_2 K_5) P_{As_2}^{-1/2} a_{Si} + (K_5^2 K_8 K_7^2 K_8 K_{10} / K_1^2 K_2^2) P_{As_2} a_{Si}} \right]^{1/2} \quad (4.3.35)$$

Thus the total equilibrium concentration of Si in the solid compound can be determined as a function of the gas phase composition and system temperature. It is seen to be a very complex function of the arsenic partial pressure and silicon activity.

Somewhat simpler expressions can be proposed under the conditions of light doping that are of interest here. At the temperature of growth the material may be considered to be intrinsic (i.e. the presence of Si in small concentrations does not contri-

bute significantly to the total ionized content of the defect structure). Furthermore, the analysis of Hurlé suggests that for GaAs the dominant ionized native defects under VPE conditions are  $e^-$  and  $V_{As}^+$ . Under these assumptions the electroneutrality conditions reduces to:

$$n \cong [V_{As}^+] \quad (4.3.36)$$

and the value of n at growth temperature can be shown to be

$$n = (K_1 K_4 / K_5)^{1/2} P_{As_2}^{1/2} \quad (4.3.37)$$

With this value for n equations 4.3.24 to 4.3.34 remain valid for the defect concentrations. With these assumptions the total Si concentration is

$$\sum [Si] = [Si_{Ga}^+] + [Si_{As}^-] + [Si_{Ga} V_{Ga}^-] + 2[Si_{Ga} Si_{As}] = (a P_{As_2}^{-1/2} + b P_{As_2}^{1/2}) a_{Si} + c a_{Si}^2 \quad (4.3.38)$$

where:

$$a = (K_1 / K_5)^{3/2} (K_9 / K_2) K_4^{1/2}$$

$$b = (K_5 / K_1)^{3/2} K_4^{-1/2} K_7 K_8 [1 + (K_4 K_6 K_7 K_{10} / K_2^2)]$$

$$c = K_7 K_8 K_9 K_{11} / K_2$$

At room temperature the intrinsic defects become negligible when compared to typical unintentional doping levels examined here ( $\sim 10^{17} / cm^3$ ). The room temperature compensation ratio then becomes

$$\frac{N_D}{N_A} = \frac{[Si_{Ga}^+]}{[Si_{As}^-] + [Si_{Ga} V_{Ga}^-]} = \frac{P_{As_2}^{3/2}}{g + h P_{As_2}^{3/2}} \quad (4.3.39)$$

where

$$g = (K_1 / K_5)^3 K_4 K_9 / (K_2 K_7 K_8)$$

$$h = K_4 K_6 K_7 K_{10} / K_2^2$$

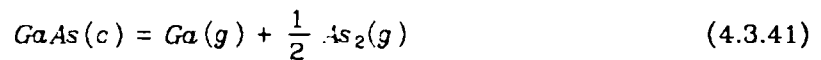
This relationship indicates that the room temperature compensation ratio does not depend on the  $a_{Si}$  and if the  $[Si_{As}^-] > [Si_{Ga} V_{Ga}^-]$  then  $N_D / N_A \propto P_{As_2}^{3/2}$  or if the reverse is

true then there should be no  $P_{As_2}$  dependence for  $N_D/N_A$ . Since the observed compensation ratio for LPE and VPE material is nearly the same, though  $P_{As_2}^-$  varies by nearly two orders of magnitude, it is suggested that the dominant acceptor is  $Si_{Ga}^- V_{Ga}^-$ . For the intentional doping of both GaAs and InP with Si in the light doping region it is found that the free carrier concentration,  $N_D - N_A$ , is directly proportional to the total ionized impurity concentration. Therefore in this region of doping the  $[Si_{Ga}^- Si_{As}^-]$  should not be important and the last term in equation 4.3.38 is negligible. In this simplified version of the defect chemistry associated with Si incorporation the total [Si] is

$$\sum [Si] \cong [Si_{Ga}^+] + [Si_{Ga}^- V_{Ga}^-] = b P_{As_2}^{3/4} a_{Si} \quad (4.3.40)$$

Thus, the concentration of Si in the compound semiconductor should increase with both the external  $As_2$  partial pressure and silicon activity.

In order to complete the thermodynamic model, a means of relating the external gas phase variables introduced above ( $P_{As_2}$  and  $a_{Si}$ ) must be related to the supersaturated external gas phase composition calculated in the deposition zone. The model stipulates a growing solid surface in equilibrium with the vapor just above it. The Ga partial pressure is determined from the equilibrium reaction



with the relation

$$P_{Ga}^s = K_{41} P_{As_2}^{5/2} \quad (4.3.42)$$

Of course all of the other species originally postulated exist above the vapor as determined from equilibrium relationships. The solid-gas interface is next assumed to be separated from the equilibrium deposition zone gas phase (supersaturated) by a mass transfer barrier. In the steady state, the flux of molecules is constant across the

barrier with the atomic flux of As equal to the Ga flux as required by stoichiometry. In addition the flux of Cl, H and O atoms is zero since there is no net incorporation of these atoms into the growing film. The flux of a specie *i* is assumed to be given by

$$J_i = K(P_i^o - P_i^s) \quad (4.3.43)$$

where  $P_i^o$  and  $P_i^s$  is the partial pressure of specie *i*, in the equilibrium bulk gas phase and at the surface, respectively. The proportionality constant is furthermore assumed to be the same for all species (e.g. for diffusion limited mass transfer  $K = -D_i / RT\delta$ , where  $D_i$  is the diffusion coefficient of specie *i* and  $\delta$  is the diffusion boundary layer thickness). With this assumption the following relations hold

$$\sum P_{Ga}^o \text{ species} - \sum P_{As}^o \text{ species} = \sum P_{Ga}^s \text{ species} + \sum P_{As}^s \text{ species} \quad (4.3.44)$$

$$\sum P_{Cl}^o \text{ species} = \sum P_{Cl}^s \text{ species} \quad (4.3.45)$$

$$\sum P_H^o \text{ species} = \sum P_H^s \text{ species} \quad (4.3.46)$$

$$\sum P_O^o \text{ species} = \sum P_O^s \text{ species} \quad (4.3.47)$$

In addition, the temperature and pressure are specified and all the equilibrium relationships solved for the gas phase deposition zone are also valid at the surface (involves all the  $P_i^s$  variables). However, an additional mixture phase has been included (the Si-GaAs defect solid solution) which is in equilibrium with the surface gas phase, with equation 4.3.42 now also valid and independent. Finally, the flux of Si atoms must be equal to the solid incorporation rate by

$$\left[ \sum P_{Si}^o \text{ species} - \sum P_{Si}^s \text{ species} \right] \sum [Si] = \sum P_{Ga}^o \text{ species} - \sum P_{Ga}^s \text{ species} \quad (4.3.48)$$

Given  $T$ ,  $P$ ,  $K_{eq}(T)$  and all  $P_i^o$ , the equations 4.3.40, 4.3.42, 4.3.44-48, and the gas phase equilibrium relations can be solved for the total concentration of Si atoms in the solid.

The above procedure was not performed here for the following reasons. The solution to these equations is extremely difficult due to their non-linear behavior. Also the distribution coefficient of Si (amount in solid/ amount in gas) is much less than unity

and thus the surface  $a_{Si}^s$  should not be much different than the bulk  $a_{Si}^g$ . Since the solid represents a "sink" for equal amounts of Ga and As atoms the  $P_{As_2}^s$  will necessarily decrease at the substrate surface. The amount by which  $P_{As_2}^s$  will differ from the bulk value,  $P_{As_2}^g$ , depends upon the III/V ratio and the supersaturation ratio.

In summary, the total concentration of Si in the growing compound can be seen to increase with  $a_{Si}$  found in the vapor phase and with the partial pressures of the Group V species. Because of a lack of knowledge of the defect reaction equilibrium constants the quantification of this dependence is not possible. However, the results of this parametric analysis should provide correct directions of change in Si content for changes in operating conditions.

## 5. THERMOCHEMICAL PROPERTIES

### 5.1 Introduction

Summarized in this section are the thermochemical properties used for the complex chemical equilibrium analysis. The proper selection of a consistent data set is of extreme importance as a small error in a property value can greatly influence the eventual calculated equilibrium composition. That this sensitivity can be important is nicely illustrated in the Si-Cl-H sub-system as discussed later. Essentially, what is required for these calculations is a means of specifying the partial molar Gibbs energy of each specie believed to be present as a function of temperature, pressure and composition. Approximately 150 species were initially examined while only those species that would be present at a mole fraction  $> 10^{-14}$  were included in the analysis. The scheme of representing the data was to fix the zero enthalpy scale at 298K and 1 atm with the pure components (standard states) Ga(c), As(c), In(c), white P(c),  $H_2(g)$ , Si(c),  $Cl_2(g)$  and  $O_2(g)$ . The enthalpy of forming the remaining components at the standard conditions from the reference components was determined. In addition, the absolute entropy at the standard conditions for each specie was selected which allows a calculation of the standard Gibbs energy change for all possible reactions at 298K and 1 atm. Finally, knowledge of the constant pressure heat capacity and assuming ideal gas behavior allows the Gibbs energy to be determined at any temperature and pressure. The gas phase was assumed to be a solution of ideal gases as is justified by the low pressure and high temperatures investigated. As a result of this simplification the pressure and composition dependence of the partial molar Gibbs energy is explicit in both formulations of the solution procedure. For the condensed solutions the pressure dependency of the thermochemical properties was neglected, however the moderate deviations from ideal behavior in the composition dependence was accounted for and represents one of the significant refinements contained in these calculations. As must be the case, this data base is sufficient for achieving a solution with either the stoichiometric or non-stoichiometric algorithms.

Thus three pieces of information were required for each species with the standard enthalpy of formation being the most critical, particularly at the lower temperatures. It is for this quantity that the most uncertainty exists in the reported values. On the other hand, the standard entropy is generally quite accurately known, either from low temperature heat capacity measurements or spectroscopic studies. The high temperature heat capacities were sometimes estimated, but there exists a partial cancellation of its effect when calculating Gibbs energy changes. Presented below is a discussion of the properties selected. It is noted that in many instances the thermochemical data presented in the JANAF (29-31) tables were used and is discussed in these tables, therefore precluding a discussion here. A summary of the selected thermochemical properties is presented in Table 5.1. In order that the stability of various species might easily be compared, the standard molar Gibbs energy of formation is listed at various temperatures in Table 5.2.

### **5.2 Pseudo-Steady State Constraint for Liquid Source Boat**

It has been observed that during VPE of GaAs and InP with a liquid source boat of pure Group III metal in the chloride process an initial transient period exists in which the composition of the gas stream leaving the source region is a function of time. Initially, the pure metal boat is dissolving the Group V atom thus producing an excess of Group III chloride. As the metal becomes saturated with the Group V element a thin crust of the compound is formed at the top surface since the density of the compound is less than that of the saturated liquid. It is observed that the crust thickness reaches a steady state value and therefore, from a simple mass balance, the vapor phase will contain all of the Group V atom in the input stream plus the amount of Group V atom generated from the saturated liquid (due to reaction of chlorine with the Group III atom). The exact amount of Group V element produced from the source boat is therefore a function of the temperature (i.e. the equilibrium Group V mole fraction in the liquid is a function of temperature and the amount of Group III atom

Table 5.1 Selected Thermochemical Values

Specie	$\Delta H_f^{\circ},_{298K}$ kcal mol <sup>-1</sup>	Ref.	$S_{298}^{\circ}$ cal mol <sup>-1</sup> K <sup>-1</sup>	Ref.	$C_p^{\circ}$ cal mol <sup>-1</sup> K <sup>-1</sup>				Form*	Ref.
					a	b×10 <sup>3</sup>	c×10 <sup>-6</sup>	d		
As(c)	0	--	8.53±0.1	1	6.736	1.50	-0.1504	-0.1967	1	1
As(g)	68.7±1.0	1	41.611±0.1	1	4.968	--	--	--	1	1
As <sub>2</sub> (g)	45.95±10.0	**	57.546±0.1	1	7.630	-0.169	-0.3708	0.212	1	1
As <sub>3</sub> (g)	52.2±1.0	1	74.121±0.1	1	13.836	-0.1365	-0.5889	0.172	1	1
As <sub>4</sub> (g)	37.5±0.6	**	78.232±0.1	1	18.616	-0.1756	-1.1128	0.218	1	1
AsCl(g)	27±3	48	66.24±2.0	48	8.878	0.0453	-0.3615	--	1	48
AsCl <sub>2</sub> (g)	14.5±4	48	72.04±2	48	13.79	0.08566	-0.3524	--	1	48
AsCl <sub>3</sub> (g)	-62.7±4.0	**	77.97±2.0	48	19.76	0.0726	-1.5766	--	1	48
AsH(g)	58±12	**	51±3	**	6.4	1.432	0.138	--	1	29(P)
AsH <sub>3</sub> (g)	16±2	14-16 52	53.22±0.8	83	10.07	5.42	-2.20	--	1	79
Cl(g)	28.992±0.002	82	39.454±0.005	82	5.779	-0.4083	-0.387	--	1	30
Cl <sub>2</sub> (g)	0	--	53.29±0.01	82	8.8	0.208	-0.67	--	1	29
Ga(c)	0	--	9.758±0.05	1	6.40	--	--	--	1	1
Ga(g)	65.0±0.05	1	40.375±0.05	1	30.138	2.09	-2.652	-3.812	1	1
GaCl(g)	-17.0±5	**	57.36±1.0	56	8.925	1.021	-0.3949	--	1	56
GaCl <sub>2</sub> (g)	59.2±5	41	72.09±1.5	56	13.84	5.15	-0.8644	--	1	56
GaCl <sub>3</sub> (g)	-107.3±3	53,54	79.93±2.0	56	19.74	0.0744	-1.690	--	1	56
Ga <sub>2</sub> Cl <sub>6</sub> (g)	-235.6±10	**	127.9±6.0	**	43.06	0.427	-4.922	--	1	29 (Al <sub>2</sub> Cl <sub>6</sub> )
H(g)	52.103±0.001	82	27.391±0.004	82	4.368	--	--	--	1	31
H <sub>2</sub> (g)	0	--	31.207±0.008	82	19.256	2.12	-0.9506	-1.462	1	29
HCl(g)	-22.063±0.03	82	44.643±0.008	82	6.224	1.29	0.3251	--	1	29
H <sub>2</sub> O(g)	-57.795±0.01	82	45.106±0.01	82	3.429	2.44	0.670	0.5682	1	29
In(c)	0	--	13.82±0.2	1	4.59	6.04	--	--	1	1
In(g)	57.3±1.0	**	41.507±0.2	1	3.775	4.426	--	-1.689×10 <sup>-6</sup>	2	1
InCl(g)	-16.8±1.0	**	59.26±0.8	78	8.93	--	-0.209	--	1	79
InCl <sub>2</sub> (g)	-58.4±1.0	80	73.4±1.0	80	13.84	0.0515	0.8644	--	1	56 (GaCl <sub>2</sub> )
InCl <sub>3</sub> (g)	-89.4±4	14	83.8±1.0	14	18.0	1.7	--	--	1	15
In <sub>2</sub> Cl <sub>6</sub> (g)	208.5±10	60	129.7±2.0	60	40.0	3.4	--	--	1	60
O(g)	59.553±0.2	82	38.467±0.005	82	5.542	0.061	0.1688	-0.0899	1	31
O <sub>2</sub> (g)	0	--	49.005±0.008	82	-7.902	-1.15	0.8877	2.504	1	29

Table 5.1 Continued

Species	$\Delta H_f^{\circ},_{298K}$ kcal mol <sup>-1</sup>	Ref.	$S_{298}^{\circ}$ cal mol <sup>-1</sup> K <sup>-1</sup>	Ref.	$C_p^{\circ}$ cal mol <sup>-1</sup> K <sup>-1</sup>				Form*	Ref.
					a	b × 10 <sup>3</sup>	c × 10 <sup>-5</sup>	d		
P(c), white	0	--	9.82±0.02	29	5.7	--	--	--	1	29
P(g)	75.62±0.25	1	38.98±0.02	1	4.968	--	--	--	1	29
P <sub>2</sub> (g)	34.34±0.9	1	52.11±0.1	1,29	8.236	8.6618	0.6036	--	1	29
P <sub>4</sub> (g)	12.58±2	**	66.89±0.1	1	19.2	0.5744	-0.2974	--	1	29
PCl(g)	31.0±2.0	29	56.8±1.0	29	7.537	-0.0581	-0.4304	0.2216	1	29
PCl <sub>3</sub> (g)	-68.67±1.4	29	74.47±0.1	29	11.291	-0.6038	-1.767	0.8773	1	29
PCl <sub>5</sub> (g)	-95.5±2	49	83.5±1.0	49	23.4	12.0	--	--	1	80
PH(g)	56.2±8	29	46.9±2.0	29	6.4	1.432	0.108	--	1	29
PH <sub>2</sub> (g)	25.9±2.0	29	50.8±2.0	29	6.524	6.237	--	-1.506×10 <sup>-6</sup>	2	29
PH <sub>3</sub> (g)	1.3±0.4	81	50.24±1.0	29	4.77	14.97	--	-4.388×10 <sup>-6</sup>	2	29
PO(g)	-5.5±1.5	30	53.218±0.005	30	-5.225	-1.256	0.7156	2.173	1	30
Si(c)	0	--	4.486±0.02	82	5.73	0.6811	-1.056	--	1	29
Si(g)	108±1.0	**	40.123±0.003	1	4.82	0.18	0.42	--	1	29
SiCl(g)	47.4±0.6	93	56.82±0.04	29	8.87	0.1387	-0.328	--	1	29
SiCl <sub>2</sub> (g)	-40.4±0.6	**	67.36±1.0	30	11.258	-0.234	-1.105	0.4081	1	30
SiCl <sub>3</sub> (g)	-93.3±0.6	93	75.17±1.5	29	12.797	-0.762	-1.761	1.112	1	29
SiCl <sub>4</sub> (g)	-158.4±0.3	30	79.07±0.05	30	14.511	-1.21	-2.416	1.778	1	30
SiH(g)	90.0±2.0	29	47.306±0.05	29	6.63	-1.423	0.0988	--	1	29
SiH <sub>4</sub> (g)	8.2±0.8	29	48.89±0.01	29	-74.824	-6.17	3.329	14.597	1	29
SiHCl <sub>3</sub> (g)	-119.5±1.0	**	74.924±2.0	29	-7.913	-2.42	-1.535	4.983	1	29
SiH <sub>2</sub> Cl <sub>2</sub> (g)	-75.5±2.0	97	68.531±2.0	29	-31.537	-3.85	-0.3446	8.408	1	29
SiH <sub>3</sub> Cl(g)	-32.7±2.5	97	59.9±2.0	29	-53.526	-5.04	1.248	11.554	1	29
SiO(g)	-24±2	29	50.54±1.0	29	-6.471	-1.39	0.4755	2.368	1	29
SiO <sub>2</sub> (c)	-217.7±0.2	82	9.91±0.05	82	31.588	14.14	-3.761	-3.703	1	29
SiO <sub>2</sub> (g)	-73±8	29	54.7±1.0	29	-14.368	-2.70	0.095	4.4884	1	29
Si <sub>2</sub> Cl <sub>6</sub>	-236±8	86	101.0±3.0	86	42.15	1.03	-8.46	--	1	86
Si <sub>2</sub> H <sub>6</sub>	17.1±3	99	70±5	**	2.247	38.20	--	-11.05×10 <sup>-6</sup>	2	C <sub>2</sub> H <sub>6</sub>
GaAs(c)	-19.52±1.0	32	15.34±0.1	42	10.16	2.8	--	--	1	43
InP(c)	-14.0±1.0	32	14.28±0.1	42	12.27	--	-0.114	298<T<910	1	68
					5.89	6.40	--	T>910	1	68

\* Form 1:  $C_p(T/K) = a + bT + c/T^2 + d \ln T$

Form 2:  $C_p(T/K) = a + bT + cT^2 + dT^3$

\*\* See text

Table 5.2 The Molar Gibbs Energy of Formation of Various Species  
(kcal mol<sup>-1</sup>)

Specie	Temperature (K)					
	273.2	873.2	973.2	1073.2	1173.2	1273.2
As(g)	59.657	38.009	34.140	30.220	25.253	22.244
As <sub>2</sub> (g)	34.880	7.467	2.436	-2.686	-7.591	-13.172
As <sub>3</sub> (g)	38.926	4.566	-1.934	-8.586	-15.376	-22.294
As <sub>4</sub> (g)	25.429	-7.959	-14.549	-21.342	-28.319	-35.465
AsCl(g)	19.204	-2.576	-6.669	-10.854	-15.121	-19.465
AsCl <sub>2</sub> (g)	11.694	0.735	-1.807	-4.491	-7.504	-10.235
AsCl <sub>3</sub> (g)	-59.852	-60.388	-61.496	-62.806	-64.300	-65.962
AsH(g)	50.652	31.956	28.451	24.866	21.207	17.479
AsH <sub>3</sub> (g)	16.570	13.767	12.613	11.305	9.649	8.255
Cl(g)	25.487	15.858	13.970	12.026	10.133	7.995
Cl <sub>2</sub> (g)	-0.009	-3.088	-4.061	-5.126	-6.275	-7.501
Ga(g)	56.629	35.966	32.200	28.376	24.500	20.578
GaCl(g)	-22.735	-38.459	-41.543	-44.719	-47.979	-51.314
GaCl <sub>2</sub> (g)	-61.684	-71.946	-74.373	-76.943	-79.641	-82.457
GaCl <sub>3</sub> (g)	-104.652	-105.596	-106.769	-108.145	-109.703	-111.430
Ga <sub>2</sub> Cl <sub>6</sub> (g)	-221.574	-205.303	-204.797	-204.734	-205.072	-205.779
H(g)	48.877	40.006	38.266	36.474	34.637	32.757
H <sub>2</sub> (g)	-0.007	-2.534	-3.326	-4.192	-5.125	-6.122
HCl(g)	-22.725	-26.697	-27.736	-28.853	-30.041	-31.295
H <sub>2</sub> O(g)	-54.907	-51.561	-51.471	-51.482	-51.587	-51.779
In(g)	49.731	31.230	27.846	24.397	20.938	17.324
InCl(g)	-21.942	-36.010	-38.793	-41.666	-44.620	-47.649
InCl <sub>2</sub> (g)	-60.132	-68.743	-70.895	-73.189	-75.612	-78.153
InCl <sub>3</sub> (g)	-86.700	-87.525	-88.669	-90.016	-91.547	-93.249
In <sub>2</sub> Cl <sub>6</sub> (g)	-195.220	-181.003	-180.857	-181.156	-181.863	-182.945
O(g)	55.732	45.999	43.528	41.505	39.436	37.324
O <sub>2</sub> (g)	-0.008	-2.662	-3.513	-4.450	-5.465	-6.553
OH(g)	8.453	3.622	2.443	1.188	-0.136	-1.524
P(g)	67.648	48.353	44.876	41.348	37.773	34.156
P <sub>2</sub> (g)	25.468	4.172	0.257	-3.743	-7.821	-11.972
P <sub>4</sub> (g)	5.020	-17.964	-22.780	-27.796	-32.994	-38.361
PCl(g)	25.436	10.119	7.102	3.994	0.802	-2.467
PCl <sub>2</sub> (g)	-64.512	-61.973	-62.552	-63.332	-64.296	-65.427
PCl <sub>3</sub> (g)	-79.260	-53.983	-51.421	-49.220	-47.358	-45.815
PH(g)	50.325	34.862	31.897	28.851	25.731	22.542
PH <sub>2</sub> (g)	23.221	14.088	12.041	9.880	7.611	5.243
PH <sub>3</sub> (g)	3.036	3.028	2.360	1.536	0.565	-0.544
PO(g)	-10.671	-24.850	-27.644	-30.526	-33.490	-36.527

Table 5.2 Continued

Species	Temperature (K)					
	273.2	873.2	973.2	1073.2	1173.2	1273.2
Si(g)	98.258	75.012	70.872	66.679	62.440	58.157
SiCl(g)	40.373	21.794	18.231	14.576	10.836	7.020
SiCl <sub>2</sub> (g)	-42.931	-53.383	-55.830	-58.419	-61.136	-63.971
SiCl <sub>3</sub> (g)	-91.064	-92.699	-93.970	-95.442	-97.197	-98.919
SiCl <sub>4</sub> (g)	-149.682	-138.946	-138.446	-138.207	-138.235	-138.420
SiF(g)	82.557	63.612	60.058	56.421	52.718	48.924
SiH <sub>4</sub> (g)	13.109	19.151	19.295	19.234	18.980	18.544
SiHCl <sub>3</sub> (g)	-112.662	-104.996	-104.889	-105.028	-105.192	-105.963
SiH <sub>2</sub> Cl <sub>2</sub> (g)	-69.928	-64.060	-64.142	-64.457	-64.855	-65.713
SiH <sub>3</sub> Cl(g)	-27.784	-22.474	-22.546	-22.835	-23.126	-24.011
SiO(g)	-29.896	-45.574	-48.611	-51.735	-54.939	-58.218
SiO <sub>2</sub> (g)	-73.342	-78.331	-79.840	-81.493	-83.276	-85.181
Si <sub>2</sub> Cl <sub>6</sub> (g)	-217.500	-190.437	-188.052	-186.103	-184.530	-183.362
Si <sub>2</sub> H <sub>6</sub> (g)	25.991	39.324	40.364	41.106	41.534	41.751
As(c)	-0.006	-2.228	-2.935	-3.714	-4.557	-5.460
Ga(c)	-0.007	-2.324	-3.047	-3.836	-4.685	-5.588
GaAs(c)	-18.727	-21.207	-22.269	-23.467	-24.790	-26.230
In(c)	-0.007	-2.665	-3.561	-4.565	-5.672	-6.878
InP(c)	-11.455	-10.040	-10.433	-10.950	-11.552	-12.317
P(c), white	-0.006	-2.070	-2.714	-3.416	-4.172	-4.977
Si(c)	-0.005	-1.969	-2.605	-3.307	-4.067	-4.883
SiO <sub>2</sub> (c)	-205.805	-184.503	-181.795	-179.288	-176.973	-174.844

leaving depends on the form in which it leaves (e.g. HCl, HCl<sub>3</sub>, H<sub>2</sub>, etc.) and the flow rate (i.e. mass transfer efficiency). The mechanism by which the Group III and V atoms reach the gas/solid interface is not known but is not required for the thermodynamic model presented here as mass transfer barriers (e.g. the crust) are assumed not to be present. All that is required is to assume a new species exists having a stoichiometry equivalent to the saturated liquid composition.

The thermodynamic properties of the hypothetical liquid species, A<sub>1-x</sub>B<sub>x</sub>(l), can be estimated in the following manner. Letting A represent the Group III atom and B the Group V atom, consider the reaction sequence:

$$(1-x) A(c) = (1-x) A(l) \tag{5.2.1}$$

$$x B(c) = x B(l) \tag{5.2.2}$$

$$(1-x) A(l) + xB(l) = A_{1-x}B_x(l) \tag{5.2.3}$$

all occurring at the source temperature, T. Since A and B are in pure state, the

Gibbs energy changes for reactions (5.2.1) and (5.2.2) are the Gibbs energies of formation for the liquid species and can be calculated from the thermodynamic sequence: solid element A or B is taken from T to its melting temperature  $T_m^A$  or  $T_m^B$ , the solid element is melted, the liquid element is taken from the melting temperature to the original temperature of interest. Assuming the heat capacity difference between the pure liquid and pure solid,  $\Delta C_p$ , is constant, the Gibbs energy change for reactions (5.2.1) and (5.2.2) are:

$$\Delta G(1) = (1-x) \left\{ \Delta H_m^A \left[ 1 - \frac{T}{T_m^A} \right] + \Delta C_p^A \left[ T - T_m^A - T \ln \left[ \frac{T}{T_m^A} \right] \right] \right\} \quad (5.2.4)$$

and

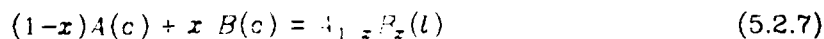
$$\Delta G(2) = x \left\{ \Delta H_m^B \left[ 1 - \frac{T}{T_m^B} \right] + \Delta C_p^B \left[ T - T_m^B - T \ln \left[ \frac{T}{T_m^B} \right] \right] \right\} \quad (5.2.5)$$

The Gibbs energy change of the third reaction is simply the Gibbs energy of mixing and, assuming a simple solution model describes the liquid behavior, results in

$$\Delta G(3) = (a+bT) x(1-x) + RT[x \ln x + (1-x) \ln(1-x)] \quad (5.2.6)$$

where a and b are adjustable parameters determined in conjunction with solid-liquid equilibrium data.

The sum of reactions (5.2.1) to (5.2.3) is the desired formation reaction



while the corresponding Gibbs energy of formation of  $A_{1-x}B_x(l)$  is the sum of  $\Delta G(1)$  to  $\Delta G(3)$ . Given the source temperature, T, the procedure is to first calculate the liquidus composition, x, from the implicit equation:

$$\frac{T}{T_m^{AB}} \Delta H_m^{AB} - R \ln[4x(1-x)] + b \left[ \frac{1}{2} - x^2 - (1-x)^2 \right] = \Delta H_m^{AB} - a \left[ \frac{1}{2} - x^2 - (1-x)^2 \right] \quad (5.2.8)$$

where  $\Delta H_m^{AB}$  and  $T_m^{19}$  are the enthalpy of fusion and melting temperature of the solid compound AB and R is the gas constant. Once the equilibrium Group V composition is determined the standard Gibbs energy of formation of  $A_{1-x}B_x(l)$  can be calculated from equations (5.2.4) to (5.2.6) given T, x and the required thermochemical properties. Tables 5.3a and 5.3b summarize the thermochemical properties used in these calculations. The adjustable parameters a and b for GaAs were determined by reduction of the liquidus measurements of Clariou et al. (102), Hall (103), Koster and Thoma (101), Muszynski and Riabeev (104) and Osamura et al. (105) using a maximum likelihood algorithm.

**Table 5.3a Thermochemical Properties of GaAs and InP required for calculating  $\Delta G_f^\circ[A_{1-x}B_x(l), T]$**

Property	GaAs	Reference	InP	Reference
$T_m^{AB}(K)$	1511	101	1332	71,72,74
$\Delta H_m^{Al}(kcal\ mol^{-1})$	25.14	43	14.4	71,72,73
a ( $cal\ mol^{-1}$ )	4,666	see text	5,055	75
b ( $cal\ mol^{-1}\cdot K^{-1}$ )	-8.74	see text	-5.0	75

**Table 5.3b Thermochemical properties of the elements Ga, In, As and P required for calculating  $\Delta G_f^\circ[A_{1-x}B_x(l), T]$**

Property	Ga	Ref.	In	Ref.	As	Ref.	P	Ref.
$T_m(K)$	302.9	1	429.76	1	1090	17	313.3	29
$\Delta H_m(kcal\ mol^{-1})$	1.336	1	0.78	1	5.123	17	0.157	29
$\Delta C_p(cal\ mol^{-1}\cdot K^{-1})$	0.27	1	-0.2	1	1.0	estimated	0.472	1

### 5.3 The Ga-As-CI-H System

The enthalpy of vaporization of As(c) has been investigated quite extensively with a reported range (1-16) of 34.4 to 38.54  $kcal\ mol^{-1}$   $As_4(g)$  and corresponds to the standard enthalpy of formation for  $As_4(g)$ . The literature has been summarized by Hultgren et al. (1) to 1973, while a more recent measurement of Kase et al. (2) by a static method produced a value of 38.14  $kcal\ mol^{-1}$ . In addition, Rau (17) has measured the total vapor pressure over solid and liquid arsenic from 550 to 1175 with a Bourdon

gauge. Analysis of the low temperature results indicated  $\Delta H_f^\circ(\text{As}_4, g, 298K) = 37.31 \pm 0.2 \text{ kcal mol}^{-1}$ . The value selected was  $37.5 \text{ kcal mol}^{-1}$  on the basis that the static methods are believed to be more reliable.

The dissociation enthalpy,  $\Delta H^\circ(\text{As}_4 = 2\text{As}_2, 298K)$ , has received considerable investigation with early mass spectrometric studies producing values in the range of 61.5 to  $73.5 \text{ kcal mol}^{-1}$  (20,24-27). These measurements are suspected of overestimating the  $\text{As}_4$  partial pressure as a result of a low condensation coefficient for  $\text{As}_4$  thus producing high  $\text{As}_4$  ion currents. More recent determinations using  $\text{WAs}_2$ ,  $\text{Mo}_2\text{As}_3$ , GaAs, InAs, and InAs + InSb sources with improved Knudsen-cell mass-spectrometer designs (18,19,21) and reduction of PVT measurements (17) have indicated a much lower value for the dissociation enthalpy ( $54.21 \pm 1.5$ ,  $54.26 \pm 1.1$ ,  $54.2 \pm 1.4$  and  $54.8 \pm 1.0 \text{ kcal mol}^{-1}$ , respectively). The value selected here is the average of these four measurements,  $54.4 \pm 1.5 \text{ kcal mol}^{-1}$ . Using the selected values from the standard enthalpies,  $\Delta H_f^\circ(\text{GaAs}, c, 298K) = 19.52 \text{ kcal mol}^{-1}$ ,  $\Delta H_f^\circ(\text{As}_4, g, 298K) = 37.5 \text{ kcal mol}^{-1}$  and the above dissociation enthalpy yields  $\Delta H^\circ(\text{GaAs}, c) = \text{Ga}(c) + \frac{1}{2} \text{As}_2(g), 298K) = 42.5 \text{ kcal mol}^{-1}$  and can be compared to the values of 44.85 (18), 45.15 (19) and 45.4 (28)  $\text{kcal mol}^{-1}$ .

The value adopted for  $\Delta H_f^\circ(\text{GaAs}, c, 298K)$  is  $-19.52 \text{ kcal mol}^{-1}$  as determined by Martosdirdjo and Pratt (32) with a precipitation calorimetric technique. This value can be compared to the emf work of Abbasov (33) and Sirota et al. (34) in which values of  $-19.4$  and  $-20.96 \text{ kcal mol}^{-1}$  were reported, respectively. These latter two values are expected to contain uncertainties due to the assumed valency of Ga in the galvanic cell and the inability to accurately determine the full temperature dependence over a relatively small temperature range of measurement. In addition a considerable number of dissociation pressure studies (18,19,21-25,27,35-40) and flow equilibration investigations with reactive gases (23,41) have been performed which contain information about solid GaAs. However, knowledge of the thermodynamic properties of other

species is required (i.e.  $As_2(g)$ ,  $As_4(g)$ ,  $GaCl(g)$ ,  $Ga_2As_{1/2}(l)$  etc.) to specify the properties of  $GaAs(c)$  and thus introduce the uncertainty in their properties in addition to those associated with the measurements. However, this work can be used to impose an internal consistency in the total data set. The standard entropy of  $GaAs$ ,  $S^\circ(GaAs, c, 298K)$  was taken from the low temperature heat capacity measurements of Piesbergen (42) while the high temperature heat capacity was taken from the measurements of Lichter and Sommelet (43) and are in good agreement with the work of Cox and Pool (39) and the estimates of Marina et al. (44) and Maslov and Maslov (45).

Very little experimental information is available for the arsenic chlorides. The reported range for the enthalpy of formation of  $AsCl_3(g)$  is  $-52$  to  $-72 \text{ kcal mol}^{-1}$  (14,16,46-51). The value adopted was  $\Delta H_f^\circ(AsCl_3, g, 298K) = -62.7 \text{ kcal mol}^{-1}$ , taken from the enthalpy of formation of the liquid and the enthalpy of vaporization. The enthalpy of formation of the mono and dichlorides were taken from the estimates of Shaulov and Mosin (48) as was the standard entropy and heat capacity. The enthalpy of formation of arsine was taken as  $\Delta H_f^\circ(AsH_3, g, 298K) = 16.0 \pm 1.5 \text{ kcal mol}^{-1}$  based on the work of Gunn (52) and reported tabulations (14-16). Finally the thermochemical properties of the remaining arsenic hydrides were estimated by comparison with the hydrides of N, P and Sb (29-31).

The thermodynamic information available for the chlorides of gallium is somewhat scarce and inconsistent. The enthalpy of formation for  $GaCl_3(g)$  was determined from  $\Delta H_f^\circ(GaCl_3, c, 298K) = -125.0 \text{ kcal mol}^{-1}$  (53) and the enthalpy of sublimation taken from the vapor pressure measurements of Kuroya et al. (54),  $\Delta H^\circ(GaCl_3(c) = GaCl_3(g), 298K) = 17.7 \text{ kcal mol}^{-1}$ , producing  $\Delta H_f^\circ(GaCl_3, g, 298K) = -107.3 \pm 3 \text{ kcal mol}^{-1}$ . The enthalpy of formation of gallium monochloride has the reported value  $\Delta H_f^\circ(GaCl, g, 298K) = -19.5 \text{ kcal mol}^{-1}$  and is taken from the dissociation energy of Barrow (55) and  $\Delta H_f^\circ(Ga, g, 298K)$  and  $\Delta H_f^\circ(Cl, g, 298K)$  values selected. However, a value of  $\Delta H_f^\circ(GaCl, g, 298K) = -12.0 \text{ kcal mol}^{-1}$  is obtained using  $\Delta H^\circ(GaAs(c) + HCl(g) = GaCl(g) + \frac{1}{4} As_4(g) + \frac{1}{2} H_2(g), 298K) = -25.2 \text{ kcal mol}^{-1}$  determined by

Battat et al. (41) and the thermochemical data selected here for the other species. These results are in sharp contrast to the vapor pressure measurements of Kuniya et al. (54) who report a second law  $\Delta H_f^\circ(\text{GaCl}_3(g) = \text{GaCl}(g) + \text{Cl}_2(g), 1083\text{K}) = 45.912 \text{ kcal mol}^{-1}$ . The value selected was  $\Delta H_f^\circ(\text{GaCl}_3(g), 298\text{K}) = -17.0 \pm 5 \text{ kcal mol}^{-1}$  is based on the first two reports, weighting the value of Barrow (55) slightly more due to the uncertainties found in the enthalpy of formation for the other species in the reaction studied by Battat et al. (41). The enthalpy of formation for gallium dichloride was taken from the measurements of Battat et al. (41) using the thermochemical data selected here and correcting the second law entropy to that calculated by Shaulov and Mosin (56). The enthalpy of dimerization has been investigated by several authors (54,57-60) with the reported enthalpy and entropy of dimerization in the range,  $\Delta H^\circ(2\text{GaCl}_3(g) = \text{Ga}_2\text{Cl}_6(g), 298\text{K}) = -22.6$  to  $-29.8 \text{ kcal mol}^{-1}$  and  $\Delta S^\circ(2\text{GaCl}_3(g) = \text{Ga}_2\text{Cl}_6(g), 298\text{K}) = -31.66$  to  $-36.0 \text{ cal mol}^{-1} \text{ K}^{-1}$ . Accepting the enthalpy and entropy of dimerization as  $-21.0 \text{ kcal mol}^{-1}$  and  $-31.0 \text{ cal mol}^{-1} \text{ K}^{-1}$ , respectively, and combining with the selected thermochemical data for  $\text{GaCl}_3$  produces  $\Delta H_f^\circ(\text{Ga}_2\text{Cl}_6, g, 298\text{K}) = -235.6 \pm 10 \text{ kcal mol}^{-1}$  and  $S^\circ(\text{Ga}_2\text{Cl}_6, g, 298\text{K}) = 127 \pm 6.0 \text{ cal mol}^{-1} \text{ K}^{-1}$ . The standard entropy and heat capacity for  $\text{GaCl}$ ,  $\text{GaCl}_2$  and  $\text{GaCl}_3$  were taken from Shaulov and Mosin (56) while the heat capacity of  $\text{Ga}_2\text{Cl}_6$  was taken as the same for  $\text{Al}_2\text{Cl}_6$  (29). In addition other species are expected to exist (i.e.  $\text{Ga}_2\text{Cl}_4$ ,  $\text{Ga}_2\text{Cl}_2$ ) (61,62) but no thermochemical data is available.

#### 5.4 The In-P-Cl-H System

The standard entropy at 298K and the constant pressure heat capacity of solid and vapor In were taken from Hultgren et al. (1). As summarized by Hultgren et al. (1), the standard enthalpy of vaporization of solid In at 298K that results from application of the third law to the vapor pressure measurements produces the range of 49.8 to 58.1  $\text{kcal mol}^{-1}$  for  $\Delta H_f^\circ(\text{In}, g, 298\text{K})$ . More recent mass spectrometric results of Fanish and Arthur (63) and Farrow (64) suggest the values 57.0 and 58.03  $\text{kcal mol}^{-1}$ , respectively, with the average value adopted here. In a similar fashion, the thermochemical

properties of phosphorus selected by Fultgen et al. (1) or the JANAF tables (29) are in agreement with the more recent results (63) and were adopted for this study. However there exists a small difference in the reported  $\Delta H_f^\circ(298K)$  of the reaction  $P_4(g) = 2P_2(g)$ . Foxon et al. (22) report a value of  $\Delta H_f^\circ(298K) = 57.9 \pm 1 \text{ kcal mol}^{-1}$  while Panish and Arthur (63) reported  $\Delta H_f^\circ(298K) = 54.8 \pm 0.8 \text{ kcal mol}^{-1}$  from third law calculations of their mass spectrometric results. The third law reduction of the mass spectrometric results of Farrow (64) produce a value of  $\Delta H_f^\circ(298K) = 58.04 \pm 0.3 \text{ kcal mol}^{-1}$ , while the JANAF tables (29) suggest  $\Delta H_f^\circ(298K) = 54.6 \pm 1.1 \text{ kcal mol}^{-1}$ . An average value was selected of  $\Delta H_f^\circ(298K) = 56.1 \pm 2.0 \text{ kcal mol}^{-1}$ .

A rather wide range in the reported values for the standard enthalpy of formation of solid InP exists ( $-13.52$  to  $-22.3 \text{ kcal mol}^{-1}$ ). As shown in Table 5.4 the value selected was the average of the two solution calorimetric determinations as this is a direct determination of the property. The results from the vapor pressure measurements are subject to uncertainties in the properties of the vapor phase species and also the heat capacity of solid InP (e.g. Panish and Arthur (63) used  $C_p$  for AlSb which produces a decrease in  $\Delta H_f^\circ(\text{InP}, c, 298K)$  of  $0.5 \text{ kcal mol}^{-1}$  when compared to  $C_p(\text{InP}, c, T)$  of Pankratz (68)). The standard entropy of InP(c) was taken from the low temperature heat capacity measurements of Piesbergen (42) while the heat capacity adopted was that measured by Pankratz (68) and is in good agreement with the 298K value of Piesbergen (42) and in fair agreement with the high temperature measurements of Cox and Pool (69) and the suggested value of Maslov and Maslov (45).

Table 5.4 The reported standard enthalpy of formation of  $\text{InP}(c)$ ,  $\Delta H_f^\circ(\text{InP}, c, 298K)$

$\Delta H_f^\circ_{298}[\text{InP}(c)]$ <i>kcal mol<sup>-1</sup></i>	Method	Reference
$-18.83 \pm 0.7^{(a)}$	flow equilibration	63
$-18.58 \pm 0.7^{(b)}$	mass spectrometry	63
$-22.3 \pm 1.5$	mass spectrometry	26
$-19.33 \pm 0.1^{(c)}$	vapor pressure	28, 65
$-17.83 \pm 1.4^{(d)}$	calculated	28
$-21.2$	calculated	66
$-20.33^{(e)}$	mass spectrometry	64
$-13.52 \pm 0.26$	solution calorimetry	32
$-21.0 \pm 2$	bomb calorimetry	67
$-21.5 \pm 1.5$	bomb calorimetry	63, 70
$-14.5 \pm 0.44$	solution calorimetry	referenced in 32

$$(a) \text{InP}(c) = \text{In}(c) + \frac{1}{2} P_2(g), \Delta H_{298}^\circ = 360 \text{ kcal mol}^{-1}$$

$$\Delta H_f^\circ_{298}[P_2(g)] \text{ taken as } 34.34 \text{ kcal mol}^{-1}$$

$$(b) \text{InP}(c) = \text{In}(c) + \frac{1}{4} P_4(g), \Delta H_{298}^\circ = 22.1 \text{ kcal mol}^{-1}$$

$$\Delta H_f^\circ_{298}[P_4(g)] \text{ taken as } 14.08 \text{ kcal mol}^{-1}$$

$$(c) \text{InP}(c) = \text{In}(c) + \frac{1}{2} P_2(g), \Delta H_{298}^\circ = 36.5 \text{ kcal mol}^{-1}$$

$$\Delta H_f^\circ_{298}[P_2(g)] \text{ taken as } 34.34 \text{ kcal mol}^{-1}$$

$$(d) \text{InP}(c) = \text{In}(c) + \frac{1}{2} P_2(g), \Delta H_{298}^\circ = 35.0 \text{ kcal mol}^{-1}$$

$$\Delta H_f^\circ_{298}[P_2(g)] \text{ taken as } 34.34 \text{ kcal mol}^{-1}$$

$$(e) \text{InP}(c) = \text{In}(c) + \frac{1}{2} P_2(g), \Delta H_{298}^\circ = 37.50 \pm 0.1 \text{ kcal mol}^{-1}$$

$$\Delta H_f^\circ_{298}[P_2(g)] \text{ taken as } 34.34 \text{ kcal mol}^{-1}$$

Barrow (55) reports the dissociation energy of  $\text{InCl}$  to be  $102.5 \text{ kcal/mol}$  and combining this with the value of the enthalpy of formation of  $\text{In}(g)$  and  $\text{Cl}(g)$  gives  $\Delta H_f^\circ(\text{InCl}, g, 298K) = -16.21 \text{ kcal mol}^{-1}$ . However the atomic fluorescence value for the dissociation energy also reported by Barrow (55) ( $D_0 = 104.6 \text{ kcal mol}^{-1}$ ) yields  $\Delta H_f^\circ(\text{InCl}, g, 298K) = -18.31 \text{ kcal mol}^{-1}$ . Klemm and Brautigan (76) reported  $\Delta H_f^\circ(\text{InCl}, c, 273K) = -44.6 \text{ kcal mol}^{-1}$  (77) and when combined with the enthalpy of sublimation,  $\Delta H_s^\circ(\text{InCl}, c, 298K) = 27.8 \text{ kcal mol}^{-1}$ , gives  $\Delta H_f^\circ(\text{InCl}, g, 298K) = -16.8 \text{ kcal mol}^{-1}$  and is the value adopted here. The standard entropy of  $\text{InCl}$  was taken from the calculations of Malakova and Pashinkin (78) while the heat capacity is that recommended by Kelly (79). The standard enthalpy of formation and entropy of  $\text{InCl}_2$

was taken from the estimate of Glassner (8) and the heat capacity is the same as listed for  $GaCl_2$ . The standard enthalpy of formation and entropy of  $GaCl_3$  was taken to be the values suggested by Muller and Hule (14) and the constant pressure heat capacity estimated by Shaw (15). The thermochemical properties of the dimer,  $In_2Cl_6$ , were taken from the values suggested by Schafer and Birnewies (16).

The standard enthalpy of formation of phosphine,  $PH_3$ , was taken from the decomposition studies of Gunn and Green (31) and the remaining properties from the JANAF tables (29,30). The JANAF tables were also used for the other phosphorous hydrides, chlorides and oxide vapor phase species listed in Table 5.1.

### 5.5 The Si-Cl-H System

The thermochemical properties of Si have been reviewed by Hultgren et al. (1) and the JANAF tables (29). In particular, there exists a rather large range in the reported third law values of the standard enthalpy of vaporization,  $\Delta H_f^\circ(Si(g), 298K) = 86.75$  to  $109.06 \text{ kcal mol}^{-1}$ . The value selected was in between the Knudsen studies of Davis et al. (84) and Grievesson and Alcock (85).

The Si-Cl-H system has received considerable attention due to its importance in the semiconductor industry. An excellent review of the literature for this system with equilibrium calculations presented is given by Hunt and Sirtl (25-27). The posture taken here is to assume that  $SiCl_4$  has the most reliable thermodynamic data with these values being fixed by the JANAF tables (29).

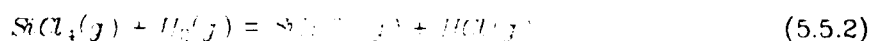
The reaction



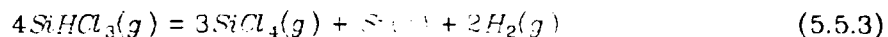
has been investigated extensively (88-93). Employing the thermochemical data for the three species in reaction (5.1) from the JANAF tables (29), third law values of  $\Delta H_f^\circ(SiCl_2(g), 298K)$  were calculated from the experimental data. The effusion-mass spectrometric determination of Fisher and Szwarc (90) is the only temperature

range of 1593K to 1792K produced the value,  $\Delta H_f^\circ(\text{SiCl}_2, g, 298K) = -40.39 \pm 0.3 \text{ kcal mol}^{-1}$  and showed no temperature dependence. This result is in good agreement with flow equilibration data of Schaffer et al. (88) (1273K to 1473K) and Teichmann and Wolf (89) (1223K to 1575K) and the static measurements of Schafer and Nickl (92) (1398K to 1573K), with third law values of  $-40.52$ ,  $-40.54$ , and  $-40.44 \text{ kcal mol}^{-1}$ , respectively. The flow equilibration values of Antipin and Sergeev (90) (1273K to 1673K) and the static values of Ishino et al. (91) (1445K to 1573K) were more negative and exhibited a marked temperature dependence. On the basis of these calculations the value,  $\Delta H_f^\circ(\text{SiCl}_2, g, 298K) = -40.4 \text{ kcal mol}^{-1}$  was selected. The values for the standard enthalpy of formation of the less stable chlorides  $\text{SiCl}$  and  $\text{SiCl}_3$  were computed from the high temperature flow equilibration studies of Farber and Srivastava (93). In the third law analysis the data previously discussed was used in conjunction with the heat capacity for  $\text{SiCl}$  and  $\text{SiCl}_3$  suggested by the JANAF tables (29) and produced the value of  $47.4 \pm 0.6$  and  $-93.3 \pm 0.5 \text{ kcal mol}^{-1}$ , respectively. These results are in agreement with the analysis of Rusin et al. (94-96) on the total pressure measurements of Schafer and Nickl (92). No additional thermodynamic studies of  $\text{Si}_2\text{Cl}_6$  are known to exist and thus the properties suggested by Hunt and Sirtl (86) were adopted and are in agreement with the analysis of Rusin et al. (94-96).

It was pointed out by Hunt and Sirtl (86) that the mole ratio of  $\text{SiCl}_4$  to  $\text{SiHCl}_3$  is very sensitive to the assumed value of the standard enthalpy of formation of  $\text{SiHCl}_3$ . Indeed this ratio is seen to vary by nearly four orders of magnitude at 1000K when bounded by the experimental determinations of  $\Delta H_f^\circ(\text{SiHCl}_3, g, 298K)$ . Since the work of Hunt and Sirtl (86) was published, two additional experimental investigations of the thermodynamic properties of  $\text{SiHCl}_3$  have been performed. Farber and Srivastava (97), from effusion-mass spectrometric measurements, determined the reaction enthalpy for



over the temperature range 1155K to 1500K. Employing the thermodynamic data listed in Table 5.1 and these results, a relatively temperature-insensitive third law value for  $\Delta H_f^\circ(\text{SiHCl}_3, g, 298K) = -119.30 \pm 1.0$  is obtained. Using both static and dynamic methods, Wolf and Teichmann (98) investigated reaction (5.5.2) and the reaction



Third law values of  $\Delta H_f^\circ(\text{SiHCl}_3, g, 298K)$  were calculated from the original results and the thermodynamic data of Table 5.1. The value obtained for reaction (5.5.3) is  $-119.47 \pm 0.40 \text{ kcal mol}^{-1}$  and for the three data sets with reaction (5.5.2) are  $-119.83 \pm 0.90$ ,  $-119.58 \pm 0.2$  and  $-119.50 \pm 0.60 \text{ kcal mol}^{-1}$  and the results are seen to be in good agreement with the measurements of Farber and Srivastava (97). Since these values are nearly  $3 \text{ kcal mol}^{-1}$  more negative than that developed by Hunt and Sirtl (86), values of  $\Delta H_f^\circ(\text{SiHCl}_3, g, 298K)$  were calculated for various experimental  $\text{SiCl}_4/\text{SiHCl}_3$  ratios in a fashion similar to Hunt and Sirtl (86). The experimental data consisted of a variety of feed mixtures (e.g.  $\text{SiCl}_4/\text{H}_2$ ,  $\text{H}_2/\text{HCl}$ ,  $\text{SiHCl}_3/\text{H}_2$ ) which were contacted with Si(c) at different temperatures during a deposition/etching process. The results of these calculations for 14 data sets suggest  $\Delta H_f^\circ(\text{SiHCl}_3, g, 298K) = -118.16 \pm 1.70 \text{ kcal mol}^{-1}$ . Based on these results and the new experimental determinations, the value adopted is  $\Delta H_f^\circ(\text{SiHCl}_3, g, 298K) = -119.5 \pm 1.5 \text{ kcal mol}^{-1}$ .

The standard enthalpy of formation of the di- and mono-chlorosilanes was taken from the recent measurements of Farber and Srivastava (97). In order to obtain a consistent data set, third law values of these quantities were calculated from the original experimental data while using the data base adopted here. The adopted values are  $\Delta H_f^\circ(\text{SiH}_2\text{Cl}_2, g, 298K) = -75.5 \pm 2 \text{ kcal mol}^{-1}$  and  $\Delta H_f^\circ(\text{SiHCl}_2, g, 298K) = -32.7 \pm 2.5 \text{ kcal mol}^{-1}$ .

No additional experimental information on the thermochemistry of  $\text{SiH}_4$  and SiH exists and thus the JANAF tabular recommendations are adopted. The standard

enthalpy of formation of disilane was taken from the calculations of Patzinger et al. (99).  $\Delta H_f^\circ(\text{Si}_2\text{H}_6, g, 298K) = 17.1 \pm 3 \text{ kcal mol}^{-1}$  and is compared with the calculations of O'Neal and Ring (100),  $\Delta H_f^\circ(\text{Si}_2\text{H}_6, g, 298K) = 19.7 \text{ kcal mol}^{-1}$  and the value of  $16.0 \text{ kcal mol}^{-1}$  obtained from the estimated enthalpy of formation for  $\text{SiH}_3$  ( $35 \text{ kcal mol}^{-1}$ ) and Si-Si ( $-54 \text{ kcal mol}^{-1}$ ). The standard entropy and heat capacity of  $\text{Si}_2\text{H}_6$  were obtained by comparison with  $\text{C}_2\text{H}_6$ .

### References: Thermochemical Properties

1. Hultgren, R., Desia, P.D., Hawkins, D.T., Gleason, M., Kelley, H.H., and Wagman, D.D., "Selected Values of the Thermodynamic Properties of the Elements," Am. Soc. Metals (1973).
2. Rusin, A.D., Agamirova, L.M., Zhukov, V.I., and Kalinnikov, V.T., Vestn. Mosk. Univ., Ser. 2; Khim., **23**, 104 (1982).
3. Herrick, C.C. and Feber, R.C., J. Phys. Chem., **72**, 1102 (1968).
4. Rosenblatt, G.M. and Lee, P.K., J. Chem. Phys., **49**, 2995 (1969).
5. Nesmeyanov, A.N., Ph.D. Thesis, Moscow State Univ. (1963).
6. Stratheer, B.A. and Judson, L.M., Trans. Am. Soc. Mining Met., **64**, 506 (1961).
7. Brewer, L. and Kasper, S., Phys. Chem., **59**, 77 (1955).
8. Wiechmann, H., Heimbarg, M. and Blatz, J., Z. anorg. allg. Chem., **240**, 129 (1938).
9. Horiba, S., Z. Physik. Chem., **106**, 275 (1922).
10. Ruff, O. and Magdon, S., Z. anorg. allg. Chem., **117**, 147 (1921).
11. Ruff, O. and Bergdahl, B., Z. anorg. allg. Chem., **106**, 76 (1921).
12. Preuner, G. and Brockmoller, E., Z. Physik. Chem., **81**, 129 (1913).
13. Gibbson, G.E., Doctoral Dissertation, Br. Slan. (1911).
14. Mullin, J.B. and Hurlle, D.J.T., J. Luminescence, **7**, 176 (1973).
15. Shaw, D.W., J. Phys. Chem. Solids, **36**, 1109 (1975).
16. Gentner, J.L., Bernard, C. and Calore, G., J. Crystal Growth, **56**, 332 (1982).
17. Rau, H., J. Chem. Therm., **7**, 27 (1975).
18. Pupp, C., Murray, J.J., and Potter, R.F., J. Chem. Thermodynamics, **6**, 123 (1974).
19. Murray, J.J., Pupp, C., and Potter, R.F., J. Chem. Phys., **58**, 2553 (1973).
20. Goldfinger, P. and Jeuhomme, M., Ann. Mass. Spectrometry, **1**, 534 (1959).
21. Drowart, J., Smoes, S., and Vanderauwera-Mahieu, A., J. Chem. Thermodynamics, **10**, 453 (1978).
22. Foxon, C.T., Joyce, B.A., Farrow, R.F.C., and Griffiths, R.M., J. Phys. D., **7**, 2422 (1974).
23. Foxon, C.T., Harvey, J.A., and Joyce, B.A., J. Phys. Chem. Solids, **34**, 1693 (1973).
24. Arthur, J.R., J. Phys. Chem. Solids, **28**, 2257 (1957).
25. Drowart, J. and Goldfinger, P., J. Chem. Phys., **55**, 721 (1958).
26. Gutbier, H., Z. Naturf., **16a**, 268 (1961).
27. DeMaria, G., Malaspina, L., and Piacentini, V., J. Chem. Phys., **52**, 1019 (1970).
28. Panish, M.B., J. Crystal Growth, **27**, 6 (1971).
29. JANAF Thermochemical Tables, National Standard Reference Data Series 37 (U.S. Bureau of Standards, Washington, D.C. 1971).
30. JANAF Thermochemical Tables, J. Phys. Chem. Ref. Data, **3**, 111 (1974).
31. JANAF Thermochemical Tables, J. Phys. Chem. Ref. Data, **4**, 1 (1975).
32. Martosudirdjo, S. and Pratt, J.N., Thermochim. Acta, **10**, 23 (1974).

33. Abbasov, A.S., Autoreferat dissertatsii, Moscow (1961).
34. Sirota, N.N. and Yushevich, N.N., "Chemical Bonds on Semiconductors and Solids," Sirota, N.N., ed., Consultants Bureau, New York, 95 (1967).
35. Rakov, V.V., Lainer, B.D., and Milvidskii, M.G., Russ. J. Phys. Chem., **44**, 922 (1970).
36. Golodushko, V.Z. and Sirota, N.N., "Chemical Bonds in Semiconductors and Solids," N.N. Sirota, ed., Consultants Bureau, New York (1967).
37. Richman, D., J. Phys. Chem. Solids, **24**, 1131 (1963).
38. Folberth, O.G., J. Phys. Chem. Solids, **7**, 295 (1959).
39. Boomgaard, J. and Schol, K., Philips Res. Rep., **12**, 127 (1957).
40. Khukhryanskii, Yu.P., Kondaurov, V.P., Nikolova, F.P., Panteleev, V.I., and Shechelev, M.L., Izv. Akad. Nauk SSSR, Neorg. Khim., **10**, 1877 (1974).
41. Battat, D., Faktor, M.M., Garrett, I., and Moss, R.H., Par. Trans. I, **12**, 2302 (1974).
42. Piesbergen, H., Z. Naturf., **16a**, 268 (1961).
43. Lichter, B.D. and Sommelet, P., Trans. AIME, **245**, 1021 (1969).
44. Marina, L.I., Nashelskii, A.Ya., and Sakharov, B.A., Chemical Bonds in Semiconductors, N.N. Sirota, ed., **3**, 124 (1972).
45. Maslov, P.G. and Maslov, Yu.P., Chemical Bonds in Semiconductors, N.N. Sirota, ed., **3**, 191 (1972).
46. Yushin, A.S. and Osipova, L.I., Russ. J. Phys. Chem., **50**, 895 (1976).
47. Chen, Y., Chung-nan K'uang Yeh Hsueh Yuan Hsueh Pao, (3), 125 (1980).
48. Shaulov, Yu.Kh. and Mosin, A.M., Russ. J. Phys. Chem., **47**, 644 (1973).
49. Steinmetz, E. and Roth, H., J. Less-Common Metals, **16**, 295 (1966).
50. Glassner, A., "The Thermochemical Properties of the Oxides, Fluorides and Chlorides to 2500°K," Argonne National Lab. Report ANL-5760 (1968).
51. Wicks, C.E. and Block, F.E., Bureau of Mines Bulletin 605 (1963).
52. Gunn, S.R., Inorg. Chem., **11**, 796 (1972).
53. Kubaschewski, O., Evans, E.LL. and Alcock, C.B., Met Thermochemistry, 4th ed., Pergamon Press (1967).
54. Kuniya, Y., Hosaka, M. and Shindo, I., Denki Kagaku, **43**, 372 (1975).
55. Barrow, R.F., Trans. Faraday Soc., **56**, 952 (1960).
56. Shaulov, Yu.Kh. and Mosin, A.M., Russ. J. Phys. Chem., **47**, 642 (1973).
57. Komshilova, O.N., Polyachehok, O.G., and Novikov, G.I., Russ. J. Inorg. Chem., **15**, 129 (1970).
58. Fischer, W. and Juber mann, O., Z. anorg. allg. Chem., **227**, 227 (1936).
59. Laubengayer, A.W. and Schirmer, F.B., J. Am. Chem. Soc., **62**, 1575 (1940).
60. Schafer, H. and Binnewies, M., Z. anorg. allg. Chem., **410**, 251 (1974).
61. Polyachehok, O.G. and Komshilova, O.N., Russ. J. Phys. Chem., **45**, 555 (1971).
62. Kuniya, Y. and Hosaka, M., J. Crystal Growth, **28**, 335 (1975).
63. Panish, M.B. and Arthur, J.R., J. Chem. Thermodynamics, **2**, 299 (1970).

64. Farrow, E.L.C., J. Phys. D., **7**, 216 (1974).
65. Bachman, K.J. and Buehler, E., J. Electrochem. Soc., **121**, 835 (1974).
66. Phillips, J.C. and Van Vecten, J.A., Phys. Rev., **B2**, 2147 (1972).
67. Sharifov, K.A. and Gadzhiev, S.N., Russ. J. Phys. Chem., **38**, 1122 (1964).
68. Pankratz, L.B., U.S. Bureau Mines Report of Investigation 6592 (1965).
69. Cox, R.F. and Pool, M.J., J. Chem. Eng. Data, **12**, 497 (1967).
70. Ermolenko, E.N. and Sirota, N.N., "Chemical Bonds in Semiconductors and Solids," N.N. Sirota, ed., Consultants Bureau, New York, 101 (1967).
71. Garbato, L. and Ledda, F., Thermochemica Acta, **19**, 267 (1977).
72. Richman, D. and Hockings, E.F., J. Electrochem. Soc., **112**, 481 (1965).
73. Shafer, M. and Weiser, K., J. Phys. Chem., **61**, 1412 (1957).
74. Boomgaard, J. and Schol, K., Phillips Res. Rep., **12**, 127 (1957).
75. Perea, E.H. and Fonstad, C.G., J. Electrochem. Soc., **127**, 313 (1980).
76. Klemm, W. and Brautigan, M., Z. anorg. allg. Chem., **163**, 227 (1927).
77. Smith, F.J. and Barrow, R.F., Trans. Faraday Soc., **54**, 826 (1958).
78. Malkova, A.S. and Pashinkin, A.S., Russ. J. Phys. Chem., **51**, 1913 (1977).
79. Kelley, K.K., U.S. Bur. Mines Bull. 584 (1961).
80. Glassner, A., Argonne Nat. Lab. Report ANL-577 (1957).
81. Gunn, S.R. and Green, L.G., J. Phys. Chem., **65**, 779 (1961).
82. Report CODATA Task Group, J. Chem. Thermodynamics, **8**, 67 (1976).
83. Wagman, D.D., Evans, W.H., Parker, V.B., Halow, R., Bailey, S.W., and Schumm, R.H., Nat. Bur. Standards Tech. Note 270-3 (1968).
84. Davis, S.G., Anthrop, D.F., and Searcy, A.W., J. Chem. Phys., **34**, 579 (1961).
85. Grievesson, P. and Alcock, C.B., "Special Ceramics," P. Popper, ed., Heywood and Co., London, 183 (1960).
86. Hunt, L.P. and Sirtl, E., J. Electrochem. Soc., **119**, 1711 (1972).
87. Sirtl, E., Hunt, L.P., and Sawyer, D.F., J. Electrochem. Soc., **121**, 830 (1974).
88. Schafer, H., Bruderreck, H., and Morcher, B., Z. anorg. allg. Chem., **352**, 122 (1967).
89. Teichmann, R. and Wolf, E., Z. anorg. allg. Chem., **347**, 145 (1966).
90. Antipin, P.F. and Sergeev, V.V., Russ. J. Appl. Chem., **27**, 737 (1954).
91. Ishino, T., Matsumoto, A., and Yamagishi, S., Kagaku Kagaku Zasshi, **68**, 252 (1965).
92. Schafer, H. and Nickl, J., Z. anorg. allg. Chem., **274**, 250 (1953).
93. Farber, M. and Srivastava, R.D., J. Chem. Soc., Faraday Trans. 1, **73**, 1672 (1977).
94. Rusin, A.D. and Yakavlev, O.P., J. Moscow Univ. Ser. 2, Chem., **13**, 70 (1972).
95. Rusin, A.D., Yakavlev, O.P., and Freshko, N.A., ibid., **14**, 39 (1973).
96. Rusin, A.D. and Yakavlev, O.P., Moskovskii Inzhenerno-Tekhnicheskii Vestnik, Ser. 3 Khimii, **20**, 530 (1973).
97. Farber, M. and Srivastava, R.D., J. Chem. Thermodynamics, **11**, 349 (1979).

98. Wolf, E. and Feichtmann, Z. anorg. allg. Chem., **30**, 5 (1959).
99. Potzinger, P., Ritter, A., and Krause, J., Z. Naturforsch., **30**, 347 (1975).
100. O'Neal, E.E. and Ring, M.A., J. Organometallic Chem., **213**, 419 (1981).
101. Rakov, V.V., Lamer, B.D., and Milvidskii, M.G., Russ. J. Phys. Chem., **44**, 922 (1970).
102. Clairou, N., Sol, J.P., Linh, N.T., and Moulin, M., J. Crystal Growth, **27**, 325 (1974).
103. Hall, R.N., J. Electrochem. Soc., **110**, 385 (1963).
104. Muzynski, Z. and Riabeev, N.G., J. Crystal Growth, **36**, 335 (1976).
105. Osamura, K., Inoue, J., and Murakami, Y., J. Elec. Soc., **119**, 103 (1972).

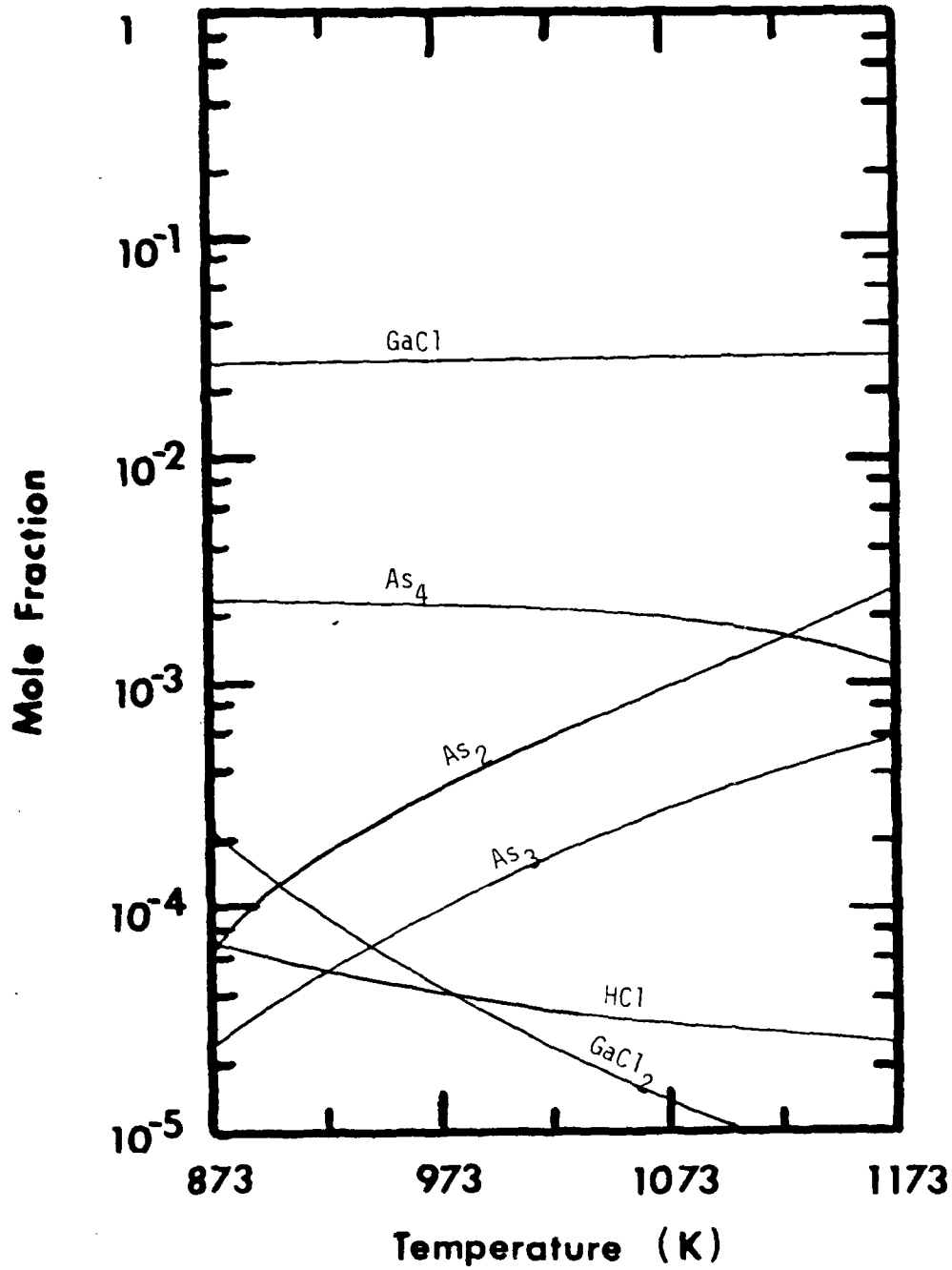
## 6. RESULTS AND DISCUSSION

### 6.1 Introduction

The product of these calculations is the equilibrium composition of the vapor phase in the presence of excess condensed phases. The composition is a function of the operating parameters: temperature, pressure, overall inlet gas composition and included condensed phases. The usual procedure was to vary one of the operating conditions while holding the remaining ones at their base values. The graphical representation of these results generally depicts the natural logarithm of the equilibrium vapor mole fractions of each specie versus the parameter varied. Since the primary objective of this study was to examine the unintentional Si incorporation levels, mole fractions are shown typically down to a level of  $10^{-10}$  (0.1 ppb). In order to show the complete detail, these plots were generally limited to fewer orders of magnitude in mole fraction. Furthermore, since the Si species were always found to be below  $10^{-5}$  mole fraction, only the lower range are given, unless the upper range is necessary to understand the results. A full parametric analysis was performed and over 160 plots were generated. In most cases the results were obvious or similar to analogous systems. Thus, this report includes only those necessary for understanding the principal phenomena observed. In interpreting these plots, it should be realized that an excess specie serves to constrain the activity of that specie to a constant value. For example, with solid  $SiO_2$  present the activity of  $SiO_2$  is fixed at unity and therefore the product of the Si and  $O_2$  partial pressures is also fixed. Thus changes in operating parameters that alter the  $O_2$  fugacity will alter the Si activity by the same degree in an inverse fashion.

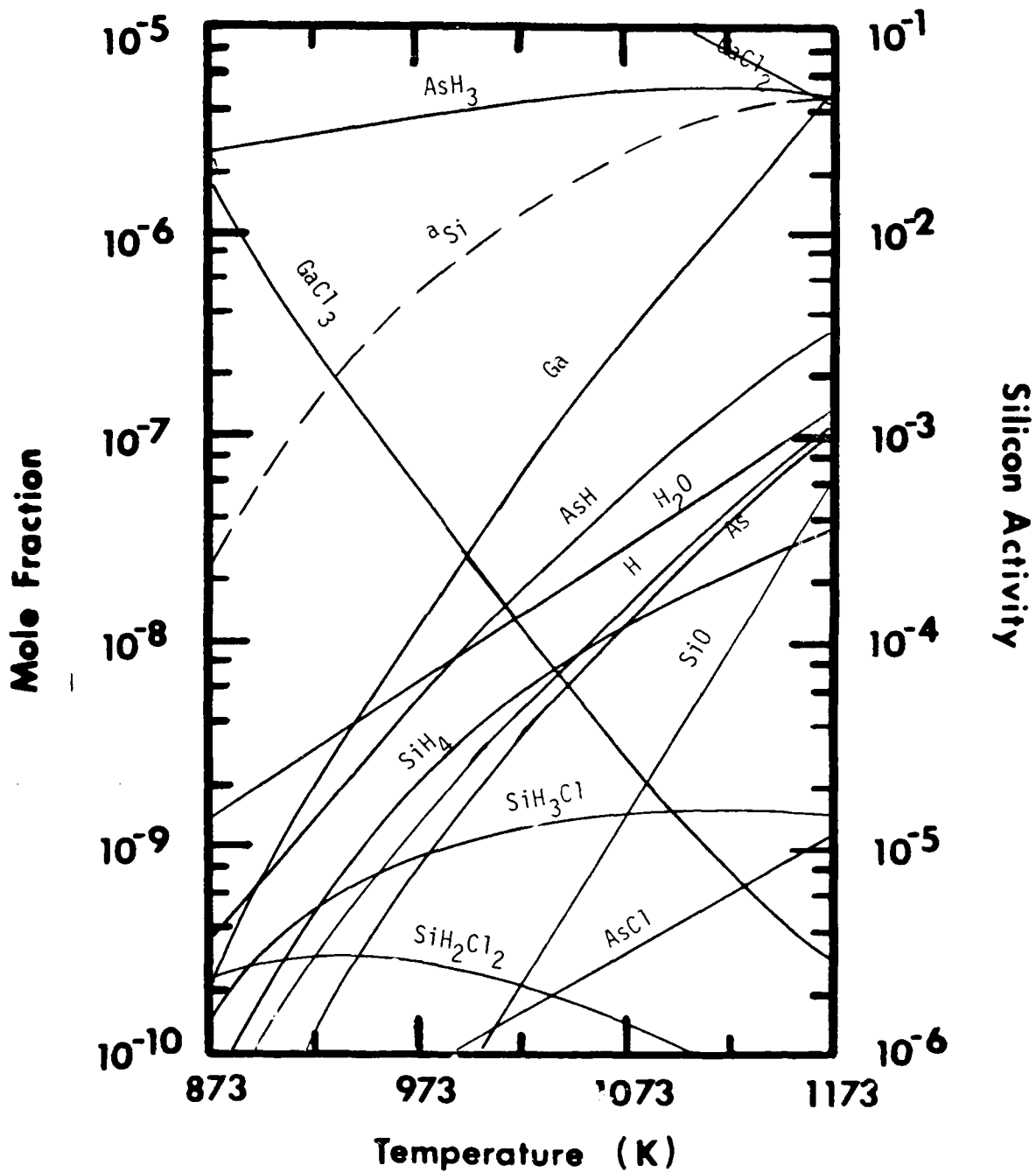
### 6.2 The GaAs Chloride System

The effect of temperature on the species present in the GaAs chloride system source zone (100 kPa pressure, inlet composition 1%  $AsCl_3$  in  $H_2$ ) is shown in Figures 6.1-6.4. Figures 6.1 and 6.2 apply to the system which used a liquid Group III source,



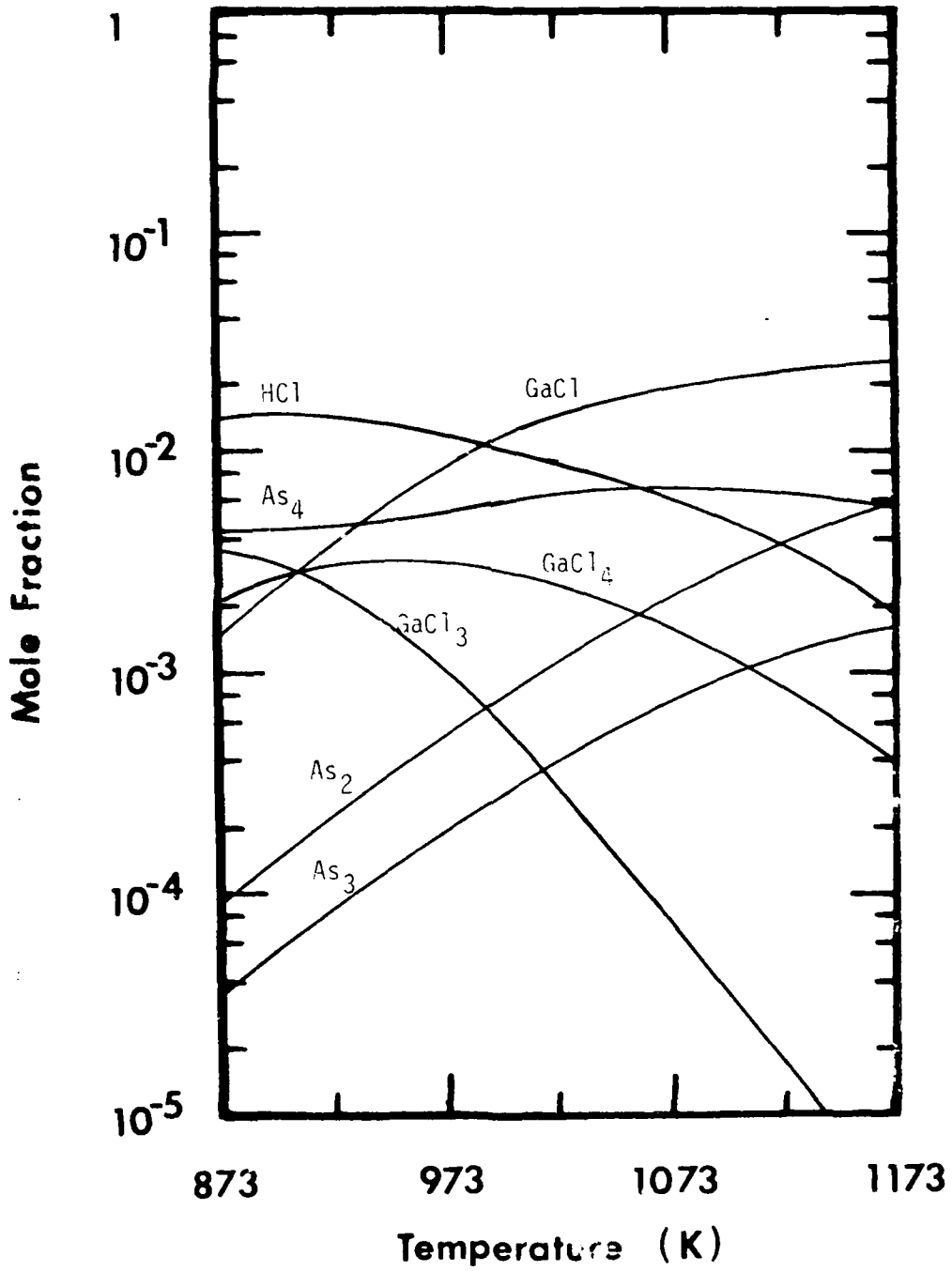
Effect of temperature in the GaAs chloride system source zone (liquid source)

Figure 9.1



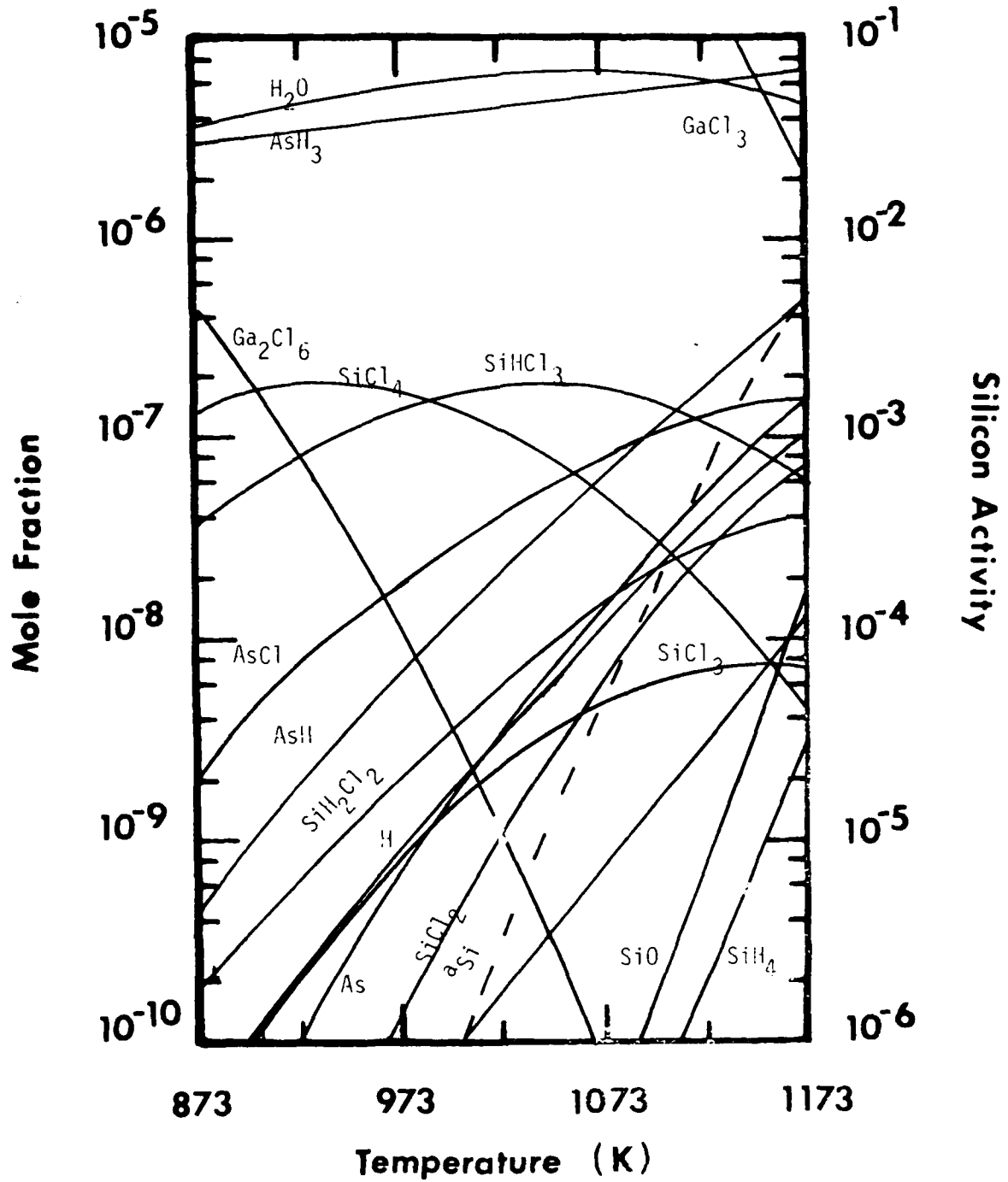
Effect of temperature in the GaAs chloride system source zone (liquid source)

Figure 11.7



Effect of temperature in the GaAs chloride system source zone (solid source)

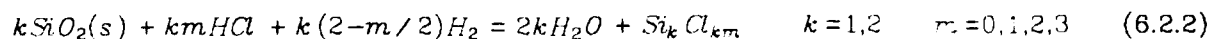
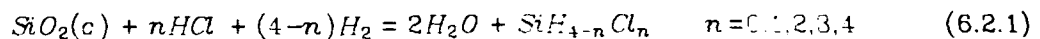
Figure 6.1



Effect of temperature in the GaAs chloride system source zone

$Ga_xAs_{1-x}$ , and Figures 6.3 and 6.4 represent the system which employed GaAs(c) as the Group III source material. At low temperatures  $GaCl_2$  and  $GaCl$  became relatively important gallium vapor species along with GaCl in the solid source system (see Fig. 6.3). In the liquid source system GaCl is the dominant gallium specie over the entire temperature range examined ( $873K \leq T \leq 1173K$ ). In both systems  $As_4$  was the dominant arsenic specie at low temperature while  $As_2$  became important at high temperatures. In contrast to previous studies [30,31], the trimer,  $As_3$ , mole fraction was not negligible. In general, comparison of the silicon activity for the two source zones revealed that the silicon activity associated with the GaAs(c) source material was much lower than that which resulted when a liquid source material was employed. The predominant silicon species in the vapor phase of the system which used a solid source were the higher silicon chlorides in contrast to the hydrogen rich silicon species found in the system which used a liquid source. An additional interesting feature is that the total mole fraction of silicon compounds in the vapor for the system which employed a solid source was greater than that for the system which employed a liquid source. At first glance this fact seems contradictory to the lower observed silicon activity.

The following reaction equations may be written to describe the formation of silicon chlorides, chlorosilanes and silane resulting from reactions with the quartz reactor wall.



Reactions 6.2.1 and 6.2.2 represent a set of independent formation reactions which describe the interplay between the dominant vapor phase silicon species present in the system. Assuming ideal gas behavior, the equilibrium constants for these reactions are as follows:

$$K_{1,n} = \frac{y_{H_2}^2 y_{SiH_4}^{1/n}}{y_{H_2}^{1-n} y_{HCl}^n P_T} \quad (6.2.3)$$

and

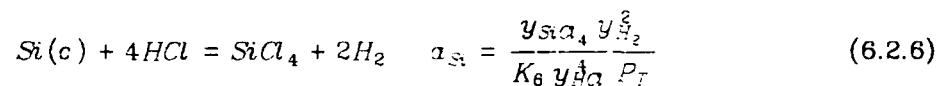
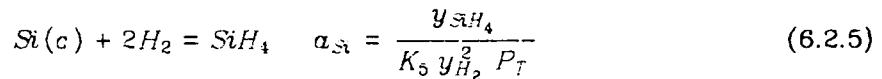
$$K_{2,k,m} = \frac{y_{H_2}^{2k} y_{Si}^k a_{km} P_T^{1-km/2}}{y_{H_2}^{k(2-m/2)} y_{HCl}^{km}} \quad (6.2.4)$$

where

$y_i$  = vapor phase mole fraction of specie i

$P_T$  = system total pressure ratio (total pressure / reference state pressure)

The activity of silicon residing in a condensed phase which is in equilibrium with the vapor phase may be calculated from any reaction using a vapor Si specie reactant and solid Si product. For example, consider the following reactions and subsequent equilibrium expressions for the activity of Si.



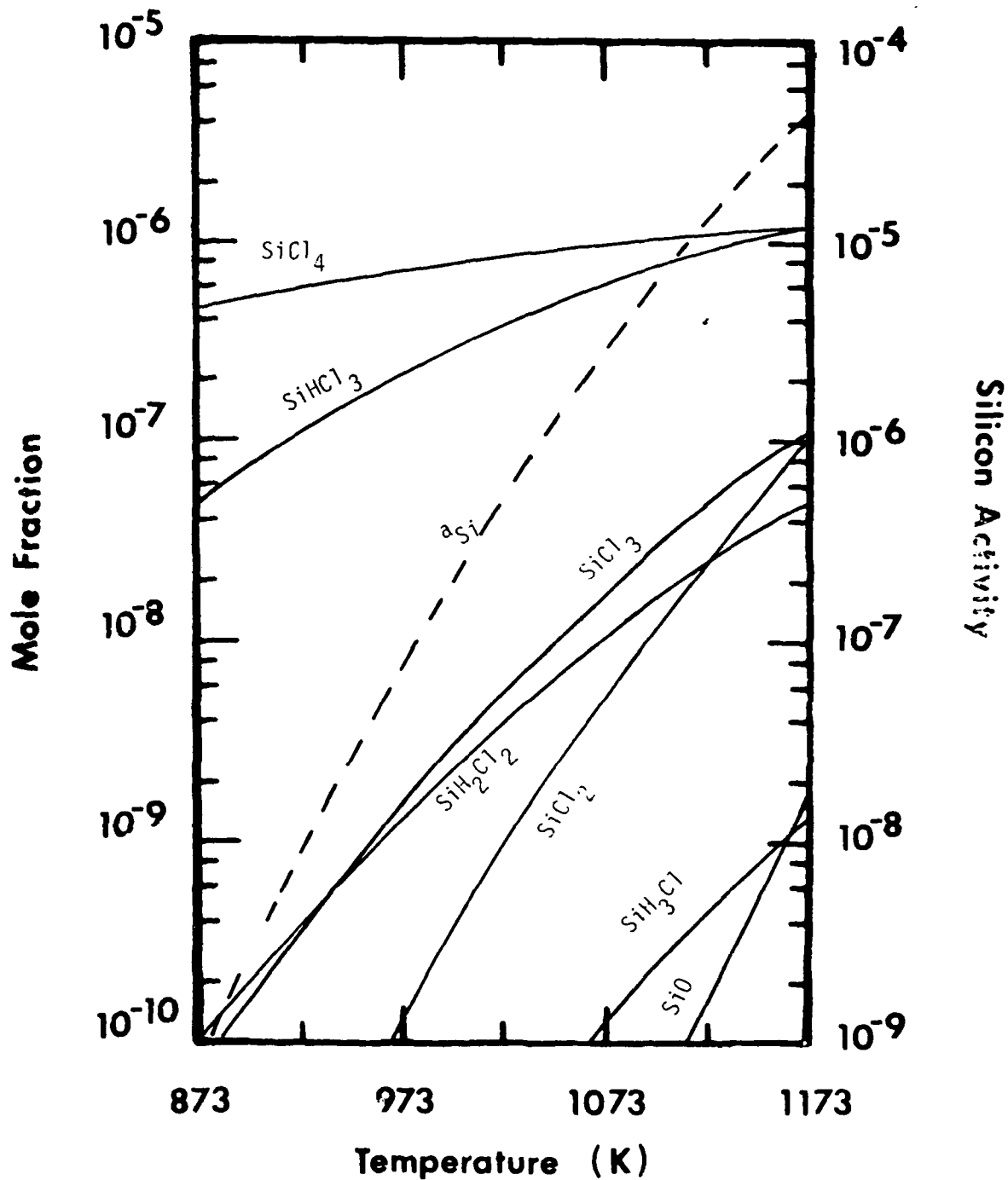
Here  $K_i$  is the equilibrium constant for reaction  $i=5$  or  $6$ . Other equivalent relations may be written in order to calculate the condensed phase silicon activity but the models suggested in equations 6.2.5 and 6.2.6 serve as convenient points of focus since either  $SiH_4$  or  $SiCl_4$  is usually a significant silicon vapor specie in the systems studied. In particular for those systems using  $H_2$  as the carrier gas, the mole fraction of  $H_2$  is nearly constant with the value unity. Therefore the  $a_{Si}$  will track the  $SiH_4$  mole fraction and is inversely proportional to the system pressure. Both models of course yield identical values for the silicon activity when applied to the same situation. The activity of Si presented in these plots can be viewed as the value found in a condensed phase in equilibrium with a vapor having the composition shown. In order to translate this into a solubility the nature of the condensed phase need be considered. Since the

same condensed phase is present (i.e. III-V compound) an increase in activity corresponds to an increase in solubility.

These thermodynamic models for the incorporation of silicon in GaAs epitaxial layers are similar to those proposed by Rai-Choudhury [27] and DiLorenzo and Moore [23]. They differ from the previously proposed models in that a more complete set of species, including condensed phases, are included in the calculation as a result of the application of a digital computer to solve the complex chemical equilibrium problem.

The lower silicon activity associated with the solid GaAs source can therefore be viewed as due to a suppressed  $SiH_4$  concentration when comparing use of the liquid source (equation 6.2.5). In the source zone which employed solid GaAs the presence of primarily higher chlorides and chlorosilanes at the lower source zone temperatures was a result of less gallium being present in the vapor phase than was present when a liquid source was employed. Ga is in excess in both sources thus constraining the activity of Ga with the liquid source having a higher activity. Thus, sufficient HCl was formed due to the decomposition of  $AsCl_3$  to enhance reactions 6.2.1 and 6.2.2 for large k and m values. Figure 6.5, which shows the chloride system pre-source zone (1%  $AsCl_3$  in  $H_2$ , no Group III source material present), further supports this analysis. The absence of Group III chlorides caused the total amount of silicon in the vapor to increase above the level observed in the solid source system while the condensed phase silicon activity decreased even further.

Table 6.1 is a list of the enthalpy of formation at 298K and the Gibbs energy of reaction at 973K for some of the vapor species described by reactions 6.2.1 and 6.2.2. The large negative enthalpies of formation are indicative of strong interatomic bonds and therefore stable species. Since equilibrium represents the lowest Gibbs energy state of the system, species with a lower Gibbs energy of reaction are favored. Therefore, providing sufficient chlorine to react with the silicon species will result in a higher total silicon concentration in the vapor phase, but, due to the stability of these



Effect of temperature on the GaAs chloride system presource zone

Figure 6.5

species, a lower activity of solid silicon in the condensed phase. The relative stability of silicon halides when compared to silicon hydrides was also recognized by Rai-Choudhury [27].

**Table 6.1. Enthalpies of Formation and Gibbs Energies of Reaction for Some Silicon Vapor Species**

Vapor Species	$\Delta H_f^{298K}$ (kcal/mol <sup>-1</sup> )	$\Delta G_{rxn}^{973K}$ (kcal/mol <sup>-1</sup> )
<i>SiCl<sub>4</sub></i>	-158.4	51.4
<i>SiHCl<sub>3</sub></i>	-119.5	60.5
<i>SiCl<sub>3</sub></i>	-93.3	69.8
<i>SiH<sub>2</sub>Cl<sub>2</sub></i>	-75.5	76.9
<i>SiCl<sub>2</sub></i>	-40.3	81.8
<i>SiH<sub>3</sub>Cl</i>	-32.7	94.0
<i>SiH<sub>4</sub></i>	8.2	111.5
SiCl	47.4	129.8
<i>Si<sub>2</sub>Cl<sub>6</sub></i>	-236.0	139.5

\*Reference state: Si(c), Cl<sub>2</sub>(v), H<sub>2</sub>(v) at 298K and 100 kPa

The outlet compositions (equilibrium composition) of the source zones using solid and liquid source materials at 973K were used as input to the mixing zone and the effect of mixing zone temperature was investigated. The system using a liquid source material displayed behavior which was nearly identical to the source zone behavior. This supports Weiner's model [9] which suggested using the outlet composition of the source zone as the inlet composition to the deposition zones. This model is only applicable, of course, if the source and mixing zones are operated at the same temperature. Justification for isothermal operation of the source and mixing zones comes from noting that the condensed phase silicon activity increases with temperature. Therefore, it is desirable to operate the mixing zone at the source zone temperature in order to minimize the silicon activity and at the same time prevent deposition of GaAs in this zone.

The behavior of the mixing zone, when fed from a source zone using solid GaAs as the source material, differs from that of the source zone alone in that the mole fractions of all of the chlorinated vapor phase silicon species increase with temperature, as does the condensed phase silicon activity. Although the silicon activity in the mixing zone increases more slowly with temperature than it does in the source zone, in the interests of attaining the lowest possible silicon activity it is again advisable to operate the mixing zone at a temperature equal to or less than that of the source zone.

The effect of temperature on the deposition zone for source and mixing zone temperatures of 973K, pressures of 100 kPa, a liquid source material and 1%  $AsCl_3$  in  $H_2$  inlet to the reactor, has shown GaCl and  $As_4$  to be the dominant Group III and V species. A measure of the supersaturation of the vapor was defined based on the reaction



using the equilibrium relationship

$$R_{sat} = \frac{P_{Ga} P_{As}}{K_{sat}} \quad (6.2.8)$$

where: 
$$K_{sat} = \exp(-\Delta G_{rxn}^{\circ} / RT)$$

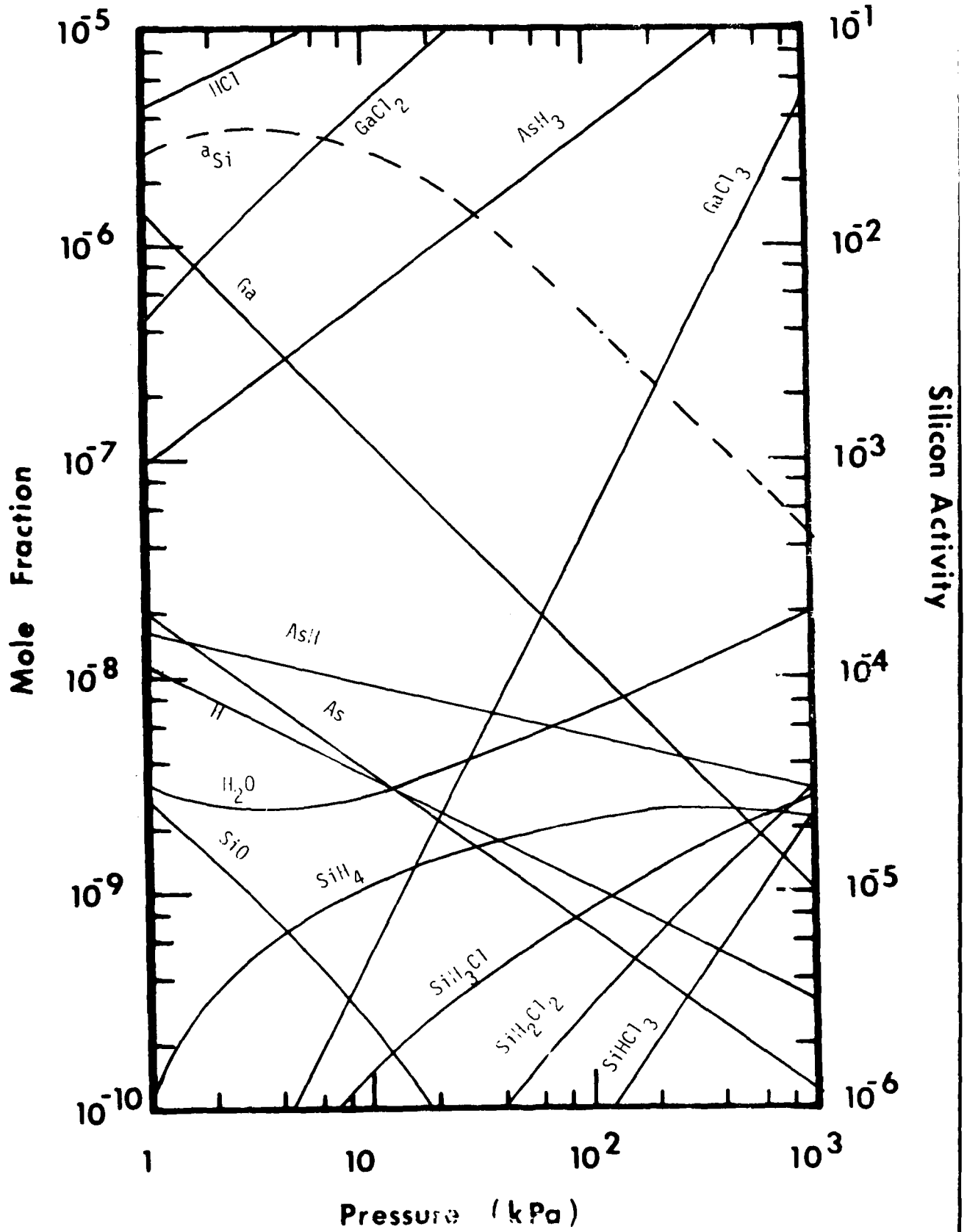
This saturation ratio was observed to decrease from  $4 \times 10^5$  at 773K to 700 at 973K which shows the vapor phase to be highly supersaturated. When  $SiO_2(c)$  was not included in the deposition zone the condensed phase silicon activity changed only slightly from  $9 \times 10^{-3}$  at 773K to  $6 \times 10^{-3}$  at 973K. Including  $SiO_2(c)$  in the deposition zone calculation resulted in the condensed phase silicon activity becoming a strong function of temperature (due to reversal of reactions 6.2.1 and 6.2.2) with the activity value at 973K remaining unchanged and the 773K value falling to  $9 \times 10^{-5}$ .

When solid GaAs was used as the Group III source material the following results were obtained for the deposition zone. The saturation ratio fell from a value of 200 at 773K to the expected value of 1 at 973K, thus showing the system to be much less supersaturated than the liquid source material counterpart. This lower degree of supersaturation was due to much less GaCl being present in the vapor. The dominant Group V specie was  $As_4$  but GaCl,  $GaCl_2$  and  $GaCl_3$  were all important contributors to the Group III vapor species. The condensed phase silicon activity was found to increase with temperature from  $9 \times 10^{-8}$  at 773K to  $7 \times 10^{-7}$  at 973K for the case where  $SiO_2(c)$  was not included in the deposition zone. When  $SiO_2(c)$  was included the silicon activity at 773K fell to  $2 \times 10^{-9}$ .

The effect of pressure was investigated over the range of 1 to 1000 kPa (temperature 973K, inlet composition: 1%  $AsCl_3$  in  $H_2$ ) for both the solid and liquid Group III source materials. Over the entire range studied GaCl was the dominant Group III vapor specie in the system using a liquid source material, while for the system using solid GaAs as the source material, GaCl became the dominant Group III specie at pressures below 100 kPa but competed with  $GaCl_2$  and  $GaCl_3$  at the higher pressures. The dominant Group V vapor specie was  $As_4$  at pressures above 10 kPa with  $As_2$  becoming important below this pressure, in agreement with Gentner et al. [31], in both the liquid and solid sourced systems.

Figures 6.6 and 6.7 show the lower five orders of magnitude in mole fraction and the condensed phase silicon activities in the liquid and solid material source zones. The silicon activity in the system using a liquid source material reaches a maximum at a pressure of 4 kPa and then decreases with increasing pressure. This behavior has not been reported in the literature presumably due to the constrained nature of previous equilibrium calculations. Referring to equation 6.2.5 reveals that the maximum in the silicon activity is due to the  $SiH_4$  mole fraction rising faster than  $P_T$  in the 1 to 10 kPa range. Applying equation 6.2.3 to the specie  $SiH_4$  ( $n=0$ ) and referring to Figure 6.6 shows that the  $SiH_4$  mole fraction dependence on pressure deviates from being linear

Effect of pressure on the GaAs chloride system source zone  
(liquid source)



Effect of pressure on the GaAs chloride system source zone (solid source)

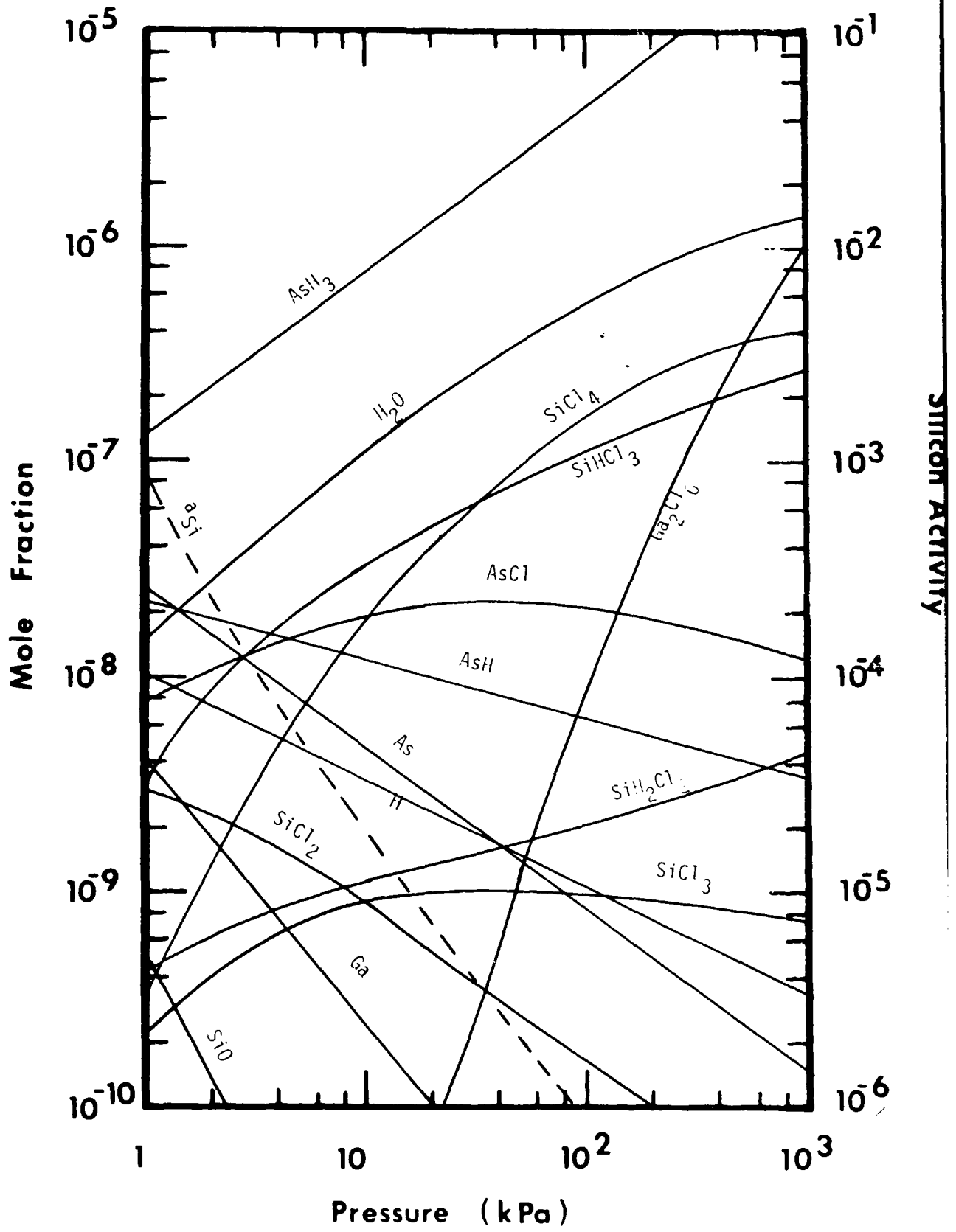
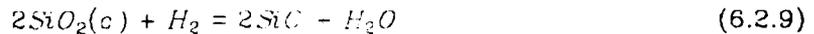


Figure 1

due to the  $H_2O$  mole fraction changes in this range ( $y_{H_2} \approx 1$ ). The change in  $H_2O$  mole fraction is due to changes in the total amount of  $SiO_2(c)$  which has reacted with the vapor. Reaction 6.2.1 is important in this system and, as the pressure increases, causes more  $SiO_2(c)$  to react which generates more  $H_2O$ .

The dominant silicon vapor specie present at the low end of the pressure range is SiO which is formed via the reaction



with the corresponding equilibrium relationship

$$K_3 = \frac{y_{SiO}^2 y_{H_2O} P^{-1}}{y_{H_2}} \quad (6.2.10)$$

Thus, the observed minimum in the  $H_2O$  mole fraction is due to the interaction between the decreasing mole fraction of SiO with the increasing system pressure from reaction 6.2.7 along with the  $H_2O$  generation from reaction 6.2.1. Reaction 6.2.2 is not important in this situation.

The source zone which used solid GaAs as the Group III source material shows a strictly decreasing condensed phase silicon activity with increasing system pressure and is best described via reactions 6.2.1 and 6.2.2 in conjunction with the silicon activity model provided by equation 6.2.6. The decrease in silicon activity is due to the 3 order of magnitude increase in  $SiCl_4$  mole fraction being offset by an order of magnitude increase in HCl mole fraction ( $a_{Si} \propto y_{HCl}^3$ ) and the  $P^{-1}$  dependence of the silicon activity. Once again the activity of silicon in the system using solid GaAs as a source material is much less than the activity resulting from using liquid  $Ga_xAs_{1-x}$  as the Group III source material.

The mixing and deposition zones were studied using only the liquid Group III source material in the source zone. The mixing zone results were again essentially the same

as those of the source zone (operated at the same temperature) and therefore do not require further discussion.

The deposition zone, shown in Figures 6.8 and 6.9, exhibited a saturation ratio of approximately  $2 \times 10^3$  at a pressure of 1 kPa rising to approximately  $2 \times 10^4$  at 1000 kPa. Thus, the deposition zone was supersaturated over the entire pressure range investigated.

The maximum value of the condensed phase silicon activity observed for the source and mixing zones was not prevalent in the deposition zone since  $SiO_2(c)$  was not included in the deposition zone model. Therefore, the silicon activity decreased with increasing pressure in accord with equation 6.2.5

The mole fraction of  $AsCl_3$  present in the feed stream was varied from 0.1% to 10% in order to determine its effect on the condensed phase silicon activity. For the source zone utilizing a liquid Group III source material most of the chlorine atoms provided by the decomposition of  $AsCl_3$  were used to generate GaCl. Therefore, the condensed phase silicon activity was not appreciably affected until large concentrations of  $AsCl_3$  were reached. The silicon activity was found to decrease from  $7 \times 10^{-3}$  at 0.1%  $AsCl_3$  to  $6 \times 10^{-3}$  at 1%  $AsCl_3$  and finally to  $7 \times 10^{-4}$  at 10%  $AsCl_3$ . These results agree qualitatively with previous calculations [23,27] and observations [20,21,22,26].

A very marked effect on the silicon activity was observed as the  $AsCl_3$  inlet concentration was varied in the system using solid GaAs as the Group III source material. Since less GaCl was generated in this system when compared to the system using a liquid Group III source, more FCl was available from the decomposition of  $AsCl_3$  to react with the silicon vapor species. Thus, the condensed phase silicon activity was found to decrease uniformly from  $9 \times 10^{-5}$  at 0.1%  $AsCl_3$  to  $1.5 \times 10^{-3}$  at 10%  $AsCl_3$  inlet concentration.

The reason less GaCl was generated in the system using solid GaAs as the Group III source is explained by the following reactions.

Effect of pressure on the GaAs chloride system deposition zone

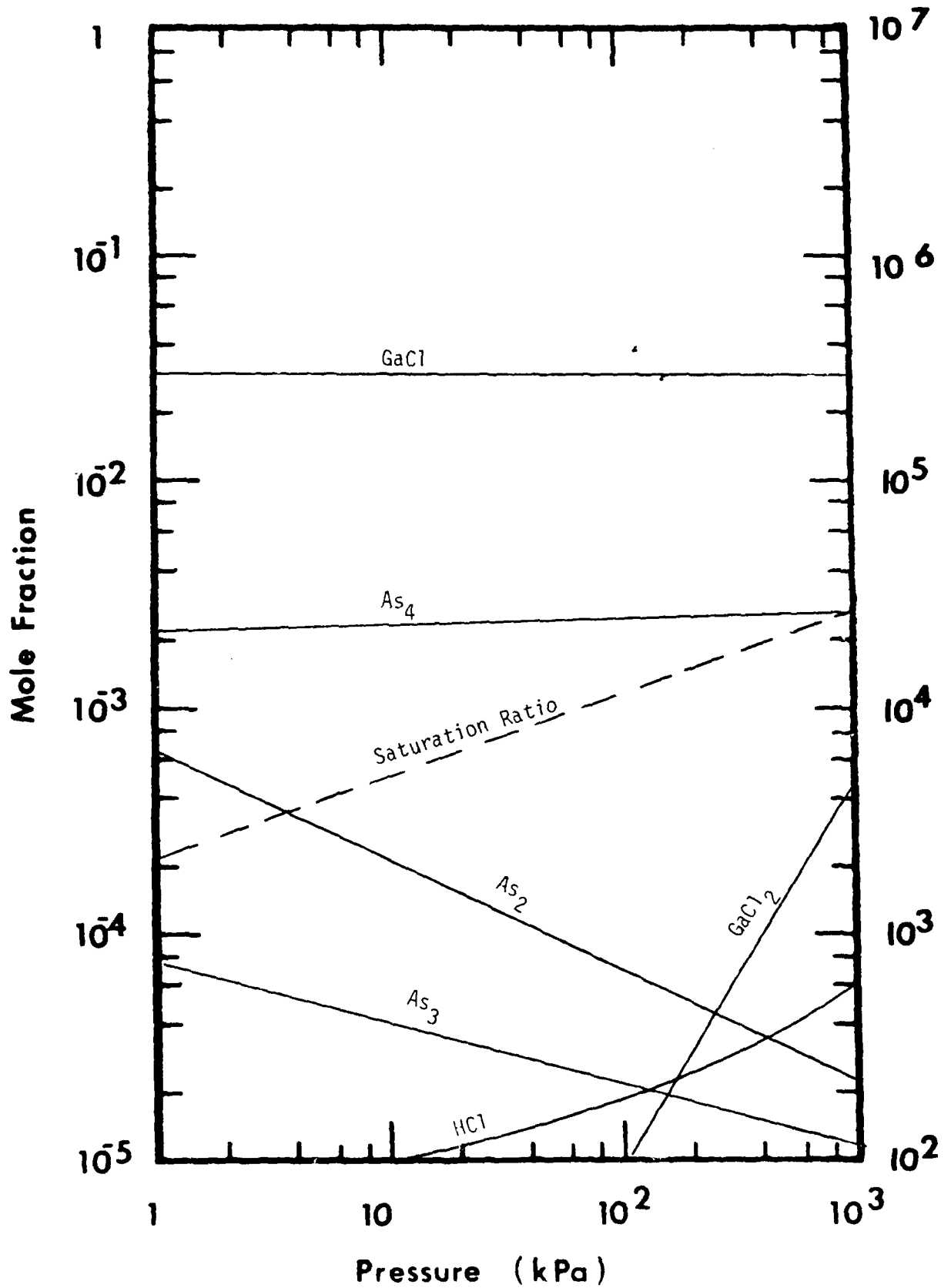
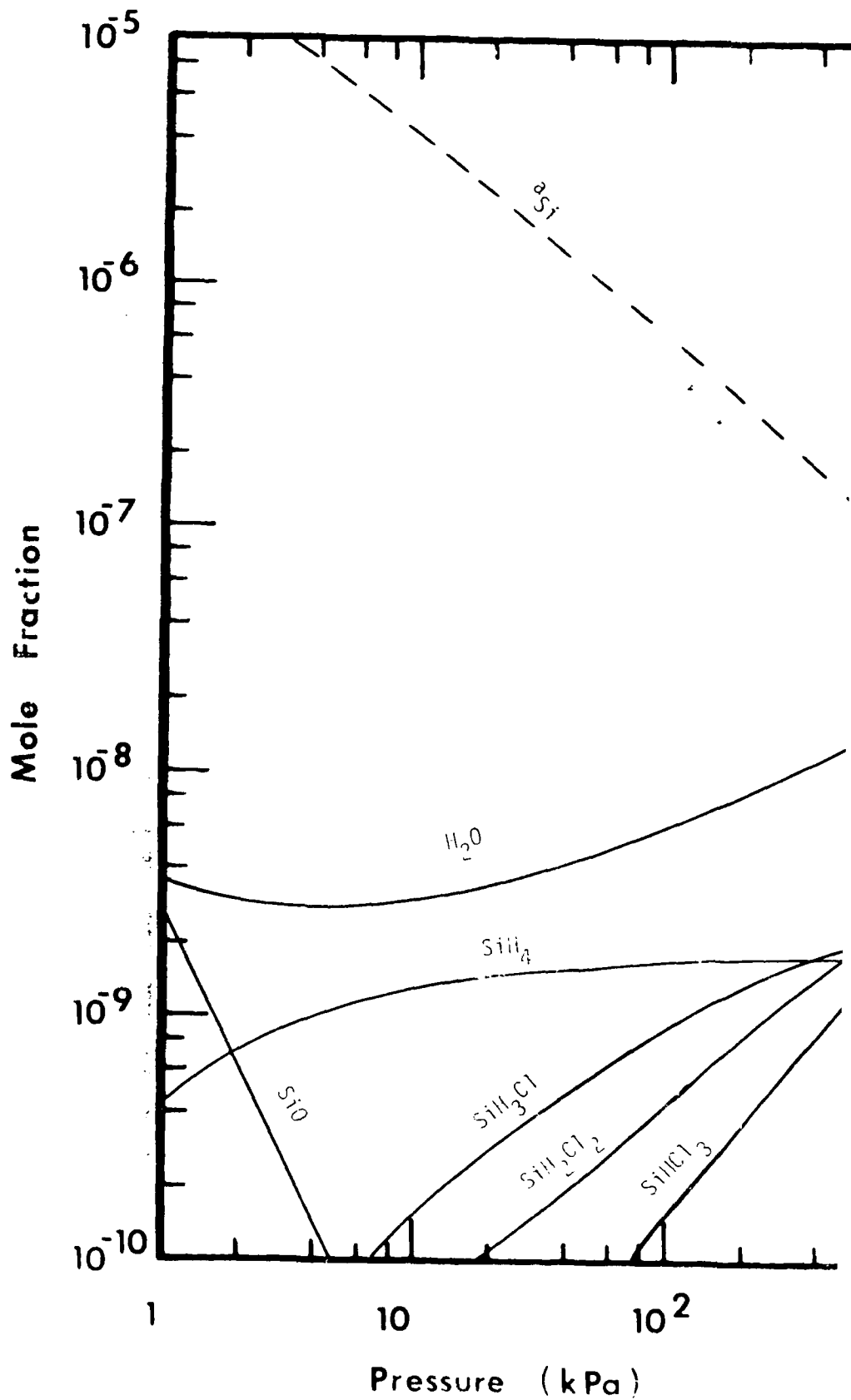
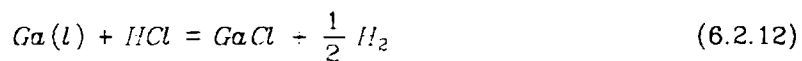
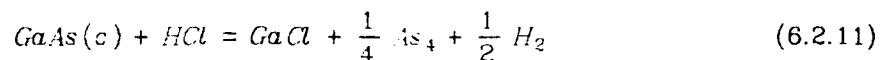


Figure 10.1

Effect of pressure on the GaAs chloride system deposition zone





Reaction 6.2.11 refers to the system using the solid source and, at 973K, has a Gibbs energy change of 3.2 kcal mole<sup>-1</sup> while reaction 6.2.12, representing the system with a liquid source, undergoes a Gibbs energy change of -9.5 kcal mole<sup>-1</sup>. The negative Gibbs energy change of reaction 6.2.10 causes the products of the reaction to be favored.

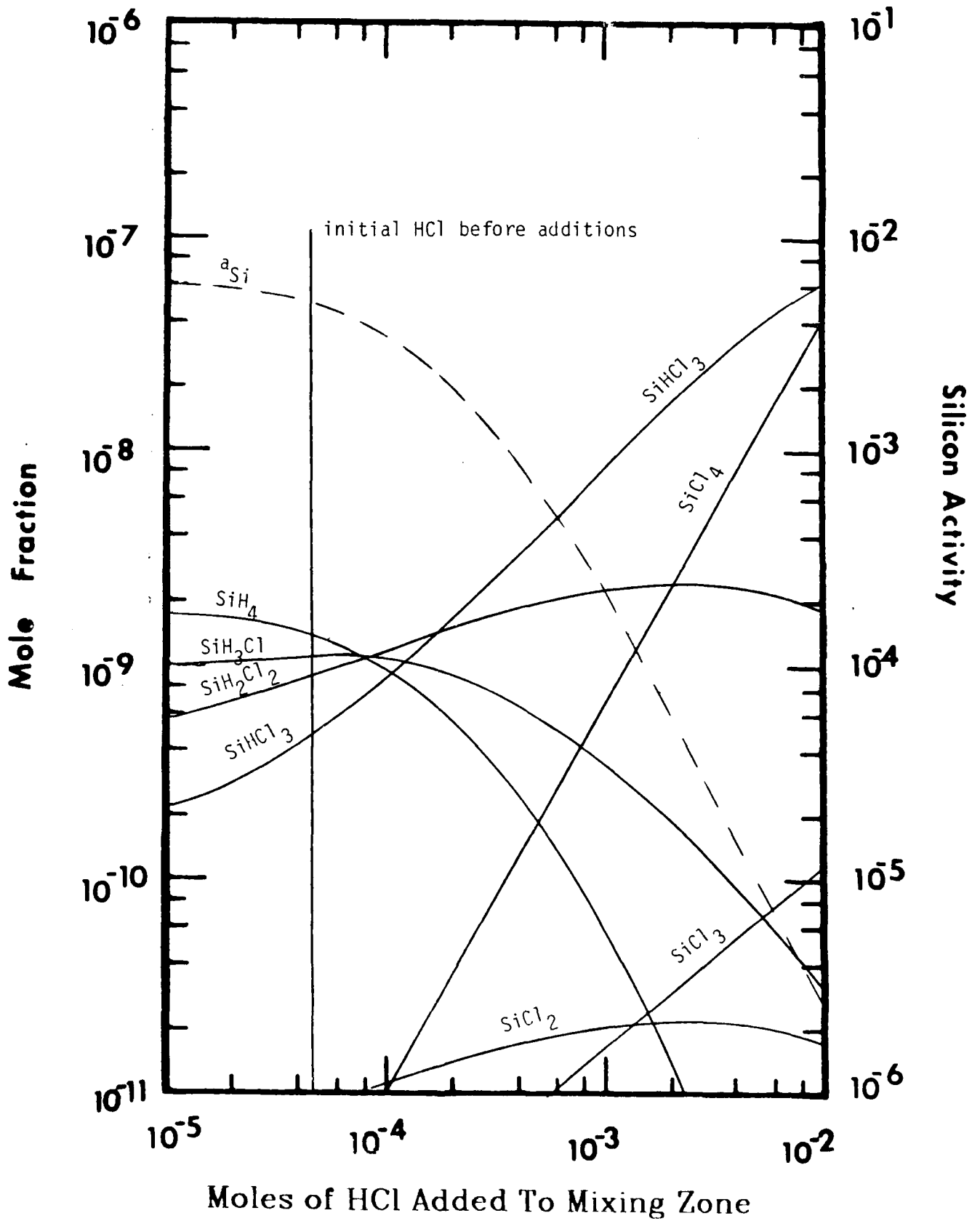
The source zone results were carried through the mixing zone and deposition zone for the system using a liquid Group III source. The mixing zone yielded the same results as the source zone (both zones operating at a temperature of 973K) and the deposition zone showed the same trends as were observed in the source and mixing zones with the values of silicon activity slightly higher due to the lower deposition zone temperature (873K).

A more effective way to reduce the silicon activity in systems using a liquid Group III source is to add HCl (or AsCl<sub>3</sub>) downstream of the source zone. This allows the chlorine atoms to react with the silicon species instead of generating additional GaCl.

Figure 6.10 shows the effect of adding small quantities of HCl to the mixing zone on the condensed phase silicon activity in the deposition zone (basis: 1 mole of vapor in the mixing zone). The initial HCl mole fraction in the deposition zone prior to the addition of any HCl was 4.5×10<sup>-6</sup>. In accord with reactions 6.2.1, 6.2.2, 6.2.5 and 6.2.6 the silicon compounds shift from being hydrogen rich to chlorine rich and the silicon activity decreases markedly. The addition of AsCl<sub>3</sub> has the same effect except that the activity decrease is slightly more pronounced since there are three chlorine atoms per molecule of AsCl<sub>3</sub> compared to one for HCl.

Another method of decreasing the condensed phase silicon activity is to add H<sub>2</sub>O to the system. This causes a decrease in the total amount of silicon in the vapor by

Effect of adding HCl on the CaAs chloride system deposition zone



shifting reactions 6.2.1 and 6.2.2 in favor of  $\text{SiO}_2(c)$ . This effect is demonstrated in Figure 6.11 for small additions of  $\text{H}_2\text{O}$  to the mixing zone (basis: 1 mole of vapor in the mixing zone) where the mole fraction of  $\text{H}_2\text{O}$  prior to the additions was  $5.5 \times 10^{-9}$ . This effect was predicted by Rai-Choudhury [27] and observed by Palm [23].

Replacing the hydrogen carrier gas with an inert gas is yet another method of reducing the condensed phase silicon activity. This method also reduces the total amount of silicon in the vapor by shifting reactions 6.2.1 and 6.2.2 in favor of  $\text{SiO}_2(c)$  as shown in Figure 6.12. Reduction of silicon incorporation using an inert to replace  $\text{H}_2$  was studied by Seki et al. [33] and observed by Ozeki et al. [34]. The curvature in the silicon activity is best understood by referring to reaction 6.2.5. As the hydrogen carrier gas is replaced by an inert the mole fractions of  $\text{H}_2$  and  $\text{SiH}_4$  decrease. The competing nature of these two mole fractions causes a maximum in the condensed phase silicon activity to occur at approximately 90% inerts after which the silane mole fraction rapidly goes to zero and the silicon activity decreases to a very small value. The silicon activity will never reach zero as predicted by 6.2.6 since reactions 6.2.1, 6.2.2, 6.2.5 and 6.2.6 are not valid models in systems devoid of hydrogen. Instead, small concentrations of  $\text{Si}(v)$ ,  $\text{SiO}(v)$  etc. will remain in the vapor to provide a nonzero but very small condensed phase silicon activity.

The use of solid GaAs as the Group III source material appears to offer an advantage over the liquid Group III source in that lower condensed phase silicon activities were predicted by these thermodynamic models. It must be emphasized, however, that the solid GaAs source was assumed to be pure (i.e. devoid of Si and other contaminants) and, from a thermodynamic point of view, that the purity of an epitaxial layer can be no better than that of the source material unless methods are employed to improve the purity (e.g. additions of  $\text{HCl}$ ,  $\text{H}_2\text{O}$ , etc.) during the CVD process.

### 6.3 The GaAs Hydride System

The effect of temperature on the silicon species present in the Group III and Group

Effect of adding  $H_2O$  on the GaAs chloride system deposition zone

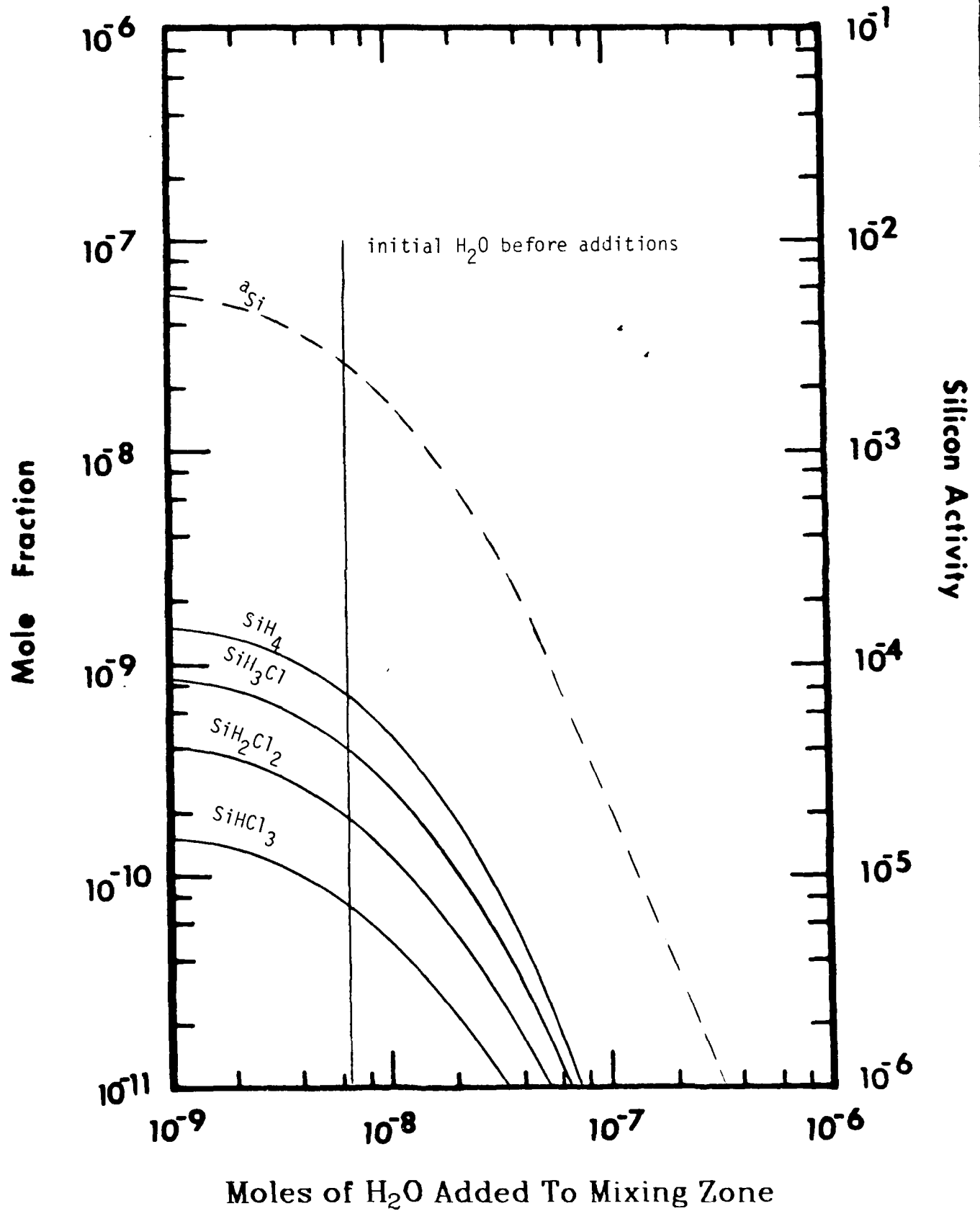


Figure 6.11

### Silicon Activity

Effect of replacing  $H_2$  with inerts on the GaAs chloride system deposition zone

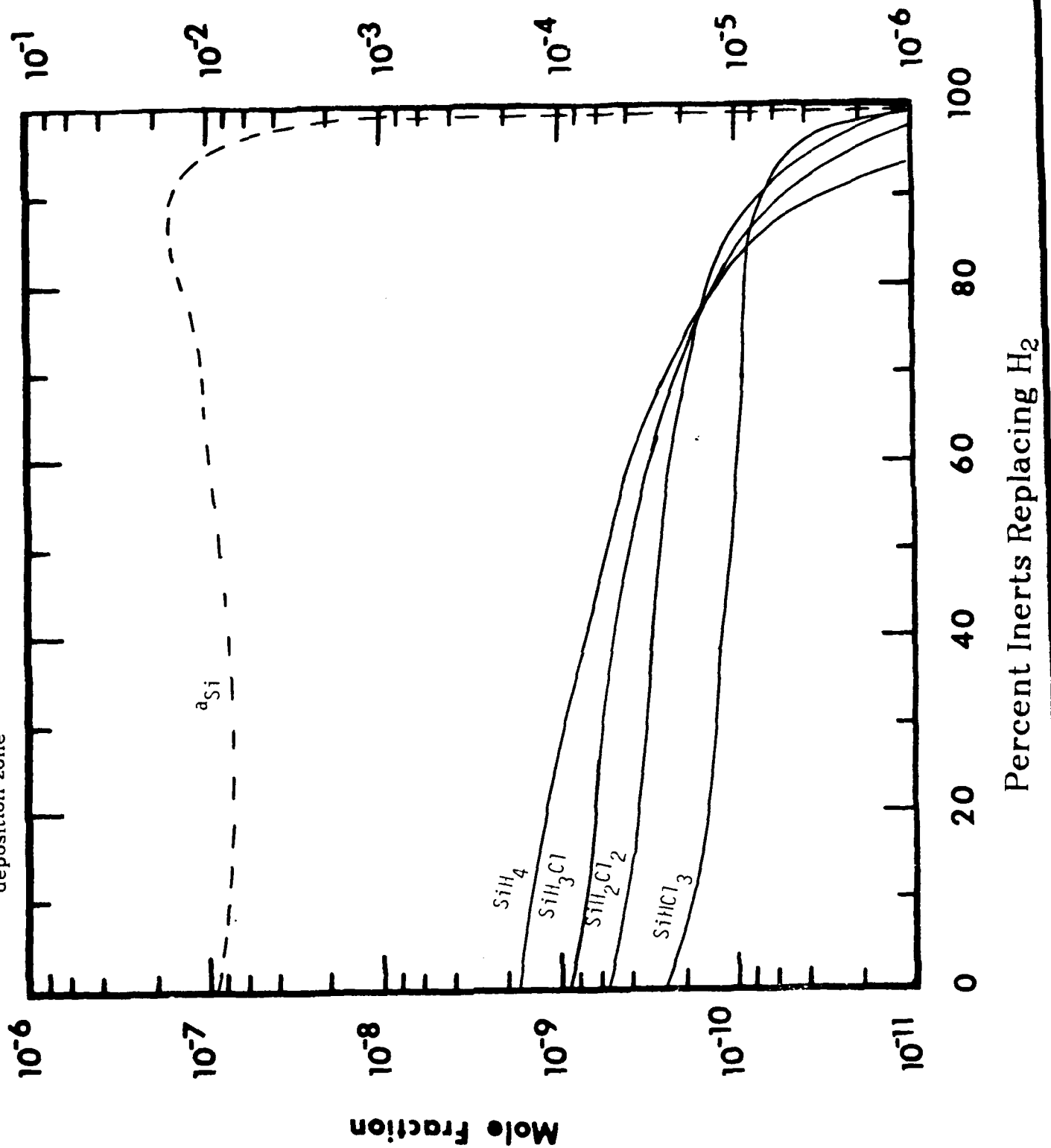
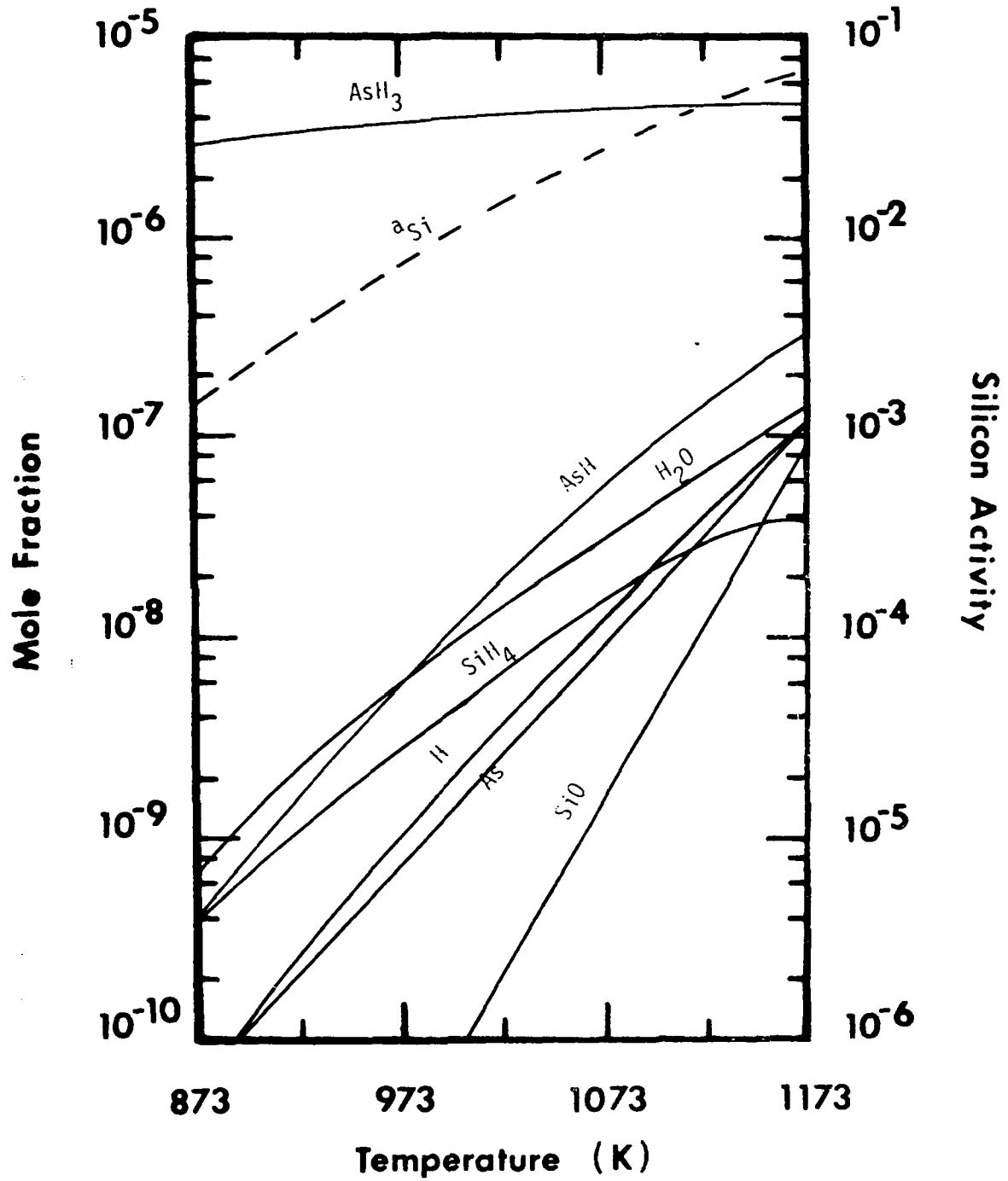


Figure 6.12

V source zones of the Ga-As-hydrogen systems as shown in Figures 6.13 and 6.14. The condensed phase silicon activity for the Group V source zone was essentially the same as that which would be observed in the Group V pre-source zone ( $AsH_3$  absent) since arsine did not compete with silicon for any atoms in the vapor other than hydrogen. The Group III source zone showed a much greater silicon activity than the Group V pre-source zone ( $Ga(l)$  absent) shown in Figure 6.15 since the liquid gallium source reacted strongly with HCl to form GaCl. This forced the silicon species to be rich in hydrogen and therefore the condensed phase silicon activity was larger. As can be seen from Figures 6.13 and 6.14, the Group V source zone was primarily responsible for the silicon activity at low temperatures while at high temperatures the Group III source zone contribution to the silicon activity also became important. As was observed in the chloride system for the liquid  $Ga_xAs_{1-x}$  source, the dominant Group III vapor specie was GaCl with  $As_4$  being the dominant Group V vapor specie at temperatures below 1073K and  $As_2$  dominant above this temperature.

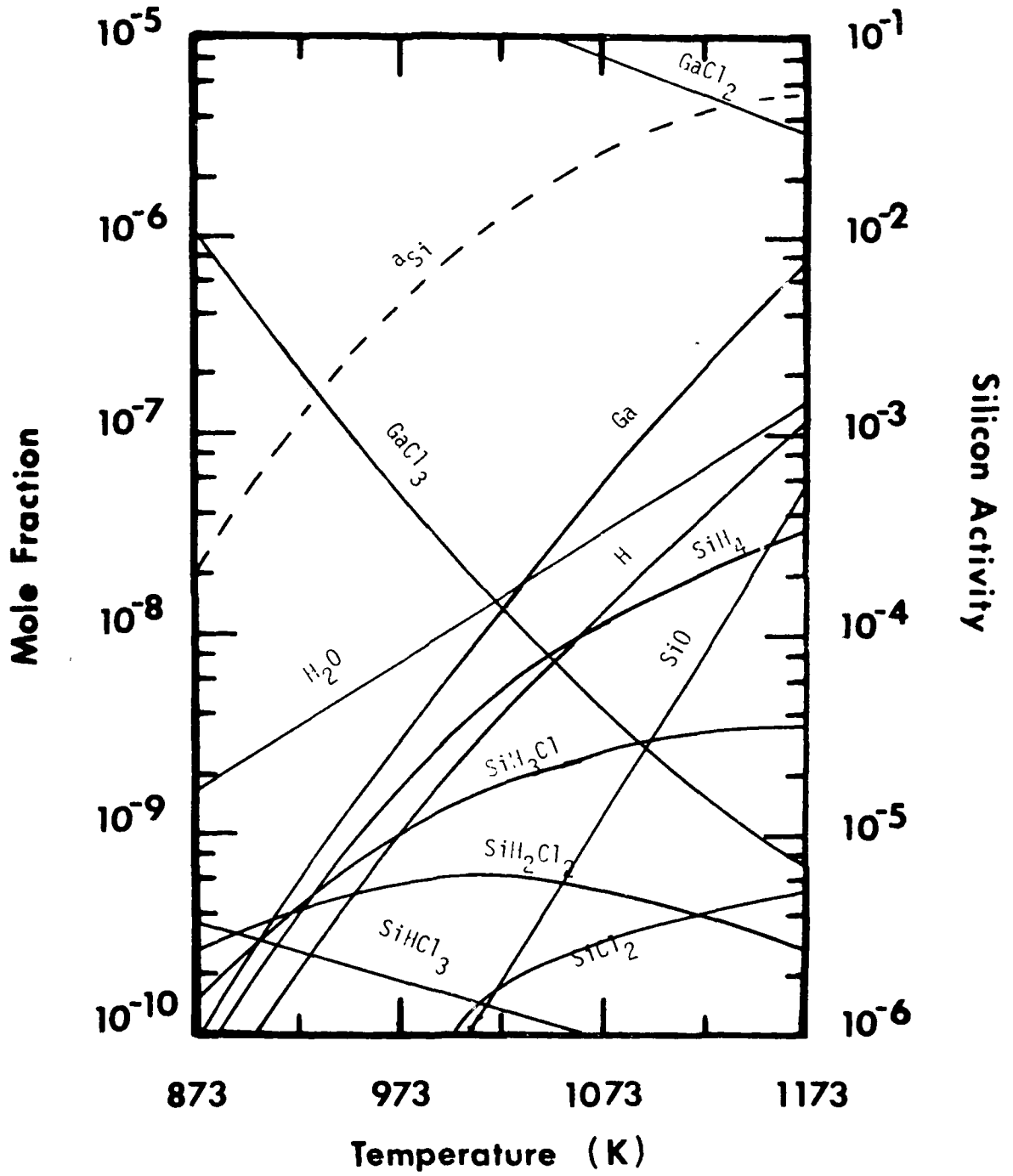
The results of these Group III and V source zone calculations at 973K were then combined and the effect of temperature in the mixing zone was investigated. Figure 6.16 shows this effect on the silicon activity and species in the lower five orders of magnitude in mole fraction. The silicon activity and silane mole fraction were found to be lower than the values for the Group V source zone alone at low temperatures due to the dilution effect of adding the two source zone streams together (equal molar flowrates were assumed in each source zone). Since the silane mole fraction and therefore the silicon activity in each source zone was approximately the same at 1173K, the resulting silicon activity in the mixing zone was the same as that at the outlet of either source zone.

Using the results from the mixing zone at 973K, the deposition zone was studied in the absence of  $SiO_2(c)$ . The saturation ratio, as defined by equation 6.1.8, was found to decrease from  $2 \times 10^4$  at 773K to 100 at 973K, indicating that the vapor was supersaturated over this entire deposition zone temperature range. The condensed phase



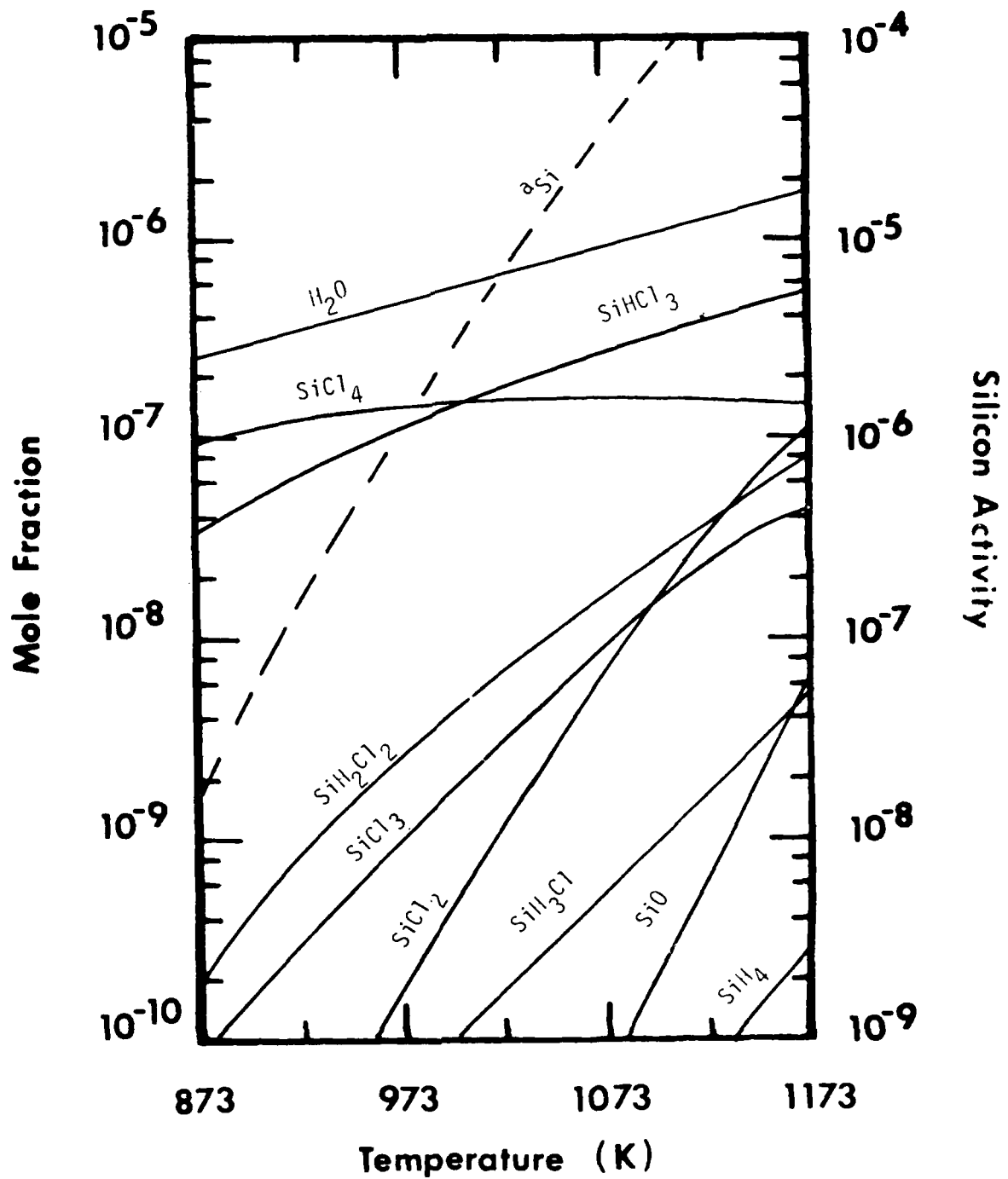
Effect of temperature on the Group V source zone of the GaAs hydride system

Figure 6.1



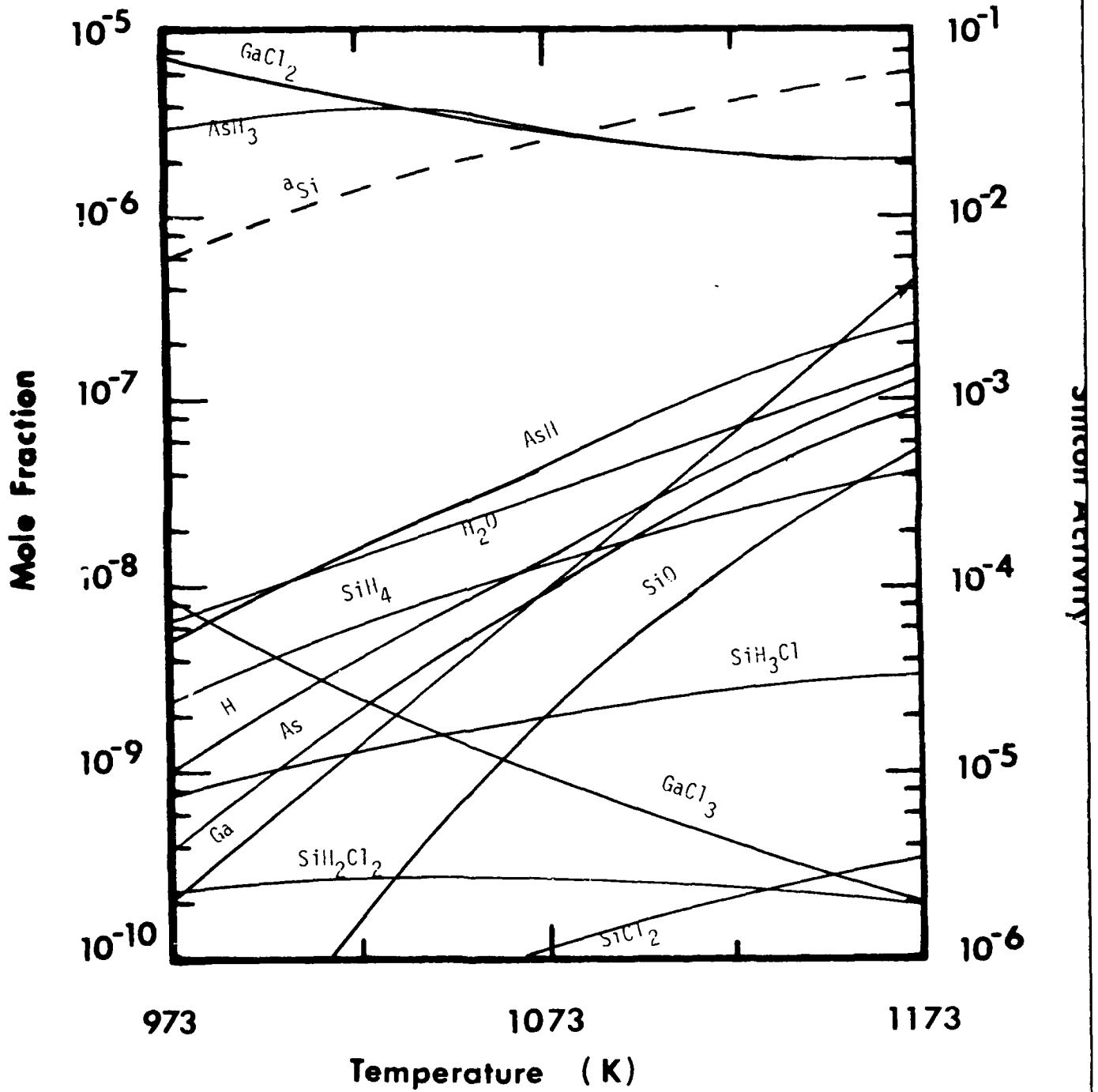
Effect of temperature on the Group III source zone of the GaAs hydride system

Figure 9.14



Effect of temperature on the Group III pre-source zone of the GaAs hydride system

Figure 6.15



Effect of temperature on the mixing zone of the GaAs hydride system

Figure 6.16

silicon activity varied only slightly, increasing from  $2 \times 10^{-3}$  at 773K to  $5 \times 10^{-3}$  at 973K, which is consistent with the effects observed in the chloride system using a liquid  $Ga_xAs_{1-x}$  Group III source. The lesser degree of supersaturation found for the hydride system when compared to the chloride system was due to the lesser amounts of Group III and V species present in the vapor. The dilution effect of adding the two source zone streams together causes the Group V vapor species to be one-half the mole fraction observed in the chloride system. The use of HCl coupled with this dilution effect reduces the rate of Group III specie transport to one-sixth of that in the chloride system.

The Group III and V source zones were investigated as functions of pressure at a temperature of 973K. The silicon activity in the Group III source zone was flat from 1 to 10 kPa then fell from a value of  $3 \times 10^{-2}$  to  $4 \times 10^{-4}$  at 1000 kPa. The Group V source zone exhibited a maximum in the condensed phase silicon activity at a pressure of 4 kPa, as did the chloride system source and mixing zones using a liquid Group III source. Upon combining the two hydride system source zones and performing the mixing zone equilibrium calculation the silicon activity in the mixing zone became a decreasing function of pressure.

The effect of pressure on the deposition zone of the hydride system very closely matched that of the chloride system. This result was expected since the source zones of the two systems are the only differences between the two and once downstream of the source zones the equilibrium chemistry of the hydride and chloride systems are the same.

The concentration of  $AsH_3$  in the feed gas stream to the Group V source zone was found to have no effect on the condensed phase silicon activity. This was due to the silicon species being rich in hydrogen and, in the presence of a large fraction of hydrogen carrier gas (> 90%), the hydrogen atoms released from the decomposition of  $AsH_3$  did not contribute significantly to the overall system hydrogen content. There-

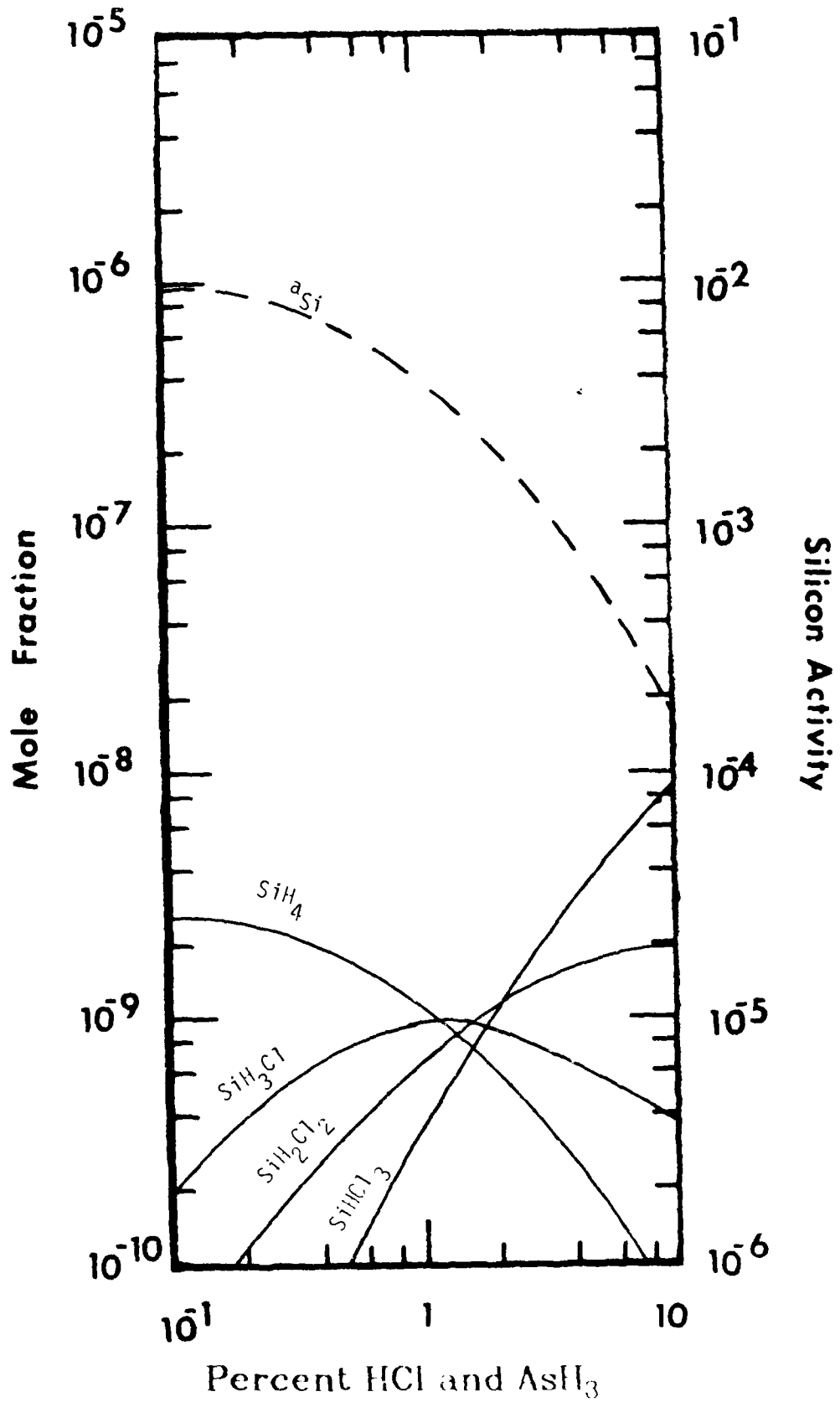
fore, the silane mole fraction was not significantly affected. In contrast Pogge and Kemlage [35] found that increased  $AsH_3$  concentrations decreased the free carrier concentrations in epitaxial GaAs. They cited kinetic effects, however, not thermodynamic limitations as the reason for their observations.

Increasing the concentration of HCl in the feed stream to the Group III source considerably decreased the condensed phase silicon activity by forming chlorine rich, as opposed to hydrogen rich, silicon species. Thus, one method of decreasing the silicon activity while maintaining a constant vapor III/V ratio is to increase both the HCl and  $AsH_3$  mole fractions in the feed streams to each source zone together. This effect is demonstrated for the deposition zone in Figure 6.17. Additionally, if various III/V ratios are desired it is advisable to operate the system with a large HCl concentration, in order to realize a low silicon activity, and vary the  $AsH_3$  concentration until the appropriate III/V ratio is attained.

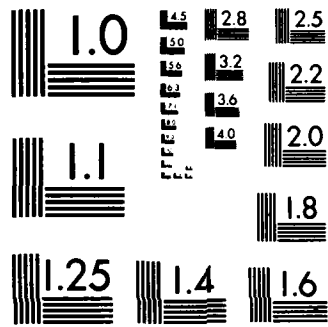
As was discussed for the chloride system, a very effective method for reducing the silicon activity is to make small additions to HCl or  $H_2O$  to the mixing zone. This preserves the system III/V ratio from the hydride system source zones and shifts reactions 6.2.1 and 6.2.2 in favor of  $SiO_2(c)$ . The results for the hydride system were essentially the same as those obtained for the chloride system and will not be discussed further.

Replacement of the hydrogen carrier gas by an inert gas was less effective in the hydride system than it was in the chloride system since hydrogen was provided by the decomposition of HCl and  $AsH_3$ . Figure 6.18 shows this effect for the deposition zone and although a very sharp bend is observed in the silicon activity, even when all of the hydrogen was replaced by inerts, the condensed phase silicon activity was approximately  $4 \times 10^{-5}$ . Therefore, replacing the hydrogen carrier gas by an inert gas was not an acceptable method to achieve low silicon activities. The addition of small amounts of HCl or  $H_2O$  to the mixing zone appears to be the most promising method of attain-

Effect of adding HCl on the GaAs hydride system deposition zone







MICROCOPY RESOLUTION TEST CHART  
NATIONAL BUREAU OF STANDARDS-1963-A

### Silicon Activity

Effect of replacing  $H_2$  with inerts on the GaAs hydride system deposition zone

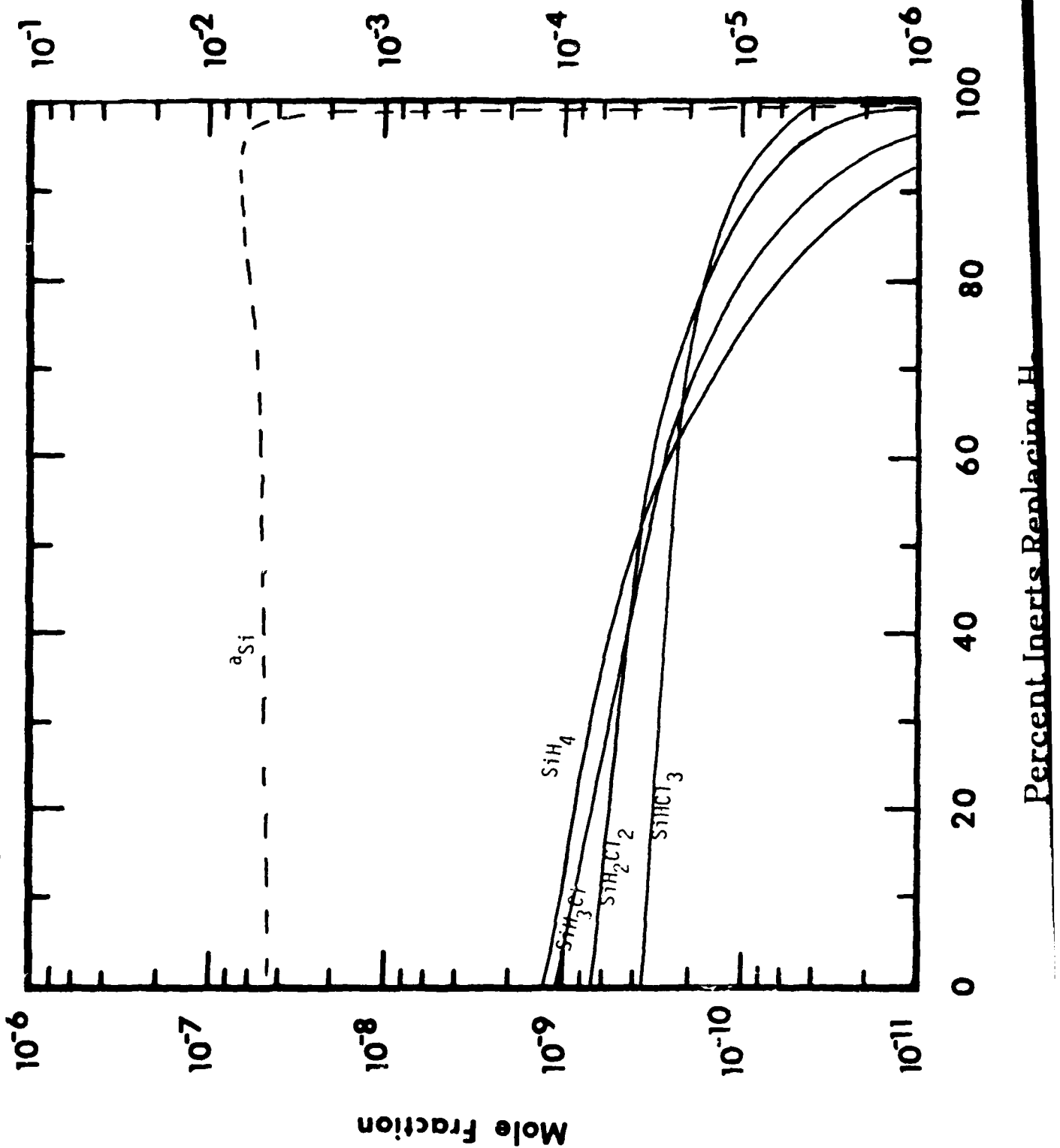


Figure 6.13

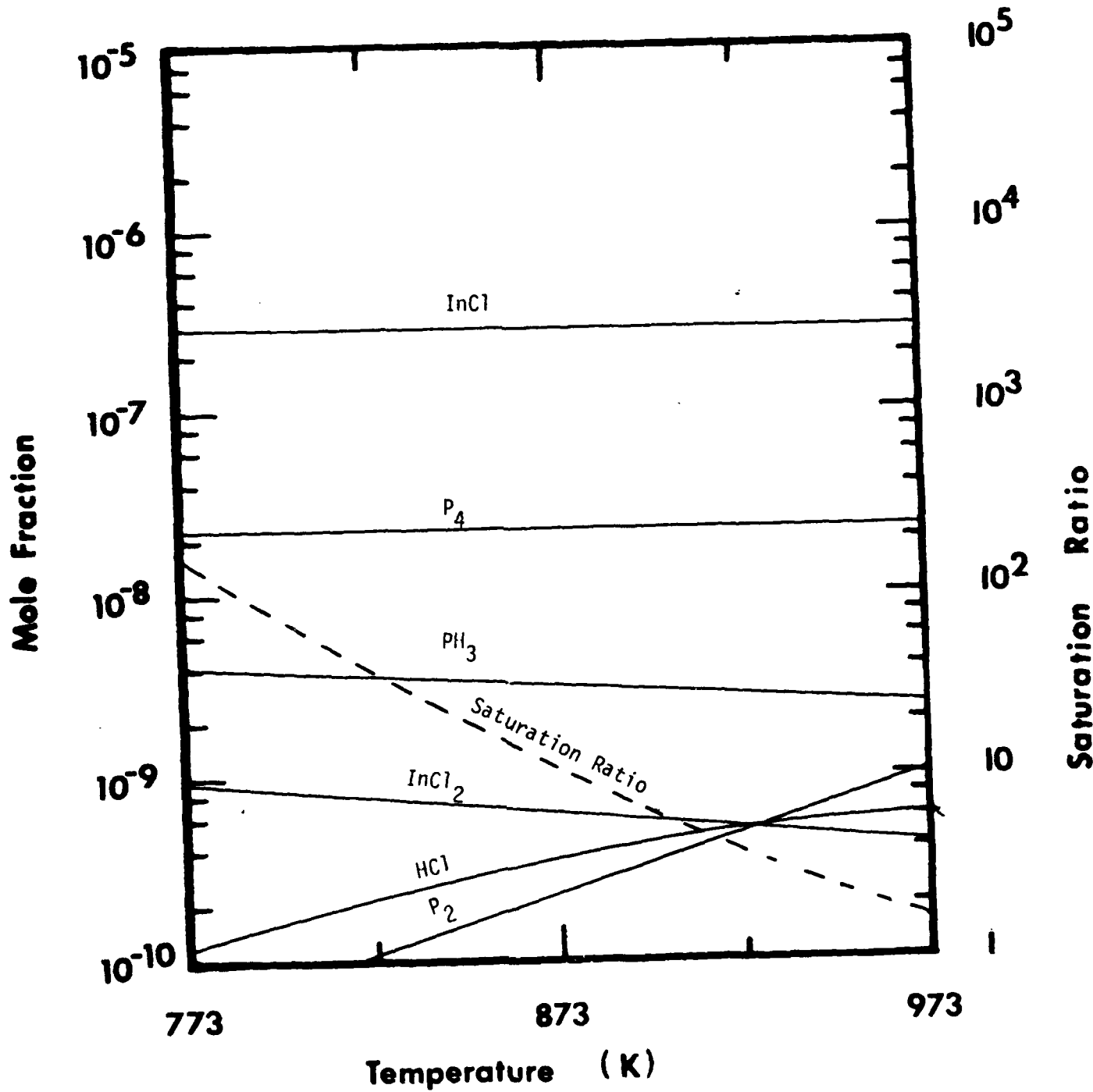
ing very low silicon activities in the hydride system.

#### 6.4 The InP Chloride System

The InP chloride system was investigated under the same conditions as the GaAs chloride system and was found to behave similarly in many respects. The source zone using liquid  $In_xP_{1-x}$  as the Group III source material was quite similar to the GaAs system in that InCl and  $P_4$  were the dominant Group III and V vapor species. One difference observed was that  $P_2$  was not as important a specie in the InP system as  $As_2$  was in the GaAs system. This may be due, however, to the equilibrium calculation being constrained as a result of the lack of a thermodynamic data set for the specie  $P_3$ . Condensed phase silicon activities for the GaAs and InP systems were found to be essentially the same. These same comments also apply to the mixing zone which was fed from this source zone.

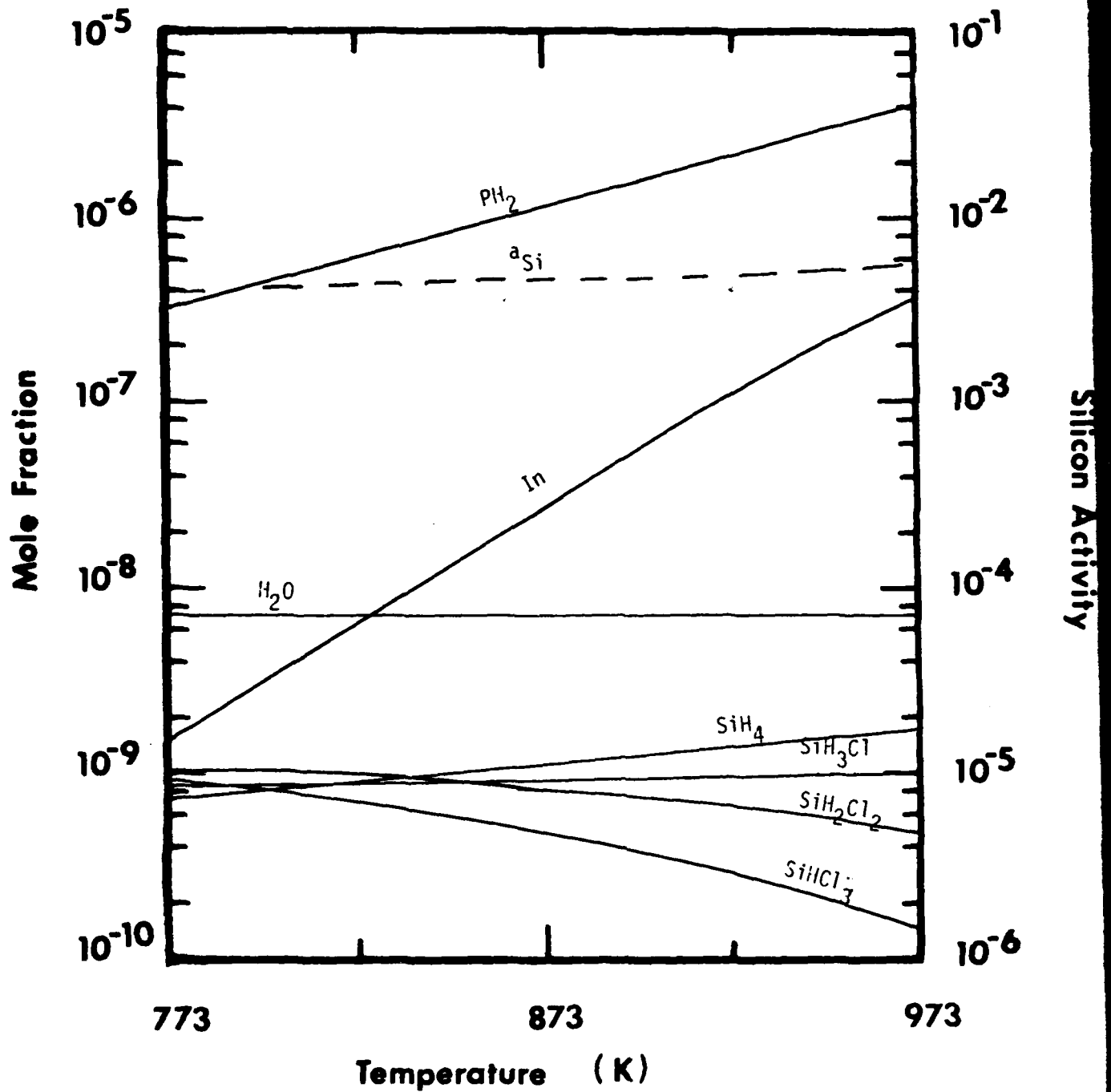
The deposition zone, shown in Figures 6.19 and 6.20 for the situation where  $SiO_2(c)$  was not included in the calculation, demonstrates several differences between the GaAs and InP systems. First, the saturation ratio for the InP system defined in analogy with equations 6.1.7 and 6.1.8, was much smaller than that of the GaAs system. The Gibbs free energy change for reaction 6.1.7 at 873K is 95.2 kcal/g-mole while the free energy change of the analogous reaction in the InP system is only 69.5 kcal/g-mole. Thus, the value of the equilibrium constant for the InP system is much larger than that for the GaAs system and, therefore, larger gas phase In and P partial pressures must be present in order to attain equal degrees of supersaturation in the two systems.

The condensed phase silicon activity for the InP system was slightly lower than that of the GaAs system, due to the lower  $SiH_4$  mole fraction, but increased slightly with temperature. Recall that the silicon activity in the GaAs system displayed a slight decrease in temperature when  $SiO_2(c)$  was not included in the calculation.



Effect of temperature on the InP chloride system deposition zone

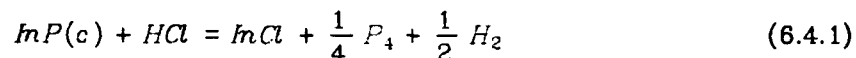
Figure 6.19



Effect of temperature on the InP chloride system deposition zone

Figure 6.20

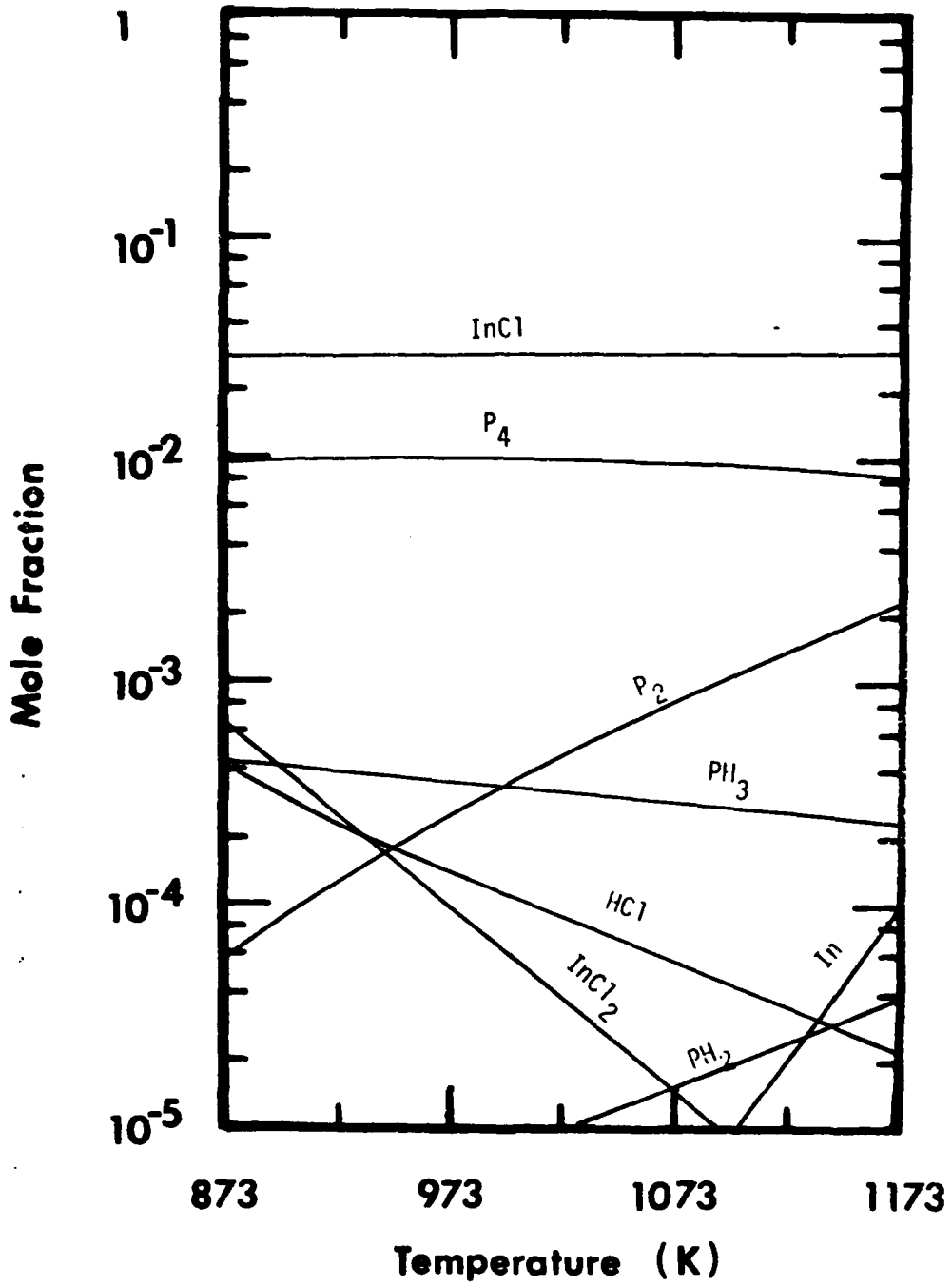
The InP source zone using solid InP as the Group III source material is shown in Figures 6.21 and 6.22. The behavior of this system was markedly different than that of the analogous GaAs system in that InCl was clearly the dominant Group III vapor specie due to the favorable Gibbs energy change (-8 kcal/g-mole at 973K) of the following reaction when compared to reaction 6.1.11 (3.2 kcal/g-mole at 973K).



The formation of a larger amount of Group III monochloride consumed much of the HCl initially present in the system and caused the vapor phase silicon species to be higher in hydrogen content than those species in the analogous GaAs system. As a result, the condensed phase silicon activity in the InP chloride system using solid InP in the source zone was found to be much larger than that of the GaAs system. These same comments also apply to the mixing and deposition zones of the InP system which follow the source zone using solid InP as the Group III source material.

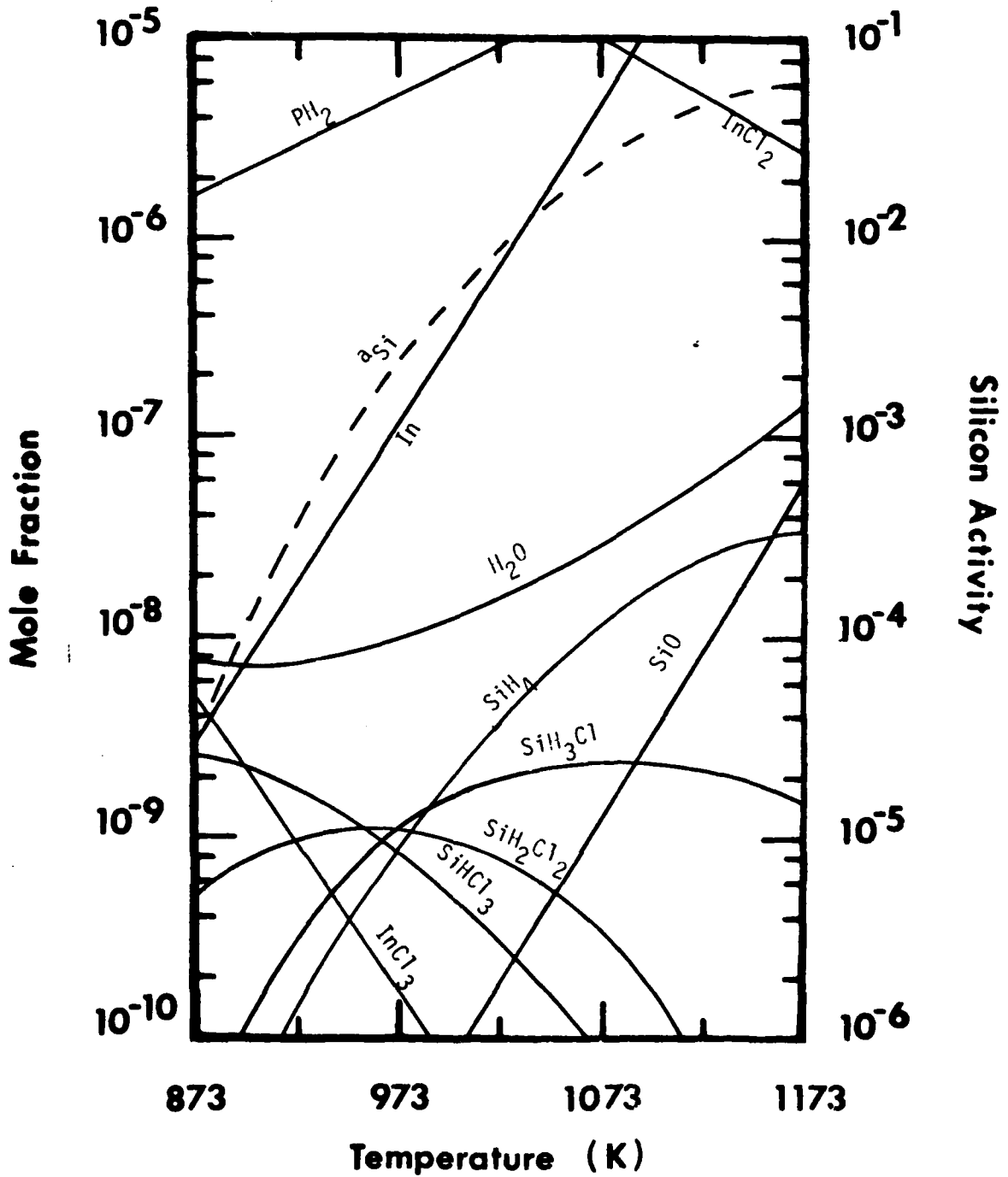
The effects of pressure on the InP chloride system follow closely those observed for the GaAs system relative to the previously discussed differences. Thus, for the system employing liquid  $\text{In}_x\text{P}_{1-x}$  as the Group III source, the condensed phase silicon activity in each zone is slightly lower than that of the GaAs system and the InP saturation ratio in the deposition zone is much less than that of the GaAs system. As in the GaAs system, maxima are observed in the condensed phase silicon activities at 4 kPa in the source and mixing zones. The chloride system using solid InP as the Group III source also displayed a pressure dependent behavior which was similar to that of the analogous GaAs system except that InCl was clearly the dominant Group III specie and the condensed phase silicon activity was much higher in the InP system due to reasons previously discussed.

The influence of  $\text{PCl}_3$  inlet concentration on the InP system was similar to that of  $\text{AsCl}_3$  in the GaAs system with the following differences. When liquid  $\text{In}_x\text{P}_{1-x}$  was used



Effect of temperature on the InP chloride system source zone (solid source)

Figure 6.21



Effect of temperature on the InP chloride system source zone (solid source)

Figure 6.22

as the Group III source material the condensed phase silicon activity was always 20% to 50% less than that of the corresponding GaAs system. This was due to  $InCl_3$  being a less important specie in the InP system than  $GaCl_3$  was in the GaAs system, which allowed more chlorine to react with the silicon vapor species. When solid InP was used as the Group III source material the silicon activity in the InP system was greater than that of the corresponding GaAs system due to the large amount of InCl formed.

Replacing the hydrogen carrier gas with an inert gas was also investigated in the InP system and the results followed the same trends as did the analogous GaAs system. The differences between the systems were consistent with the previous discussions, i.e. the condensed phase silicon activity for the InP system using solid InP for a source was larger than the GaAs system and the liquid source InP system showed a slightly reduced silicon activity in the deposition zone relative to the GaAs system.

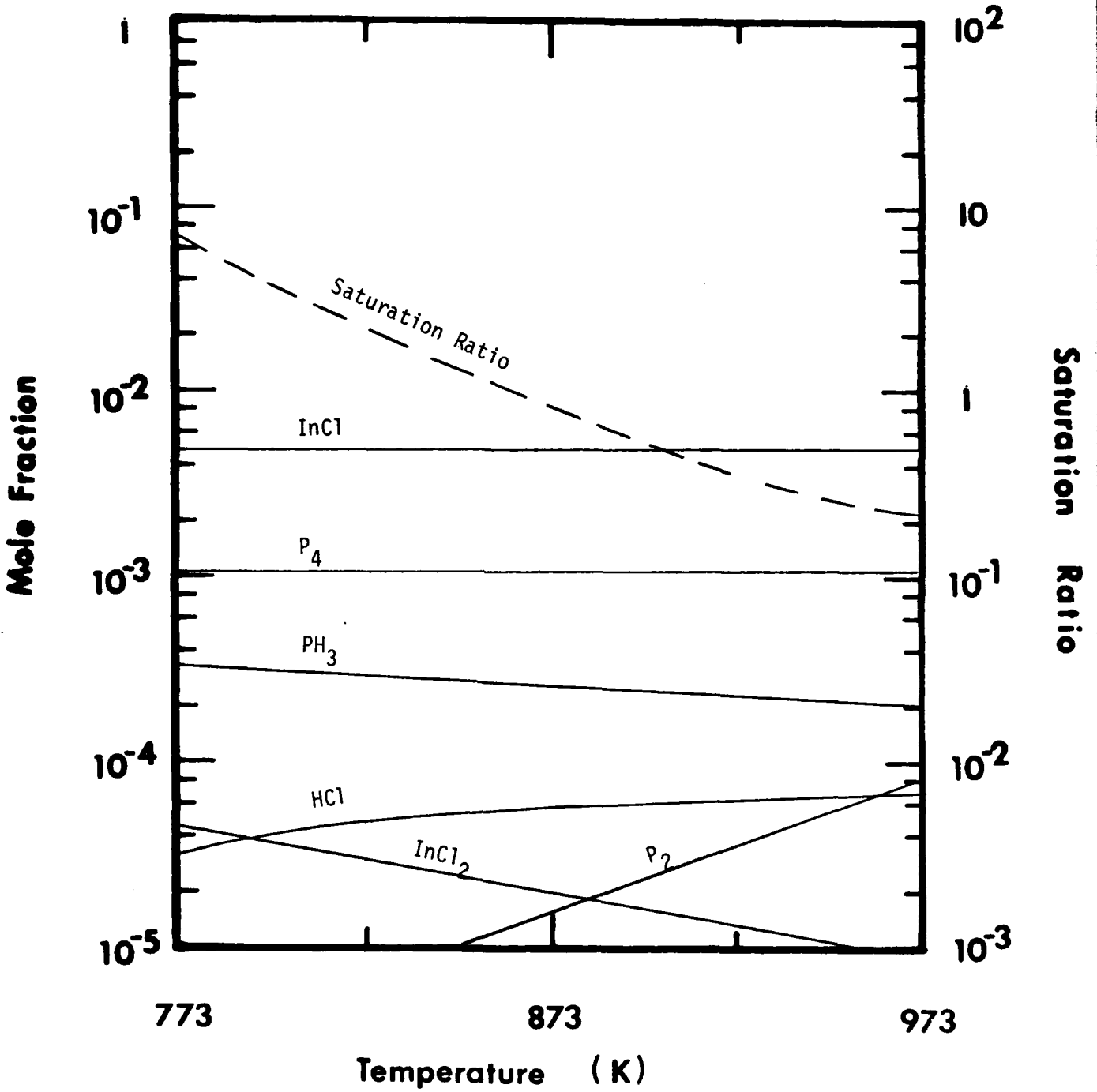
Additions of HCl,  $H_2O$ , and  $PCl_3$  to the mixing zone of the InP system were also studied. The trends observed were the same as those in the GaAs system.

### 6.5 The InP Hydride System

The results of a parametric analysis of the InP chloride system were similar to those of the GaAs hydride system discussed previously. The condensed phase silicon activity in the InP system was found to be consistently less than that in the GaAs system under all analogous conditions. At very low inlet HCl concentrations ( $\sim 0.1\%$ ) the silicon activities were nearly the same while at large inlet HCl concentrations ( $\sim 10\%$ ) the InP system exhibited silicon activities which were half the value of those in the GaAs system. This was primarily due to the smaller (more negative) Gibbs energy of formation of GaCl ( $-41.5 \text{ kcal/mol}^{-1}$  at 973K) which caused a greater production of GaCl via reaction 6.1.12 than InCl in the analogous reaction where In is the Group III specie. The differences in the Gibbs energies of formation at 973K for  $Ga(l)$  and  $In(l)$  were not significant. Thus, more HCl was available in the InP system to form chlorine rich silicon vapor species via reaction 6.1.1 which in turn lowered the condensed

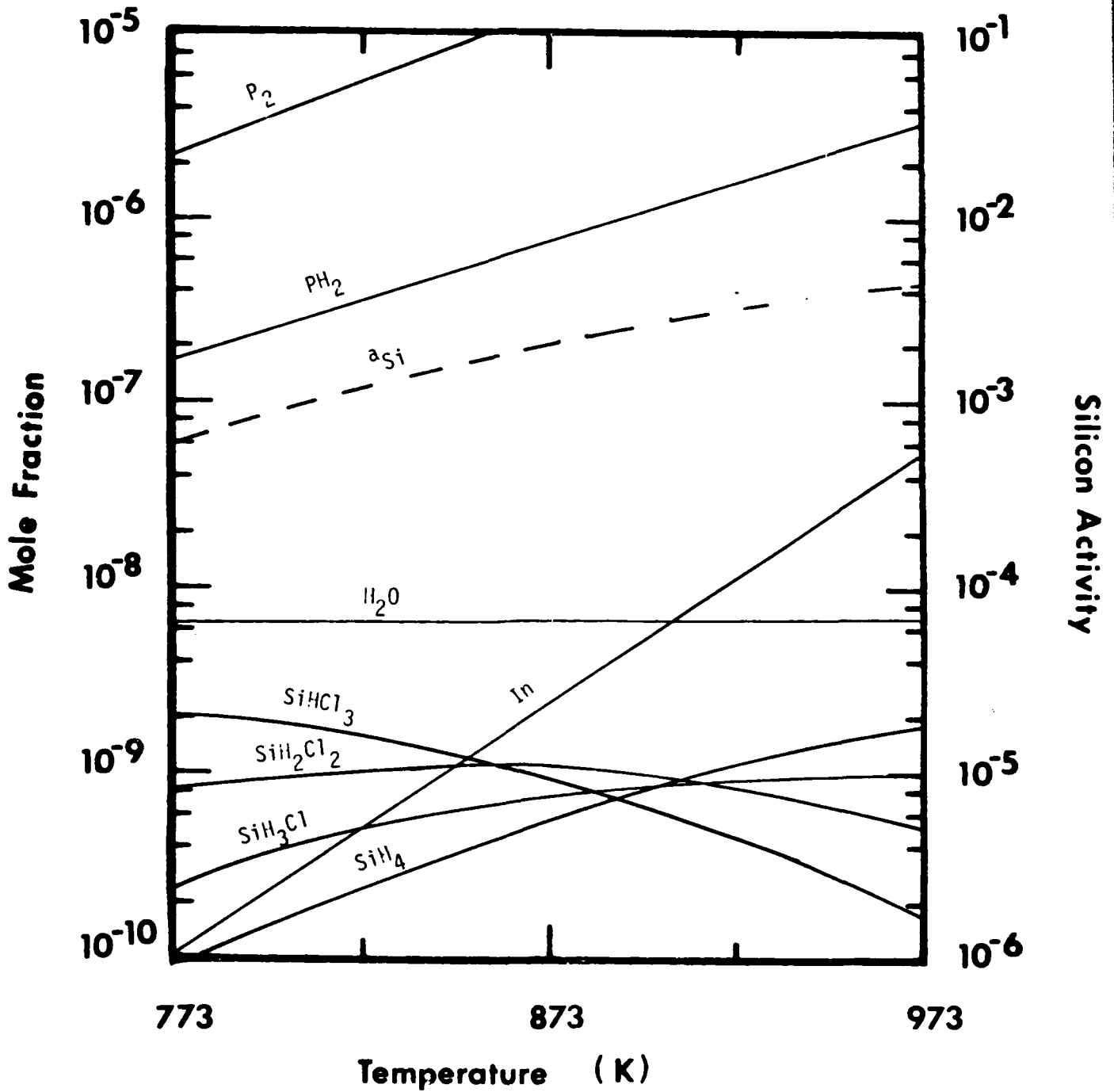
phase silicon activity relative to the GaAs system.

Figures 6.23 and 6.24 show the effect of temperature on the deposition zone of the InP system. As observed in the chloride systems, the saturation ratio for InP was much smaller than that for GaAs. The hydride system showed that, for the source zone conditions shown in the figures, the InP system did not become supersaturated until the temperature was below 860K. Alternatively, supersaturation at 873K can be achieved by increasing the system pressure from 100 kPa to 200 kPa or by increasing the  $PH_3$  and HCl inlet compositions. These results are in contrast to those observed in the InP chloride system and both GaAs systems which displayed supersaturated conditions in the deposition zone under all situations studied.



Effect of temperature on the InP hydride system deposition zone

Figure 6.23



Effect of temperature on the InP hydride system deposition zone

Figure 6.1.1

## 7. CONCLUSIONS

Parametric analyses of the chemical reaction thermodynamics pertaining to the chemical vapor deposition of GaAs and InP in the chloride and hydride systems have revealed some of the dissimilarities between these systems. Within the chloride system the condensed phase silicon activity resulting from the use of solid III-V material as the Group III source was shown to be much smaller than that obtained when a liquid Group III source was used. This difference was more pronounced for the GaAs system than it was for the InP system. The silicon activity for the InP system using a liquid source was slightly less than that of the analogous GaAs system while the GaAs system using the solid source exhibited a much smaller silicon activity than did the InP system using a solid source. Small additions of HCl,  $H_2O$  or  $VCl_3$  to the mixing zones of these chloride systems were very effective in reducing the silicon activity. Replacing the hydrogen carrier gas with an inert gas was found to be an effective method of reducing the silicon activity only if greater than 98% of the hydrogen was replaced. The degree of supersaturation in the deposition zone was much larger for the GaAs system than for the InP system. Also, the use of a liquid Group III source material led to greater supersaturations than the use of a solid III-V compound as the Group III source.

The hydride system was found to be substantially less supersaturated than the chloride system under typical operating conditions and the condensed phase silicon activity was less by approximately one order of magnitude for the hydride system when compared to the chloride system. Replacement of the hydrogen carrier gas with an inert was not as effective a method of reducing the silicon activity in the hydride system as it was in the chloride system due to the  $H_2$  liberated from the decomposition of HCl and  $VH_3$ . The condensed phase silicon activity was found to decrease with increasing pressure in the deposition zones while maxima in the silicon activity were found in the source and mixing zones at approximately 4 kPa pressure for systems using liquid source materials. Increasing the temperature was found to strongly

increase the silicon activity in the source and cooling zones. The influence of inlet composition on silicon activity was not as strong as that of temperature, pressure, replacement of  $H_2$  by inerts or the addition of species downstream of the source zone. Reduced silicon activities occurred as the inlet composition of chlorine containing species was increased.

In general it was found that shifting the vapor phase silicon species from those which are hydrogen rich to chlorine rich species markedly reduced the condensed phase silicon activity. This effect was so pronounced that even in systems where the total amount of silicon in the vapor phase as chlorinated species was much greater than that of hydrogen rich species in other systems, the condensed phase silicon activity was still sharply reduced.

## 8. REFERENCES

1. Smith W.R., Ind. Eng. Chem. Fund., **19**, 1, 1980
2. Clasen, R.J., Memorandum RM-4345-PR, 1965 The Rand Corporation
3. Cruise D.R., J. Phys. Chem., **68**, 12, 3797, 1964
4. Anderson T.J., Proposal to the Department of the Air Force
5. Smith W.R., Theoretical Chemistry: Advances and Perspectives, Vol. 5, 1980 Academic Press Inc.
6. Hunt L.P. and Sirtl E., J. Electrochem. Soc. **119**, 12, 1741, 1972
7. Shaw D.W., J. Crystal Growth, **8**, 117, 1971
8. Blakemore J.S., J. Appl. Phys., **53**, 10, 1982
9. Weiner M.E., J. Electrochem. Soc., **119**, 4, 496, 1972
10. Streetman B.G., Solid State Electronic Devices, Prentice Hall, 1972
11. Foyt A.G., Proc. 1980 NATO InP Workshop, Hanscom AFB, RADC-TM-80-07
12. Kressel H., Ettenberg M., Wittke J.P., Ladany I., Topics in Applied Physics: Semiconductor Devices for Optical Comm., 39, H. Kressel Editor
13. Ploog K., MBE, Ann. Rev. Mater. Sci., **11**, 171, 1981
14. Heyen M., Balk P., Proc. 8th Intl. Conf. on Chem. Vapor. Dep., Electrochem. Soc., 291, 1981
15. Seeger K., Semiconductor Physics, Springer-Verlag, 1973
16. Knight J.R., Effer D. and Evans P.R., Solid State Electron., **8**, 178, 1965
17. Effer D., J. Electrochem. Soc., **112**, 1020, 1965
18. Enstrom R.E. and Peterson C.C., Trans. Metall. Soc., AIME 239, 418, 1967
19. Wolfe C.M. and Stillman G.E., 1970 Symp. on GaAs, 3
20. Cairns B. and Fairman R., J. Electrochem. Soc., **115**, 3276, 1968
21. Cairns B. and Fairman R., J. Electrochem. Soc., **117**, 197C, 1970
22. DiLorenzo J.V., Moore G.E. and Machala A.E., J. Electrochem. Soc., **117**, 102C, 1970
23. DiLorenzo J.V. and Moore G.E., J. Electrochem. Soc., **118**, 11, 1823, 1971
24. Wolfe C.M., Stillman G.E., Korn D.M., Inst. Phys. Conf. Ser., #33b, 120, 1977
25. Solomon R., Gallium Arsenide and Related Compounds, Inst. Phys. Conf. Ser. 7, 1968
26. Ashen D.J., Dean P.J., Hurle D.T.J., Mullin J.B., Royle A., White A.M., Proc. 5th Intl. Symp. on GaAs, Inst. Phys. Conf. Ser. 34, 1975
27. Rai-Choudhury P., J. Crystal Growth, **11**, 113, 1971
28. Palm L., Bruch H., Bachem K., Balk D., J. Electronic Mat., **8**, 5, 555, 1979
29. Beiden V.E., Dyachkova N.M., Ivanyatin L.A., Nishanov D., Izves. Akad. Nauk SSSR, Neorgan. Mat., **12**, 8, 1114, 1974
30. Boucher A. and Hollan L., J. Electrochem. Soc., **117**, 932, 1970
31. Gentner J.L., Bernard C., Cadoret R., J. Crystal Growth, **56**, 332, 1982
32. Cadoret R., Current Topics in Mat. Sci., Vol. 5, Editor E. Kaldic, 1980

33. Seki H., Koukito A., Seki H., Fujimoto M., *J. Crystal Growth*, **43**, 153, 1978
34. Ozeki M., Kitahara K., Nakai K., Shibatomi A., Dazai K., Okawa S., and Ryuzan O., *Japan. J. Applied Physics*, **16**, 9, 1617, 1977
35. Pogge F.B. and Kemlage B.M., *J. Crystal Growth*, **31**, 183, 1975
36. Kennedy J.K., Potter W.D., and Davies D.E., *J. Crystal Growth*, **24/25**, 233, 1974
37. Enstrom R.E. and Appert J., *Electrochem. Soc.*, **129**, 11, 2566, 1982
38. Skromme B.J., Low T.J., Roth T.J., Stillman G.E., Kennedy J.K., and Abrokewah J.K., *J. Electronic Mat.*, **12**, 2, 433, 1983
39. Putz N., Venhoff E., Bachen K-H., Balk P., and Luth E., *J. Electrochem. Soc.*, **128**, 10, 2202, 1981
40. Clarke, R.C., Joyce B.D., and Wilgoss W.H.E., *Solid State Comm.*, **8**, 1125, 1970
41. Hales H.C., Knight J.R., and Wilkins C.W., 1970 Symposium on GaAs, 50
42. Joyce B.D. and Williams E.W., 1970 Symposium on GaAs, 57
43. Clarke R.C., *J. Crystal Growth*, **23**, 166, 1974
44. Clarke R.C., *Inst. Phys. Conf. Ser. No. 45*, 19
45. Easton B.C., *Acta Electronica*, **21**, 2, 151, 1978
46. Fairhurst K., Lee D., Robertson D.S., Parfitt E.T., and Wilgoss W.H.E., *Proc. 1980 NATO Sponsored InP Workshop*, 313 RADC-TM-80-07
47. Hales M.C. and Knight J.R., *J. Crystal Growth* **46**, 582, 1979
48. Chevrier J., Huber A., and Linh N.T., *J. Crystal Growth*, **47**, 267, 1979
49. Cardwell M.J., Giles P.L., Hales M.C., and Stirland D.J., *Proc. 1980 NATO InP Workshop*, Hascom AFB, 285 RADC-TM-80-07
50. Shaw D.W., *J. Phys. Chem. Solids*, **36**, 111, 1975
51. Olsen G.E., *Proc. 1980 NATO InP Workshop*, Hascom AFB, RADC-TM-80-07
52. Hyder S.B., *Proc. 1980 NATO InP Workshop*, Hascom AFB, RADC-TM-80-07
53. Zinkiewicz L.M., Roth T.J., Skromme B.J., and Stillman G.E., *Inst. Phys. Conf. Ser.*, **56**, 19, 1981
54. Anderson T.J., *Research Report USAF Rome Air Development Center*, F49620-79-C-0038
55. Jones K.A., *J. Crystal Growth*, **60**, 313, 1982
56. Bans V.S. and Ettenberg M., *J. Phys. Chem. Solids*, **34**, 1119, 1973
57. Usui A., and Watanabe, H., *J. Electronic Mat.*, **12**, 5, 891, 1983
58. Kupper P., Bruch H., Keyen, M., and Balk, P., *J. Elect. Mat.*, **5**, 5, 455, 1976
59. Ashen D.J., Dean P.J., Hurle D.T.J., Mullin J.B., White A.M., and Greene P.D., *J. Phys. Chem. Solids*, **36**, 1041, 1975
60. Cox, H.M., and DiLorenzo J.V., *Inst. Phys. Conf. Ser.*, **33b**, 11, 1977
61. Komeno J., Nogami M., Shibatomi A., and Ohkawa S., *Inst. Phys. Conf. Ser.*, **56**, 9, 1981
62. Mizuno O., *Japan. J. Appl. Phys.*, **14**, 4, 451, 1975
63. Fairman R.D. Omori M., and Fank F.B., *Inst. Phys. Conf. Ser.*, **33b**, 45, 1977

64. Vohl P., J. Crystal Growth, **54**, 101, 1981
65. Veuhoff E., Maier M., Bachem K.H., and Balk P., J. Crystal Growth, **53**, 598, 1981
66. Erstfeld T.E., and Quinlan K.P., J. Elec. Mat., **11**, 4, 647, 1982
67. Hurle, D.T.J., J. Phys. Chem. Solids, **40**, 613, 1979
68. Hurle, D.T.J., *ibid.*, 627, 1979
69. Hurle, D.T.J., *ibid.*, 639, 1979
70. Hurle, D.T.J., *ibid.*, 647, 1979

9. Appendix A. MCMPEC.RAND: A Computer Code For Calculating Chemical Equilibrium Using A Nonstoichiometric Algorithm

A.1 Introduction

A.2 The Main Program

- A.2.1 Array Dimensions, Expandability and Initialization
- A.2.2 Data Input
- A.2.3 Preparation for the Iterative Solution
- A.2.4 Iterative Solution for Equilibrium Compositions
- A.2.5 Output of Results
- A.2.6 Main Program Listing

A.3 A Description of the Major Variables in MCMPEC.RAND

A.4 A Description of the Subroutines

- A.4.1 STSTCP
- A.4.2 ESTMTE
- A.4.3 STEADY
- A.4.4 IDPTEQ
- A.4.5 TESTD
- A.4.6 ADDR MV
- A.4.7 ACTCOF
- A.4.8 RAND
- A.4.9 CNVFRC and DGDLAM
- A.4.10 RESTOR
- A.4.11 GIBBS
- A.4.12 CALCQ
- A.4.13 TOSI
- A.4.14 RATIO
- A.4.15 WRAPUP
- A.4.16 DEBUG
- A.4.17 PRNTAB
- A.4.18 IMSL Subroutines LINVIF, LEQTIF, LUDATF, LUELMF

A.5 Theoretical Development of the RAND Algorithm

A.6 Example Calculation: The Ga, As, H System

## Appendix A

MCMPEC.RAND: A Computer Code for Calculating Chemical  
Equilibrium Using a Nonstoichiometric Algorithm

## A.1 Introduction

The calculation of chemical equilibrium using a nonstoichiometric algorithm (the Rand algorithm) is based on the work of Clasen [1]. A nonstoichiometric algorithm adjusts the amount of each specie present in the system without referring to a specific set of chemical reaction equations. The overall system mass is conserved by constraining the amount of each element present to a constant value. Equilibrium is attained when the free energy of the system is minimized. A development of the Rand algorithm, extended to include a solution phase and pure condensed phases in addition to a vapor phase, is presented in section A.5. Since CVD systems are operated at constant pressure the Gibbs Free Energy was chosen as the appropriate free energy function.

The algorithm consists of a set of linearized finite difference equations which are formed from the overall system free energy function and the elemental abundance constraints. These equations are solved to predict changes in the amount of each specie which will yield a decrease in the overall system free energy. The vapor phase is assumed to be ideal although activity coefficients (which are set to unity) are included in the equations. The solution phase includes options for ideal behavior, a binary system simple solution theory model or inclusion of a Henry's Law constant. An inert specie in the vapor phase is also available as an option.

The use of linear algebra techniques to solve the system of linear equations results in three complications. First, a vapor phase must always be present in order to prevent the coefficient matrix from becoming singular. Therefore, systems consisting of only pure condensed phases and a solution phase cannot be solved using this algorithm. Second, pure condensed phases which have compositions that vanish must be removed from the calculation in order to prevent the coefficient matrix from becoming singular. This results in the addition of some rather intricate logic and a considerable amount of "book keeping" in order to remove the phase, shift the equation order and then perform tests to determine whether the phase needs to be reinserted later in the calculation. Finally, a considerable amount of computer storage is required (about 111 k-bytes on an IBM 370 for 50 species) in order to execute the code.

The code includes options to allow temperature, pressure and inlet composition loops in order to generate the data required for parametric analyses.

Currently there is evidence which suggests that the liquid solution in the source zone of the CVD halide system is at steady state [2]. Therefore, an option has been included to model this situation in the Ga/As and In/P systems. Several data output options and debugging aids have also been included. The reader is referred to subsection A.2.2 for a discussion of these options.

The structure of the main program along with data input and output are discussed in section A.2. A description of the major variables used in the code is presented in section A.3 and each subroutine is discussed separately in Section A.4. As was previously mentioned, the theoretical development of this extended version of the Rand algorithm is presented in section A.5 and an example calculation is located in section A.6.

## A.2 The Main Program

A flowsheet for MCMPEC.RAND is shown in Figure A1. The primary functions of the main program are to set array dimensions, provide a framework for calling the subroutines and to take care of data input and output. Thus the actual looping parameters for the temperature, pressure and composition options are located in the main program as are the loop and convergence test for determining the equilibrium compositions. All of the data input and output are performed in the main program. Subroutines DEBUG and PRINTAB write out information useful for debugging purposes and execution diagnostics pertaining to the various subroutines are written out directly from the appropriate subroutine. Also, subroutine WRAPUP writes out a concise wrapup file when the option is active.

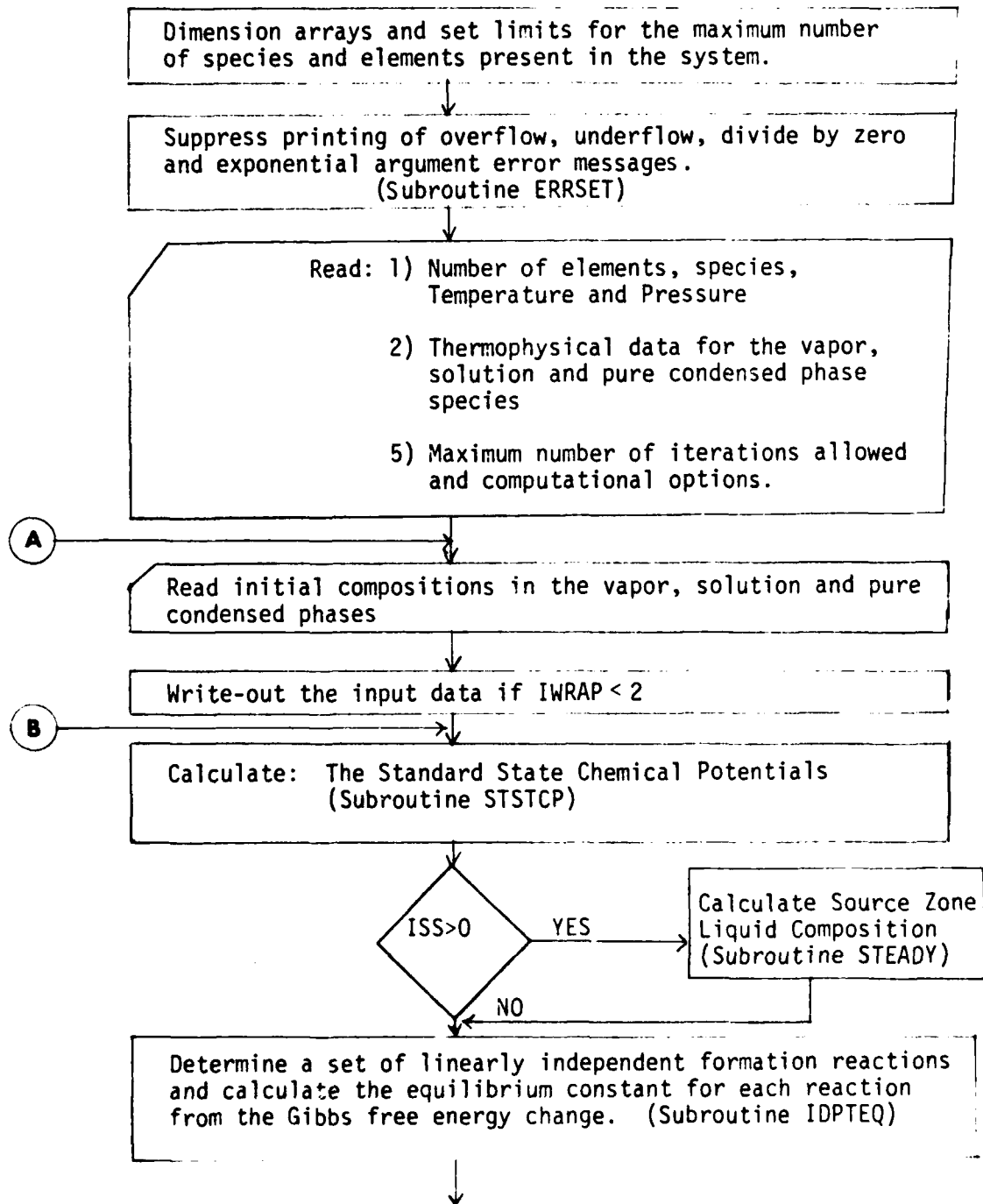
A listing of the main program is located in subsection A.2.6.

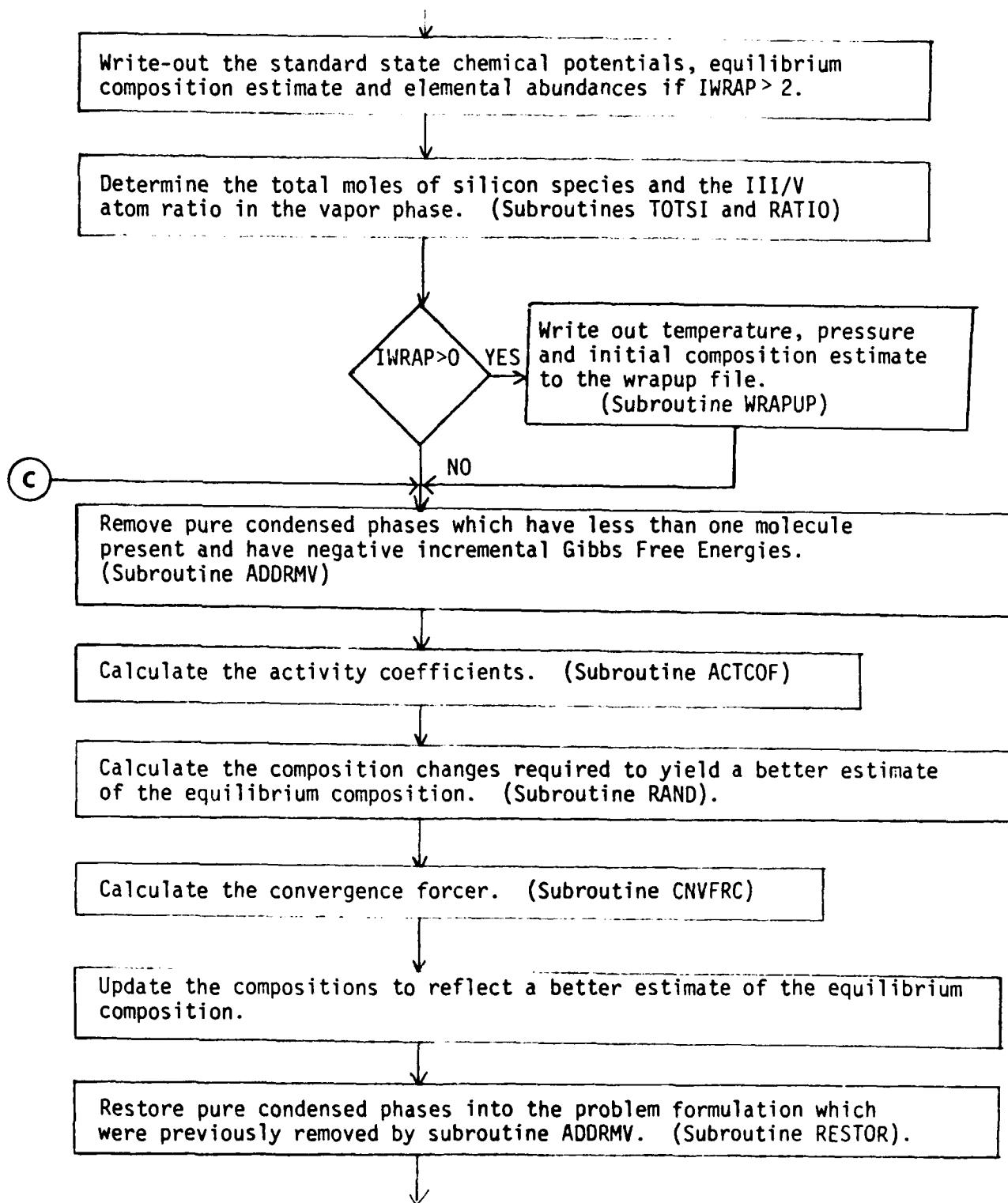
### A.2.1 Array Dimensions, Expandability and Initialization

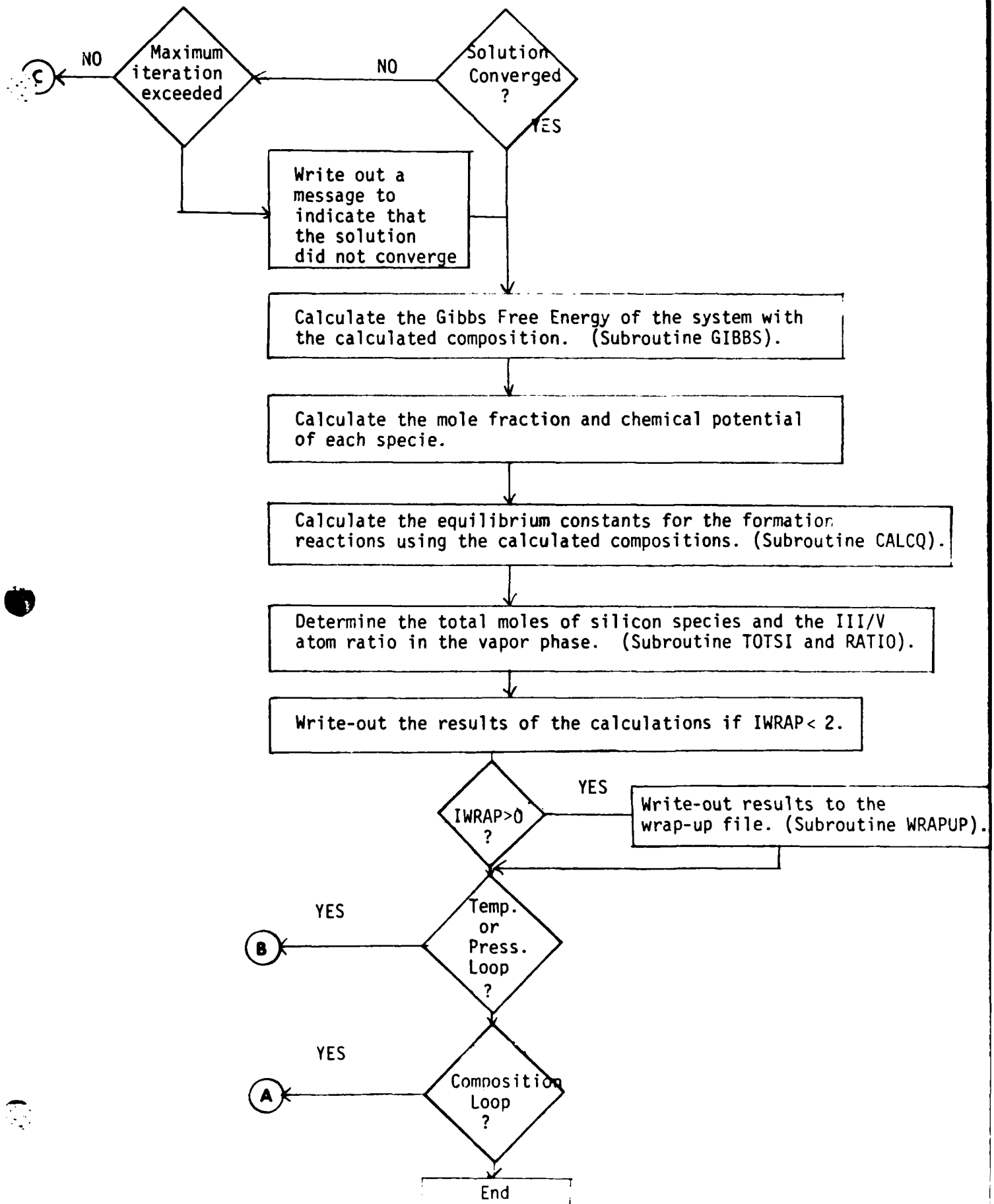
The arrays used in MCMPEC.RAND are dimensioned in lines 5 through 17. Currently these arrays are dimensioned to accommodate systems containing up to 50 different species comprised of a maximum of 13 different elements. The variables IDIM1, IDIM2 and IDIM3, which are initialized in lines 36, 37 and 38, are used to set the array dimensions in the subroutines. Therefore, the code can be expanded to accommodate larger systems simply by changing the array dimensions and the values of IDIM1 and IDIM2 in the main program. The double precision arrays ALEQ,

Figure A1

## Main Program Flowsheet for MCMPEC.RAND







BLEQ and WKA are dimensioned  $IDIM1 + IDIM2$  and therefore must be modified accordingly. It is suggested that the element dimension  $IDIM2$  not be increased beyond 13 as this will cause output line lengths in excess of 132 characters which will either be lost or difficult to read as a result of printer "wrap around". There are no restrictions (other than available computer memory) to the number of species which the code may be expanded to accommodate.

Character strings used to build the output for the reaction formation equations are initialized at lines 11 through 16. The vapor, solution and condensed phase identifying character strings are also initialized here.

The logical unit designators for the input file, printed output and the wrap-up file are initialized at 5, 6 and 2 respectively in lines 33 through 36.

Lines 43 and 44 call the system subroutine ERRSET to suppress the printing of overflow, underflow, divide by zero and exponential argument error messages. These errors occur commonly in the IMSL matrix routine LEQTIF and since this routine internally tests for the number of significant figures in the results it is unnecessary to receive these system warnings. The exponential argument error message occurs quite frequently in the calculation of equilibrium constants from composition (subroutine CALCQ). This is a result of species having very small concentrations being included in the formation reactions. The equilibrium constants are calculated for comparison purposes only and therefore do not effect the calculated compositions. Discrepancies between the equilibrium

constants as calculated from composition and Gibbs Free Energy usually result from exceeding the numerical range of the computer.

#### A.2.2 Data Input

Data input is accomplished in lines 45 through 146. A summary of the input data set is shown in Table A.1 and a description of each input variable is located in Table A.2.

The first input record consists of a data set title which may be up to 80 characters in length. The second record consists of the number of elements in the system, the number of species in the vapor ( $V > 0$ ), solution and pure condensed phases, followed by the system temperature and pressure. The last two pieces of information on this record are the reference temperature and pressure for the enthalpies and entropies of formation. The symbols for each element are on the third record. Two characters are allowed for each element symbol.

The next  $3V$  records contain information regarding the species present in the vapor phase. The first record contains a 12 character specie name and the enthalpy and entropy of formation at temperature  $T_0$  and pressure  $P_0$  for this specie. Heat capacity correlation information is contained on the second record and the number of atoms of each element which are present in a single molecule of the specie are on the third record. Records  $3V + 1$  to  $3V + 3$  contain this same information for an inert specie in the vapor phase. The inert specie information must always be present in the data set. When it is desired to perform a calculation without the inert, its initial concentration is simply set to zero. This same information must also be provided for each specie in the solution phase and each pure condensed phase.

Table A.1  
Input Data Set for MCMPEC.RAND

Record	Comments	Format
Title (1),.... TITLE (20)	80 Character Title	20A4
E, V, S, C, T, P, T <sub>0</sub> , P <sub>0</sub>		4I5, 4F10.0
ELMNT (1), ELMNT (2) .... ELMNT (E)	Element Symbols	13 (1X, A2)
SPECIE (I,K), DMO(I), DSO(I)	Each vapor phase specie	3A4, 2E12.5
AO(I), A1(I), A2(I), A3(I), ICP(I)		4E12.5, I2
A(I,1), A(I,2).... A(I,E)		13(F5.0, 1X)
Inert(K), DHOZ, DSOZ	Inert vapor phase specie	3A4, 12E12.5
AOZ, -A1Z, A2Z, A3Z, ICPZ		4E12.5, I2
IDUMMY		13(F5.0, 1X)
SPECIE(I, K), DHO(I), DSO(I)	Each solution phase specie	3A4, 12E12.5
AO(I), A1(I), A2(I), A3(I), ICP(I)		4E12.5, I2
A(I,1), A(I,2),...A(I,E)		13(F5.0,1X)
SPECIE(I,K), A2(I), A3(I), ICP(I)	Each pure condensed phase	3A4, 12E12.5
AO(I), A1(I), A2(I), A3(I), ICP(I)		4E12.5, I2
A(I,1), A(I,2)...A(I,E)		13(F5.0,1X)
IDEBUG, IOPT, ISS, IWRAP, MAXIT, NMAX CNVG, TINC, PINC		6I5, 3F10.0
TOTMV		E12.5
FRAC(1), FRAC(2).... FRAC(V), FRACZ		6E12.5
TOTMS		E12.5
FRAC(V+1), FRAC(V+2)... FRAC(V+S)		6E12.5
IXSCOR, AXS, BXS		I5, 2E12.5
TOTMC(V+S+1)...TOTMC(V+S+C)		6E12.5

Table A.2

Description of Input Variables

<u>Variable</u>	<u>Description</u>
TITLE (20)	80 Character data set <del>title</del>
E	Number of elements ( $E \leq 13$ )
V	Number of vapor species excluding the inert
S	Number of solution species
C	Number of pure condensed phases
T	System Temperature (K)
P	System Pressure (Pa)
T0	Reference Temperature for $\Delta H$ and $\Delta S$ formation
P0	Reference Pressure for $\Delta H$ and $\Delta S$ formation
ELMNT (13)	2 character symbol for each element (right justified)
SPECIE (50, 3)	12 character symbol for each specie
A (50, 13)	Elemental abundance matrix
DH0 (50)	Enthalpy of formation (kcal/g-mole) for each specie at Temperature T0 and Pressure P0.
DS0 (50)	Entropy of formation (kcal/g-mole-K) for each specie at Temperature T0 and Pressure P0.
A0 (50)	Heat capacity correlation parameter (kcal/g-mole-K)
A1 (50)	Heat capacity correlation parameter (kcal/g-mole-K <sup>2</sup> )
A2 (50)	Heat capacity correlation parameter (see Table)
A3 (50)	Heat capacity correlation parameter (see Table)
ICP (50)	Heat capacity correlation parameter (see Table)

Heat Capacity Correlations

<u>ICP (I)</u>	<u>A2 (I)</u>	<u>A3 (I)</u>	<u>Correlation</u>
0	kcal-K/g-mole	kcal/g-mole-K- $\ln(k)$	$A0+A1*T+A2/T^2+A3*\ln(T)$
1	kcal/g-mole-K <sup>3</sup>	kcal/g-mole-K <sup>4</sup>	$A0+A1*T+A2*T^2+A3*T^3$

INERT (3) 12 character name for inert vapor specie

DHOZ Inert specie enthalpy of formation

DSOZ Inert specie entropy of formation

AOZ	}	Inert specie heat capacity correlation parameters
A1Z		
A2Z		
A3Z		
ICPZ		

IDEBUG Debugging output parameter

<u>IDEBUG</u>	<u>FUNCTION</u>
0	warning messages are printed when problems are encountered in the IMSL subroutines
1	Prints IDEBUG = 0 option plus composition changes and Gibbs Free Energy for each iteration.
2	Prints IDEBUG = 1 option plus matrices and vectors ALEQ, BLEQ and X for each iteration.

IOPT Looping option parameter

<u>IOPT</u>	<u>FUNCTION</u>
0	One pass through routine
1	Temperature loop
2	Pressure loop
3	Composition loop

ISS Source zone steady state option parameter

<u>ISS</u>	<u>FUNCTION</u>
0	Steady state option is inactive
1	Ga/As liquid composition is at steady state with GaAs solid
2	In/P liquid composition is at steady state with InP solid.

IWRAP	Data output option parameter										
	<table> <thead> <tr> <th><u>IWRAP</u></th> <th><u>FUNCTION</u></th> </tr> </thead> <tbody> <tr> <td>0</td> <td>Write-out input data, execution diagnostics and results to printer</td> </tr> <tr> <td>1</td> <td>IWRAP=0 function plus writes-out a concise wrap-up file.</td> </tr> <tr> <td>2</td> <td>No printer output just a wrap-up file</td> </tr> <tr> <td>3</td> <td>Write a wrap-up to the printer</td> </tr> </tbody> </table>	<u>IWRAP</u>	<u>FUNCTION</u>	0	Write-out input data, execution diagnostics and results to printer	1	IWRAP=0 function plus writes-out a concise wrap-up file.	2	No printer output just a wrap-up file	3	Write a wrap-up to the printer
<u>IWRAP</u>	<u>FUNCTION</u>										
0	Write-out input data, execution diagnostics and results to printer										
1	IWRAP=0 function plus writes-out a concise wrap-up file.										
2	No printer output just a wrap-up file										
3	Write a wrap-up to the printer										
MAXIT	maximum number of iterations allowed for the equilibrium composition to converge										
NMAX	maximum number of loops allowed for the IOPT parameter										
CNVG	convergence criterion										
TINC	temperature increment for each loop if IOPT=1										
PINC	pressure increment for each loop if IOPT=2										
TOTMV	total moles in the vapor phase										
TOTMS	total moles in the solution phase										
TOTMC (I)	total moles in each pure condensed phase										
FRAC (I)	1<I<V mole fraction of specie i in vapor V+1<I<V+s mole fraction of specie i in solution										
FRACZ	mole fraction of inert in vapor										
IXSCOR	activity coefficient correlation parameter for the solution phase										
	<table> <thead> <tr> <th><u>IXSCOR</u></th> <th><u>Correlation</u></th> </tr> </thead> <tbody> <tr> <td>0</td> <td>ideal solution</td> </tr> <tr> <td>1</td> <td>binary simple solution</td> </tr> <tr> <td>2</td> <td>Henry's Law</td> </tr> </tbody> </table>	<u>IXSCOR</u>	<u>Correlation</u>	0	ideal solution	1	binary simple solution	2	Henry's Law		
<u>IXSCOR</u>	<u>Correlation</u>										
0	ideal solution										
1	binary simple solution										
2	Henry's Law										
AXS, BXS	activity coefficient correlation coefficients for the solution phase										
	<table> <thead> <tr> <th><u>IXSCOR</u></th> <th><u>Correlation</u></th> </tr> </thead> <tbody> <tr> <td>0</td> <td>ideal solution</td> </tr> <tr> <td>1</td> <td><math>G^E = (AXS + BXS * T) * \chi_1 * \chi_2</math></td> </tr> <tr> <td>2</td> <td><math>H = AXS * EXP (BXS/T)</math></td> </tr> </tbody> </table>	<u>IXSCOR</u>	<u>Correlation</u>	0	ideal solution	1	$G^E = (AXS + BXS * T) * \chi_1 * \chi_2$	2	$H = AXS * EXP (BXS/T)$		
<u>IXSCOR</u>	<u>Correlation</u>										
0	ideal solution										
1	$G^E = (AXS + BXS * T) * \chi_1 * \chi_2$										
2	$H = AXS * EXP (BXS/T)$										

Following the data for each individual specie is a record describing the various options available and numerical methods information. Parameter IDEBUG should be set to zero for production type jobs but may be set to 1 or 2 to provide information which allows the calculations to be examined in a step by step fashion.

Parameter IOPT allows the code to be looped in order to generate temperature, pressure or composition parametric curves. NMAX sets the number of loops to be carried out while TINC and PINC are the temperature and pressure increments per loop. If a composition loop is desired a new initial composition data set must be provided for each loop.

Parameter ISS is used to activate the steady state liquid source option. If ISS is set to 1 the composition of a liquid containing Ga and As in equilibrium with GaAs solid is calculated. This liquid is inserted as the last pure condensed phase in the system. Thus when the value of C (number of pure condensed phases) is specified it must include a steady state phase if  $ISS > 0$  otherwise the last pure condensed phase in the system will be replaced with the steady state liquid. Setting  $ISS = 2$  will model a liquid of In and P in equilibrium with InP solid.

The parameter IWRAP is used to choose the amount of data output desired. When  $IWRAP = 0$  the input data is written out in tabulated form along with a description of the options chosen, execution diagnostics, equilibrium compositions, reaction formation equations and a comparison between the equilibrium constants for these equations as calculated from the free energy changes and the compositions. With  $IWRAP = 1$  a concise wrap-up file is written to logical unit designator IFILE ( $IFILE = 2$ )

in addition to the IWRAP = 0 option. These two output options are quite useful when one is becoming acquainted with the code as they provide an echo of the input data set and a verification of the results. Options IWRAP = 2 and IWRAP = 3 provide only wrapup file output to IFILE and IWRT respectively.

MAXIT sets the maximum number of iterations to be performed for calculating the equilibrium compositions. Typically MAXIT is set to 1000.

The equilibrium compositions are considered converged when, after two successive iterations, the largest fractional change in any significant specie concentration is less than CNVG. A significant specie is one which is present in a concentration of  $1 \cdot 10^{-50}$  moles or greater. A typical value for CNVG is  $10^{-4}$ .

The inlet compositions for the vapor, solution and pure condensed phases are next in the input data set. The total moles in the vapor are on one record and the following records contain the mole fractions of each component in the vapor, the last value being the mole fraction of the inert. The solution phase inlet compositions are done the same way except that there is no inert. Following the solution phase mole fractions is a record which determines the activity coefficient model to be used in the solution phase. For IXSCOR = 0 the solution is considered to be ideal. Setting IXSCOR = 1 yields a binary simple solution model for the excess Gibbs Free Energy. A Henry's Law constant for the first component in the solution phase is activated by setting IXSCOR = 2. The parameters AXS and BXS are used in the activity coefficient models as shown in Table A.2.

The final records of the input data set contain the number of moles in each pure condensed phase.

## A.2.3. Preparation for the Iterative solution

The limits for the temperature, pressure and composition loops are set in lines 126 through 129. The composition loop (IOPT = 3) starts at line 130.

The input specie order is saved so that the results may be output in this order. This step is necessary since pure condensed phases may be removed and reinstated during the calculational procedure and it is convenient to compare the equilibrium results to the input concentrations in the original sequence.

The specie names along with their associated enthalpy of formation, entropy of formation and heat capacity correlation data are then written to IWRT if IWRAP < 2. Also, the temperature and pressure of the reference state, maximum number of iterations, convergence criterion and the debug, steady-state and solution phase excess free energy correlation options are identified.

The temperature and pressure loops (IOPT = 1 or IOPT = 2) start at line 205. Subroutine STSTCP is called to calculate the standard state chemical potential of each specie. Subroutine ESTMTE is then called to provide an estimate to the equilibrium composition during the first pass through the temperature/pressure loop. Succeeding passes through this loop utilize the equilibrium composition of the preceding pass as an estimate of the current equilibrium composition when ISS = 0.

If the steady state option is activated (ISS > 0) subroutine STEADY inserts as the last pure condensed phase a liquid phase composed of group III and V elements which has a composition determined by the liquidus line of the III-V system at the specified temperature. The total moles of each element present are then calculated based on the initial estimate of the equilibrium composition.

Subroutine IDPTEQ calculates a set of independent reaction formation equations and the equilibrium constants for each of these equations based on the Gibbs Free Energy change associated with each reaction. This result is later compared with equilibrium constants calculated using the "converged" equilibrium compositions to assure that convergence has been attained.

The initial composition estimate, standard chemical potential and elemental abundance vector for each specie along with the amount of each element present in the system are written out if IWRAP < 2. This occurs in lines 244 through 287. Headings for a page containing execution diagnostics are set up in lines 289 through 293 and the standard state chemical potentials are divided by R and T in accord with the derivation in section A.5.

During the first pass through the temperature or pressure loop the total moles of silicon compounds and the group III to group V atom ratio in the vapor phase are calculated in subroutine TOTSI and RATIO. The specie initial concentration along with the total silicon and III-V atom ratio in the vapor are then written to a wrap-up file if IWRAP > 0.

#### A.2.4 Iterative Solution for Equilibrium Composition

The iteration scheme for determining equilibrium compositions is located in lines 313 through 362. Before entering the loop RELMAX and IACFF are initialized to prevent calculation of activity coefficients during the first iteration. If a nonideal solution option is chosen activity coefficients are calculated only after RELMAX has reached a value of less than 0.1. This greatly reduces the chance that the numerical solution will diverge.

At the top of the loop subroutine ADDRMV is called to remove pure condensed phases from the calculation which have compositions of less than  $1.65 \times 10^{-25}$  g-moles. ADDRMV then reinserts one molecule of the pure condensed phase which has the smallest negative incremental Gibbs Free Energy of those which have been removed. Subroutine ACTCOF is called to calculate activity coefficients for each of the species followed by RAND which calculates the change in composition for each specie which will yield a closer approximation to the system equilibrium composition.

A convergence forcer is calculated in subroutine CNVFC. The purpose of the convergence forcer is to assure that negative compositions do not occur and, if IALG = 1, to provide a correction to the predicted composition changes which will help eliminate numerical instabilities. Lines 338 through 341 apply the convergence forcer to update the current estimate of the equilibrium composition. The minimum composition any specie in the vapor or solution phases may attain is set to  $10^{-50}$  g-moles in line 340.

Subroutine RESTOR is called to replace any pure condensed phases which were removed by ADDRMV back into the problem in the original sequence. Subroutines GIBBS and DEBUG provide diagnostic information if IDEBUG > 1.

Lines 352 through 360 test for convergence of the solution. The maximum fractional change of all species with compositions greater than  $10^{-50}$  g-moles over two successive iterations is compared with CNVG. The solution is considered converged if the largest fractional change is less than CNVG.

The iteration process will also be terminated if the maximum number of iterations, MAXIT, is exceeded or if ISTOP = 1. The parameter ISTOP is set to unity if the coefficient matrix in subroutine RAND is found to be algorithmically singular which prohibits the solution of the set of linear equations. A message is printed in line 363 if the numerical solution does not converge.

#### A.2.5 Output of Results

Following the loop for determining the equilibrium compositions subroutine GIBBS is called to calculate the final system Gibbs Free Energy. Lines 369 through 409 then determine mole fractions and chemical potentials for each of the species. Subroutine CALCQ is called to calculate equilibrium constants for the reaction formation equations using the compositions determined by the RAND algorithm. Subroutines TOTSI and RATIO then determine the total silicon concentrations and the group III-V atom ratio in the vapor phase.

The results of the equilibrium calculations are written out in lines 422 through 470 if IWRAP < 2. A wrap-up file is written at line 472 if IWRAP > 0. If a temperature, pressure or composition loop option has been chosen (IOPT > 0) the program jumps to the bottom of this loop at line 553. Otherwise the set of independent formation reaction equations are written out followed by a comparison of the equilibrium constants for these reactions as calculated by the free energy change and the equilibrium compositions.

## A.2.6 Listing of The Main Program

```

1 C MCMPEC.RAND .... MULTICOMPONENT MULTIPHASE EQUILIBRIUM CODE
2 C RAND ALGORITHM
3 C
4 C
5     DOUBLE PRECISION ALEQ(63,63),BLEQ(63),D(13,13),DPRMF(13,13),
6     & DINV(13,13),WKA1(13),WKA(63)
7     DIMENSION A(50,13),A0(50),A1(50),A2(50),A3(50),ACOEFF(50),B(13),
8     & BCALC(50),CHMPT(50),COEFF(6),DELN(50),DG(50),
9     & DTST(50),DHO(50),DSO(50),FRAC(50),FRACIN(50),GNU(50,13)
10    & ICP(50),IDXBAS(50),INERT(3),Q(50),STDCP(50),TOTMC(50)
11    INTEGER ISPCE(50,3),PHASE(50,3),SPECIE(50,3),STRING(6,4),
12    & TITLE(20),V,S,C,E,VP1,VPS,VPSP1,VSC,VSC,EPCP2,
13    & ELMNT(13)/13*' '/*,VAPOR(3)/* 'V','APO','R '/*,
14    & SOLN(3)/*SOL','UTI','ON '/*,COND(3)/*CON','DEN','SED'/*,
15    & RSPS/' ' + '/*,RPAS/' ' <= '/*,RPBL/' ' '/*,SSPS/' ' + '/*,
16    & BLNKS/' ' /*,LP/' ' (/*
17    REAL N(50),KEQ(50),NV,NS,LAMBDA
18 C
19 C A(I,J) : ELEMENTAL ABUNDANCE MATRIX
20 C B(J) : TOTAL NUMBER OF GRAM-MOLES OF ELEMENT J
21 C DHO(I) : ENTHALPY OF FORMATION OF SPECIES I
22 C DSO(I) : ENTROPY OF FORMATION OF SPECIES I
23 C STDCP(I) : STANDARD CHEMICAL POTENTIAL OF SPECIES I
24 C
25 C ***** HEAT CAPACITY CORRELATIONS *****
26 C ICP(I)=0 : CP(I) = A0(I) + A1(I)*T + A2(I)/T**2 + A3(I)*ALOG(T)
27 C ICP(I)=1 : CP(I) = A0(I) + A1(I)*T + A2(I)*T**2 + A3(I)*T**3
28 C
29 C *****
30 C * DOUBLE PRECISION IS USED IN THE MATRIX ROUTINE LEQ1F *
31 C *****
32 C
33     IRD=5
34     IWRT=6
35     IFILE=2
36     IDIM1=50
37     IDIM2=13
38     IDIM3=IDIM1+IDIM2
39 C
40 C SUPPRESS PRINTING OF OVERFLOW, UNDERFLOW, DIVIDE BY ZERO
41 C AND EXPONENTIAL ARGUMENT ERROR MESSAGES
42 C
43     CALL ERRSET(207,0,-1,0,0,209)
44     CALL ERRSET(252,0,-1,0,0,253)
45 C
46 C READ TITLE
47 C
48     READ(IRD,5) (TITLE(K),K=1,20)
49     5 FORMAT(20A4)
50 C
51 C NUMBER OF ELEMENTS, VAPOR SPECIES, SOLUTION SPECIES,
52 C CONDENSED PURE PHASES, SYSTEM TEMPERATURE (K) AND PRESSURE (PA)
53 C
54     READ(IRD,10) E,V,S,C,T,P,TO,PO

```

```

55     10 FORMAT(4I5,4F10.0)
56     IF(V.EQ.0) WRITE(IWRT,11) V
57     11 FORMAT('0',50('*'),/,1X,'PROBLEM CANNOT BE SOLVED USING THE ',
58     &'RAND ALGORITHM',/,1X,'NUMBER OF VAPOR PHASE SPECIES = ',I2,
59     &/,1X,50('*'))
60     IF(V.EQ.0) GO TO 3000
61     VP1=V+1
62     VPS=V+S
63     VPSP1=V+S+1
64     VSC=V+S+C
65     VSCE=V+S+C+E
66     EPCP2=E+C+2
67     IF(S.EQ.0) EPCP2=E+C+1
68 C
69 C READ ELEMENTS
70 C
71     READ(IRD,15) (ELMNT(J),J=1,E)
72     15 FORMAT(13(1X,A2))
73 C
74 C VAPOR SPECIES INFORMATION
75 C
76     DO 110 I=1,V
77     READ(IRD,20) (SPECIE(I,K),K=1,3),DH0(I),DS0(I)
78     READ(IRD,21) A0(I),A1(I),A2(I),A3(I),ICP(I)
79     READ(IRD,22) (A(I,J),J=1,E)
80     20 FORMAT(3A4,2E12.5)
81     21 FORMAT(4E12.5,I2)
82     22 FORMAT(13(F5.0,1X))
83     DO 110 J=1,3
84     PHASE(I,J)=VAPOR(J)
85     110 CONTINUE
86 C
87 C INERT VAPOR SPECIE DATA
88 C
89     READ(IRD,20) (INERT(K),K=1,3),DH0Z,DS0Z
90     READ(IRD,21) A0Z,A1Z,A2Z,A3Z,ICPZ
91     READ(IRD,22) IDUMMY
92 C
93 C SOLUTION SPECIES INFORMATION
94 C
95     IF(S.EQ.0) GO TO 125
96     DO 120 I=VP1,VPS
97     READ(IRD,20) (SPECIE(I,K),K=1,3),DH0(I),DS0(I)
98     READ(IRD,21) A0(I),A1(I),A2(I),A3(I),ICP(I)
99     READ(IRD,22) (A(I,J),J=1,E)
100    DO 120 J=1,3
101    PHASE(I,J)=SOLN(J)
102    120 CONTINUE
103    125 CONTINUE
104 C
105 C CONDENSED PHASE DATA
106 C
107     IF(C.EQ.0) GO TO 135
108     DO 130 I=VPSP1,VSC

```

```

109      READ(IRD,20) (SPECIE(I,K),K=1,3),DH0(I),DS0(I)
110      READ(IRD,21) A0(I),A1(I),A2(I),A3(I),ICP(I)
111      READ(IRD,22) (A(I,J),J=1,E)
112      DO 130 J=1,3
113      PHASE(I,J)=COND(J)
114 130 CONTINUE
115 135 CONTINUE
116 C
117 C MAXIMUM NUMBER OF ITERATIONS, CONVERGENCE CRITERION AND OPTIONS
118 C
119      READ(IRD,136) IDEBUG,IOPT,ISS,IWRAP,MAXIT,NMAX,CNVG,TINC,PINC
120 136 FORMAT(6I5,3F10.0)
121      IF(IWRAP.EQ.3) IFILE=IWRIT
122 C
123 C SET THE LOOP LIMITS FOR THE TEMPERATURE, PRESSURE AND COMPOSITION
124 C LOOPS. THE COMPOSITION LOOP STARTS HERE
125 C
126      NCMP=1
127      NTP=1
128      IF(IOPT.EQ.1.OR.IOPT.EQ.2) NTP=NMAX
129      IF(IOPT.EQ.3) NCMP=NMAX
130      DO 2000 ICM=1,NCMP
131 C
132 C TOTAL NUMBER OF MOLES OF VAPOR AND MOLE FRACTIONS
133 C
134      READ(IRD,137) TOTMV
135      READ(IRD,137) (FRACIN(I),I=1,V),FRCZIN
136 137 FORMAT(6E12.5)
137 C
138 C TOTAL NUMBER OF MOLES OF SOLUTION SPECIES, MOLE FRACTIONS
139 C AND EXCESS FREE ENERGY CORRELATION PARAMETERS
140 C
141      IF(S.EQ.0) GO TO 139
142      READ(IRD,137) TOTMS
143      READ(IRD,137) (FRACIN(I),I=VP1,VPS)
144      READ(IRD,138) IXSCOR,AXS,BXS
145 138 FORMAT(15,2E12.5)
146 139 CONTINUE
147 C
148 C TOTAL NUMBER OF MOLES IN PURE CONDENSED PHASES
149 C
150      IF(C.EQ.0) GO TO 140
151      READ(IRD,137) (TOTMC(I),I=VPSP1,VSC)
152 140 CONTINUE
153 C
154 C SAVE THE ORIGINAL SPECIE ORDER SO THAT THE PROBLEM CAN BE PLACED
155 C IN THIS ORDER IF ANY PURE CONDENSED PHASES ARE REMOVED OR SHIFTED
156 C
157      DO 165 I=1,VSC
158      DO 165 K=1,3
159      ISPCE(I,K)=SPECIE(I,K)
160 165 CONTINUE
161      IF(ICMP.GT.1.OR.IWRAP.EQ.3) GO TO 187
162 C

```

```

163 C WRITE-OUT SOME OF THE INPUT DATA
164 C
165     IPAGE=1
166     WRITE(IWRT,400) (TITLE(K),K=1,20),IPAGE
167     WRITE(IWRT,410) T,P
168     IF(IWRAP.GT.1) GO TO 187
169     WRITE(IWRT,170)
170 170 FORMAT('0',/,1X,T55,'HEAT CAPACITY CORRELATION COEFFICIENTS',
171           &/,1X,T16,'ENTHALPY OF',T33,'ENTROPY OF',T58,'ICP=0: CP = A0',
172           &' + A1*T + A2/T**2 + A3*LN(T)',/,1X,T17,'FORMATION',T33,'FORMAT',
173           &'ION',T58,'ICP=1: CP = A0 + A1*T + A2*T**2 + A3*T**3',/,1X,T4,
174           &'SPECIE',T20,'DH0',T37,'DS0',T54,'A0',T73,'A1',T93,'A2',T113,
175           &'A3',T122,'ICP',/,1X,T4,'SYMBOL',T15,'(KCAL/G-MOLE)',T30,
176           &'(KCAL/G-MOLE-K)',T47,'(KCAL/G-MOLE-K)',T65,'(KCAL/G-MOLE-K**2)',
177           &T86,'(.....)',T106,'(.....)',T122,'(-)',
178           &/,+',.12(' '),T15,13(' '),T30,15(' '),T47,15(' '),
179           &T65,18(' '),T86,15(' '),T106,15(' '),T122,3(' '))
180     DO 180 I=1,VSC
181     WRITE(IWRT,175) (SPECIE(I,K),K=1,3),DH0(I),DS0(I),A0(I),A1(I),
182           &           A2(I),A3(I),ICP(I)
183 175 FORMAT(1X,3A4,T17,F9.3,T33,F9.6,T50,F9.6,T68,E12.5,T88,E12.5,
184           &T108,E12.5,T123,I1)
185     IF(I.EQ.V) WRITE(IWRT,175) (INERT(K),K=1,3),DH0Z,DS0Z,A0Z,A1Z,
186           &           A2Z,A3Z,ICPZ
187 180 CONTINUE
188     WRITE(IWRT,184) T0,P0,MAXIT,CNMG,IDEBUG
189 184 FORMAT('0',/,'0',T10,'THE ENTHALPY AND ENTROPY OF FORMATION ',
190           &'REFERENCE TEMPERATURE AND PRESSURE ARE:',5X,'T0 = ',F6.1,' K',
191           &5X,'P0 = ',F9.1,' PA',/,',0',T35,'MAXIMUM NUMBER OF ITERATIONS ',
192           &'ALLJWD = ',I5,/,',0',T50,'CONVERGENCE CRITERION = ',E12.4,
193           &/,',0',T48,'OUTPUT PARAMETER IDEBUG = ',I2)
194     IF(S.GT.1) WRITE(IWRT,185) IXSCOR,AXS,BXS
195 185 FORMAT('0','EXCESS FREE ENERGY CORRELATION :',2X,'IXSCOR = ',
196           &           I5.5X,'AXS = ',E12.5,5X,'BXS = ',E12.5)
197     IF(ISS.GT.0) WRITE(IWRT,186) ISS
198 186 FORMAT('0',T24,'ISS= ',I2,' THE III-V LIQUID SOLUTION IS AT ',
199           &'EQUILIBRIUM WITH THE III-V STOICHIOMETRIC SOLID')
200 187 CONTINUE
201 C
202 C CALCULATE THE STANDARD STATE CHEMICAL POTENTIALS
203 C AND AN INITIAL ESTIMATE OF THE EQUILIBRIUM COMPOSITION
204 C
205     DO 2000 ITP=1,NTP
206     IF(IOPT.EQ.1.AND.)ITP.GT.1) T=T+TINC
207     IF(IOPT.EQ.2.AND.)ITP.GT.1) P=P+PINC
208     CALL STSTCP(A0,A1,A2,A3,A0Z,A1Z,A2Z,A3Z,DH0,DS0,DH0Z,DS0Z,
209           &           STDCP,STDCPZ,ICP,ICPZ,T0,T,IDIMI,V,S,C)
210     IF(ITP.GT.1.AND.ISS.EQ.0) GO TO 195
211     DO 190 I=1,VPS
212     FRAC(I)=FRACIN(I)
213 190 CONTINUE
214     FRACZ=FRCZIN
215     CALL ESTMTE(TOTMV,TOTMS,TOTMC,FRAC,N,FRACZ,ZV,
216           &           IDIMI,V,S,C)

```

```

217 195 CONTINUE
218 C
219 C SOURCE ZONE STEADY-STATE LIQUID COMPOSITION MODEL
220 C
221     IF(ISS.GT.0) CALL STEADY(SPECIE,A,STDCP,ELMNT,XIII,T,TO,V,S,C,
222     & IDIM1,IDIM2,ISS,IWRT)
223 C
224 C CALCULATE THE TOTAL GRAM-MOLES OF EACH ELEMENT
225 C BASED ON THE INITIAL COMPOSITION ESTIMATES IN THE PHASES
226 C
227     DO 200 J=1,E
228     BCALC(J)=0.
229     DO 200 I=1,VSC
230     BCALC(J)=A(I,J)*N(I)+BCALC(J)
231     B(J)=BCALC(J)
232 200 CONTINUE
233 C
234 C DETERMINE A SET OF INDEPENDENT REACTION EQUATIONS,
235 C THE GIBBS FREE ENERGY CHANGE FOR THESE REACTIONS
236 C AND THE REACTION EQUILIBRIUM CONSTANTS
237 C
238     RT=0.0019872*T
239     CALL IDPTEQ(A,D,OPRME,DINV,STDCP,GNU,IDXBAS,KEQ,WKA1,DG,
240     & RT,IDIM1,IDIM2,V,S,C,E,IWRT)
241     IF(IWRAP.GT.1) GO TO 476
242     IF(ITP.GT.1) GO TO 472
243 C
244 C WRITE-OUT THE INITIAL COMPOSITION ESTIMATES, STANDARD STATE
245 C CHEMICAL POTENTIALS AND THE ELEMENTAL ABUNDANCE MATRIX
246 C
247     IPAGE=IPAGE+1
248     WRITE(IWRT,400) (TITLE(K),K=1,20),IPAGE
249 400 FORMAT('1',/, '0',T38,'RAND ALGORITHM FOR DETERMINING ',
250     & 'EQUILIBRIUM COMPOSITIONS',/, '0',T30,20A4,T120,
251     & 'PAGE ',I2)
252     WRITE(IWRT,410) T,P
253 410 FORMAT('0',T43,'TEMPERATURE = ',F6.1,' K',5X,'PRESSURE = ',F12.5,
254     & ' PA')
255     WRITE(IWRT,420) (ELMNT(K),K=1,13)
256 420 FORMAT('0',/,T48,'INPUT DATA AND INITIAL COMPOSITION ESTIMATES',
257     &/, '0',T29,'INITIAL',T43,'STANDARD',/,1X,T27,'COMPOSITION',
258     &T43,'CHEMICAL',/,1X,T4,'SPECIE',T29,'ESTIMATE',T42,'POTENTIAL',
259     &T72,'ELEMENTAL ABUNDANCE MATRIX',/,1X,T4,'SYMBOL',T17,'PHASE',
260     &T28,'(G-MOLES)',T40,'(KCAL/G-MOLE)',T55,13(A2,4X),/, '+',
261     &12(' '),T15,9(' '),T25,14(' '),T40,13(' '),T55,78(' '))
262     DO 440 I=1,VSC
263     WRITE(IWRT,430) (SPECIE(I,K),K=1,3),(PHASE(I,K),K=1,3),N(I),
264     & STDCP(I),(A(I,J),J=1,E)
265 430 FORMAT(1X,3A4,T15,3A3,T25,E14.7,T42,F9.3,T55,13(F5.3,1X))
266     IF(I.EQ.V) WRITE(IWRT,430) (INERT(K),K=1,3),
267     & (PHASE(I,K),K=1,3),ZV,STDCPZ
268 440 CONTINUE
269     IF(ISS.GT.0) WRITE(IWRT,445) XIII
270 445 FORMAT(4X,'X=' ,F6.4)

```

```

271      WRITE(IWRT,450)
272 450 FORMAT('0',/, '0',T44,'TOTAL GRAM-MOLES OF EACH ELEMENT FROM IN',
273 &      'PUT DATA',/,1X,T40,'AND AS CALCULATED FROM THE INITIAL',
274 &      'COMPOSITION ESTIMATES',/, '0',4(4X,'INPUT DATA',3X,
275 &      'CALCULATED',5X))
276      NPRT=E/4
277      NCHK=NPRT*4
278      IF(NCHK.NE.E) NPRT=NPRT+1
279      ISTRT=1
280      DO 470 K=1,NPRT
281      NEND=ISTRT+3
282      IF(NEND.GT.E) NEND=E
283      WRITE(IWRT,460) (ELMNT(J),B(J),BCALC(J),J=ISTRT,NEND)
284 460 FORMAT(1X,4(A2,1X,E12.5,1X,E12.5,4X))
285      ISTRT=NEND+1
286 470 CONTINUE
287 472 CONTINUE
288      IPAGE=IPAGE+1
289      WRITE(IWRT,400) (TITLE(K),K=1,20),IPAGE
290      WRITE(IWRT,410) T,P
291      WRITE(IWRT,475)
292 475 FORMAT('0',T58,'EXECUTION DIAGNOSTICS',/, '+',T58,9('_','),1X,
293 &      '11('_','),/, '0')
294 476 CONTINUE
295 C
296 C   DIVIDE THE STANDARD STATE CHEMICAL POTENTIALS BY RT
297 C
298      DO 480 I=1,VSC
299      STDCP(I)=STDCP(I)/RT
300 480 CONTINUE
301      STDCPZ=STDCPZ/RT
302 C
303 C   CALCULATE THE TOTAL SILICON AND THE III/V RATIO IN THE VAPOR
304 C   AND WRITE-OUT THE INITIAL RESULTS TO THE WRAPUP FILE
305 C
306      IF(ITP.GT.1) GO TO 485
307      CALL TOTS1(A,ELMNT,FRAC,N,SITOT,SIMF,IDIM1,IDIM2,V,E)
308      CALL RATIO(A,ELMNT,FRAC,R1IIV,IDIM1,IDIM2,V,E)
309      IF(IWRAP.GT.0) CALL WRAPUP(TITLE,SPECIE,INERT,N,FRAC,ZV,FRACZ,
310 &      SITOT,SIMF,R1IIV,CNMG,CNMG,ISS,XIII,
311 &      T,P,IDATA,IDIM1,IFILE,V,VSC)
312 485 CONTINUE
313 C
314 C   ITERATIVE SOLUTION FOR THE EQUILIBRIUM COMPOSITIONS
315 C
316      RELMAX=100.0
317      IACFF=0
318      DO 600 I=1,MAXIT
319      ITER=I
320 C
321 C   REMOVE OR ADD PURE CONDENSED PHASES INTO THE CALCULATION
322 C   BASED ON THEIR INCREMENTAL GIBBS FREE ENERGIES
323 C
324      CALL ADDRNV(A,N,DGTST,STDCP,BLEQ,SPECIE,DELN,VPSP1,VSC,F,C,

```

```

325      E          EPCP2, IOUT, IDIM1, IDIM2, IDIM3)
326      CALL ACTCOF(N, ACOEF, ZACT, IDIM1, IXSCOR, AXS, BXS, T, V, S, C, IACFF,
327      E          RELMAX)
328      CALL RAND(A, S, BCALC, N, DELN, STDCP, ALEQ, BLEQ, WKA, ACOEF,
329      E          ZACT, V, S, C, E, VSC, EPCP2, IDIM1, IDIM2, IDIM3, ITER, PO, P, ZV,
330      E          ISTOP, IWRT, IDEBUG, IWRAP)
331 C
332 C   CALCULATE THE CONVERGENCE FORCER
333 C   AND THE NEW ESTIMATE TO THE EQUILIBRIUM COMPOSITION
334 C
335      IALG=1
336      CALL CNVFRG(STDCP, N, DELN, ACOEF, V, S, C, IDIM1, IALG, ZV,
337      E          P, PO, RT, LAMBDA, ITER, IWRT)
338      DO 510 II=1, VSC
339      N(II)=N(II)+LAMBDA*DELN(II)
340      IF(II.LT.VPS.AND.N(II).LE.1.0E-50) N(II)=1.0E-50
341 510 CONTINUE
342 C
343 C   RESTORE THE CONSTANTS AND ARRAYS TO THE ORIGINAL PROBLEM FORMULATION
344 C   (THIS UNDOES THE SHIFTING DONE IN SUBROUTINE ADDRNV)
345 C
346      CALL RESTOR(A, SPECIE, ISPCE, STDCP, N, DELN, IDIM1, IDIM2, VSC,
347      E          EPCP2, C, VPSP1, E, IOUT)
348      IF(IDEBUG.GE.1) CALL GIBBS(N, STDCP, STDCPZ, ACOEF, ZACT, ZV, T, P, PO,
349      E          IDIM1, V, S, C, GFE)
350      IF(IDEBUG.GE.1) CALL DEBUG(N, DELN, DGTST, VSC, IDIM1, ITER, LAMBDA,
351      E          GFE, RELMAX, IWRT)
352 C
353 C   CHECK FOR CONVERGENCE OF THE EQUILIBRIUM COMPOSITIONS
354 C
355      RELMAX=0.
356      DO 520 II=1, VSC
357      IF(N(II).GT.0.0) RELERR=DELN(II)/N(II)
358      IF(ABS(RELERR).GT.RELMAX.AND.N(II).GT.1.0E-50)
359      E          RELMAX=ABS(RELERR)
360 520 CONTINUE
361      IF(RELMAX.LT.CNVG.OR.ISTOP.EQ.1) GO TO 610
362 600 CONTINUE
363      IF(IWRAP.LT.3) WRITE(IWRT, 605) MAXIT
364 605 FORMAT('0', '***** AFTER ', I5, ' ITERATIONS THE EQUILIBRIUM ',
365      E 'COMPOSITION DID NOT CONVERGE')
366 610 CONTINUE
367      CALL GIBBS(N, STDCP, STDCPZ, ACOEF, ZACT, ZV, T, P, PO, IDIM1, V, S, C, GFE)
368 C
369 C   CALCULATE NV, NS, MOLE FRACTIONS, AND THE CHEMICAL POTENTIALS
370 C
371      NV=ZV
372      DO 800 I=1, V
373      NV=NV+N(I)
374 800 CONTINUE
375      NS=0.
376      IF(S.EQ.0) GO TO 815
377      DO 810 I=VP1, VPS
378      NS=NS+N(I)

```

```

379      810 CONTINUE
380      815 CONTINUE
381          DO 820 I=1,V
382          CHMPT(I)=0.
383          FRAC(I)=N(I)/NV
384          ARG=ACDEF(I)*FRAC(I)
385          IF(ARG.LT.1.0E-50) ARG=1.0E-50
386          CHMPT(I)=RT*(STDCP(I)+ALOG(ARG))
387      820 CONTINUE
388          IF(S.EQ.0) GO TO 835
389          DO 830 I=VP1,VPS
390          CHMPT(I)=0.
391          FRAC(I)=N(I)/NS
392          ARG=ACDEF(I)*FRAC(I)
393          IF(ARG.LT.1.0E-50) ARG=1.0E-50
394          CHMPT(I)=RT*(STDCP(I)+ALOG(ARG))
395      830 CONTINUE
396      835 CONTINUE
397          IF(C.EQ.0) GO TO 845
398          DO 840 I=VPSP1,VSC
399          FRAC(I)=1.
400          IF(N(I).LT.1.0E-50) FRAC(I)=0.0
401          CHMPT(I)=STDCP(I)*RT
402      840 CONTINUE
403      845 CONTINUE
404          FRACZ=ZV/NV
405          DZV=0.
406          CHMPTZ=0.
407          IF(FRACZ.LE.0.0) GO TO 850
408          CHMPTZ=(STDCPZ+ALOG(ZACT*FRACZ))*RT
409      850 CONTINUE
410 C
411 C   CALCULATE THE EQUILIBRIUM CONSTANTS FROM COMPOSITION
412 C
413         CALL CALCO(GNU,N,ACDEF,FRAC,IDXBAS,Q,
414         &          P,P0,V,S,C,E, IDIM1, IDIM2)
415 C
416 C   CALCULATE THE TOTAL SILICON AND THE III/V RATIO IN THE VAPOR
417 C
418         CALL TOTSI(A,ELMNT,FRAC,N,SITOT,SIMF, IDIM1, IDIM2,V,E)
419         CALL RATIO(A,ELMNT,FRAC,RIIIIV, IDIM1, IDIM2,V,E)
420         IF(IWRAP.GT.1) GO TO 971
421 C
422 C   WRITE-OUT THE RESULTS
423 C
424         IPAGE=IPAGE+1
425         WRITE(IWRT,400) (TITLE(K),K=1,20),IPAGE
426         WRITE(IWRT,410) T,P
427         WRITE(IWRT,900) ITER,GFE,RELMAX,CNVG,LAMBDA
428      900 FORMAT('0',/,1X,T45,'EQUILIBRIUM COMPOSITIONS AFTER ',I5,
429         & ' ITERATIONS',/, '0',T42,'SYSTEM GIBBS FREE ENERGY = ',E14.7,
430         & ' (KCAL)',
431         & /, '0', 'RELATIVE ERROR = ',E12.5,5X, 'CONVERGENCE CRITERION = ',
432         & E12.5,5X, 'RELAXATION PARAMETER AT LAST ITERATION = ',E12.5,

```

```

433      & /,'0',T57,'ESTIMATED',/,1X,T25,'EQUILIBRIUM',T39,'EQUILIBRIUM',
434      & T56,'COMPOSITION',T92,'CHEMICAL',
435      & /,1X,T4,'SPECIE',T29,'MOLE',T39,'COMPOSITION',T56,
436      & 'UNCERTAINTY',T91,'POTENTIAL',T109,'ACTIVITY',
437      & /,1X,T4,'SYMBOL',T17,'PHASE',T27,'FRACTION',T40,'(G-MOLES)',
438      & T57,'(G-MOLES)',T90,'(KCAL/G-MOLE)',T107,'COEFFICIENT',
439      & /,'+',12(' '),T15,9(' '),T25,12(' '),T37,14(' '),T54,
440      & 14(' '),T89,14(' '),T106,12(' '))
441      DO 920 I=1,VSC
442      WRITE(IWRT,910) (SPECIE(I,K),K=1,3),(PHASE(I,K),K=1,3),FRAC(I),
443      & N(I),DELN(I),CHMPT(I),ACDEF(I)
444      910 FORMAT(1X,3A4,T15,3A3,T24,E12.5,T37,E14.7,T54,E14.7,T92,F9.3,
445      & T106,E12.5)
446      IF(I.EQ.V) WRITE(IWRT,910) (INERT(K),K=1,3),(PHASE(I,K),K=1,3),
447      & FRACZ,ZV,DZV,CHMPTZ,ZACT
448      920 CONTINUE
449      IF(ISS.GT.0) WRITE(IWRT,445) XIII
450      WRITE(IWRT,930) SIMF
451      930 FORMAT('0',T35,'MOLE FRACTION OF SILICON SPECIES IN ',
452      & 'VAPOR PHASE = ',E12.5)
453      WRITE(IWRT,940) RIIIIV
454      940 FORMAT('0',T50,'III/V RATIO IN THE VAPOR PHASE = ',F9.4)
455      WRITE(IWRT,950)
456      950 FORMAT('0',/,'0',T44,'TOTAL GRAM-MOLES OF EACH ELEMENT FROM IN',
457      & 'PUT DATA',/,1X,T42,'AND AS CALCULATED FROM THE EQUILIBRIUM',
458      & ' COMPOSITIONS',/,'0',4(4X,'INPUT DATA',3X,
459      & 'CALCULATED',5X))
460      NPRT=E/4
461      NCHK=NPRT*4
462      IF(NCHK.NE.E) NPRT=NPRT+1
463      ISTRT=1
464      DO 970 K=1,NPRT
465      NEND=ISTRT+3
466      IF(NEND.GT.E) NEND=E
467      WRITE(IWRT,960) (ELMNT(J),B(J),BCALC(J),J=ISTRT,NEND)
468      960 FORMAT(1X,4(A2,1X,E12.5,1X,E12.5,4X))
469      ISTRT=NEND+1
470      970 CONTINUE
471      971 CONTINUE
472      IF(IWRAP.GT.0) CALL WRAPUP(TITLE,SPECIE,INERT,N,FRAC,ZV,FRACZ,
473      & SITOT,SIMF,RIIIIV,RELMAX,CNVG,ISS,XIII,T,P,I0DATA,IDIM1,IFILE,
474      & V,VSC)
475      IF((ITP.GT.1.OR.ICMP.GT.1.OR.IWRAP.GT.1) GO TO 1900
476 C
477 C WRITE-OUT THE INDEPENDENT EQUATIONS
478 C
479      IPAGE=IPAGE+1
480      WRITE(IWRT,400) (TITLE(K),K=1,20), IPAGE
481      WRITE(IWRT,410) T,P
482      WRITE(IWRT,980)
483      980 FORMAT('0',T38,'A SET OF INDEPENDENT REACTION EQUATIONS FOR ',
484      & ' THIS SYSTEM IS AS FOLLOWS:',/,'0')
485      DO 1100 I=1,VSC
486 C

```

```

487 C DETERMINE THE NUMBER OF BASIS SPECIES IN EACH FORMATION REACTION
488 C
489     NSPEC=0
490     DO 990 K=1,E
491     IF(I.EQ.IDXBAS(K)) GO TO 1100
492     IF(ABS(GNU(I,K)).LT.1.0E-6) GO TO 990
493     NSPEC=NSPEC+1
494 990 CONTINUE
495 C
496 C FILL THE CHARACTER ARRAY "STRING" WITH THE FORMATION REACTION SPECIES
497 C
498     NLOOP=1
499     IF(NSPEC.GT.4) NLOOP=FLOAT(NSPEC)/4.0+0.9
500     DO 1000 K=1,3
501     STRING(1,K)=SPECIE(I,K)
502 1000 CONTINUE
503     STRING(1,4)=RPAS
504     COEFF(1)=1.0
505     IST=1
506     ICNT=0
507     DO 1060 ILOOP=1,NLOOP
508     NCNT=NSPEC-ICNT+1
509     IF(NCNT.GT.5) NCNT=5
510     DO 1020 IDX=2,NCNT
511     ICNT=ICNT+1
512     DO 1015 IBASE=IST,E
513     IF(ABS(GNU(I,IBASE)).LT.1.0E-6) GO TO 1015
514     IDXB=IDXBAS(IBASE)
515     DO 1010 K=1,3
516     STRING(IDX,K)=SPECIE(IDXB,K)
517 1010 CONTINUE
518     COEFF(IDX)=GNU(I,IBASE)
519     STRING(IDX,4)=RPSPS
520     GO TO 1018
521 1015 CONTINUE
522 1018 IST=IBASE+1
523 1020 CONTINUE
524     STRING(NCNT,4)=RPBL
525     IF(ILOOP.EQ.1) WRITE(IWRT,1040)(LP,COEFF(IJK),
526     & (STRING(IJK,K),K=1,4),IJK=1,NCNT)
527 1040 FORMAT('0',A1,F5.2,4A4,4(A1,E10.3,4A4))
528     IF(ILOOP.GT.1) WRITE(IWRT,1050) SSPTS,(LP,COEFF(IJK),
529     & (STRING(IJK,K),K=1,4),IJK=2,NCNT)
530 1050 FORMAT(1X,T20,A4,4(A1,E10.3,4A4))
531 1060 CONTINUE
532 1100 CONTINUE
533 C
534 C WRITE-OUT A COMPARISON BETWEEN THE EQUILIBRIUM CONSTANTS
535 C AS CALCULATED BY THE GIBBS FREE ENERGY CHANGE AND BY COMPOSITION
536 C
537     IPAGE=IPAGE+1
538     WRITE(IWRT,400) (TITLE(K),K=1,20), IPAGE
539     WRITE(IWRT,410) T,P
540     WRITE(IWRT,1110)

```

```
541 1110 FORMAT('0'./,1X,T40,'EQUILIBRIUM CONSTANTS FOR THE INDEPENDENT',
542 6' REACTIONS'./,'0'.T20,'GIBBS FREE ENERGY CHANGE'.T47,
543 6'EQUILIBRIUM CONSTANT'.T73,'EQUILIBRIUM CONSTANT'./,1X,
544 6'REACTION PRODUCT'.T25,'(KCAL/G-MOLE)'.T46,'FROM GIBBS FREE ',
545 6'ENERGY'.T70,'FROM PREDICTED COMPOSITION'./,'+'.16('_').T20,
546 624('_').T46,22('_').T70,26('_'))
547 DO 1200 I=1,VSC
548 WRITE(IWRT,1120) (SPECIE(I,K),K=1,3),DG(I),KEQ(I),Q(I)
549 1120 FORMAT(1X,3A4,T28,F8.3,T51,E12.5,T77,E12.5)
550 1200 CONTINUE
551 IF(ISS.GT.0) WRITE(IWRT,445) XIII
552 1900 IF(ISTOP.EQ.1) GO TO 3000
553 2000 CONTINUE
554 3000 STOP
555 END
```

### A.3 A Description of the Major Variables in MCMPEC.RAND

Variables which are used in the IMSL subroutines LINVIF, LEQTIF, LUDATF and LUELMF are not included in this list. FORTRAN default typing applies unless otherwise specified.

<u>Variable</u>	<u>Description</u>	<u>Units</u>
A (I,J)	elemental abundance matrix	$\frac{\text{atoms of element } j}{\text{molecule of specie } i}$
ACOE (I)	activity coefficient of specie i	-
ALEQ (I, J)	matrix containing coefficients in the RAND algorithm	variable
AMAX	maximum value the convergence forcer may attain	-
AMIN	minimum value the convergence forcer may attain	-
AXS	activity coefficient correlation parameter	variable
A0 (I)	heat capacity correlation parameter	kcal/g-mole-K
A1 (I)	heat capacity correlation parameter	kcal/g-mole-K <sup>2</sup>
A2 (I)	heat capacity correlation parameter	variable
A3 (I)	heat capacity correlation parameter	variable
A0Z	inert specie heat capacity correlation parameter	kcal/g-mole-K
A1Z	inert specie heat capacity correlation parameter	kcal/g-mole-K <sup>2</sup>
A2Z	inert specie heat capacity correlation parameter	variable
A3Z	inert specie heat capacity correlation parameter	variable

<u>Variable</u>	<u>Description</u>	<u>Units</u>
B (J)	moles of element J specified in the system	g-moles
BCALC (J)	moles of element J as calculated by algorithm	g-moles
BK (J)	same as BCALC (J)	g-moles
BLEQ (I)	vector containing the right-hand-side of the RAND algorithm	variable
BXS	activity coefficient correlation parameter	variable
C	number of pure condensed phases (integer)	-
CHMPT (I)	chemical potential of specie i	kcal/g-mole
CHMPTZ	chemical potential of the inert	kcal/g-mole
CNVG	composition convergence criterion	-
COND (3)	vector containing the character string 'CONDENSED'	-
D (I, J)	matrix of basis species	$\frac{\text{atoms of } j}{\text{molecule of } i}$
DELH	total enthalpy change	kcal/g-mole
DELN (I)	change in moles of specie i	g-mole
DELS	total entropy change	kcal/g-mole-K
DG (I)	Gibbs Free Energy change of reaction i	kcal/g-mole
DGDL	change in system Gibbs Free Energy with respect to the convergence forcer	kcal/g-mole

<u>Variable</u>	<u>Description</u>	<u>Units</u>
DGTST (I)	incremental change in Gibbs free energy for specie i	kcal/g-mole
DHO (I)	enthalpy of formation of specie i	kcal/g-mole
DHOZ	enthalpy of formation of the inert specie	kcal/g-mole
DINV (I, J)	inverse of matrix D	-
DPRME (I, J)	Gram-Schmidt orthogonalization of matrix D	-
DSO (I)	entropy of formation of specie i	kcal/g-mole-K
DSOZ	entropy of formation of the inert specie	kcal/g-mole-K
E	number of elements in the system (integer)	-
ELIII (K)	vector containing character string of group III elements	-
ELMNT (J)	vector containing character strings of the elements present in the system	-
ELV (K)	vector containing character strings of group V element	-
EPCP2	$E + C + 2$ (integer)	-
EP3	$E + 3$ (integer)	-
EP3PC	$E + 3 + C$ (integer)	-
FRAC (I)	mole fraction of specie i in its phase	-
FRACZ	mole fraction of inert in the vapor	-

<u>Variable</u>	<u>Description</u>	<u>Units</u>
GNU (I, J)	formation reaction coefficient matrix	g-mole
GFE	Gibbs Free Energy of the system	kcal/g-mole
GSTAR	GFE divided by RT	-
IACFF	activity coefficient switch	-
IALG	convergence forcer algorithm switch	-
ICMP	index for the composition loop	-
ICP (I)	heat capacity correlation parameter	-
IDATA	switch used with the wrap-up file	-
IDGT	number of significant figures in each matrix element	-
IDIM1	maximum number of species allowed in system	-
IDIM2	maximum number of elements allowed in system	-
IDIM3	IDIM1 + IDIM2	-
IDEBUG	option to aid in trouble-shooting	-
IDXBAS (J)	vector containing the index of each basis specie	-
IFILE	logical unit designator of the wrap-up file	-
INERT (3)	vector containing the inert specie name	-

<u>Variable</u>	<u>Description</u>	<u>Units</u>
IOPT	parameter to allow various computational options	-
IOUT	number of pure condensed phases removed by subroutine ADDR MV	-
IRD	logical unit designator for data input	-
ISPCE (I, J)	array containing the original specie order	-
ISS	steady state option parameter	-
ISTOP	switch which halts the computation if problems develop	-
ITER	current iteration number in the equilibrium calculation	-
ITP	index for the temperature and pressure loop	-
ITST	parameter which indicates linear dependence in the basis specie matrix	-
IWRAP	switch used with the wrap-up file	-
IWRT	logical unit designator for data output	-
IXSCOR	parameter which chooses the solution phase activity coefficient model	-
KEQ (I)	equilibrium constant for formation reaction i as calculated from the Gibbs Free Energy change (real)	-
LAMBDA	convergence forcer (real)	-
MAXIT	maximum number of iterations to be used	-
N (I)	moles of specie i (real)	g-moles
NMAX	total number of loops to be made in the composition or temperature and pressure loops	-

<u>Variable</u>	<u>Description</u>	<u>Units</u>
NS	total moles in solution (real)	g-moles
NSPEC	number of species in the formation reaction	-
NV	total moles in the vapor (real)	g-moles
P	system pressure	Pa
PHASE (I, 3)	matrix containing a character string to denote the phase of each specie	-
PINC	pressure increment for each loop	Pa
PO	formation data reference pressure	Pa
Q (I)	equilibrium constant for formation reaction i as calculated from composition	-
RELERR	fractional change in composition resulting from one iteration	-
RELMAX	maximum fractional change in composition of all species resulting from one iteration	-
RIIIV	vapor phase III/V atomic ratio	-
RT	product of the ideal gas constant and the temperature	kcal/g-mole
S	total number of species in the solution phase	-
SIMF	mole fraction of silicon species in the vapor	-
SITOT	moles of silicon species in the vapor	g-moles
SOLN (3)	vector containing the character string 'SOLUTION'	-

<u>Variable</u>	<u>Description</u>	<u>Units</u>
SPECIE (I, 3)	matrix of character strings containing the names of each specie	-
STDCP (I)	standard chemical potential of specie i	kcal/g-mole
STDCPZ	standard chemical potential of the inert	kcal/g-mole
SUMIII	total moles of group III atoms in the vapor	g-mole
SUMV	total moles of group V atoms in the vapor	g-mole
T	system temperature	K
TITLE (K)	vector containing an 80 character title	-
TINC	temperature increment for each loop	K
TOTMC (I)	total moles of pure condensed phase i as input	g-moles
TOTMOL	total moles in a single phase	g-moles
TOTMS	total moles in the solution phase	g-moles
TOTMV	total moles in the vapor phase	g-moles
TO	formation data reference temperature	K
US	coefficient for the solution species	-
UV	coefficient for the vapor species	-
V	total number of species in the vapor (integer)	-
VAPOR (3)	vector containing the character string 'VAPOR'	-

<u>Variable</u>	<u>Description</u>	<u>Units</u>
WKA	work area for LEQT1F	
WKA1	work area for LINV1F	
XIII	group III specie fraction in the steady state liquid "pure" condensed phase	-
ZV	moles of inert in the system	g-moles
ZACT	activity coefficient of the inert	-

#### A.4 A Description of the Subroutines

The subroutine calling sequence is shown in Figure A2. All of the subroutines in MCMPEC.RAND are discussed separately in the following sections with the exception of subroutine ERRSET and the IMSL subroutines LINVIF and LEQTIF. Subroutine ERRSET is a system subroutine which is used to suppress printing of certain execution time error messages. This subroutine may not be available at all computer installations and therefore the two calls to ERRSET may have to be removed if this code is to be implemented on other systems. The IMSL subroutines are briefly described in section A.4.18.

##### A.4.1 STSTCP

A listing of subroutine STSTCP is shown in Figure A3. STSTCP calculates the standard state chemical potentials for each specie in the system. The reference state is the system temperature  $T$ , the formation pressure  $P_0$ , and pure component in the phase in which the specie is present.

The pure component Gibbs Free Energy (standard chemical potential) of specie  $i$  at temperature  $T_0$  and pressure  $P_0$  is:

$$\mu_i^\circ(T_0, P_0) = G_i^\circ = \Delta H_f^\circ - T_0 \Delta S_f^\circ \quad (1)$$

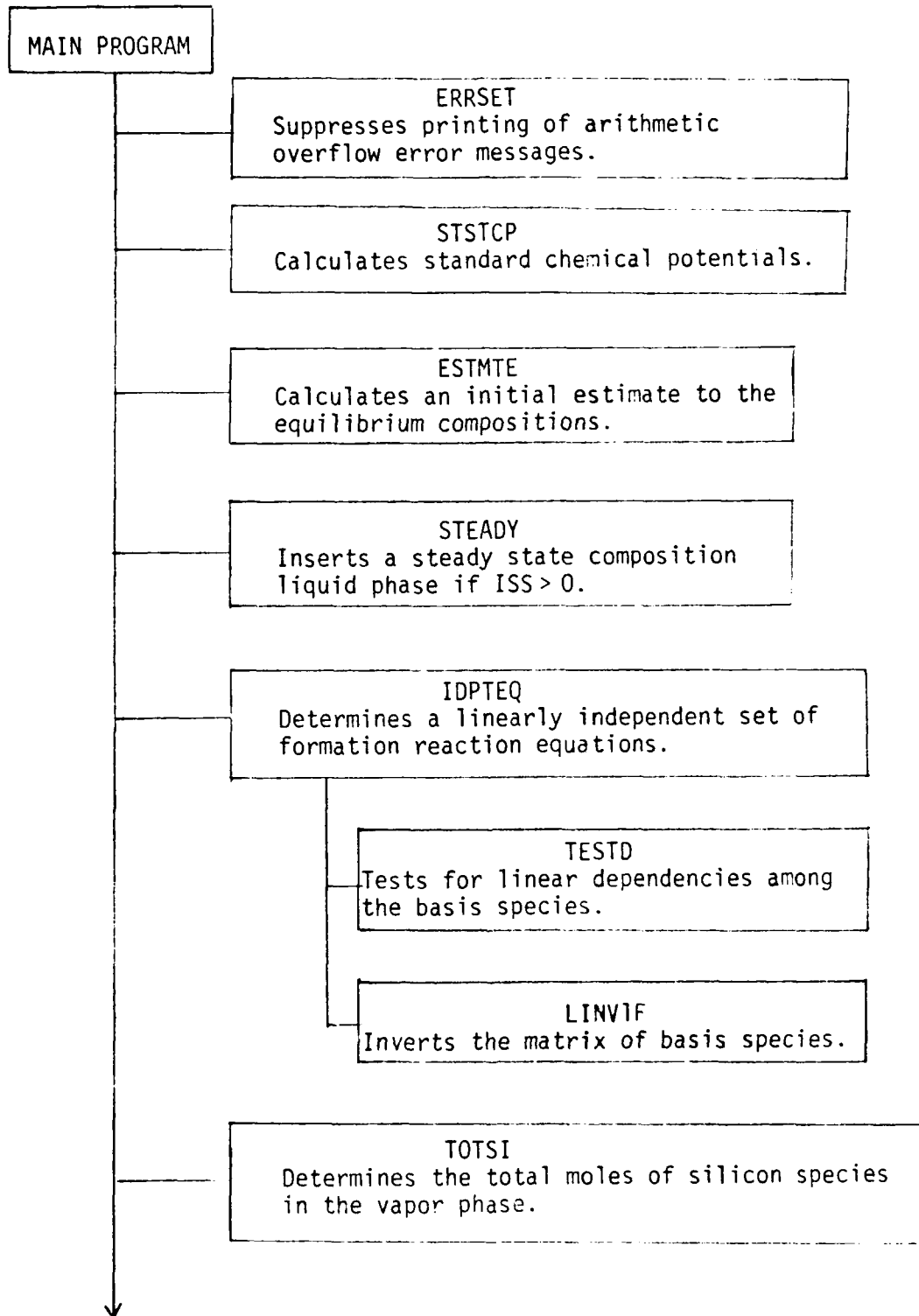
For a system temperature  $T$  the standard chemical potential of specie  $i$  is given by:

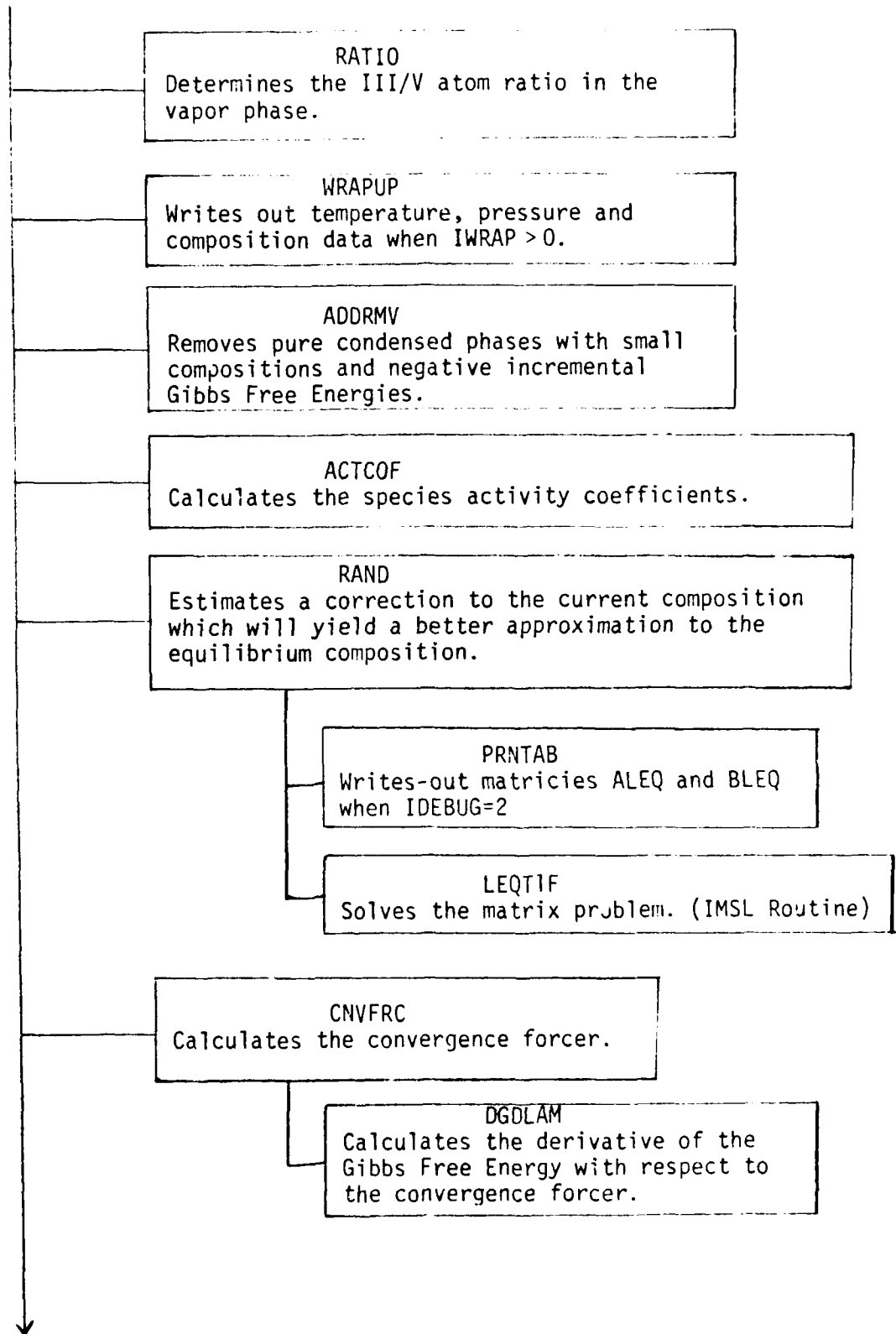
$$\mu_i^\circ(T, P_0) = \Delta H_f^i(T_0) + \int_{T_0}^T C_p^i dT - T \left[ \Delta S_f^i(T_0) + \int_{T_0}^T \frac{C_p^i}{T} dT \right] \quad (2)$$

Two heat capacity correlations are available and are chosen by the

Figure A2

## Subprogram Structure of MCMPEC.RAND





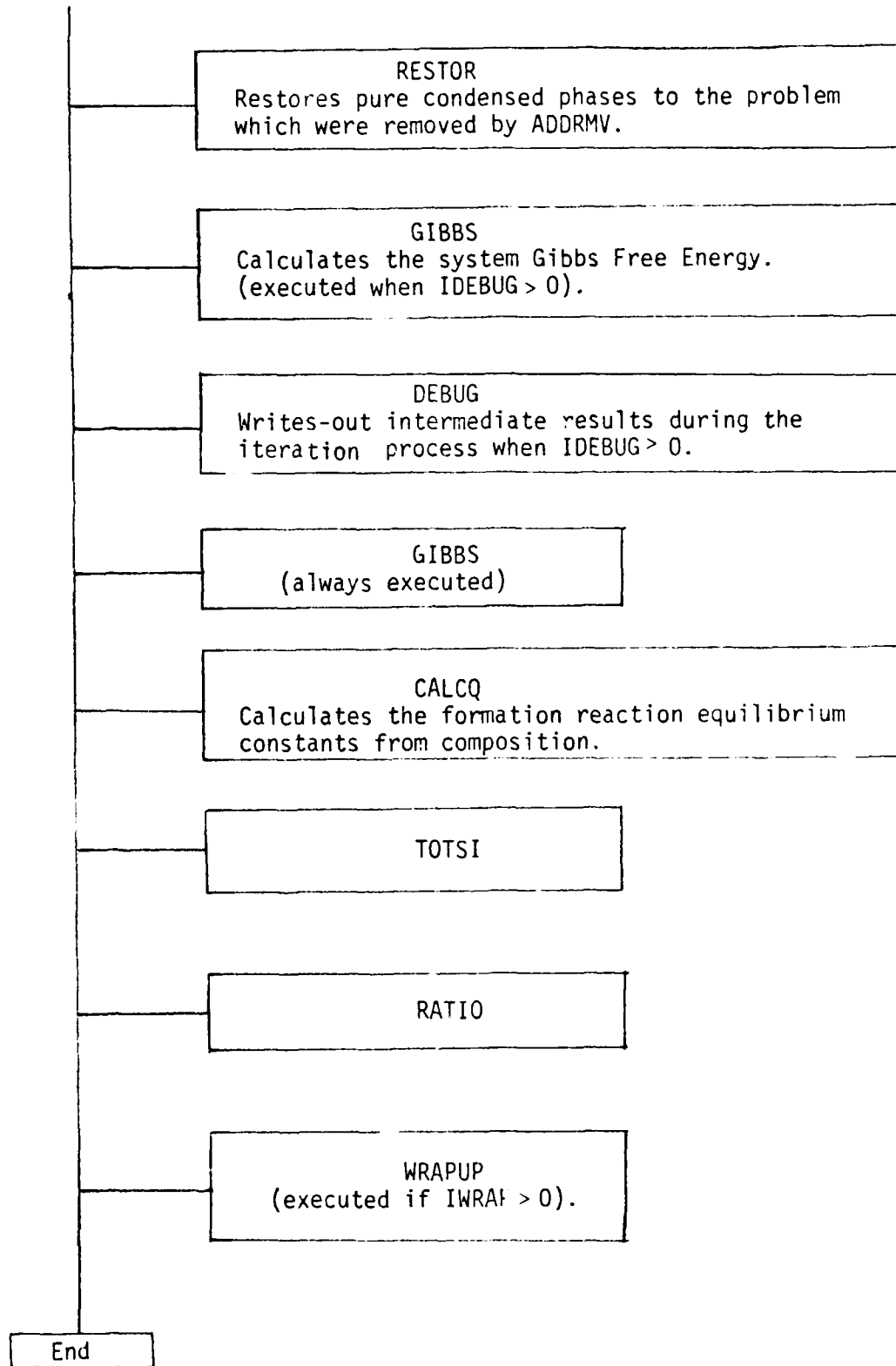


Figure A3. Subroutine STSTCP

```

1      SUBROUTINE STSTCP(A0,A1,A2,A3,A0Z,A1Z,A2Z,A3Z,DH0,DS0,DH0Z,DS0Z,
2      C      STDCP,STDCPZ,ICP,ICPZ,T0,T,IDIM1,V,S,C)
3      C
4      C THIS SUBROUTINE CALCULATES THE STANDARD STATE CHEMICAL POTENTIALS
5      C REFERENCE STATE: PURE COMPONENT (APPROPRIATE PHASE)
6      C AT TEMPERATURE T.
7      C
8      DIMENSION A0(IDIM1),A1(IDIM1),A2(IDIM1),A3(IDIM1),DH0(IDIM1),
9      C      DS0(IDIM1),STDCP(IDIM1),ICP(IDIM1)
10     INTEGER V,S,C,VSC
11     VSC=V+S+C
12     DT=T-T0
13     DT2=T**2-T0**2
14     DT3=T**3-T0**3
15     DT4=T**4-T0**4
16     DTM1=1.0/T-1.0/T0
17     DTM2=1.0/T/T-1.0/T0/T0
18     DLNT=ALOG(T)-ALOG(T0)
19     DLNT2=ALOG(T)**2-ALOG(T0)**2
20     DTLNT=T*ALOG(T)-T0*ALOG(T0)
21     C
22     C CHEMICAL POTENTIALS FOR THE VAPOR, SOLUTION AND CONDENSED PHASES
23     C
24     DO 100 I=1,VSC
25     DELH=A0(I)*DT+A1(I)*DT2/2.-A2(I)*DTM1+A3(I)*(DTLNT-DT)
26     DELS=A0(I)*DLNT+A1(I)*DT-A2(I)*DTM2/2.+A3(I)*DLNT2/2.
27     IF(ICP(I).EQ.1) DELH=A0(I)*DT+A1(I)*DT2/2.+A2(I)*DT3/3.
28     C      +A3(I)*DT4/4.
29     IF(ICP(I).EQ.1) DELS=A0(I)*DLNT+A1(I)*DT+A2(I)*DT2/2.
30     C      +A3(I)*DT3/3.
31     STDCP(I)=DH0(I)+DELH-T*(DS0(I)+DELS)
32     100 CONTINUE
33     C
34     C CHEMICAL POTENTIAL FOR THE INERT COMPONENT IN THE VAPOR PHASE
35     C
36     DELH=A0Z*DT+A1Z*DT2/2.-A2Z*DTM1+A3Z*(DTLNT-DT)
37     DELS=A0Z*DLNT+A1Z*DT-A2Z*DTM2/2.+A3Z*DLNT2/2.
38     IF(ICPZ.EQ.1) DELH=A0Z*DT+A1Z*DT2/2.+A2Z*DT3/3.
39     C      +A3Z*DT4/4.
40     IF(ICPZ.EQ.1) DELS=A0Z*DLNT+A1Z*DT+A2Z*DT2/2.
41     C      +A3Z*DT3/3.
42     STDCPZ=DH0Z+DELH-T*(DS0Z+DELS)
43     RETURN
44     END

```

parameter ICP. These correlations are:

<u>ICP</u>	<u>Heat Capacity Correlation</u>	
0	$C_p (T) = a_0 + a_1 T + a_2 T^{-2} + a_3 \ln (T)$	(3)

1	$C_p (T) = a_0 + a_1 T + a_2 T^2 + a_3 T^3$	(4)
---	---	-----

Obviously various other correlations (constant, linear, quadratic, etc.) may be generated from these two functions by simply setting the appropriate coefficients to zero.

Lines 12 through 20 calculate the necessary limit differentials which result from performing the indicated integrations in Equation 2 using the heat capacity correlations in Equations 3 and 4. The integrals are evaluated as DELH and DELS and the standard chemical potential for each specie, STDCP(I) is then calculated.

#### A.4.2 ESTMTE

A listing of subroutine ESTMTE is provided in Figure A4. ESTMTE simply calculates the number of moles of each specie from the specie mole fraction and the total number of moles in the phase. ESTMTE is provided as a subroutine to allow the inclusion of an algorithm which will yield an estimate to the equilibrium composition and therefore reduce the number of iterations required to obtain convergence. Currently the inlet composition is used as this initial estimate.

#### A.4.3 STEADY

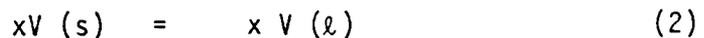
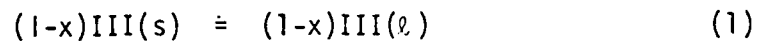
Subroutine STEADY inserts a pure condensed phase into the system in order to model a III-V liquid solution with a steady state composition. The composition of this liquid is that which would exist at equilibrium

FIGURE A4. Subroutine ESTMTE

```
1      SUBROUTINE ESTMTE(TOTMV,TOTMS,TOTMC,FRAC,N,FRACZ,ZV,IDIM1,
2      &
3      C
4      C THIS SUBROUTINE CALCULATES AN INITIAL ESTIMATE
5      C TO THE SYSTEM EQUILIBRIUM COMPOSITIONS
6      C
7      DIMENSION TOTMC(IDIM1),FRAC(IDIM1)
8      INTEGER V,S,C,VS,VS1,VSC
9      REAL N(IDIM1)
10     VS=V+S
11     VS1=VS+1
12     VSC=V+S+C
13     TOTMOL=TOTMV
14     DO 50 I=1,VS
15     IF(I.GT.V) TOTMOL=TOTMS
16     N(I)=TOTMOL*FRAC(I)
17     50 CONTINUE
18     ZV=FRACZ*TOTMV
19     IF(C.EQ.0) RETURN
20     DO 60 I=VS1,VSC
21     N(I)=TOTMC(I)
22     60 CONTINUE
23     RETURN
24     END
```

with the stoichiometric III-V solid at the system temperature. This subroutine is invoked when  $ISS > 0$ , a Ga/As liquid phase being inserted for  $ISS = 1$  and an In/P liquid phase for  $ISS = 2$ . This phase is inserted as the last pure condensed phase in the system (specie V+S+C).

A solid liquid equilibrium model for a binary liquid with the mole fraction of group V specie designated as X is obtained by writing the following reactions.



Reaction 4, which is the sum of the previous three reactions, represents the formation of a liquid solution having a composition  $(1-x)III$  and  $xV$ .

The Gibbs Free Energies of reactions 1 and 2 are simply those due to melting at  $T_m$  corrected for the temperature,  $T$ , of the solution.

$$\Delta G_1 = (1-x) \left[ \Delta S_m^{III} (T_m^{III} - T) + \Delta C_p^{III} (T - T_m^{III} - T \ln \frac{T_m^{III}}{T}) \right] \quad (5)$$

$$\Delta G_2 = x \left[ \Delta S_m^V (T_m^V - T) + \Delta C_p^V (T - T_m^V - T \ln \frac{T_m^V}{T}) \right] \quad (6)$$

where it has been assumed that  $\Delta C_p$ , the difference between the liquid and solid heat capacities, may be approximated as a constant.

The Gibbs Free Energy of reaction 3 is that due to the mixing of the group III and V liquids. This free energy consists of an ideal free energy of mixing (comprised of a configurational entropy term) and an excess Gibbs Free Energy term due to nonidealities. Applying a simple solution theory model for the excess Gibbs Free Energy yields [4]:

$$\Delta G_3 = RT [x \ln x + (1-x) \ln (1-x)] + (A_{xs} + B_{xs} T) x (1-x) \quad (7)$$

The Gibbs Free Energy of the liquid solution represented by reaction 4 is therefore given by:

$$\Delta G_4 = \Delta G_1 + \Delta G_2 + \Delta G_3 \quad (8)$$

Determination of the mole fraction of group V atoms in the melt,  $X$ , is accomplished by solving the implicit equation developed by Veiland [10] modified to include a simple solution rather than a regular solution model.

$$T = \frac{T_m^{IIIV} \Delta S_m^{IIIV} - A_{xs} (2x - 2x^2 - 0.5)}{\Delta S_m^{IIIV} - R \ln 4x(1-x) + B_{xs} (2x - 2x^2 - 0.5)} \quad (9)$$

The thermodynamic constants necessary for the evaluation of equations 8 and 9 are listed in Table A.3. Figures A5 and A6 demonstrate how well the theory predicts the liquidus temperature in the Ga/As and In/P systems.

Table A.3

Thermodynamic Data for the Ga/As and In/P Systems.

	$\Delta S_m$ (cal/g-mole-K)	$T_m$ (K)	$\Delta C_p$ (cal/g-mole-K)	$A_{xs}$ (cal/g-mole)	$B_{xs}$ (cal/g-mole-K)
Ga	4.411	302.9	-0.05	4666	-8.741
As	4.7	1090	1.0		
GaAs	16.64	1511	0		
In	1.815	429.8	-0.2	32750	-23.95
P	0.5011	313.3	0.47		
InP	10.81	1332.2	0		

Figure A5  
The Ga/As System Liquidus Line  
(Data refs. 3, 14, 15)

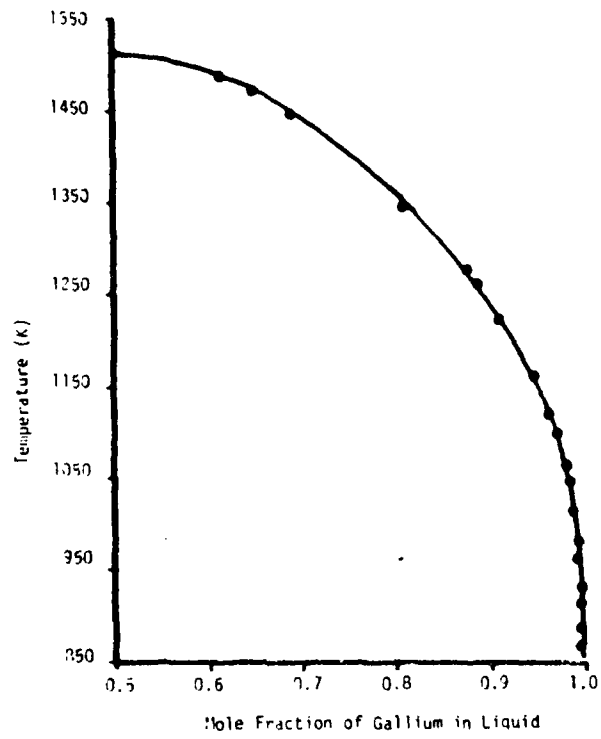
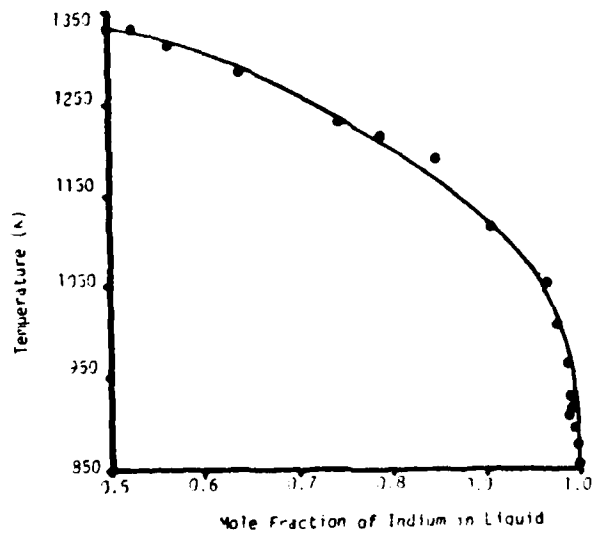


Figure A6  
The In/P System Liquidus Line  
(Data refs. 5, 11, 12, 13)



A listing of subroutine STEADY is shown in Figure A7. Lines 16 and 17 define a statement function which corresponds to the right hand side of Equation 9. Hollerith strings are assigned to the specie identifier matrix in lines 19 through 21. The melting temperature, entropies and excess Gibbs Free Energy correlation parameters for the Ga/As and In/P systems are assigned in lines 29 through 54.

An "interval halving" root finding algorithm for solving the implicit equation is located at lines 57 through 80. The iteration is considered to have converged when the two sides of the equation differ by less than 0.01%.

The standard state chemical potential of the liquid solution is calculated in lines 86 through 91. Finally, the elemental abundance matrix is assigned the appropriate values which reflect the elemental composition of the liquid solution in lines 93 through 107.

#### A.4.4 IDPTEQ

Subroutine IDPTEQ constructs a set of linearly independent formation reaction equations for the species in the system and then calculates the equilibrium constants for each of these reactions from the Gibbs Free Energy change of each reaction. A flowsheet and a listing of this subroutine are shown in Figures A8 and A9 respectively.

Lines 15 through 33 construct a matrix D which contains a linearly independent set of basis species using an algorithm similar to that of Cruise [6]. A matrix GNU, which contains the stoichiometric coefficients of all of the formation reactions, is then calculated in lines 39 through 57 using the relation

$$\text{GNU} = \text{A D}^{-1} \quad (1)$$

A50  
Figure A7. Subroutine STEADY

```

1      SUBROUTINE STEADY(SPECIE,A,STDCP,ELMNT,XIII,T,T0,V,S,C,IDIM1,
2      &
3      C      [DIM2,ISS,[WRT]
4      C      SUBROUTINE TO CALCULATE THE SOLID-LIQUID EQUILIBRIUM COMPOSITIONS
5      C      FOR USE IN THE STEADY-STATE APPROXIMATION IN THE SOURCE ZONE
6      C
7      C      ISS      SYSTEM
8      C      1      GA(L)-AS(L)/GA-AS (S)
9      C      2      IN(L)-P(L)/IN-P (S)
10     C
11     DIMENSION A(IDIM1,IDIM2),STDCP(IDIM1)
12     INTEGER SPECIE(IDIM1,3),ELMNT(IDIM2),IIIEL(2),VEL(2),V,S,C,VSC,
13     &      LAST/'1-X)/,GA/'GA'/,AS/'AS'/,IN/'IN'/,P/'P'/
14     DATA IIIEL(1)/' GAX'/,IIIEL(2)/' INX'/,
15     &      VEL(1)/'-AS('/,VEL(2)/'- P('/
16     THETA2(XV)=(TMIIIV*DSIIIV-AXS*(0.5-XV**2-(1.-XV)**2))/
17     &      (DSIIIV-R*ALOG(4.*XV*(1.-XV))+BXS*(0.5-XV**2-(1.-XV)**2))
18     VSC=V+S+C
19     SPECIE(VSC,1)=IIIEL(ISS)
20     SPECIE(VSC,2)=VEL(ISS)
21     SPECIE(VSC,3)=LAST
22     DT=T-T0
23     DT2=T**2-T0**2
24     DTM1=1.0/T-1.0/T0
25     DTM2=1.0/T**2-1.0/T0**2
26     DLNT=ALOG(T/T0)
27     IF(ISS.EQ.2) GO TO 50
28     C
29     C      GA-AS SYSTEM
30     C
31     TMIII=302.9
32     TMV=1090.
33     TMIIIV=1511.
34     DSIII=0.004411
35     DSV=0.0047
36     DSIIIV=0.01664
37     DCIII=-0.00005
38     DCV=0.001
39     AXS=4.666
40     BXS=-0.008741
41     GO TO 60
42     C
43     C      IN-P SYSTEM
44     C
45     50 TMIII=429.8
46     TMV=317.3
47     TMIIIV=1343.2
48     DSIII=0.00185
49     DSV=0.000498
50     DSIIIV=0.0152
51     DCIII=-0.0024
52     DCV=0.000592
53     AXS=0.0
54     BXS=0.0

```

```

55      60 CONTINUE
56 C
57 C   BINARY ROOT FINDING ROUTINE FOR THE GROUP III AND V COMPOSITIONS
58 C
59      XV=0.5
60      XMIN=0.0
61      XMAX=1.0
62      R=0.0019872
63      THETA1=T
64      XOLD=0.4
65      THTOLD=THETA2(XOLD)
66      DO 100 I=1,50
67      THET2=THETA2(XV)
68      ERR=(THET2-THETA1)/THETA1
69      IF(ABS(ERR).LT.0.0001) GO TO 200
70      SWTCH=(THET2-THTOLD)/(XV-XOLD)
71      THTOLD=THET2
72      XOLD=XV
73      IF(SWTCH.GT.0.AND.THET2.LT.THETA1) GO TO 80
74      IF(SWTCH.LT.0.AND.THET2.GT.THETA1) GO TO 80
75      XMAX=XV
76      XV=0.5*(XMIN+XV)
77      GO TO 100
78      80 XMIN=XV
79      XV=0.5*(XMAX+XV)
80      100 CONTINUE
81      WRITE(IWRT,120)
82      120 FORMAT('0','***** SUBROUTINE STEADY: ITERATION FOR SOURCE ',
83      &          'COMPOSITION DID NOT CONVERGE')
84      200 CONTINUE
85 C
86 C   CALCULATE THE STANDARD CHEMICAL POTENTIAL OF THE SOURCE SOLUTION
87 C
88      DGA=(1.0-XV)*(DSIII*(TMIII-T)+DCIII*(T-TMIII-T*ALOG(T/TMIII)))
89      DGB=XV*(DSV*(TMV-T)+DCV*(T-TMV-T*ALOG(T/TMV)))
90      DGC=(AXS+BXS*T)*XV*(1.-XV)+R*T*(XV*ALOG(XV)+(1.-XV)*ALOG(1.-XV))
91      STDCP(VSC)=DGA+DGB+DGC
92 C
93 C   LOCATE THE GROUP III AND V ELEMENTS IN THE ELEMENTAL ABUNDANCE ARRAY
94 C   AND INSERT THE CALCULATED ABUNDANCES INTO THIS ARRAY
95 C
96      IDX3=0
97      IDX5=0
98      DO 300 I=1,IDIM2
99      IF(ISS.EQ.2) GO TO 250
100     IF(ELMNT(I).EQ.G4) IDX3=I
101     IF(ELMNT(I).EQ.AS) IDX5=I
102     GO TO 300
103     250 IF(ELMNT(I).EQ.IN) IDX3=I
104     IF(ELMNT(I).EQ.P) IDX5=I
105     300 CONTINUE
106     A(VSC,IDX3)=1.0-XV
107     A(VSC,IDX5)=XV
108     XIII=1.0-XV
109     RETURN
110     END

```

Figure A8

## Flowsheet for Subroutine IDPTEQ

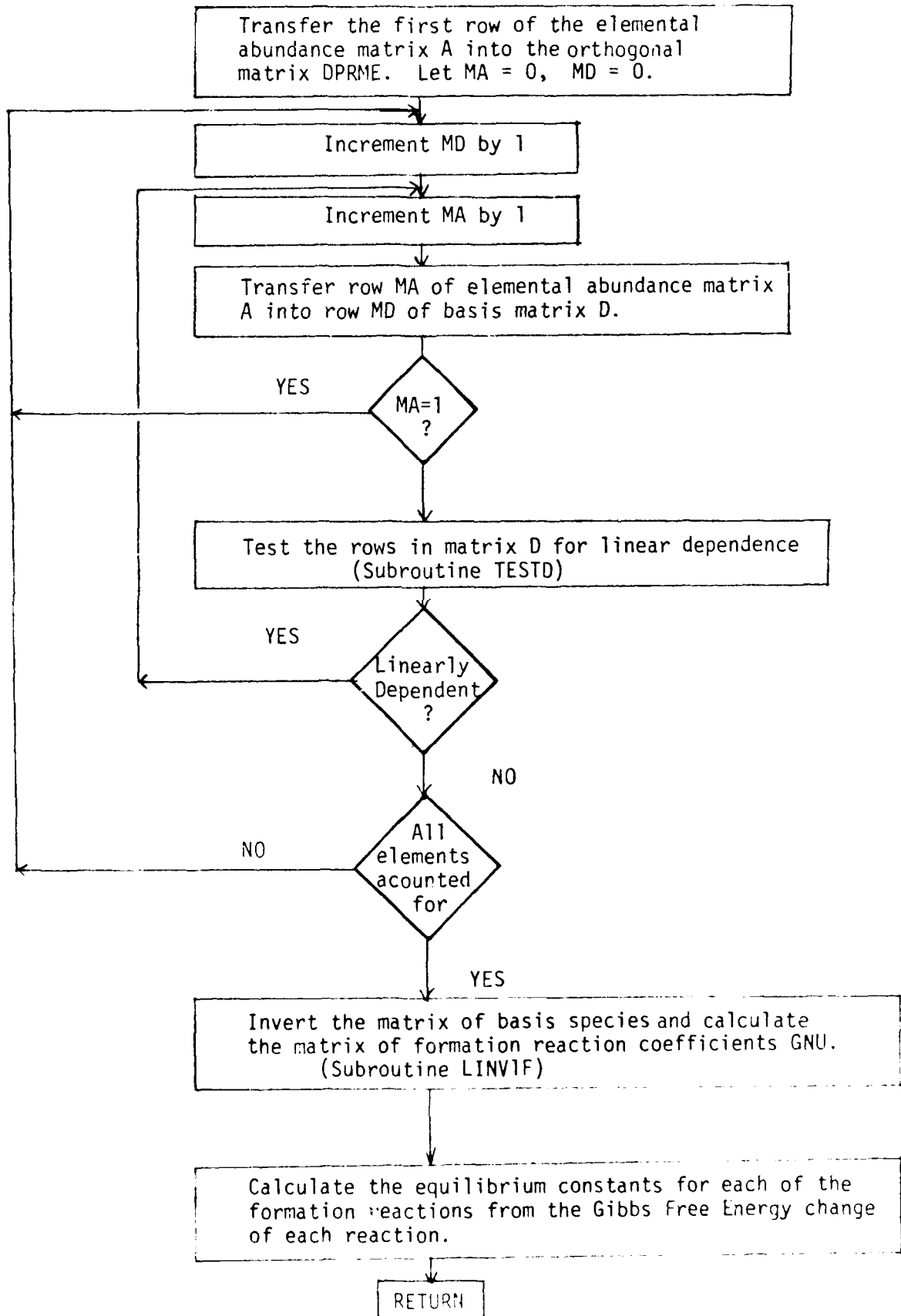


Figure A9. Subroutine IDPTEQ

```

1      SUBROUTINE IDPTEQ(A,D,DPRME,DINV,STDCP,GNU,IDXBAS,KEQ,WKA,DG,
2      &
3      C
4      C THIS SUBROUTINE DETERMINES A SET OF LINEARLY INDEPENDENT REACTION EQ
5      C AND CALCULATES THE EQUILIBRIUM CONSTANTS FOR THESE REACTIONS FROM TH
6      C GIBBS FREE ENERGY CHANGE OF EACH REACTION.
7      C
8      C DOUBLE PRECISION D,DPRME,DINV,WKA
9      C DIMENSION D(IDIM2,IDIM2),DPRME(IDIM2,IDIM2),DINV(IDIM2,IDIM2),
10     & WKA(IDIM2),IDXBAS(IDIM2),STDCP(IDIM1),DG(IDIM1),GNU(IDIM1,IDIM2)
11     & A(IDIM1,IDIM2)
12     REAL KEQ(IDIM1)
13     INTEGER V,S,C,E,VSC
14     VSC=V+S+C
15     C
16     C BUILD THE D MATRIX WHICH WILL CONTAIN THE LINEARLY INDEPENDENT BASIS
17     C
18     DO 100 J=1,E
19     DPRME(1,J)=A(1,J)
20     100 CONTINUE
21     MA=0
22     DO 200 MD=1,E
23     140 MA=MA+1
24     IF(MA.GT.VSC) GO TO 250
25     DO 150 J=1,E
26     D(MD,J)=A(MA,J)
27     150 CONTINUE
28     IDXBAS(MD)=MA
29     IF(MD.EQ.1) GO TO 200
30     CALL TESTD(D,DPRME,MD,E,IDIM2,ITST)
31     IF(ITST.EQ.0) GO TO 140
32     200 CONTINUE
33     GO TO 280
34     250 WRITE(IWRT,260)
35     260 FORMAT('0','***** A COMPLETE SET OF BASIS SPECIES COULD NOT BE *
36     & 'FOUND IN SUBROUTINE IDPTEQ')
37     280 CONTINUE
38     C
39     C INVERT MATRIX D USING IMSL SUBROUTINE LINVIF
40     C AND CALCULATE THE REACTION COEFFICIENT MATRIX GNU
41     C
42     IDGT=4
43     CALL LINVIF(D,E,IDIM2,DINV,IDGT,WKA,IER)
44     IF(IER.EQ.34) WRITE(IWRT,310) IDGT
45     310 FORMAT('0','***** ACCURACY TEST FAILED DURING MATRIX INVERSION *
46     & 'IN SUBROUTINE IDPTEQ.... IDGT=',I2)
47     IF(IER.EQ.129) WRITE(IWRT,320)
48     320 FORMAT('0','***** MATRIX D IS SINGULAR IN SUBROUTINE IDPTEQ')
49     DO 400 I=1,VSC
50     DO 400 J=1,E
51     TEMP=0.0
52     DO 350 JJ=1,E
53     TEMP=TEMP+A(I,JJ)*DINV(JJ,J)
54     350 CONTINUE

```

```
55      GNU(I,J)=TEMP
56  400 CONTINUE
57 C
58 C  CALCULATE THE EQUILIBRIUM CONSTANTS FOR THE FORMATION REACTIONS
59 C
60      DO 500 I=1,VSC
61      ARG=(-1.0)*STDCP(I)
62      DO 450 K=1,E
63      IDXB=IDXBAS(K)
64      ARG=ARG+GNU(I,K)*STDCP(IDXB)
65  450 CONTINUE
66      DG(I)=(-1.0)*ARG
67      ARG=ARG/RT
68      KEQ(I)=EXP(ARG)
69  500 CONTINUE
70      RETURN
71      END
```

The equilibrium constants for each reaction are then calculated in lines 58 through 70 by

$$K_{eqi} = \text{EXP} \left[ \left( \sum_{j=1}^E v_{ij} \mu_j^{\circ} - \mu_i^{\circ} \right) / RT \right] \quad (2)$$

Where  $\mu_j^{\circ}$  is the standard chemical potential of basis specie  $j$  and  $v_{ij}$  is the stoichiometric coefficient of basis specie  $j$  in formation reaction  $i$ .

#### A.4.5 TESTD

Subroutine TESTD tests the rows of the D matrix for linear independence by building a Gram-Schmidt orthogonalized matrix DPRME from D. The Gram-Schmidt orthogonalization procedure essentially subtracts away the projection of all the rows in the matrix which are above the row being orthogonalized. If the resulting orthogonalized row is composed of all zeros then this row was linearly dependent upon at least one of the above rows in the matrix. The equations used to construct matrix DPRME from matrix D are [7]:

$$d'_{1j} = d_{1j} \quad (1)$$

$$d'_{ij} = d_{ij} - \sum_{\ell=1}^{i-1} d'_{\ell j} \left[ \frac{\sum_{k=1}^E d_{ik} d'_{\ell k}}{\sum_{k=1}^E (d'_{\ell k})^2} \right] \quad (2)$$

Where:  $i=2,3,\dots,m_d$  = row index

$j = 1, 2, \dots, E$  = column index

$m_d$  = current row index in matrix D

$E$  = total # of elements in the system

$d'_{ij}$ ,  $d_{ij}$  are matrix elements in DPRME and D respectively.

A listing of TESTD is provided in Figure A10.

#### A.4.6 ADDR MV

During the iterative calculation to determine chemical equilibrium it is possible that pure condensed phases may be entirely consumed. This situation will cause an entire row in matrix ALEQ (subroutine RAND) to fill with zeros and therefore this matrix becomes singular. In order to allow the iterations to continue these zero composition pure condensed phases must be removed from the calculation and the ALEQ matrix is then reconstructed without them. As the calculation proceeds it is necessary to test the zero composition pure condensed phases at each iteration to see if they should be reinstated since the disappearance of a phase may be only a temporary occurrence as a result of the path taken to reach equilibrium. Phases with negative incremental values of Gibbs Free Energy are reinserted into the calculation since their presence lowers the Gibbs Free Energy of the entire system.

A listing of subroutine ADDR MV is shown in Figure A11. Lines 14 through 27 set to zero the composition of any pure condensed phase which has less than one molecule present. An incremental Gibbs Free Energy is calculated for each of the zero composition pure condensed phases at lines 28 through 32. The incremental Gibbs Free Energy, DGTST(I), is given by [8].

$$DGTST_i = \mu_i^o - \sum_{j=1}^E a_{ij} \pi_j \quad (1)$$

Where  $\pi_j$  is a Lagrange multiplier determined from the solution of the matrix problem in subroutine RAND,  $a_{ij}$  is defined in section A.5 and E is the number of elements in the system.

Figure A10. Subroutine TESTD

```
1      SUBROUTINE TESTD(D,DPRME,MD,E, IDIM2, ITST)
2 C
3 C THIS SUBROUTINE TESTS THE D MATRIX FOR LINEAR DEPENDENCE
4 C USING A GRAM-SCHMIDT ORTHOGONALIZATION ALGORITHM
5 C
6      DOUBLE PRECISION D,DPRME,ANUM,DENOM
7      DIMENSION D(IDIM2, IDIM2),DPRME(IDIM2, IDIM2)
8      INTEGER E
9      ITST=0
10     DO 100 J=1,E
11     DPRME(MD,J)=D(MD,J)
12     100 CONTINUE
13     MDM1=MD-1
14     DO 400 L=1,MDM1
15     DENOM=0.0
16     ANUM=0.0
17     DO 200 K=1,E
18     ANUM=ANUM+D(MD,K)*DPRME(L,K)
19     DENOM=DENOM+DPRME(L,K)**2
20     200 CONTINUE
21     DO 300 J=1,E
22     DPRME(MD,J)=DPRME(MD,J)-DPRME(L,J)*ANUM/DENOM
23     300 CONTINUE
24     400 CONTINUE
25     DO 500 J=1,E
26     IF(DABS(DPRME(MD,J)).GT.1.0E-5) ITST=ITST+1
27     500 CONTINUE
28     RETURN
29     END
```

A58  
Figure A11. Subroutine ADDR MV

```

1      SUBROUTINE ADDR MV(A,N,DGTST,STDCP,BLEQ,SPECIE,DELN,VPSP1,
2      &
3      C      VSC,E,C,EPCP2,IOUT,IDIM1,IDIM2,IDIM3)
4      C      SUBROUTINE TO ADD OR REMOVE PURE CONDENSED PHASES
5      C      IN THE EQUILIBRIUM CALCULATION BASED ON THE INCREMENTAL
6      C      GIBBS FREE ENERGY OF THESE PHASES
7      C
8      C      DOUBLE PRECISION BLEQ(IDIM3)
9      C      DIMENSION A(IDIM1,IDIM2),DELN(IDIM1),DGTST(IDIM1),STDCP(IDIM1)
10     C      REAL N(IDIM1)
11     C      INTEGER SPECIE(IDIM1,3),VPSP1,VSC,E,EPCP2,C
12     C      INDEX=0
13     C      IOUT=0
14     C
15     C      ZERO THE COMPOSITION OF ANY PURE CONDENSED PHASE WHICH CURRENTLY
16     C      HAS LESS THAN ONE MOLECULE (1.65E-24 G-MOLES) PRESENT.
17     C      DETERMINE THE INCREMENTAL CHANGE IN GIBBS FREE ENERGY
18     C      FOR EACH OF THESE ZERO COMPOSITION PURE CONDENSED PHASES
19     C
20     C      DO 50 I=1,VSC
21     C      DGTST(I)=0.
22     C      50 CONTINUE
23     C      IF(C.EQ.0) GO TO 500
24     C      DO 200 I=VPSP1,VSC
25     C      IF(N(I).GT.1.65E-24) GO TO 200
26     C      IOUT=IOUT+1
27     C      N(I)=0.0
28     C      DELN(I)=0.0
29     C      DGTST(I)=STDCP(I)
30     C      DO 100 J=1,E
31     C      DGTST(I)=DGTST(I)-A(I,J)*BLEQ(J)
32     C      100 CONTINUE
33     C      IF(DGTST(I).LT.0.0) INDEX=I
34     C      200 CONTINUE
35     C      IF(INDEX.EQ.0) GO TO 400
36     C
37     C      FIND THE ZERO COMPOSITION PURE CONDENSED PHASE WITH THE SMALLEST NEGATIVE
38     C      INCREMENTAL GIBBS FREE ENERGY AND ADD ONE MOLECULE OF IT
39     C      INTO THE EQUILIBRIUM CALCULATION
40     C
41     C      DGMIN=DGTST(INDEX)
42     C      DO 300 I=VPSP1,VSC
43     C      IF(N(I).GT.1.65E-24) GO TO 300
44     C      IF(DGTST(I).GT.0.0.OR.DGTST(I).LT.DGMIN) GO TO 300
45     C      INDEX=I
46     C      DGMIN=DGTST(I)
47     C      300 CONTINUE
48     C      N(INDEX)=1.66E-24
49     C      IOUT=IOUT-1
50     C      400 CONTINUE
51     C
52     C      REMOVE PURE CONDENSED PHASES WITH ZERO COMPOSITION
53     C      AND SHIFT NONZERO PURE CONDENSED PHASES UP IN THE ARRAYS
54     C

```

```
55      DO 500 I=VPSP1,VSC
56      IF(N(I).GT.1.65E-24) GO TO 500
57      IP1=I+1
58      IF(IP1.GT.VSC) IP1=VSC
59      DO 450 IJ=IP1,VSC
60      IF(N(IJ).LT.1.65E-24) GO TO 450
61      TMPVAR=N(I)
62      N(I)=N(IJ)
63      N(IJ)=TMPVAR
64      TMPVAR=STDCP(I)
65      STDCP(I)=STDCP(IJ)
66      STDCP(IJ)=TMPVAR
67      TMPVAR=DELN(I)
68      DELN(I)=DELN(IJ)
69      DELN(IJ)=TMPVAR
70      DO 420 J=1,E
71      TMPVAR=A(I,J)
72      A(I,J)=A(IJ,J)
73      A(IJ,J)=TMPVAR
74  420  CONTINUE
75      DO 430 K=1,3
76      ITMPV=SPECIE(I,K)
77      SPECIE(I,K)=SPECIE(IJ,K)
78      SPECIE(IJ,K)=ITMPV
79  430  CONTINUE
80      GO TO 500
81  450  CONTINUE
82  500  CONTINUE
83      C=C-IOUT
84      VSC=VSC-IOUT
85      EPCP2=EPCP2-IOUT
86      RETURN
87      END
```

The zero composition pure condensed phase which has the smallest negative incremental Gibbs Free Energy is determined in lines 36 through 50 and one molecule of it is inserted into the calculation. This treatment allows pure condensed phases to be reinserted in the calculation while minimizing any perturbation between iterations.

Lines 51 through 85 reformulate the equilibrium problem without the zero composition pure condensed phases by eliminating these phases from matrix ALEQ. The elimination is achieved by shifting the data in these phases to the last positions in arrays A and SPECIE, and in vectors N, DELN, and STDCP. The value of C, VSC and EPCP2 are then reduced to reflect the number of phases which were removed.

#### A.4.7 ACTCOF

A listing of subroutine ACTCOF, which calculates the activity coefficients for each specie, is shown in Figure A12. Initially all of the activity coefficients are set to unity. The iteration process for the equilibrium composition proceeds under this assumption of an ideal system until RELMAX, the convergence test parameter, becomes less than 0.1. At this point three options become available for the solution phase. The first option (IXSCOR = 0) simply assumes an ideal solution phase. The second option (IXSCOR = 1) treats the solution phase using simple solution theory and is applicable to binary solutions only. The activity coefficient for specie  $i$  is given by:

$$\gamma_i = \exp [ (A_{XS} + B_{XS}) (1-X_i)^2 / RT ] \quad (1)$$

The third option (IXSCOR = 2) allows the first specie in the solution phase to have an activity coefficient described by Henry's constant, H.

Figure A12. Subroutine ACTCOF

```

1      SUBROUTINE ACTCOF(N,ACOE, ZACT, IDIM1, IXSCOR, AXS, BXS, T, V, S, C,
2      &
3      C
4      C SUBROUTINE TO CALCULATE ACTIVITY COEFFICIENTS FOR EACH COMPONENT
5      C
6      C IXSCOR ALGORITHM
7      C   1 BINARY SIMPLE SOLUTION THEORY GE=(AXS+BXS*T)*X1*X2
8      C   2 HENRY'S CONSTANT FOR THE FIRST SOLUTION SPECIE H=AXS*EXP(BXS
9      C
10     DIMENSION ACOEF(IDIM1)
11     REAL N(IDIM1), NS
12     INTEGER V, S, C, VP1, VPS, VSC
13     VP1=V+1
14     VPS=V+S
15     VSC=V+S+C
16     ZACT=1.0
17     DO 100 I=1, VSC
18     ACOEF(I)=1.0
19 100 CONTINUE
20     IF(RELMAX.LT.0.1) IACFF=1
21     IF(IXSCOR.EQ.2) IACFF=1
22     IF(IXSCOR.LT.1.OR. IXSCOR.GT.2.OR.S.LE.1) IACFF=0
23     IF(IACFF.EQ.0) GO TO 900
24     RT=0.0019872*T
25     NS=0.0
26     DO 150 I=VP1, VPS
27     NS=NS+N(I)
28 150 CONTINUE
29     IF(IXSCOR.EQ.2) GO TO 200
30 C
31 C BINARY SIMPLE SOLUTION THEORY
32 C
33     X1=N(VP1)/NS
34     X2=1.0-X1
35     ARG1=(AXS+BXS*T)*X2**2/RT
36     ARG2=(AXS+BXS*T)*X1**2/RT
37     ACOEF(VP1)=EXP(ARG1)
38     ACOEF(VPS)=EXP(ARG2)
39     GO TO 900
40 C
41 C HENRY'S CONSTANT FOR THE FIRST SOLUTION SPECIE
42 C
43 200 ACOEF(VP1)=AXS*EXP(BXS/T)
44 900 RETURN
45     END

```

$$Y_{v+1} = H = A_{XS} \exp [ B_{XS}/T] \quad (2)$$

The vapor phase is always assumed to be ideal.

#### A.4.8 RAND

Subroutine RAND, shown in Figure A13, calculates a step change in each specie composition using the Rand algorithm developed in section A.5. This subroutine is used to solve the set of linear equations described by equations 17, 21, 22 and 23 in section A.5. Details of the matrix formulation are shown in Figures A14 and A15.

Matrix ALEQ is filled in accordance with Figures A14 and A15 in lines 26 through 105. Lines 106 through 175 fill vector BLEQ. The matrix problem

$$\text{ALEQ} \cdot X = \text{BLEQ} \quad (1)$$

is then solved in line 182 using the double precision version of IMSL routine LEQT1F. Warning messages are written out from lines 183 to 193 if matrix ALEQ is algorithmically singular or if less than three significant figures are present in the solution vector. Parameter ISTOP is set to unity if matrix ALEQ is found to be algorithmically singular (IER = 129). The value of ISTOP is tested in the main program at line 369 and execution is halted if ISTOP = 1.

In order to save on storage space the solution vector X is actually returned in BLEQ. Lines 201 through 238 determine the  $\delta n_j$  values from the solution vector and assign them to their appropriate position in the DELN vector.

Figure A13. Subroutine RAND

```

1      SUBROUTINE RAND(A,B,BK,N,DELN,STDCP,ALEQ,BLEQ,WKA,ACOE,
2      &                ZACT,V,S,C,E,VSC,EPCP2,IDIM1,IDIM2,IDIM3,ITER,PO,
3      &                P,ZV,ISTOP,IWRT,IDEBUG,IWRAP)
4 C
5 C  RAND ALGORITHM TO MINIMIZE THE GIBBS ENERGY OF A
6 C  MULTIPHASE, MULTICOMPONENT SYSTEM CONTAINING A VAPOR PHASE INERT
7 C
8 C  *****
9 C  * DOUBLE PRECISION IS USED TO EVALUATE THE MATRIX PROBLEM *
10 C *****
11 C
12      DOUBLE PRECISION ALEQ(IDIM3,IDIM3),BLEQ(IDIM3),WKA(IDIM3),
13      &                US,UV,TMPVAR
14      DIMENSION A(IDIM1,IDIM2),B(IDIM2),BK(IDIM2),DELN(IDIM1),
15      &                STDCP(IDIM1),ACOEF(IDIM1)
16      INTEGER V,S,C,E,VSC,EPCP2,VPS,VP1,EP3,EP3PC,
17      &                VPSP1
18      REAL N(IDIM1),NV,NS
19      ISTOP=0
20      VPS=V+S
21      VPSP1=V+S+1
22      VP1=V+1
23      EP3=E+3
24      EP3PC=E+3+C
25      50 CONTINUE
26 C
27 C  ZERO MATRIX ALEQ BEFORE ASSIGNING VALUES
28 C
29      DO 100 I=1,EPCP2
30      DO 100 J=1,EPCP2
31      ALEQ(I,J)=0.
32  100 CONTINUE
33 C
34 C  FILL THE UPPER E ROWS OF MATRIX ALEQ FROM EQUATION 21
35 C  THE FIRST E COLUMNS ARE THE LAGRANGE MULTIPLIER COEFFICIENTS
36 C
37      DO 180 I=1,E
38      DO 140 J=1,E
39      TMPVAR=0.
40      DO 130 K=1,VPS
41      TMPVAR=TMPVAR+A(K,I)*A(K,J)*N(K)
42  130 CONTINUE
43      ALEQ(I,J)=TMPVAR
44  140 CONTINUE
45 C
46 C  COLUMNS E+1 AND E+2 IN MATRIX ALEQ ARE THE
47 C  COEFFICIENTS FOR VARIABLES UV AND US RESPECTIVELY
48 C
49      IEP1=E+1
50      IEP2=E+2
51      TMPVAR=0.
52      DO 150 K=1,V
53      TMPVAR=TMPVAR+A(K,I)*N(K)
54  150 CONTINUE

```

```

55     ALEQ(I,IEP1)=TMPVAR
56     IF(S.EQ.0) GO TO 165
57     TMPVAR=0.
58     DO 160 K=VP1,VPS
59     TMPVAR=TMPVAR+A(K,I)*N(K)
60 160 CONTINUE
61     ALEQ(I,IEP2)=TMPVAR
62 165 CONTINUE
63 C
64 C THE FINAL C COLUMNS OF ALEQ ARE FOR THE DELTA-N
65 C COEFFICIENTS RELATING TO THE PURE CONDENSED PHASES
66 C
67     IADD=2
68     IF(S.EQ.0) IADD=1
69     IF(C.EQ.0) GO TO 180
70     DO 170 K=VPSP1,VSC
71     INDEX=K-VPS+E+IADD
72     ALEQ(I,INDEX)=A(K,I)
73 170 CONTINUE
74 180 CONTINUE
75 C
76 C FILL THE NEXT TWO ROWS (ROWS E+1 AND E+2) OF MATRIX ALEQ
77 C BASED ON EQUATIONS 22 AND 23
78 C
79     DO 250 J=1,E
80     TMPVAR=0.
81     DO 230 K=1,V
82     TMPVAR=TMPVAR+A(K,J)*N(K)
83 230 CONTINUE
84     ALEQ(IEP1,J)=TMPVAR
85     IF(S.EQ.0) GO TO 250
86     TMPVAR=0.
87     DO 240 K=VP1,VPS
88     TMPVAR=TMPVAR+A(K,J)*N(K)
89 240 CONTINUE
90     ALEQ(IEP2,J)=TMPVAR
91 250 CONTINUE
92     ALEQ(IEP1,IEP1)=(-1.0)*ZV
93 C
94 C THESE FINAL C ROWS IN MATRIX ALEQ ARE FILLED BY EQUATION 17
95 C
96     EP3=E+1+IADD
97     EP3PC=EP3+C
98     IF(C.EQ.0) GO TO 300
99     INDEX=VPS
100    DO 290 I=EP3,EP3PC
101    INDEX=INDEX+1
102    DO 290 J=1,E
103    ALEQ(I,J)=A(INDEX,J)
104 290 CONTINUE
105 300 CONTINUE
106 C
107 C CALCULATE BK, NV AND NS VALUES FROM THE PREVIOUS ESTIMATE OF N
108 C

```

```

109      DO 360 J=1,E
110      TMPVAR=0.
111      DO 350 I=1,VSC
112      TMPVAR=A(I,J)*N(I)+TMPVAR
113 350 CONTINUE
114      BK(J)=TMPVAR
115 360 CONTINUE
116      NV=ZV
117      DO 365 I=1,V
118      NV=NV+N(I)
119 365 CONTINUE
120      NS=0.
121      IF(S.EQ.0) GO TO 375
122      DO 370 I=VP1,VPS
123      NS=NS+N(I)
124 370 CONTINUE
125 375 CONTINUE
126 C
127 C NOW ASSIGN VALUES TO VECTOR BLEQ
128 C THE FIRST E VALUES ARE FROM EQUATION 21
129 C
130      DO 400 J=1,E
131      TMPVAR=B(J)-BK(J)
132      DO 380 I=1,V
133      ARG=ACOE(I)*N(I)*P/P0/NV
134      IF(ARG.LE.1.0E-50) ARG=1.0E-50
135      TMPVAR=TMPVAR+A(I,J)*N(I)*((STDCP(I)+ALOG(ARG)))
136 380 CONTINUE
137      IF(S.EQ.0) GO TO 395
138      DO 390 I=VP1,VPS
139      ARG=ACOE(I)*N(I)/NS
140      IF(ARG.LE.1.0E-50) ARG=1.0E-50
141      TMPVAR=TMPVAR+A(I,J)*N(I)*((STDCP(I)+ALOG(ARG)))
142 390 CONTINUE
143 395 CONTINUE
144      BLEQ(J)=TMPVAR
145 400 CONTINUE
146 C
147 C THE NEXT 2 POSITIONS IN VECTOR BLEQ (POSITIONS E+1 AND E+2)
148 C ARE FROM EQUATIONS 22 AND 23
149 C
150      TMPVAR=0.
151      DO 410 I=1,V
152      ARG=ACOE(I)*N(I)*P/P0/NV
153      IF(ARG.LE.1.0E-50) ARG=1.0E-50
154      TMPVAR=TMPVAR+N(I)*((STDCP(I)+ALOG(ARG)))
155 410 CONTINUE
156      BLEQ(I+1)=TMPVAR
157      TMPVAR=0.
158      IF(S.EQ.0) GO TO 425
159      DO 420 I=VP1,VPS
160      ARG=ACOE(I)*N(I)/NS
161      IF(ARG.LE.1.0E-50) ARG=1.0E-50
162      TMPVAR=TMPVAR+N(I)*((STDCP(I)+ALOG(ARG)))

```

```

163 420 CONTINUE
164     BLEQ(IEP2)=TMPVAR
165 425 CONTINUE
166 C
167 C THE FINAL C POSITIONS OF VECTOR BLEQ ARE FROM EQUATION 17
168 C
169     IF(C.EQ.0) GO TO 435
170     INDEX=VPS
171     DO 430 I=EP3,EP3PC
172     INDEX=INDEX+1
173     BLEQ(I)=STDCP(INDEX)
174 430 CONTINUE
175 435 CONTINUE
176     IF(IDDEBUG.EQ.2) CALL PRNTAB(ALEQ,BLEQ,EPCP2,IDIM3,IWRT)
177 C
178 C SOLVE THE MATRIX PROBLEM USING SUBROUTINE LEQTF
179 C
180     M=1
181     IDGT=3
182     CALL LEQTF(ALEQ,M,EPCP2,IDIM3,BLEQ,IDGT,WKA,IER)
183     IF(IER.NE.34.AND.IER.NE.129) GO TO 490
184     IF(ISTOP.EQ.1) GO TO 490
185     WRITE(IWRT,438) ITER
186 438 FORMAT('0','***** ITERATION ',I5,' *****')
187     IF(IER.EQ.34.AND.IWRAP.LT.2) WRITE(IWRT,440) IER,IDGT
188 440 FORMAT(1X,'***** ACCURACY TEST IN SUBROUTINE LEQTF',
189 6      '   ' FAILED..... IER=',I3,' IDGT=',I2,' *****',
190 6      '/.1X,' ')
191     IF(IER.EQ.129) WRITE(IWRT,450) IER
192 450 FORMAT(1X,'***** MATRIX ALEQ IN SUBROUTINE RAND IS SINGULAR',
193 6      '   ' IER = ',I3,' *****')
194     IF(IER.EQ.129) ISTOP=1
195     IDBG=IDDEBUG
196     IF(IER.EQ.129) IDDEBUG=2
197     IF(IDBG.LT.2.AND.IER.EQ.129) GO TO 50
198 490 CONTINUE
199     IF(IDDEBUG.EQ.2) WRITE(IWRT,495) (BLEQ(K),K=1,EPCP2)
200 495 FORMAT('0','THE TRANSPOSED X VECTOR IS:',/.1X,10(D11.4,2X))
201 C
202 C FILL THE DELN VECTOR FROM BLEQ USING EQUATIONS 19 AND 20
203 C THE FIRST E VALUES IN BLEQ ARE NOW THE LAGRANGE MULTIPLIERS;
204 C THE NEXT 2 VALUES ARE UV AND US RESPECTIVELY;
205 C THE LAST C VALUES ARE THE DELN VALUES FOR THE PURE CONDENSED PHASES
206 C
207     UV=BLEQ(IEP1)
208     DO 510 I=1,V
209     ARG=ACDEF(I)*N(I)*P/P0/NV
210     IF(ARG.LE.1.0E-50) ARG=1.0E-50
211     TMPVAR=UV-STDCP(I)-ALOG(ARG)
212     DO 500 J=1,E
213     TMPVAR=TMPVAR+BLEQ(J)*A(I,J)
214 500 CONTINUE
215     DELN(I)=TMPVAR*N(I)
216 510 CONTINUE

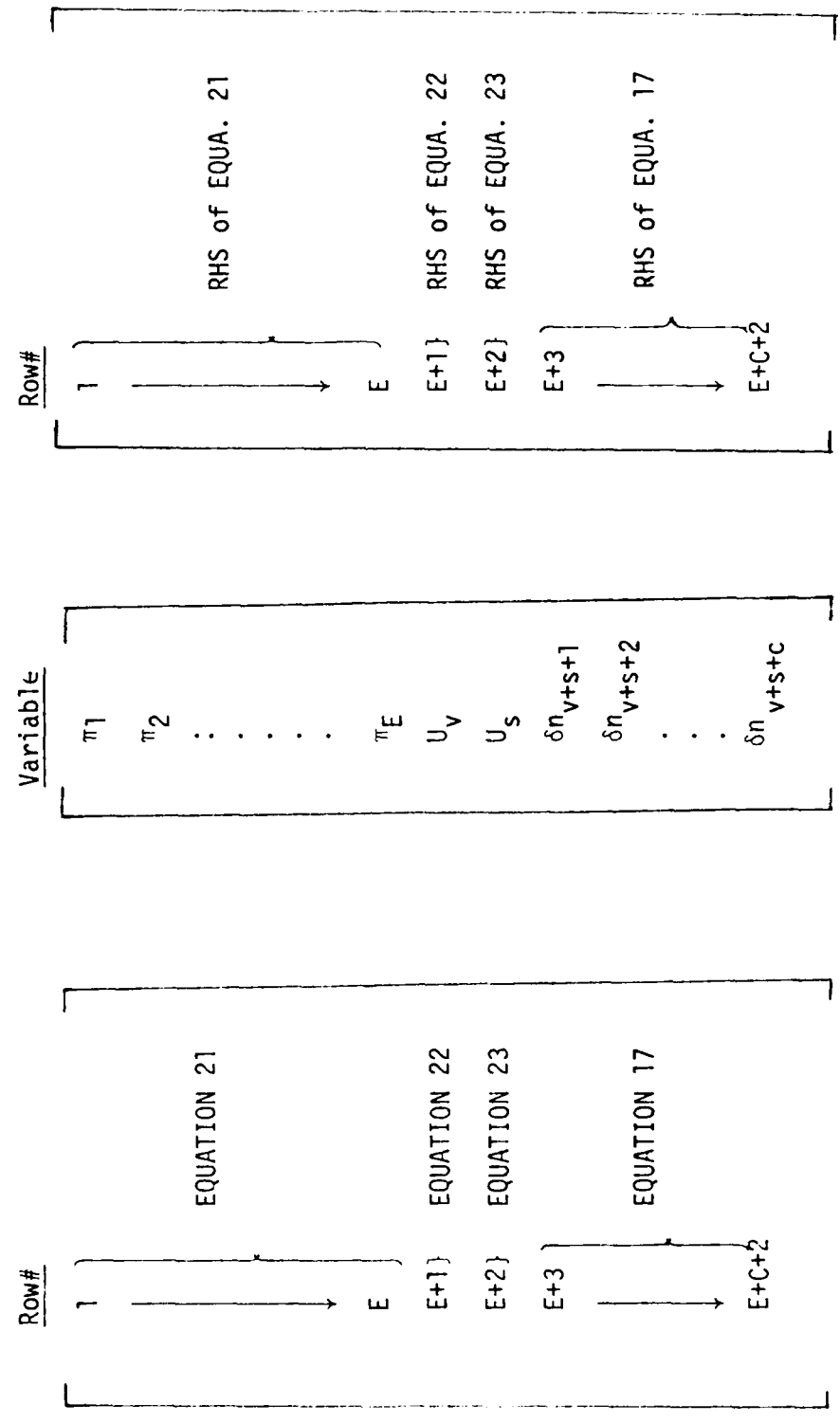
```

```
217      IF(S.EQ.0) GO TO 535
218      US=BLEQ(IEP2)
219      DO 530 I=VP1,VPS
220      ARG=ACDEF(I)*N(I)/NS
221      IF(ARG.LE.1.0E-50) ARG=1.0E-50
222      TMPVAR=US-STDCP(I)-ALOG(ARG)
223      DO 520 J=1,E
224      TMPVAR=TMPVAR+BLEQ(J)*A(I,J)
225      520 CONTINUE
226      DELN(I)=TMPVAR*N(I)
227      530 CONTINUE
228      535 CONTINUE
229 C
230 C THE FINAL C DELN VALUES ARE THE LAST C VALUES OF BLEQ
231 C
232      IF(C.EQ.0) GO TO 550
233      INDEX=E+IADD
234      DO 540 I=VPSP1,VSC
235      INDEX=INDEX+1
236      DELN(I)=BLEQ(INDEX)
237      540 CONTINUE
238      550 CONTINUE
239      RETURN
240      END
```

Figure A14

OVERVIEW OF MATRIX FORMULATION

(Equation numbers refer to section A.5)



ALEQ

X

BLEQ

(Note: RHS = Right Hand Side)

Figure A15

Detailed MATRIX FORMULATION of Linear EquationsSOLVE:  $\underline{ALEQ} \cdot \underline{X} = \underline{BLEQ}$  for  $\underline{X}$ 

$$\begin{array}{l}
 \underline{X} = \begin{bmatrix} \pi_1 \\ \pi_2 \\ \vdots \\ \pi_E \\ U_V \\ U_S \\ \delta n_{v+s+1} \\ \delta n_{v+s+2} \\ \vdots \\ \delta n_{v+s+c} \end{bmatrix} \\
 \\
 \underline{BLEQ} = \begin{bmatrix} b_1 - b_1^k + \sum_{i=1}^v a_{ii} n_i \left[ \mu_i^\circ + \ln \left( \frac{n_i^P}{n_V^P \rho} \right) \right] + \sum_{i=v+1}^{v+s} a_{ii} n_i \left[ \mu_i^\circ + \ln \left( \frac{n_i}{n_S} \right) \right] \\ \vdots \\ b_E - b_E^k + \sum_{i=1}^v a_{iE} n_i \left[ \mu_i^\circ + \ln \left( \frac{n_i^P}{n_V^P \rho} \right) \right] + \sum_{i=v+1}^{v+s} a_{iE} n_i \left[ \mu_i^\circ + \ln \left( \frac{n_i}{n_S} \right) \right] \\ \sum_{i=1}^v n_i \left[ \mu_i^\circ + \ln \left( \frac{n_i^P}{n_V^P \rho} \right) \right] \\ \sum_{i=v+1}^{v+s} n_i \left[ \mu_i^\circ + \ln \left( \frac{n_i}{n_S} \right) \right] \\ \mu_{v+s+1}^\circ \\ \mu_{v+s+2}^\circ \\ \vdots \\ \vdots \\ \mu_{v+s+c}^\circ \end{bmatrix}
 \end{array}$$

$$\begin{array}{l}
 \sum_{i=1}^{v+s} a_{i1} a_{i1}^{n_i} > \sum_{i=1}^{v+s} a_{i1} a_{i2}^{n_i} \dots \sum_{i=1}^{v+s} a_{i1} a_{iE}^{n_i} > \sum_{i=1}^v a_{i1} a_{iE}^{n_i} > \sum_{i=v+1}^{v+s} a_{i1}^{n_i} > a_{v+s+1,1} > \dots > a_{v+s+c,1} \\
 \cdot \\
 \cdot \\
 \cdot \\
 \cdot \\
 \sum_{i=1}^{v+s} a_{iE} a_{i1}^{n_i} > \sum_{i=1}^{v+s} a_{iE} a_{i2}^{n_i} \dots \sum_{i=1}^{v+s} a_{iE} a_{iE}^{n_i} > \sum_{i=1}^v a_{iE} a_{iE}^{n_i} > \sum_{i=v+1}^{v+s} a_{iE}^{n_i} > a_{v+s+1,E} > \dots > a_{v+s+c,E} \\
 \sum_{i=1}^v a_{i1}^{n_i} > \sum_{i=1}^v a_{i2}^{n_i} \dots \sum_{i=1}^v a_{iE}^{n_i} > -Z_v > 0 > \dots > 0 \\
 \sum_{i=v+1}^{v+s} a_{i1}^{n_i} > \sum_{i=v+1}^{v+s} a_{i2}^{n_i} \dots \sum_{i=v+1}^{v+s} a_{iE}^{n_i} > 0 > 0 > \dots > 0 \\
 a_{v+s+1,1} > a_{v+s+1,2} \dots a_{v+s+1,E} > 0 > 0 > \dots > 0 \\
 \cdot \\
 \cdot \\
 \cdot \\
 \cdot \\
 a_{v+s+c,1} > a_{v+s+c,2} > \dots > a_{v+s+c,E} > 0 > 0 > \dots > 0
 \end{array}$$

MATRIX ALEQ

## A.4.9 CNVFRC and DGD LAM

Subroutine CNVFRC calculates the convergence forcer for the iterative solution and is shown in Figure A16. The convergence forcer is used when the composition estimate is updated during each iteration according to the formula:

$$n_i' = n_i + \lambda \delta n_i \quad (1)$$

Where:  $n_i'$  = updated estimate to the equilibrium, composition  
 $n_i$  = previous estimate of equilibrium, composition  
 $\delta n_i$  = step change in composition as calculated in subroutine RAND  
 $\lambda$  = convergence forcer

The convergence forcer is also used to prevent negative compositions from appearing. Lines 13 through 22 determine the maximum value of the convergence forcer which will yield positive values for all of the specie molar amounts with the constraint that the convergence forcer must be between zero and one. If parameter IALG is zero this maximum value yielding positive compositions is used for the convergence forcer. If IALG is unity, an optimum value is calculated in lines 29 through 39 using the method of Smith and Missen [9]. This method entails the evaluation of  $dG/d\lambda$  at the maximum and minimum allowable values of  $\lambda$  where  $G$  is the system Gibbs Free Energy. An estimate to the optimum value of the convergence forcer is then obtained by

$$\lambda \approx \frac{\left(\frac{dG}{d\lambda}\right)_{\lambda=0}}{\left(\frac{dG}{d\lambda}\right)_{\lambda=0} - \left(\frac{dG}{d\lambda}\right)_{\lambda=MAX}} \quad (2)$$

Figure A16. Subroutine CNVFRC and Function DGDLAM

```

1      SUBROUTINE CNVFRC(STDCP,N,DELN,ACDEF,V,S,C,IDIM1,IALG,ZV,
2      &                  P,PO,RT,LAMBDA,ITER,IWRT)
3      C
4      C THIS SUBROUTINE CALCULATES THE CONVERGENCE FORCER
5      C FOR THE CURRENT ITERATION
6      C
7      DIMENSION STDCP(,IDIM1),ACDEF(IDIM1),DELN(IDIM1)
8      REAL N(IDIM1),LAMBDA
9      INTEGER V,S,C,VSC
10     VSC=V+S+C
11     AMIN=0.
12     AMAX=1.
13     C
14     C LIMIT THE MAXIMUM VALUE OF THE CONVERGENCE FORCER
15     C BY APPLYING THE CONSTRAINT OF NON-NEGATIVE COMPOSITION
16     C
17     DO 50 I=1,VSC
18     IF(ABS(DELN(I)).LT.1.0E-50) GO TO 50
19     LAMBDA=(-1.0)*N(I)/DELN(I)
20     IF(LAMBDA.GT.0.0.AND.LAMBDA.LT.AMAX) AMAX=LAMBDA
21 50 CONTINUE
22     LAMBDA=AMAX
23     C
24     C IF IALG=0 OR ATEST IS SMALL THE MAXIMUM RELAXATION PARAMETER IS USED
25     C
26     IF(IALG.EQ.0) RETURN
27     ATEST=AMAX-AMIN
28     IF(ATEST.LT.0.01) RETURN
29     C
30     C ESTIMATE THE OPTIMUM VALUE OF THE CONVERGENCE FORCER
31     C
32     DGDMAX=DGDLAM(N,DELN,STDCP,ACDEF,ZV,P,PO,RT,AMAX,
33     &             IDIM1,V,S,C)
34     DGDMIN=DGDLAM(N,DELN,STDCP,ACDEF,ZV,P,PO,RT,AMIN,
35     &             IDIM1,V,S,C)
36     IF(DGDMIN.EQ.DGDMAX) DGDMAX=0.0
37     LAMBDA=DGDMIN/(DGDMIN-DGDMAX)
38     IF(LAMBDA.GT.AMAX) LAMBDA=AMAX
39     IF(LAMBDA.LT.AMIN) LAMBDA=0.05
40     RETURN
41     END
42     FUNCTION DGDLAM(N,DELN,STDCP,ACDEF,ZV,P,PO,RT,ALAM,
43     &             IDIM1,V,S,C)
44     C
45     C EVALUATION OF DG/DLAMBDA FOR DETERMINING THE CONVERGENCE FORCER
46     C
47     DIMENSION ACDEF(IDIM1),DELN(IDIM1),STDCP(IDIM1)
48     REAL N(IDIM1),NV,NS
49     INTEGER V,S,C,VP1,VPS,VSC,VS1
50     VP1=V+1
51     VPS=V+S
52     VS1=VPS+1
53     VSC=VPS+C
54     NV=ZV

```

```
55      DO 100 I=1,V
56      NV=NV+N(I)
57      100 CONTINUE
58      IF(S.EQ.0) GO TO 210
59      NS=0.0
60      DO 200 I=VP1,VPS
61      NS=NS+N(I)
62      200 CONTINUE
63      210 CONTINUE
64      C
65      C   CALCULATE DG/DLAMBDA
66      C
67      DGDL=0.0
68      DO 300 I=1,VPS
69      ARG=ACDEF(I)*(N(I)+ALAM*DELN(I))*P/P0/NV
70      IF(I.GT.V) ARG=ACDEF(I)*(N(I)+ALAM*DELN(I))/NS
71      DGDL=DGDL+DELN(I)*(STDCP(I)+ALOG(ARG))
72      300 CONTINUE
73      IF(C.EQ.0) GO TO 410
74      DO 400 I=VS1,VSC
75      DGDL=DGDL+DELN(I)*STDCP(I)
76      400 CONTINUE
77      410 DGDLAM=DGDL*RT
78      RETURN
79      END
```

This equation is essentially a single iteration of a Regula-Falsi root finding algorithm and yields a sufficiently close approximation to the optimum value of  $\lambda$ . The value of  $\lambda$  chosen is further constrained to be between 0.05 and the maximum value which yields positive molar amounts. The lower limit of 0.05 allows the iterative process to continue when zero or negative values for the convergence factor are predicted.

The derivatives are calculated in function subroutine DGD LAM shown in lines 42 through 79 and are given by

$$\frac{dG}{d\lambda} = RT \left\{ \sum_{i=1}^v \delta n_i \left[ \mu_i^{\circ} + \lambda n \left( \frac{n_i' P}{P_0 n_v} \right) \right] + \sum_{i=v+1}^{v+s} \delta n_i \left[ \mu_i^{\circ} + \lambda n \left( \frac{n_i'}{n_s} \right) \right] + \sum_{i=v+s+1}^{v+s+c} \delta n_i \mu_i^{\circ} \right\} \quad (3)$$

#### A.4.10 RESTOR

Subroutine RESTOR, shown in Figure A17, restores the arrays and vectors which were shifted in subroutine ADDR MV to the original order in the problem formulation. This is accomplished by comparing array SPECIE, which has the shifted order of the species, to array ISPCE, which contains the original specie order. The data in the arrays and vectors are then shifted to reflect the original specie order. The constants C, VSC and EPCP2 are also restored to their original values.

#### A.4.11 GIBBS

Subroutine GIBBS, shown in Figure A13, calculates the system Gibbs Free Energy using equation 1 in section A.5. This subroutine is called after the iteration for equilibrium has terminated and also during debugging (IDEBUG > 1).

Figure A17. Subroutine RESTOR

```

1      SUBROUTINE RESTOR(A, SPECIE, ISPCE, STDCP, N, DELN, IDIM1, IDIM2,
2      &                   VSC, EPCP2, C, VPSP1, E, IOUT)
3      C
4      C THIS SUBROUTINE RESTORES MATRICES AND VECTORS A, SPECIE, STDCP,
5      C N AND DELN ALONG WITH CONSTANTS VSC, C AND EPCP2 TO THEIR ORIGINAL
6      C ORDER AND VALUES IN THE INITIAL PROBLEM FORMULATION
7      C
8      DIMENSION A(IDIM1, IDIM2), STDCP(IDIM1), DELN(IDIM1), ISPCE(IDIM1, 3)
9      INTEGER SPECIE(IDIM1, 3), VSC, F, EPCP2, C, VPSP1, VSCM1
10     REAL N(IDIM1)
11     IF(IOUT.EQ.0) GO TO 400
12     EPCP2=EPCP2+IOUT
13     C=C+IOUT
14     VSC=VSC+IOUT
15     VSCM1=VSC-1
16     C
17     C DO A CHARACTER STRING COMPARISON OF SPECIE WITH ISPCE AND PUT
18     C THE ARRAYS AND VECTORS INTO THEIR ORIGINAL ORDERS
19     C
20     DO 300 I=VPSP1, VSCM1
21     IP1=I+1
22     IF(IP1.GT.VSC) IP1=VSC
23     DO 200 II=IP1, VSC
24     IF((ISPCE(I, 1).EQ.SPECIE(II, 1)).AND.
25     &  ISPCE(I, 2).EQ.SPECIE(II, 2)).AND.
26     &  ISPCE(I, 3).EQ.SPECIE(II, 3)) GO TO 50
27     GO TO 200
28     50 TEMP=N(I)
29     N(I)=N(II)
30     N(II)=TEMP
31     TEMP=STDCP(I)
32     STDCP(I)=STDCP(II)
33     STDCP(II)=TEMP
34     TEMP=DELN(I)
35     DELN(I)=DELN(II)
36     DELN(II)=TEMP
37     DO 100 J=1, E
38     TEMP=A(I, J)
39     A(I, J)=A(II, J)
40     A(II, J)=TEMP
41     100 CONTINUE
42     DO 120 K=1, 3
43     ITEMP=SPECIE(I, K)
44     SPECIE(I, K)=SPECIE(II, K)
45     SPECIE(II, K)=ITEMP
46     120 CONTINUE
47     GO TO 300
48     200 CONTINUE
49     300 CONTINUE
50     400 RETURN
51     END

```



## A.4.12 CALCQ

A listing of CALCQ is shown in Figure A19. This subroutine calculates the equilibrium constants for each of the independent formation reactions based on the composition of the system. These equilibrium constants are given by:

$$Q_i = \gamma_i X_i P_{poi} / \prod_{k=1}^E (\gamma_k X_k P_{pok})^{\nu_{ik}} \quad (1)$$

Where:

$\gamma_i$  = activity coefficient of specie i

$X_i$  = mole fraction of specie i in its phase

$\nu_j$  = stoichiometric reaction coefficient

$$P_{poi} = \begin{cases} 1 & \text{for solution or pure condensed phase} \\ P/P_0 & \text{for vapor phase} \end{cases}$$

The product in the denominator is taken over the basis species used in the formation reaction equations.

## A.4.13 TOTSI

Subroutine TOTSI, shown in Figure A20 calculates the total moles and mole fraction of silicon species in the vapor phase. A character string comparison is made to determine which member of vector ELMNT is assigned the string 'SI'. Then the moles of all vapor species with a nonzero value in their elemental abundance vector corresponding to this position are summed.

## A.4.14 RATIO

Subroutine RATIO, shown in Figure A21 calculates the group III/V atom ratio in the vapor phase. All of the elements in columns III and V

A78  
Figure A19. Subroutine CALCQ

```
1     SUBROUTINE CALCQ(GNU,N,ACDEF,FRAC,IDXBAS,Q,  
2     E  
3     C  
4     C SUBROUTINE TO CALCULATE EQUILIBRIUM CONSTANTS FROM COMPOSITION  
5     C  
6     DIMENSION GNU(IDIM1,IDIM2),ACDEF(IDIM1),FRAC(IDIM1),  
7     E  
8     IDXBAS(IDIM2),Q(IDIM1)  
9     INTEGER V,S,C,E,VSC  
10    REAL N(IDIM1)  
11    VSC=V+S+C  
12    C  
13    C CALCULATE THE EQUILIBRIUM CONSTANTS  
14    C  
15    DO 400 I=1,VSC  
16    PP0=1.0  
17    IF(I.LE.V) PP0=P/P0  
18    Q(I)=ACDEF(I)*FRAC(I)*PP0  
19    DO 300 J=1,E  
20    K=IDXBAS(J)  
21    PP0=1.0  
22    IF(K.LE.V) PP0=P/P0  
23    Q(I)=Q(I)/(ACDEF(K)*FRAC(K)*PP0)**GNU(I,J)  
24    300 CONTINUE  
25    400 CONTINUE  
26    RETURN  
27    END
```

Figure A20. Subroutine TOTS1

```
1      SUBROUTINE TOTS1(A,ELMNT,FRAC,N,SITOT,SIMF,IDIM1,IDIM2,V,F)
2 C
3 C      SUBROUTINE TO CALCULATE THE TOTAL SI IN THE VAPOR PHASE
4 C
5      DIMENSION A(IDIM1,IDIM2),FRAC(IDIM1)
6      INTEGER ELMNT(IDIM2),V,F,SIVPR/'SI'/
7      REAL N(IDIM1)
8      SITOT=0.0
9      SIMF=0.0
10     DO 100 J=1,E
11     KSI=J
12     IF(ELMNT(J).EQ.SIVPR) GO TO 130
13 100 CONTINUE
14     GO TO 150
15 130 CONTINUE
16     DO 140 I=1,V
17     IF(A(I,KSI).LT.0.001) GO TO 140
18     SITOT=SITOT+N(I)
19     SIMF=SIMF+FRAC(I)
20 140 CONTINUE
21 150 CONTINUE
22     RETURN
23     END
```

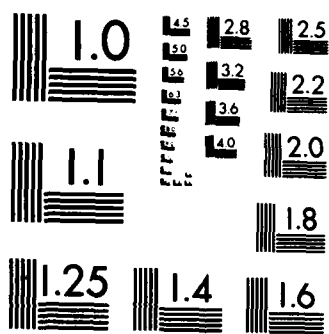
Figure A21. Subroutine RATIO

```

1      SUBROUTINE RATIO(A,ELMNT,FRAC,RIIIV,IDIM1,IDIM2,V,E)
2 C
3 C   THIS SUBROUTINE CALCULATES THE VAPOR III/V RATIO
4 C
5      DIMENSION A(IDIM1,IDIM2),FRAC(IDIM1),KIII(5),KV(5)
6      INTEGER ELMNT(IDIM2),ELIII(5),ELV(5),V,E
7      DATA ELIII(1)/' B'/,ELIII(2)/'AL'/,ELIII(3)/'GA'/,ELIII(4)/'IN'/,
8 C      ELIII(5)/'TL'/,ELV(1)/' N'/,ELV(2)/' P'/,ELV(3)/'AS'/,
9 C      ELV(4)/'SB'/,ELV(5)/'BI'//
10 C
11 C   DETERMINE WHICH INDECIES CORRESPOND TO COLUMN III AND V ELEMENTS
12 C
13      DO 100 K=1,5
14      KIII(K)=0
15      KV(K)=0
16      DO 100 J=1,E
17      IF(ELMNT(J).EQ.ELIII(K)) KIII(K)=J
18      IF(ELMNT(J).EQ.ELV(K)) KV(K)=J
19 100 CONTINUE
20 C
21 C   SUM-UP THE GROUP III AND V SPECIES AND CALCULATE THE RATIO
22 C
23      SUMIII=0.0
24      SUMV=0.0
25      DO 200 I=1,V
26      DO 200 K=1,5
27      IDXIII=KIII(K)
28      IDXV=KV(K)
29      IF(IDXIII.EQ.0) GO TO 120
30      SUMIII=SUMIII+A(I,IDXIII)*FRAC(I)
31 120 CONTINUE
32      IF(IDXV.EQ.0) GO TO 200
33      SUMV=SUMV+A(I,IDXV)*FRAC(I)
34 200 CONTINUE
35      RIIIV=1.0E10
36      IF(SUMV.GT.0.0) RIIIV=SUMIII/SUMV
37      RETURN
38      END

```





MICROCOPY RESOLUTION TEST CHART  
NATIONAL BUREAU OF STANDARDS-1963-A

of the periodic table are included. This results in a total III/V ratio which does not distinguish between the various elements in each group. Since character string comparisons are made in order to locate the positions of the appropriate elements in vector ELMNT it is essential that all group III and V elements which have single letter representations (B, N, P) be entered right justified in the input data set.

#### A.4.15 WRAPUP

Subroutine WRAPUP, shown in Figure A22, writes a wrap-up file to logical unit designator IFILE. This subroutine is accessed when parameter IWRAP > 0. For IWRAP = 1 or 2 the value of IFILE is set to 2. For IWRAP = 3 IFILE is set equal to IWRT which is the line printer logical unit designator. This subroutine provides concise data output and is quite useful when the input data set has been verified to be correct and parametric studies are desired.

#### A.4.16 DEBUG

Subroutine DEBUG is accessed when parameter IDEBUG > 1. This subroutine provides an output of the convergence forcer, system Gibbs Free Energy, the relative state of convergence, specie molar amounts, changes in specie molar amounts and the incremental Gibbs Free Energy of each specie at each iteration. A listing of DEBUG is shown in Figure A23.

#### A.4.17 PRNTAB

Subroutine PRNTAB, shown in Figure A24 writes out matrix ALEQ and vector BLEQ for diagnostic purposes when parameter IDEBUG = 2. This subroutine is accessed from line 176 of subroutine RAND.

Figure A22. Subroutine WRAPUP

```

1     SUBROUTINE WRAPUP(TITLE,SPECIE,INERT,N,FRAC,ZV,FRACZ,SITOT,SIMF,
2     &                   RIII,RELMAX,CNVG,ISS,XIII,T,P,IDATA,IDIM1,IFILE,
3     &                   V,VSC)
4     C
5     C SUBROUTINE TO WRITE-OUT A SUMMARY OF THE RESULTS TO A FILE
6     C
7     DIMENSION INERT(3),FRAC(IDIM1)
8     INTEGER TITLE(20),SPECIE(IDIM1,3),V,VSC
9     REAL N(IDIM1)
10    IF(IDATA.EQ.0) WRITE(IFILE,50) (TITLE(K),K=1,20)
11    50 FORMAT(20A4)
12    WRITE(IFILE,55) T,P
13    55 FORMAT('TEMPERATURE = ',F7.1,' K',/, 'PRESSURE = ',E12.5,' PA')
14    IF(ABS(RELMAX).GT.CNVG.AND.IDATA.NE.0)WRITE(IFILE,58) RELMAX,CN
15    58 FORMAT(66('*'),/, '* ',5X, 'ITERATION FOR EQUILIBRIUM COMPOSITION
16    &         'DID NOT CONVERGE',5X, '* ',/, '* ',1X, 'MAXIMUM ERROR = ',
17    &         E12.5,2X, 'CONVERGENCE CRITERION = ',E12.5,1X, '* ',
18    &         /,66('*'))
19    IF(IDATA.EQ.0) WRITE(IFILE,60)
20    60 FORMAT(13X, 'INITIAL COMPOSITIONS')
21    IF(IDATA.EQ.1) WRITE(IFILE,70)
22    70 FORMAT(13X, 'EQUILIBRIUM COMPOSITIONS')
23    IF(IDATA.EQ.0) WRITE(IFILE,80)
24    80 FORMAT('SPECIE',7X, 'MOLE FRACTION',4X, 'GRAM MOLES')
25    DO 200 I=1,VSC
26    WRITE(IFILE,100) (SPECIE(I,K),K=1,3),FRAC(I),N(I)
27    IF(I.EQ.V) WRITE(IFILE,100) (INERT(K),K=1,3),FRACZ,ZV
28    100 FORMAT(3A4,2X,E12.5,2X,E12.5)
29    IF(I.EQ.V) WRITE(IFILE,105) RIII
30    105 FORMAT('VAPOR III/V ',10X,F9.4)
31    IF(I.EQ.V) WRITE(IFILE,110) SIMF,SITOT
32    110 FORMAT('SI IN VAPOR ',2X,E12.5,2X,E12.5)
33    200 CONTINUE
34    IF(ISS.GT.0) WRITE(IFILE,205) XIII
35    205 FORMAT(3X, 'X=' ,F6.4)
36    WRITE(IFILE,210)
37    210 FORMAT(' ')
38    IDATA=1
39    RETURN
40    END

```

Figure A23. Subroutine DEBUG

```
1      SUBROUTINE DEBUG(N,DELN,DGTST,VSC,IDIM1,ITER,LAMBDA,GFE,
2      &
3      C          RMX,IWRT)
4      C  ROUTINE TO WRITE-OUT N, DELN, ALMBDA DURING THE ITERATON PROCESS
5      C
6      REAL LAMBDA,N(IDIM1),DGTST(IDIM1),DELN(IDIM1)
7      INTEGER VSC
8      WRITE(IWRT,10) ITER,LAMBDA,GFE,RMX
9      10 FORMAT('0',' ITERATION = ',I5.5X,'LAMBDA = ',E14.7,
10     &        5X,'GIBBS FREE ENERGY = ',E14.7,' KCAL',
11     &        5X,'RELATIVE ERROR = ',E12.5,'/0.1X,
12     &        'N-VALUES',T20,'DELTA-N VALUES',
13     &        T40,'DGTST VALUES')
14      DO 50 I=1,VSC
15      WRITE(IWRT,20) N(I),DELN(I),DGTST(I)
16      20 FORMAT(1X,E14.7,T20,E14.7,T40,E14.7)
17      50 CONTINUE
18      RETURN
19      END
```

Figure A24. Subroutine PRNTAB

```
1      SUBROUTINE PRNTAB(A,B,N,IDIM3,IWRT)
2 C
3 C  MATRIX OUTPUT ROUTINE FOR DIAGNOSTIC USE
4 C
5      DOUBLE PRECISION A(IDIM3,IDIM3),B(IDIM3)
6      MAX=N/10+1
7      LINE=0
8      IST=1
9      DO 50 I=1,MAX
10     LINE=LINE+N+2
11     IEND=IST+9
12     IF(IEND.GT.N) IEND=N
13     IF(LINE.GT.80) WRITE(IWRT,10) IST,IEND
14     IF(I.EQ.1) WRITE(IWRT,10) IST,IEND
15     IF(LINE.LE.80.AND.I.GT.1) WRITE(IWRT,20) IST,IEND
16     10 FORMAT('1','COLUMNS ',I2,' THROUGH ',I2,' OF MATRIX ALEQ:')
17     20 FORMAT('0','COLUMNS ',I2,' THROUGH ',I2,' OF MATRIX ALEQ:')
18     IF(LINE.GT.80) LINE=0
19     DO 40 ILIN=1,N
20     WRITE(IWRT,30) (A(ILIN,J),J=IST,IEND)
21     30 FORMAT(1X,10(D11.4,2X))
22     40 CONTINUE
23     IST=IEND+1
24     IF(IST.GT.N) GO TO 60
25     50 CONTINUE
26     60 CONTINUE
27     WRITE(IWRT,70)
28     70 FORMAT('0','THE TRANSPOSED BLEQ VECTOR IS:')
29     IST=1
30     DO 90 I=1,MAX
31     IEND=IST+9
32     IF(IEND.GT.N) IEND=N
33     WRITE(IWRT,80) (B(J),J=IST,IEND)
34     80 FORMAT(1X,10(D11.4,2X))
35     IST=IEND+1
36     IF(IST.GT.N) RETURN
37     90 CONTINUE
38     RETURN
39     END
```

A.4.18 IMSL Subroutines  
LINV1F, LEQT1F, LUDATF, LUELMF

The calling sequence of the IMSL subroutines is shown in Figure A25 and a listing of these subroutines is provided in Figure A26. These IMSL subroutines are used to perform matrix inversions and solve the matrix problem

$$A X = B \quad (1)$$

for vector  $X$ . The matrix inversion subroutine, LINV1F, is called from line 43 of subroutine IDPTEQ. LINV1F defines  $B$  to be a matrix instead of a vector and simply puts ones on the diagonal of this matrix and zeros elsewhere. Subroutine LEQT1F is then called upon to solve the matrix problem

$$A AINV = B \quad (2)$$

to yield the inverted  $A$  matrix AINV.

Subroutine LEQT1F is called from line 182 of subroutine RAND to solve the linear algebra problem in equation 1 for the vector  $X$ . The  $X$  vector solution is then returned as vector  $B$  in order to save on storage requirements. Double precision arithmetic is used in the calculations and the routines check for IDGT significant figures in the answers. If less than IDGT significant figures are found parameter IER is returned as 34. If matrix  $A$  is singular IER is returned as 129.

Figure A25

## IMSL Subroutine Calling Sequence

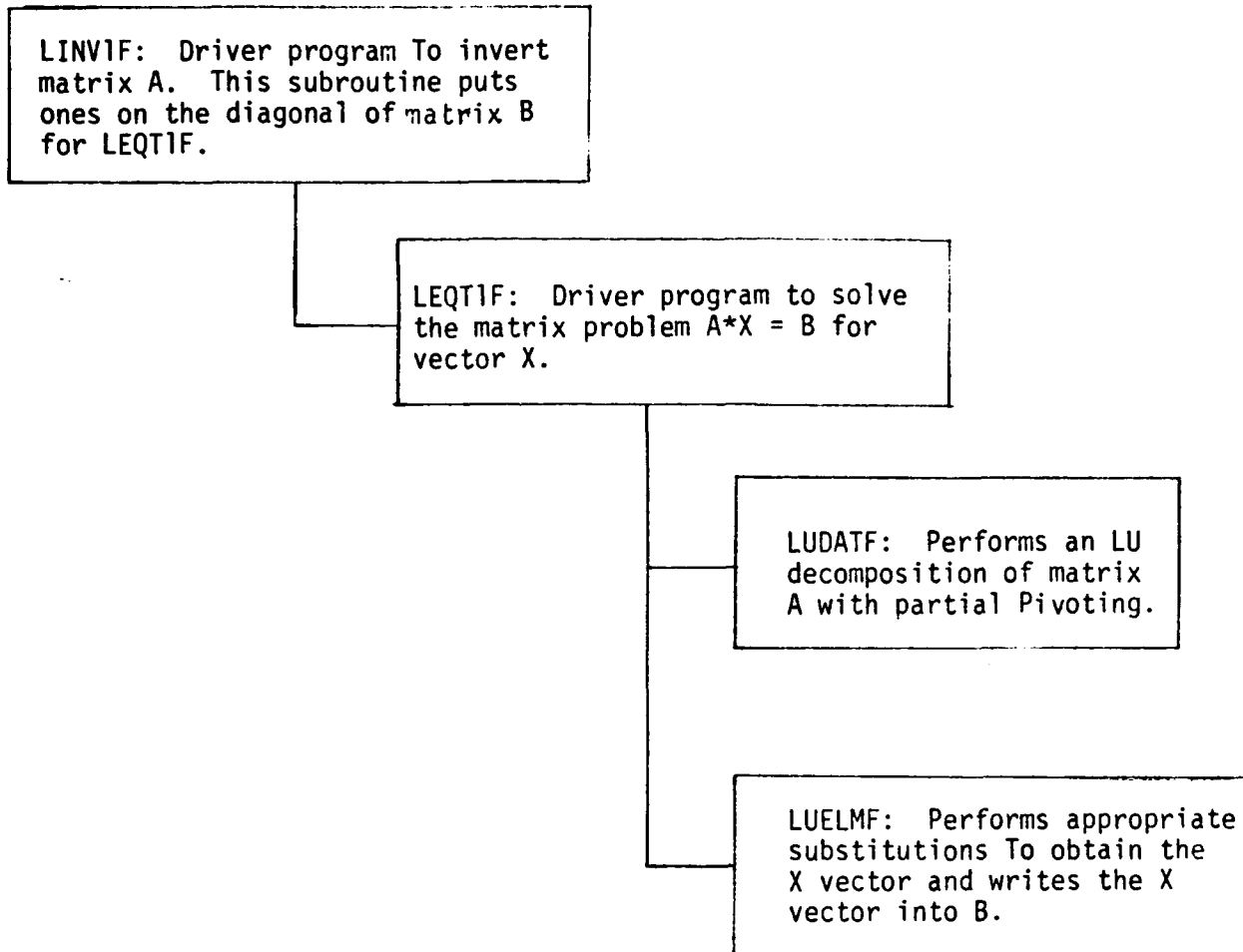


Figure A26. IMSL Subroutines LINVIF, LEQTIF, LUDATF and LUELMF.

```
1      SUBROUTINE LINVIF (A,N,IA,AINV,IDGT,WKAREA,IER)
2 C
3 C  IMSL SUBROUTINE FOR INVERTING REAL MATRICIES
4 C
5      DOUBLE PRECISION A(IA,N),AINV(IA,N),WKAREA(1),ZERO,ONE
6      DATA              ZERO/0.000/,ONE/1.000/
7      IER=0
8      DO 10 I=1,N
9          DO 5 J=1,N
10             AINV(I,J) = ZERO
11     5      CONTINUE
12             AINV(I,I) = ONE
13 10 CONTINUE
14      CALL LEQTIF (A,N,N,IA,AINV,IDGT,WKAREA,IER)
15      IF (IER .EQ. 0) GO TO 9005
16 9000 CONTINUE
17 9005 RETURN
18      END
```

```
1      SUBROUTINE LEQT1F (A,M,N,IA,B, IDGT,WKAREA,IER)
2 C
3 C      IMSL SUBROUTINE LEQT1F FOR SOLVING THE MATRIX PROBLEM A*X=B
4 C
5      DIMENSION          A(IA,1),B(IA,1),WKAREA(1)
6      DOUBLE PRECISION  A,B,WKAREA,D1,D2,WA
7 C                          INITIALIZE IER
8 C                          FIRST EXECUTABLE STATEMENT
9      IER=0
10 C                          DECOMPOSE A
11      CALL LUDATF (A,A,N,IA, IDGT,D1,D2,WKAREA,WKAREA,WA,IER)
12      IF (IER .GT. 128) GO TO 9005
13 C                          CALL ROUTINE LUELMF (FORWARD AND
14 C                          BACKWARD SUBSTITUTIONS)
15      DO 10 J=1,M
16          CALL LUELMF (A,B(1,J),WKAREA,N,IA,B(1,J))
17      10 CONTINUE
18      9005 RETURN
19      END
```

```

1      SURROUTINE LUDATF (A,LU,N,IA,IOGT,D1,D2,IPVT,EQUIL,WA,IER)
2 C
3 C THIS SUBROUTINE IS USED WITH SUBROUTINE LEOTIF
4 C
5      DIMENSION      A(IA,1),LU(IA,1),IPVT(1),EQUIL(1)
6      DOUBLE PRECISION A,LU,D1,D2,EQUIL,WA,ZERO,ONE,FOUR,SIXTN,SIXTH
7      *
8      DATA          RN,WREL,BIGA,BIG,P,SUM,AI,WI,T,TEST,Q
9      *              ZERO,ONE,FOUR,SIXTN,SIXTH/0.00,1.00,4.00,
10     *              16.00,.062500/
10 C
11 C
12     IER = 0
13     RN = N
14     WREL = ZERO
15     D1 = ONE
16     D2 = ZERO
17     BIGA = ZERO
18     DO 10 I=1,N
19         BIG = ZERO
20         DO 5 J=1,N
21             P = A(I,J)
22             LU(I,J) = P
23             P = DABS(P)
24             IF (P .GT. BIG) BIG = P
25     5 CONTINUE
26     IF (BIG .GT. BIGA) BIGA = BIG
27     IF (BIG .EQ. ZERO) GO TO 110
28     EQUIL(I) = ONE/BIG
29 10 CONTINUE
30     DO 105 J=1,N
31         JM1 = J-1
32         IF (JM1 .LT. 1) GO TO 40
33 C
34     DO 35 I=1,JM1
35         SUM = LU(I,J)
36         IM1 = I-1
37         IF (IOGT .EQ. 0) GO TO 25
38 C
39         AI = DABS(SUM)
40         WI = ZERO
41         IF (IM1 .LT. 1) GO TO 20
42         DO 15 K=1,IM1
43             T = LU(I,K)*LU(K,J)
44             SUM = SUM-T
45             WI = WI+DABS(T)
46     15 CONTINUE
47     LU(I,J) = SUM
48     20 WI = WI+DABS(SUM)
49     IF (AI .EQ. ZERO) AI = BIGA
50     TEST = WI/AI
51     IF (TEST .GT. WREL) WREL = TEST
52     GO TO 35
53 C
54     25 WITHOUT ACCURACY
55     IF (IM1 .LT. 1) GO TO 35

```

```

55          DO 30 K=1,IM1
56          SUM = SUM-LU(I,K)*LU(K,J)
57 30      CONTINUE
58          LU(I,J) = SUM
59 35      CONTINUE
60 40      P = ZERO
61 C          COMPUTE U(J,J) AND L(I,J), I=J+1.....
62          DO 70 I=J,N
63          SUM = LU(I,J)
64          IF (IDGT .EQ. 0) GO TO 55
65 C          WITH ACCURACY TEST
66          AI = DABS(SUM)
67          WI = ZERO
68          IF (JMI .LT. 1) GO TO 50
69          DO 45 K=1,JMI
70          T = LU(I,K)*LU(K,J)
71          SUM = SUM-T
72          WI = WI+DABS(T)
73 45      CONTINUE
74          LU(I,J) = SUM
75 50      WI = WI+DABS(SUM)
76          IF (AI .EQ. ZERO) AI = BIGA
77          TEST = WI/AI
78          IF (TEST .GT. WREL) WREL = TEST
79          GO TO 65
80 C          WITHOUT ACCURACY TEST
81 55      IF (JMI .LT. 1) GO TO 65
82          DO 60 K=1,JMI
83          SUM = SUM-LU(I,K)*LU(K,J)
84 60      CONTINUE
85          LU(I,J) = SUM
86 65      Q = EQUIL(I)*DABS(SUM)
87          IF (P .GE. Q) GO TO 70
88          P = Q
89          IMAX = I
90 70      CONTINUE
91 C          TEST FOR ALGORITHMIC SINGULARITY
92          IF (RN+P .EQ. RN) GO TO 110
93          IF (J .EQ. IMAX) GO TO 80
94 C          INTERCHANGE ROWS J AND IMAX
95          D1 = -D1
96          DO 75 K=1,N
97          P = LU(IMAX,K)
98          LU(IMAX,K) = LU(J,K)
99          LU(J,K) = P
100 75      CONTINUE
101          EQUIL(IMAX) = EQUIL(J)
102 80      IPVT(J) = IMAX
103          D1 = D1*LU(J,J)
104 85      IF (DABS(D1) .LE. ONE) GO TO 90
105          D1 = D1*SIXTH
106          D2 = D2+FOUR
107          GO TO 85
108 90      IF (DABS(D1) .GE. SIXTH) GO TO 95

```

```
109         D1 = D1*SIXTN
110         D2 = D2-FOUR
111         GO TO 90
112     95     CONTINUE
113         JP1 = J+1
114         IF (JP1 .GT. N) GO TO 105
115 C                                     DIVIDE BY PIVOT ELEMENT U(J,J)
116         P = LU(J,J)
117         DO 100 I=JP1,N
118             LU(I,J) = LU(I,J)/P
119     100     CONTINUE
120     105     CONTINUE
121 C                                     PERFORM ACCURACY TEST
122         IF (IDGT .EQ. 0) GO TO 9005
123         P = 3*N+3
124         WA = P*WREL
125         IF (WA+10.00**(-IDGT) .NE. WA) GO 9005
126         IER = 34
127         GO TO 9005
128 C                                     ALGORITHMIC SINGULARITY
129     110     IER = 129
130         D1 = ZERO
131         D2 = ZERO
132     9005     RETURN
133         END
```

```

1      SUBROUTINE LUELMF (A,B,IPVT,N,IA,X)
2 C
3 C THIS SUBROUTINE IS USED WITH SUBROUTINE LEOTIF
4 C
5      DIMENSION      A(IA,1),B(1),IPVT(1),X(1)
6      DOUBLE PRECISION  A,B,X,SUM
7 C                                FIRST EXECUTABLE STATEMENT
8 C                                SOLVE LY = B FOR Y
9      DO 5 I=1,N
10     5 X(I) = B(I)
11     IW = 0
12     DO 20 I=1,N
13         IP = IPVT(I)
14         SUM = X(IP)
15         X(IP) = X(I)
16         IF (IW .EQ. 0) GO TO 15
17         IM1 = I-1
18         DO 10 J=IW,IM1
19             SUM = SUM-A(I,J)*X(J)
20     10 CONTINUE
21         GO TO 20
22     15 IF (SUM .NE. 0.00) IW = I
23     20 X(I) = SUM
24 C                                SOLVE UX = Y FOR X
25     DO 30 IB=1,N
26         I = N+1-IB
27         IP1 = I+1
28         SUM = X(I)
29         IF (IP1 .GT. N) GO TO 30
30         DO 25 J=IP1,N
31             SUM = SUM-A(I,J)*X(J)
32     25 CONTINUE
33     30 X(I) = SUM/A(I,I)
34     RETURN
35     END

```

## A.5 Theoretical Development of the Rand algorithm

A variety of methods have been proposed for calculating compositions in multiphase, reacting systems at equilibrium. The technique derived here employs the Newton-Raphson method to minimize the Gibbs Energy of an ideal system. The problem may be formulated as follows: Given the initial mole numbers of all species, the temperature, and the pressure, determine the composition which minimizes the Gibbs Energy of an ideal mixture subject to atom balance constraints. The system considered here allows for the presence of a gas phase (with an inert species permitted), multiple pure condensed phases, and a condensed solution phase all existing in equilibrium. If we assume all mixtures behave in an ideal manner, the total Gibbs energy of the system,  $G^*(T, P, n_i)$ , can be expressed in terms of the temperature (T), pressure (P) and chemical

$$G^*(T, P, n_i)/RT = G = \sum_{i=1}^{v+s} n_i \left[ \mu_i^\circ + \ln \frac{n_i P}{n_v} \right] + Z_v \left[ \mu_z^\circ + \ln \frac{Z_v P}{n_v} \right] + \sum_{i=v+1}^{v+s} n_i \left[ \mu_i^\circ + \ln \frac{n_i}{n_s} \right] + \sum_{i=v+s+1}^{v+s+c} n_i \mu_i^\circ \quad (1)$$

In this expression the following notation is used:

$n_i$  = moles of species  $i$

$Z_v$  = moles of inert specie in the vapor phase

$n_v = \sum_{i=1}^v n_i + Z_v$  = total moles of vapor

$n_s = \sum_{i=v+1}^{v+s} n_i$  = total moles of condensed solution

$\mu_i^\circ$  = standard state chemical potential divided by RT

$v$  = number of vapor specie

$s$  = number of solution specie

$c$  = number of pure condensed phases present

The minimization problem is constrained by the conservation of atomic elements such that

$$\sum_{i=1}^{v+s+c} a_{ji} n_i - b_j = 0, \quad (2)$$

where  $a_{ji}$  is the number of atoms of element  $j$  per molecule of species  $i$  and  $b_j$  is the total number of gram-atoms of each of the  $E$  elements present in the system.

The first step involves an expansion of  $G$  in a quadratic Taylor series about a solution estimate  $\underline{n}^k$  as

$$G^{k+1} \approx G^k + \sum_{i=1}^{v+s+c} \delta n_i \frac{\partial G^k}{\partial n_i} + \frac{1}{2} \sum_{i=1}^{v+s+c} \sum_{\lambda=1}^{v+s+c} \delta n_i \delta n_\lambda \frac{\partial^2 G^k}{\partial n_i \partial n_\lambda} \quad (3)$$

where  $n_i = n_i^{k+1} - n_i^k$ . The partial derivatives required in Equation (3) are found by analytical differentiation of Equation 1. After differentiation and simplification the results are:

For  $i = 1, \dots, v$

$$\partial G^k / \partial n_i = \mu_i^\circ + \lambda n \frac{n_i^P}{n_v} \quad (4)$$

$$\frac{\partial^2 G^k}{\partial n_i^2} = \frac{1}{n_i} - \frac{1}{n_v} \quad (5)$$

and

$$\frac{\partial^2 G^k}{\partial n_i \partial n_{\ell \neq i}} = -1/n_v \quad (6)$$

For  $i = v+1, \dots, v+s$

$$\partial G^k / \partial n_i = \mu_i^\circ + \lambda n \frac{n_i}{n_s} \quad (7)$$

$$\partial^2 G^k / \partial n_i^2 = 1/n_i - 1/n_s \quad (8)$$

$$\partial^2 G^k / \partial n_i \partial n_{\ell \neq i} = -1/n_s \quad (9)$$

and

For  $i = v+s+1, \dots, v+s+c$

$$\partial G^k / \partial n_i = \mu_i^{\circ} \quad (10)$$

$$\partial^2 G^k / \partial n_i^2 = \frac{\partial^2 G^k}{\partial n_i \partial n_{\ell \neq i}} = 0 \quad (11)$$

Upon substituting Equations 4 - 11 into 3 and simplifying the following result is found

$$\begin{aligned} G^{k+1} = G^k &+ \sum_{i=1}^v \delta n_i \left[ \mu_i^{\circ} + \ell n \frac{n_i P}{n_v} \right] + \frac{1}{2} \sum_{i=1}^v \left[ \frac{\delta n_i^2}{n_i} - \frac{\delta n_i \delta n_v}{n_v} \right] \\ &+ \frac{1}{2} \sum_{i=v+1}^{v+s} \left[ \frac{\delta n_i^2}{n_i} - \frac{\delta n_i \delta n_s}{n_s} \right] + \sum_{i=v+s+1}^{v+s+c} \delta n_i \mu_i^{\circ} \quad (12) \end{aligned}$$

Since the atom balance must also be satisfied for the new solution estimate,  $\underline{n}^{k+1}$ , the subtraction of  $\sum_{i=1}^{v+s+c} a_{ji} n_i^{k+1} - b_j$  for all elements E from  $G^{k+1}$  will not change its value as is easily ascertained from Equation 2. An unconstrained objective function,  $\phi^{k+1}$ , results when using Lagrange multipliers for each atom balance,  $\pi_j$  ( $j=1, 2, \dots, E$ ).

$$\phi^{k+1} = G^{k+1} + \sum_{j=1}^E \pi_j \left( - \sum_{i=1}^{v+s+c} a_{ji} n_i^{k+1} + b_j \right) \quad (13)$$

The problem has now been reduced to minimizing  $\phi^{k+1}$  as:

$$\frac{\partial \phi^{k+1}}{\partial n_i^{k+1}} = 0 \quad (14)$$

$$= \mu_i^{\circ} + \ell n \frac{n_i P}{n_v} + \frac{\delta n_i}{n_i} - \sum_{j=1}^v \frac{\delta n_j}{n_v} - \sum_{j=1}^E \pi_j a_{ji} \quad \text{for } 1 \leq i \leq v \quad (15)$$

$$= \mu_i^{\circ} + \ell n \frac{n_i}{n_s} + \frac{\delta n_i}{n_i} - \sum_{j=v+1}^s \frac{\delta n_j}{n_s} - \sum_{j=1}^E \pi_j a_{ji} \quad \text{for } v+1 < i < v+s \quad (16)$$

$$= \mu_i^{\circ} - \sum_{j=1}^E \pi_j a_{ji} \quad \text{for } v+s+1 < i < v+s+c \quad (17)$$

with the addition of Equation 2 rewritten as

$$\sum_{i=1}^{v+s+c} a_{ji} (\delta n_i + n_i) = b_j \quad \text{for } 1 < j < E \quad (18)$$

we now have  $v+s+c+E$  linear equations (Equations 15 - 18) in the same number of unknowns ( $v+s+c$   $\delta n_i$ 's and  $E$   $\pi_j$ 's). The number of independent linear equations that must be solved simultaneously can be reduced by hand elimination of  $v+s-2$  equations as follows: Solving Equations 15 and 16 for  $\delta n_i$  yields

$$\delta n_i = n_i \left[ \sum_{j=1}^v \frac{\delta n_j}{n_v} + \sum_{j=1}^E \pi_j a_{ji} - \mu_i^{\circ} - \ln \frac{n_i^p}{n_v} \right] \quad \text{for } 1 < i < v \quad (19)$$

and

$$\delta n_i = n_i \left[ \sum_{j=v+1}^{v+s} \frac{\delta n_j}{n_s} + \sum_{j=1}^E \pi_j a_{ji} - \mu_i^{\circ} - \ln \frac{n_i}{n_s} \right] \quad \text{for } v+1 < i < v+s \quad (20)$$

Equations 19 and 20 contain only  $\delta n_i$  on the right hand side in terms of  $\sum_{j=1}^v \frac{\delta n_j}{n_v}$  and  $\sum_{j=v+1}^{v+s} \frac{\delta n_j}{n_s}$  and we shall designate these two summations as the new variables  $u_v$  and  $u_s$ , respectively. With Equations 19 and 20

$\delta n_i$  for  $1 < i < v+s$  can be eliminated in Equation 18 with the result

$$\sum_{\ell=1}^E \pi_{\ell} \sum_{i=1}^{v+s} a_{ji} a_{\ell i} n_i + u_v \sum_{i=1}^v a_{ji} n_i + u_s \sum_{i=v+1}^{v+s} a_{ji} n_i + \sum_{i=v+s+1}^{v+s+c} a_{ji} \delta n_i =$$

$$b_j - b_j^k + \sum_{i=1}^v a_{ji} n_i \left[ \mu_i^{\circ} + \ln \frac{n_i^p}{n_v} \right] + \sum_{i=v+1}^{v+s} \left[ \mu_i^{\circ} + \ln \frac{n_i}{n_s} \right] a_{ji} n_i \quad \text{for } 1 < j < E \quad \dots(21)$$

where  $b_j^k$  is the gram-atoms of element  $j$  in system as determined by the mole numbers  $\underline{n}_i^k$  and  $b_j$  is provided by the initial condition.

Besides Equations 17 and 21, two additional equations are required.

As only  $v+s-2$   $\delta n_i$  variables were hand eliminated, the remaining two equations must be a linear combination of this set, for example  $\sum_{i=1}^v \delta n_i$  and  $\sum_{i=v+1}^{v+s} \delta n_i$  results in

$$\sum_{\ell=1}^E \pi_{\ell} \sum_{i=1}^v a_{\ell i} n_i - z_v u_v = \sum_{i=1}^v n_i \left( \mu_i^0 + z_n \frac{n_i P}{n_v} \right) \quad (22)$$

and

$$\sum_{\ell=1}^E \pi_{\ell} \sum_{i=v+1}^{v+s} a_{\ell i} n_i = \sum_{i=v+1}^{v+s} n_i \left( \mu_i^0 + z_n \frac{n_i}{n_s} \right) \quad (23)$$

Thus the final set of linear equations to be solved includes Equations 17, 21 - 23 ( $E + c + 2$  equations) for unknowns  $\pi_{\ell}$  ( $1 < \ell < E$ ),  $\delta n_i$  ( $v+s+1 < i < v+s+c$ ),  $U_v$  and  $u_s$ .

The procedure is thus to input the temperature, pressure, all species possibly present along with their standard state chemical potential and formula vector ( $a_{ji}$ ), total gram-atoms of each element present ( $b_j$ ), and an initial guess of the equilibrium composition. The solution of Equations 17 and 21 - 23 for  $\pi_{\ell}$ ,  $u_v$ ,  $u_s$  and the  $C$   $\delta n_i$ 's allows the computation of the remaining  $v+s$   $\delta n_i$ 's with Equations 19 and 20. A new solution estimate can now be obtained as

$$n_i^{k+1} = n_i^k + \delta n_i \quad (24)$$

This procedure is repeated with the new solution estimate until the composition converges to within a specified increment of the last two solutions estimates.

#### A.6 Example Calculation: The Ga, As, H System.

Figure A27 shows the results of an equilibrium calculation for the Ga, As and H system. The wrap-up file output is shown in Figure A28 and the data file which yielded these results is shown in Figure A29. This calculation determines the equilibrium composition of a system which initially consisted of 10% As, 10% Ga, 10% H<sub>2</sub> and 70% inert in the vapor phase. The calculation was performed for a temperature of 1000 C at one atmosphere pressure.

This example is provided as a demonstration of the data file required and type of output received. It is not intended to represent a CVD process.





RAND ALGORITHM FOR DETERMINING EQUILIBRIUM COMPOSITIONS  
THE GAS/LIQUID SYSTEM WITH AN INERT PRESENT A TEST OF MCHPEC.MAND.  
TEMPERATURE = 1273.2 K PRESSURE = 0.101325 06 PA  
EXECUTION DIAGNOSTICS



PAGE 5

RAND ALGORITHM FOR DETERMINING EQUILIBRIUM COMPOSITIONS  
 THE CAVAS/H SYSTEM WITH AN INERT PRESENT A TEST OF MCIPREC RAND  
 TEMPERATURE = 1273.2 K PRESSURE = 0.10132506 PA  
 A SET OF INDEPENDENT REACTION EQUATIONS FOR THIS SYSTEM IS AS FOLLOWS

```
( 1.00 AS2 (V)      ) - ( 0.200E 01 AS (V)      )
( 1.00 AS3 (V)      ) - ( 0.300E 01 AS (V)      )
( 1.00 AS4 (V)      ) - ( 0.400E 01 AS (V)      )
( 1.00 AS-H2 (V)    ) - ( 0.200E 01 AS (V)      ) + ( 0.200E 01 AS-H (V)    )
( 1.00 H (V)       ) - ( 0.100E 01 AS (V)      ) + ( 0.100E 01 AS-H (V)    )
( 1.00 H2 (V)      ) - ( 0.200E 01 AS (V)      ) + ( 0.200E 01 AS-H (V)    )
( 1.00 GA-H2 (S)   ) - ( 0.100E 01 AS (V)      ) + ( 0.100E 01 GA (V)      )
```

RAND ALGORITHM FOR DETERMINING EQUILIBRIUM COMPOSITIONS  
 OF A GAS/SM SYSTEM WITH AN INERT PRESENT A TEST OF MCPPEC RAND  
 TEMPERATURE = 1273.2 K PRESSURE = 0.101325 06 PA

EQUILIBRIUM CONSTANTS FOR THE INDEPENDENT REACTIONS

REACTION PRODUCT	FREE ENERGY CHANGE (KCAL/MOLE)	EQUILIBRIUM CONSTANT FROM SUPPLIED ENERGY	EQUILIBRIUM CONSTANT FROM PREDICTED COMPOSITION
AS2 (V)	0	0 100000E 00	0 78742E 10
AS3 (V)	27 640	0 17911E 10	0 17109E 16
AS4 (V)	-19 025	0 17109E 16	0 27926E 22
AS4 H (V)	-14 440	0 27926E 22	0 97979E 00
AS4 H2 (V)	0	0 10000E 01	0 98635E 00
AS4 H3 (V)	0 105	0 10000E 01	0 10000E 01
AS4 (V)	0	0 28356E-05	0 28356E-06
H2 (V)	0	0 28012E 00	0 28012E 00
SA-AS (S)	57 051	0 71259E 12	0 71259E 12





References

1. Clasen R. J., The RAND Corporation, RM-4345-PR, Jan. 1965.
2. Shaw D.W., J. Crystal Growth, 8, 1971.
3. Thurmond C.D., J. Phys. Chem. Solids, 26, 1965.
4. Prausnitz J.M., Molecular Thermodynamics of Fluid-Phase Equilibrium, Prentice Hall, 1969.
5. Shafer M. and Weiser K., J. Phys. Chem. 61, 1957.
6. Cruise, D.R., J. Phys. Chem., 8, 18, 1964.
7. Clark M. and Hansen K., Numerical Methods of Reactor Analysis, Academic Press, 1964.
8. Smith W.R. and, Ind. Eng. Chem. Fund., 19, 1980.
9. Smith W.R. and Missen R. W., Canad. J. of Chem. Eng., 46, 1968.
10. Vieland L.J., Acta Metallurgica, 11, 1963.
11. Perea and Fonstad, J. Electrochem. Soc. 127, 2, 1980.
12. Boomgard and Schol, Philips Res. Rep., 12, 127, 1957.
13. Sol, Claviou, Linh, Moulin, J. Cryst. Growth, 127, 325.
14. Hall, J. Electrochem. Soc., 110, 385, 1963.
15. Koster and Thoma, Z. Metall. 46, 291, 1955.

## 10. Appendix B. MCMPEC.STOIC: A Computer Code for Calculating Chemical Equilibria Using a Stoichiometric Algorithm

### B.1 Introduction

### B.2 The Main Program

- B.2.1 Array Dimensions, Expandability and Initialization
- B.2.2 Data Input
- B.2.3 Preparation for the Iterative Solution
- B.2.4 Iterative Solution for the Equilibrium Composition
- B.2.5 Output of Results
- B.2.6 Listing of the Main Program

### B.3 A Description of the Major Variables in MCMPEC.STOIC

### B.4 Descriptions of the Subroutines

- B.4.1 STSTCP
- B.4.2 ESTMTE
- B.4.3 STEADY
- B.4.4 TOSI
- B.4.5 RATIO
- B.4.6 OPTBAS
- B.4.7 TESTD
- B.4.8 EQCON
- B.4.9 ACTCOF
- B.4.10 CALCO
- B.4.12 CNVFC and DGDLM
- B.4.13 CORMOL
- B.4.14 ORDER
- B.4.15 WRAPUP
- B.4.16 DEBUG
- B.4.17 GIBBS
- B.4.18 PMAT, DPMAT, PVEC and IPVEC
- B.4.19 IMSL Subroutines LINVIF, LEQTIF, LUELMF, LUDATF

### B.5 Theoretical Development of the Stoichiometric Algorithm

### B.6 Example Calculation: The Ga/As system source zone

## Appendix B

## MCMPEC.STOIC: A Computer Code for Calculating Chemical Equilibria Using a Stoichiometric Algorithm.

B.1 Introduction

The calculation of chemical equilibrium using a stoichiometric algorithm is based on the work of Cruise [1] and Smith and Missen [2]. The stoichiometric algorithm requires a set of formation reaction equations for each specie of the form

$$S_i = \sum_{j=1}^E v_{ij} S_j^b \quad (1)$$

where:  $S_i$  = specie being formed

$S_j^b$  = basis specie in the system

$v_{ij}$  = reaction coefficient

$E$  = number of elements in the system

An optimum set of basis species is chosen by selecting those species which represent all of the elements present in the system, are linearly independent from each other and are present in the greatest molar amounts. Employing this set of optimum basis species minimizes the number of iterations required in the numerical solution.

The iterative solution for equilibrium composition proceeds by calculating equilibrium constants for each formation reaction using the Gibbs Free Energy change of the reaction and the current estimate to the equilibrium composition. These two values are compared and the extents of each formation reaction are then adjusted to yield a better approximation to the system equilibrium composition. Since the formation reactions are initially balanced the conservation of mass constraint is implicitly included.

The application of an explicit set of formation reaction equations results in a greater flexibility for stoichiometric algorithms as compared to nonstoichiometric algorithms. There are no restrictions upon the types of phases which must be present, i.e. systems which do not include a vapor phase are solvable. Also, it is not necessary to remove pure condensed phases as their compositions vanish since the reaction extents simply vanish. The storage requirements for this stoichiometric algorithm are much less than those of the Rand algorithm in Appendix A. Only 87 k-bytes are required for a system consisting of 50 species composed of up to 13 elements.

MCMPEC.STOIC assumes the vapor phase to be ideal and includes an inert specie. The solution phase may have nonidealities described by Henry's Law, simple solution theory or may be modelled as ideal. The code includes options to allow temperature, pressure and inlet composition loops in order to generate data for parametric analyses.

Currently there is evidence which suggests that the liquid solution in the source zone of the CVD halide system is at steady state [3]. An option has therefore been included to model this situation in the Ga/As and In/P systems. Several data output and debugging options have also been included and are discussed in subsection B.2.2.

The structure of the main program along with data input and output are discussed in section B.2. A description of the major variables in the code is located in section B.3 and discussions of each subroutine are presented in section B.4. The theoretical development of the stoichiometric algorithm is presented in section B.5 and an example calculation is located in section B.6.

## B.2 The Main Program

A flowsheet for MCMPEC.STOIC is shown in Figure B1. The main program sets array dimensions, provides a framework for calling the subroutines and performs data input and output. The temperature, pressure and composition loops, for generating parametric data, and the iteration loop for determining the equilibrium composition are also located in the main program. Data output which does not take place in the main program occurs in subroutines DEBUG, PMAT, DPMAT, PVEC, IPVEC and WRAPUP. Output which is useful for debugging purposes is written by DEBUG, PMAT, DPMAT, PVEC and IPVEC while WRAPUP writes out a concise file which summarizes the results. Also, execution diagnostics which pertain to the various subroutines are written out by the appropriate subroutine.

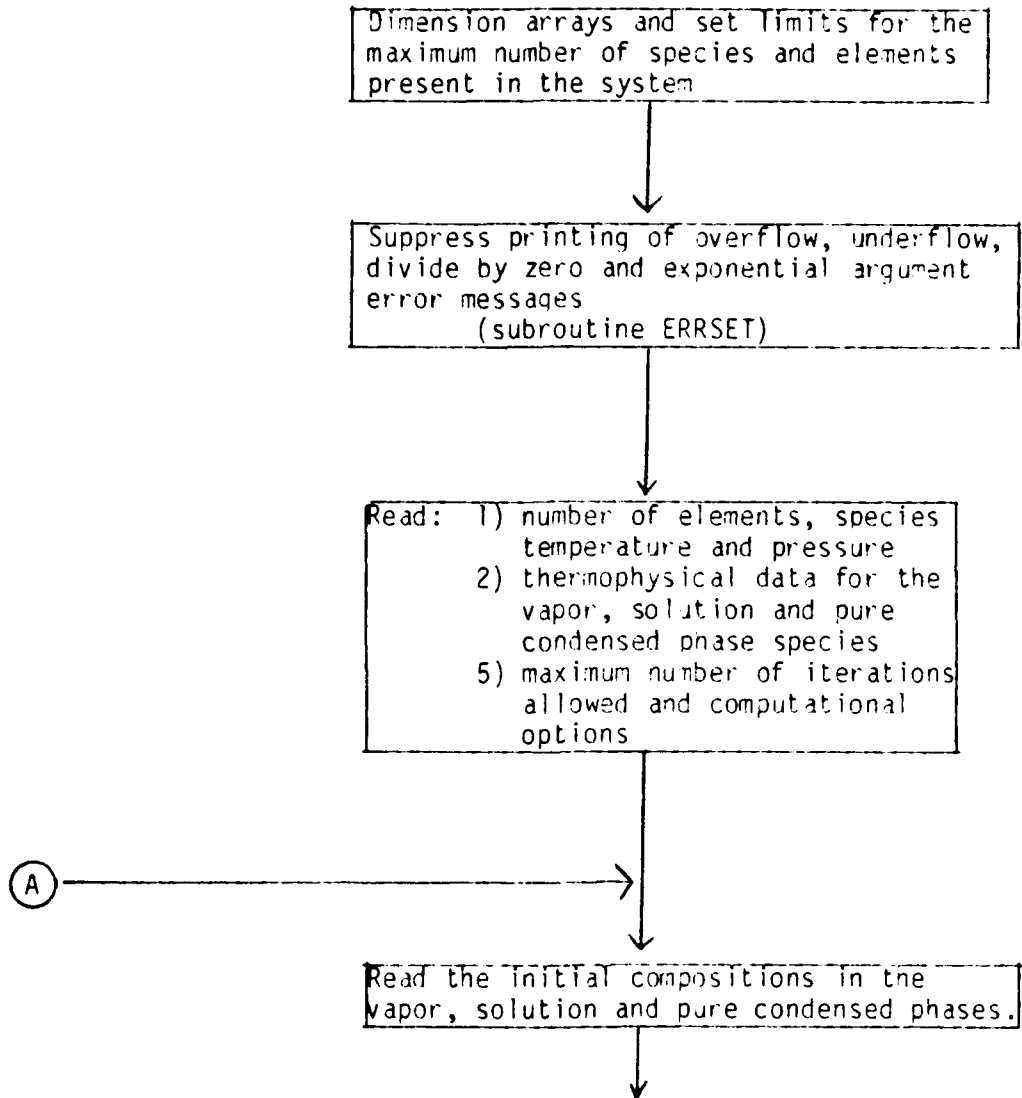
A listing of the main program is located in section B.2.6.

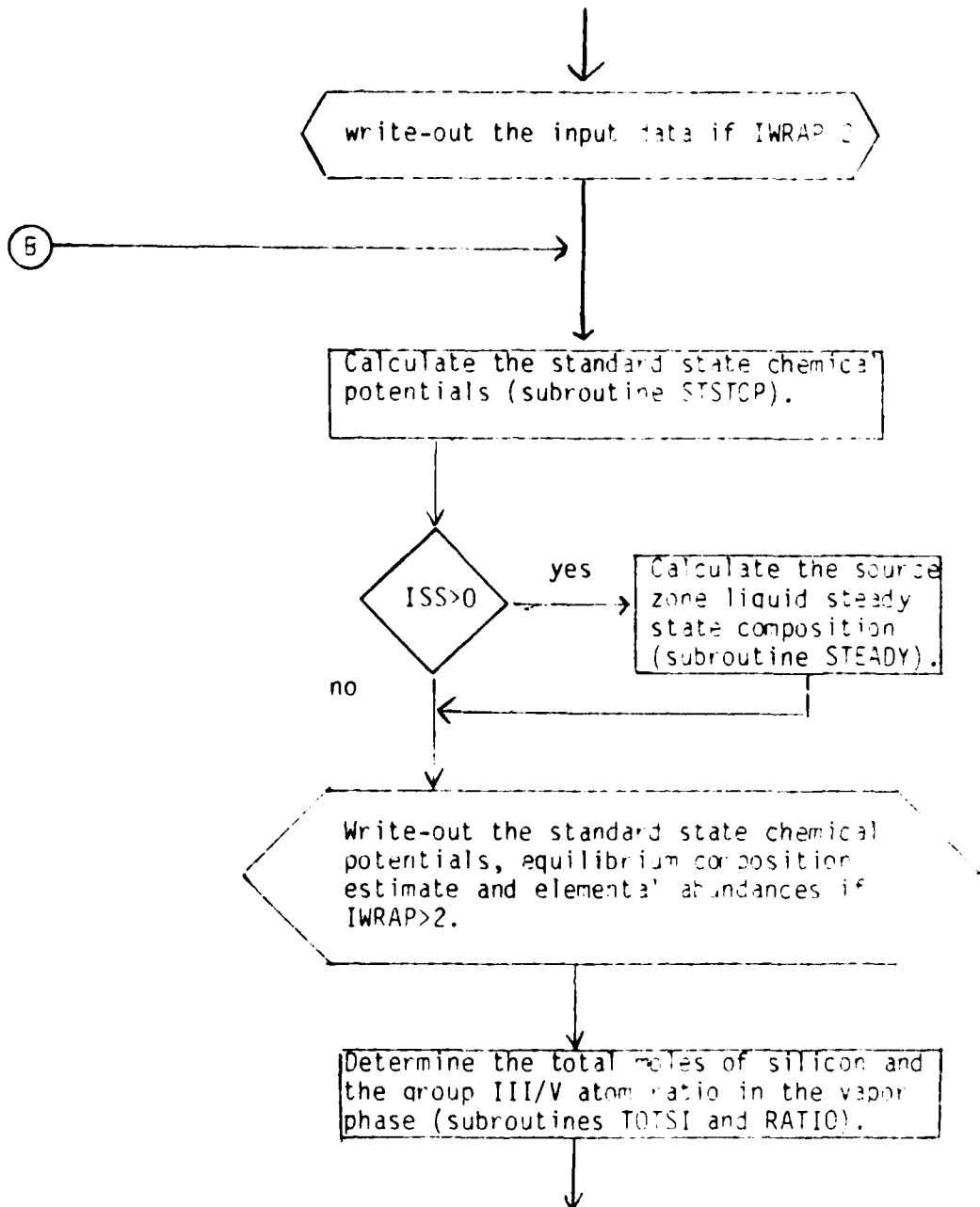
### B.2.1. Array Dimensions, Expandability and Initialization.

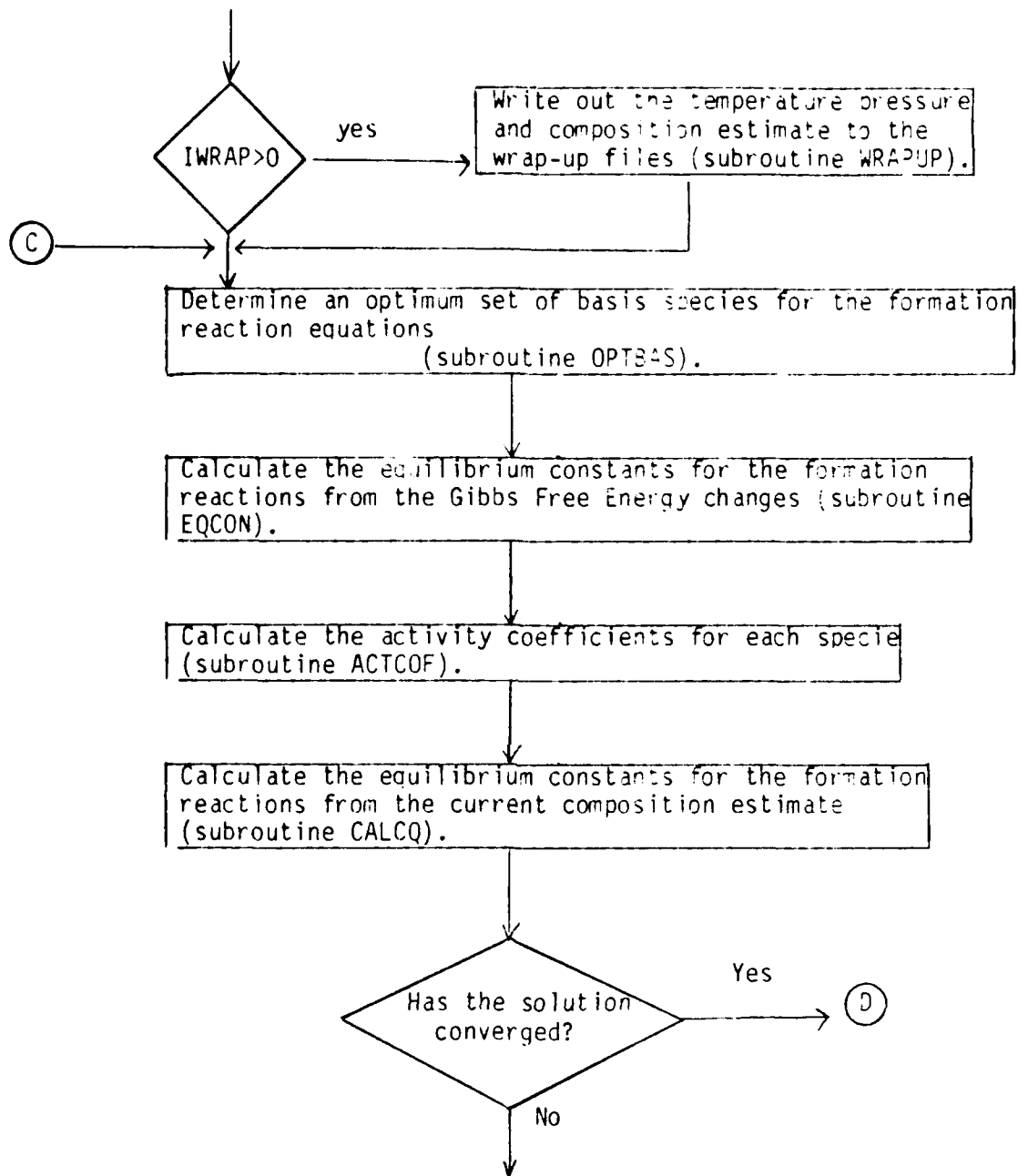
The arrays used in MCMPEC.STOIC are dimensioned in lines 5 through 19. Currently, systems containing up to 50 different species comprised of up to 13 different elements may be modelled. The variables IDIMI and IDIM2, which are initialized in lines 35 and 36, are used to set the array dimensions in the subroutines. Therefore, the code may be expanded to accommodate larger systems simply by modifying the array dimensions in the main program and the values of IDIMI and IDIM2. It is suggested that the element dimension IDIM2 not be increased beyond 13 as this will result in output line lengths greater than 132 characters which will be difficult to read as a result of printer "wrap-around". There are no restrictions (other than available computer memory) to the number of species which the code may be expanded to accommodate.

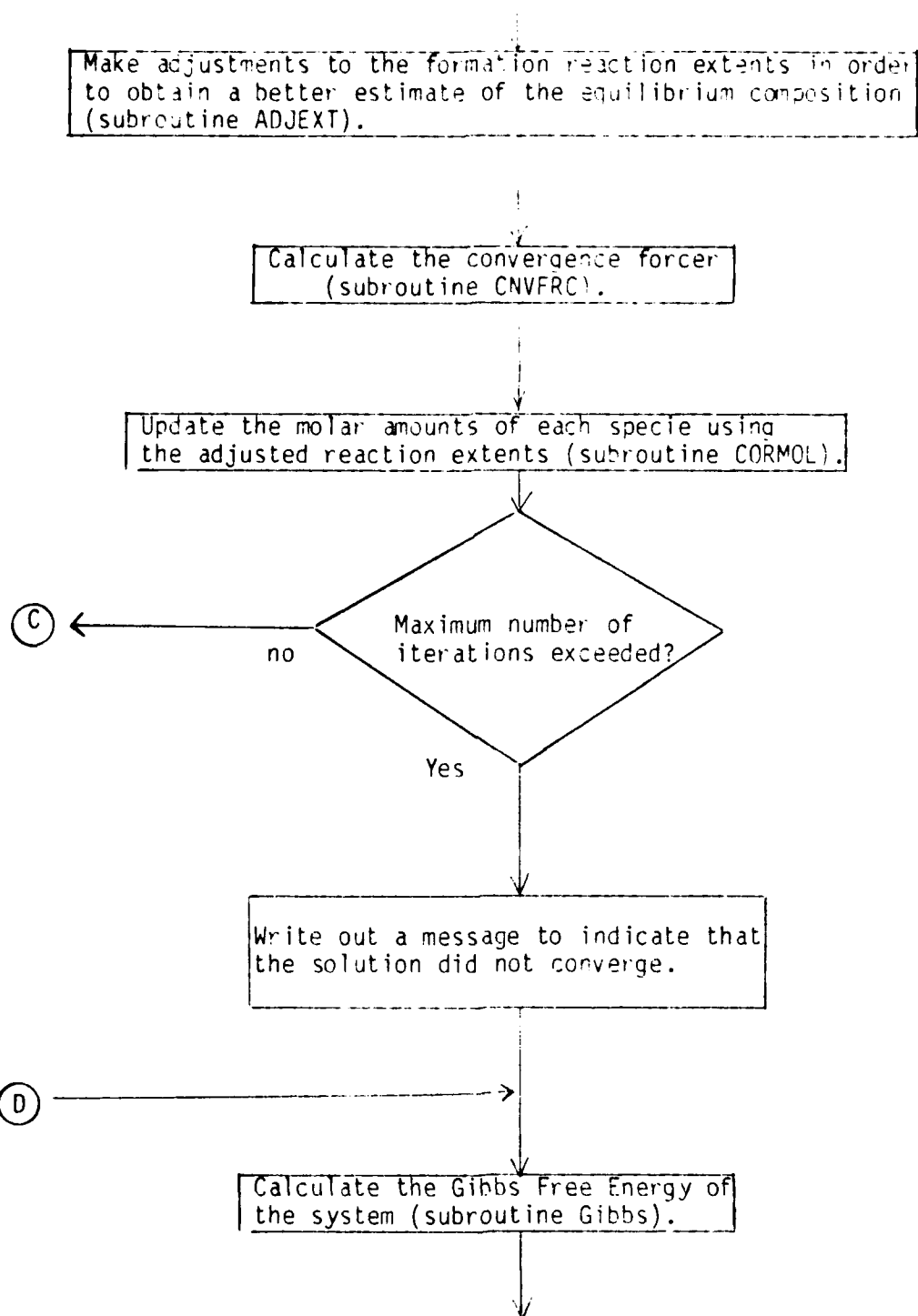
The logical unit designators for the input file, printed output and the wrap-up file are initialized at lines 32, 33 and 34.

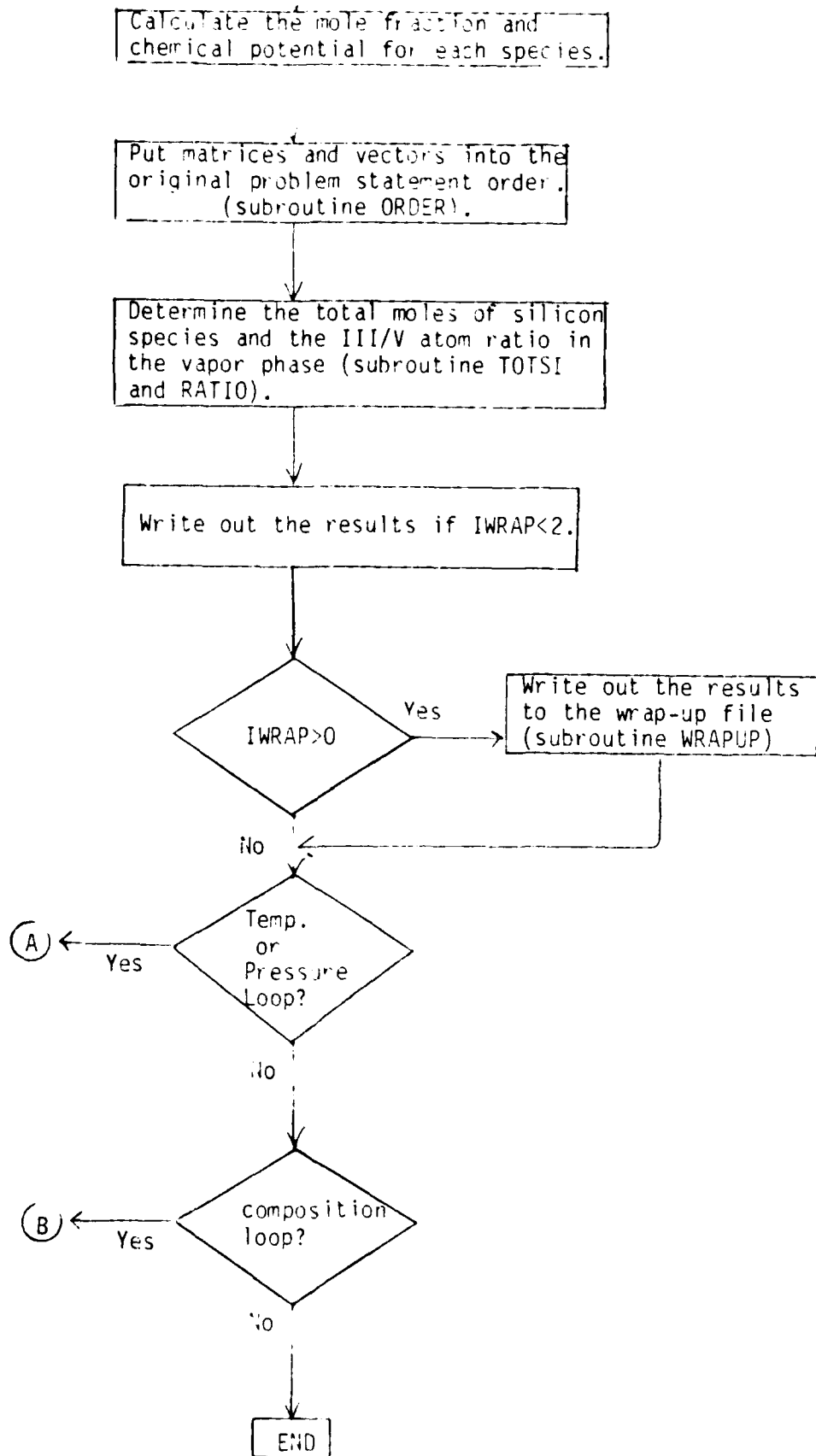
Figure 31

Main Program Flowsheet for MCMPEC.STOIC









Lines 49 and 50 call the system subroutine ERRSET to suppress printing of overflow, underflow, divide by zero and exponential argument error messages. These errors occur quite frequently in subroutine CALCQ during the first few iterations as a result of the small initial concentrations of some of the species.

### B.2.2 Data Input

Data input is accomplished in lines 51 through 159. A summary of the input data set is shown in Table B.1 and a description of each input variable is located in Table B.2.

The first input record consists of a data set title which may be up to 80 characters in length. The second record consists of the number of elements in the system, the number of species in the vapor, solution and pure condensed phases, followed by the system temperature and pressure. The last two pieces of information on this record are the reference temperature and pressure for the enthalpies and entropies of formation. The symbols for each element are on the third record. Two characters are allowed for each element symbol.

The next  $3V$  records contain information regarding the species present in the vapor phase. The first record contains a 12 character specie name and the enthalpy and entropy of formation at temperature  $T_0$  and pressure  $P_0$  for this specie. Heat capacity correlation information is contained on the second record and the number of atoms of each element which are present in a single molecule of the specie are on the third record. Records  $3V+1$  to  $3V+3$  contain this same information for an inert specie in the vapor phase. The inert specie information must always be present in the data set. When it is desired to perform a calculation without the inert, its initial concentration is simply set to zero. This same information must also be provided for each specie in the solution phase and each pure condensed phase.

Table B.1  
Input Data Set for MCMPEC.STOIC

Record	Comments	Format
Title (1),.... TITLE (20)	80 Character Title	20A4
E, V, S, C, T, P, T <sub>0</sub> , P <sub>0</sub>		4I5, 4F10.0
ELMNT (1), ELMNT (2) .... ELMNT (E)	Element Symbols	13 (1X, A2)
SPECIE (I,K), DMO(I), DSO(I)		3A4, 2E12.5
AO(I), AI(I), A2(I), A3(I), ICP(I)	Each vapor phase specie	4E12.5, I2
A(I,1), A(I,2).... A(I,E)		13(F5.0, 1X)
Inert(K), DHOZ, DSOZ		3A4, 12E12.5
AOZ, AIZ, A2Z, A3Z, ICPZ	Inert vapor phase specie	4E12.5, I2
IDUMMY		13(F5.0, 1X)
SPECIE(I, K), DHO(I), DSO(I)		3A4, 12E12.5
AO(I), AI(I), A2(I), A3(I), ICP(I)	Each solution phase specie	4E12.5, I2
A(I,1), A(I,2),...A(I,E)		13(F5.0,1X)
SPECIE(I,K), A2(I), A3(I), ICP(I)		3A4, 12E12.5
AO(I), AI(I), A2(I), A3(I), ICP(I)	Each pure condensed phase	4E12.5, I2
A(I,1), A(I,2)...A(I,E)		13(F5.0,1X)
IDERUG, IOPT, ISS, IWRAP, MAXIT, NMAX CNVG, TINC, PINC, RLXMIN		6I5, 4F10.0
TOTMV		E12.5
FRAC(1), FRAC(2).... FRAC(V), FRACZ		6E12.5
TOTMS		E12.5
FRAC(V+1), FRAC(V+2)... FRAC(V+S)		6E12.5
IXSCOR, AXS, BXS		15, 2E12.5
TOTMC(V+S+1)...TOTMC(V+S+C)		6E12.5

Table B.2

Description of Input Variables

<u>Variable</u>	<u>Description</u>
TITLE (20)	80 Character data set title
E	Number of elements ( $E \leq 13$ )
V	Number of vapor species excluding the inert
S	Number of solution species
C	Number of pure condensed phases
T	System Temperature (K)
P	System Pressure (Pa)
T0	Reference Temperature for $\Delta H$ and $\Delta S$ formation
P0	Reference Pressure for $\Delta H$ and $\Delta S$ formation
ELMNT (13)	2 character symbol for each element (right justified)
SPECIE (50, 3)	12 character symbol for each specie
A (50, 13)	Elemental abundance matrix
DHO (50)	Enthalpy of formation (kcal/g-mole) for each specie at Temperature T0 and Pressure P0.
DSO (50)	Entropy of formation (kcal/g-mole-K) for each specie at Temperature T0 and Pressure P0.
A0 (50)	Heat capacity correlation parameter (kcal/g-mole-K)
A1 (50)	Heat capacity correlation parameter (kcal/g-mole-K <sup>2</sup> )
A2 (50)	Heat capacity correlation parameter (see Table)
A3 (50)	Heat capacity correlation parameter (see Table)
ICP (50)	Heat capacity correlation parameter (see Table)

Heat Capacity Correlations

<u>ICP (I)</u>	<u>A2 (I)</u>	<u>A3 (I)</u>	<u>Correlation</u>
0	kcal-K/g-mole	kcal/g-mole-K-2n(k)	$A0+A1*T+A2/T^2+A3*2n(T)$
1	kcal/g-mole-K <sup>3</sup>	kcal/g-mole-K <sup>4</sup>	$A0+A1*T+A2*T^2+A3*T^3$

INERT(3)		12 Character name for inert vapor specie
DHOZ		Inert Specie enthalpy of formation
DSOZ		Inert Specie entropy of formation
A0Z	}	Inert specie heat capacity correlation parameter
A1Z		
A2Z		
A3Z		
ICPZ		
IDEBUG		Debugging Output parameter
	<u>IDEBUG</u>	<u>Function</u>
	0	Warning messages are printed when problems are encountered in the IMSL subroutines
	1	Prints IDEBUG=0 option plus composition changes and Gibbs energy for each iteration.
	2	Prints IDEBUG=1 option plus matrices and vectors D, DPRME, KEQ and Q for each iteration
IOPT		Looping Option Parameter
	<u>IOPT</u>	<u>Function</u>
	0	One pass through routine
	1	Temperature loop
	2	Pressure loop
	3	Composition loop
ISS		Source Zone Steady State Option Parameter
	<u>ISS</u>	<u>Function</u>
	0	Steady state option is inactive
	1	Ga/As liquid composition is at steady state with GaAs solid.
	2	In/P liquid composition is at steady state with InP solid.

	Data output option	parameter	
IWRAP	<u>IWRAP</u>	<u>Function</u>	
	0	Write-out input data, execution diagnostics and results to printer	
	1	IWRAP=0 function plus writes-out a concise wrap-up file.	
	2	No printer output, just a wrap-up file	
	3	Write a wrap-up to the printer	
MAXIT	Maximum number of iterations allowed for the equilibrium composition to converge		
NMAX	maximum number of loops allowed for the IOPT parameter		
CNVG	convergence criterion		
TINC	temperature increment for each loop if IOPT=1		
PINC	pressure increment for each loop if IOPT=2		
TOTMV	total moles in the vapor phase		
TOTMS	total moles in the solution phase		
TOTMC(I)	total moles in each pure condensed phase		
FRAC(I)	mole fraction of specie i in vapor ( $1 \leq I \leq V$ )		
	mole fraction of specie i in solution ( $V+1 \leq I \leq V$ )		
FRACZ	mole fraction of inert in vapor		
IXSCOR	<u>IXSCOR</u>	<u>Correlation</u>	activity coefficient correlation parameter for the solution phase
	0	ideal solution	
	1	binary simple solution	
	2	Henry's law	
AXS, BXS	<u>IXSCOR</u>	<u>Correlation</u>	activity coefficient correlation coefficient for the solution phase
	0	ideal solution	
	1	$G^E = (AXS + BXS * T) * X1 * X2$	
	2	$H = AXS * EXP (BXS/T)$	
RLYMIN	minimum value of the convergence factor		

Following the data for each individual specie is a record describing the various options available and numerical methods information. Parameter IDEBUG should be set to zero for production jobs but may be set to 1 or 2 to provide information which allows the code to be examined in a step by step fashion.

Parameter IOPT allows the code to be looped in order to generate temperature, pressure or composition parametric curves. NMAX sets the number of loops to be executed while TINC and PINC are the temperature and pressure increments per loop. If a composition loop is desired a new initial composition data set must be provided for each loop.

Parameter ISS is used to activate the steady state liquid source option. If ISS is set to 1 the composition of a liquid containing Ga and As in equilibrium with GaAs solid is calculated. This liquid is inserted as the last pure condensed phase in the system. Thus when the value of C (number of pure condensed phases) is specified it must include a steady state phase if ISS>0 otherwise the last pure condensed phase in the system will be replaced with the steady state liquid. Setting ISS=2 will model a liquid of In and P in equilibrium with InP solid.

The parameter IWRAP is used to choose the amount of data output desired. When IWRAP=0 the input data is written out in tabulated form along with a description of the options chosen, execution diagnostics, equilibrium compositions, reaction formation equations and a comparison between the equilibrium constants for these equations as calculated from the free energy changes and the compositions. With IWRAP=1 a concise wrap-up file is written to logical unit designator IFILE (IFILE=2) in addition to the IWRAP=0 option. These two output options are quite useful when one is becoming acquainted with the code as they provide an echo of the input data set and a verification of the results. Options IWRAP=2 and IWRAP=3 provide only wrap-up file output to IFILE and IWRT respectively.

MAXIT sets the maximum number of iterations to be performed for calculating the equilibrium compositions. Typically MAXIT is set to 1000. The equilibrium compositions are considered converged when the relative difference between the equilibrium constants, as calculated from the Gibbs Free Energy change of the formation reactions and from the estimate to the equilibrium composition, is less than CNVG. A typical value for CNVG is  $10^{-4}$ .

The inlet compositions for the vapor, solution and pure condensed phases are next in the input data set. The total moles in the vapor are on one record and the following records contain the mole fractions of each component in the vapor, the last value being the mole fraction of the inert. The solution phase inlet compositions are done the same way except that there is no inert. Following the solution phase mole fractions is a record which determines the activity coefficient model to be used in the solution phase. For IXSCOR=0 the solution is considered to be ideal. Setting IXSCOR=1 yields a binary simple solution model for the excess Gibbs Free Energy. A Henry's Law constant for the first component in the solution phase is activated by setting IXSCOR=2. The parameters AXS and BXS are used in the activity coefficient models as shown in Table B.2.

The final records of the input data set contain the number of moles in each pure condensed phase.

### B.2.3. Preparation for the Iterative Solution

The limits for the temperature, pressure and composition loops are set at lines 126 through 133. The composition loop (IOPT=3) starts at line 134.

The input specie order is saved so that the results may be output in this order. This step is necessary since the specie order is shifted during the iterative procedure in order to obtain an optimum set of basis species and it is convenient to compare the equilibrium results to the input concentrations in the same sequence.

The specie names along with their associated enthalpy of formation, entropy of formation and heat capacity correlation data are then written to IWRT if IWRAP<2. Also, the temperature and pressure of the reference state, maximum number of iterations, convergence criterion and the debugging, steady-state and solution phase excess free energy correlation options are identified.

The temperature and pressure loops (IOPT=1 or IOPT=2) start at line 209. Subroutine STSTCP is called to calculate the standard state chemical potential of each specie. Subroutine ESTMTE is then called to provide an estimate to the equilibrium composition during the first pass through the temperature/pressure loop. Succeeding passes through this loop utilize the equilibrium composition of the preceding pass as an estimate of the current equilibrium composition when ISS=0.

If the steady state option is activated (ISS>0) subroutine STEADY inserts, as the last pure condensed phase, a liquid phase composed of group III and V elements which has a composition determined by the liquidus line of the III-V system at the specified temperature. The total moles of each element present is then calculated based on the estimate of the equilibrium compositions. This result is later written out along with the previous determination of each element to provide a means of verifying that mass has been conserved in the calculations.

The initial composition estimate, standard chemical potential and elemental abundance vector for each specie along with the amount of each element present in the system are written out if IWRAP<2. This occurs in lines 245 through 286. Headings for a page containing execution diagnostics are set up in lines 289 through 294 and the standard state chemical potentials are divided by R and T in accordance with the derivation in section B.5.

During the first pass through the temperature or pressure loop the total moles of silicon compounds and the group III to group V atom ratio in the vapor phase are calculated in subroutines TOTSI and RATIO. The specie initial concentrations along with the total silicon and III-V atom ratio in the vapor are then written to a wrap-up file if IWRAP>0.

#### B.2.4 Iterative Solution for the Equilibrium Composition.

The iterative scheme for determining the equilibrium compositions is located at lines 319 through 421. Before entering the loop RELMAX, the relative maximum error between the actual and approximated equilibrium constants, is set to a large number and IACFF is set to zero to prevent the inclusion of nonidealities in the solution phase until a close approximation to the equilibrium composition is attained.

Subroutine OPTBAS is called to determine the optimum set of basis species for the current iteration. If a complete set of basis species cannot be found parameter ISTOP is set to unity and program execution is halted. If parameter ICHNG is returned as zero the optimum set of basis species for the current iteration is the same as the previous iteration and an unnecessary recalculation of the equilibrium constants for the formation reactions is omitted. If ICHNG is not zero subroutine EQCON is called to calculate the equilibrium constants for each formation reaction from the Gibbs Free Energy change of the reaction. Parameter ISTOP is set to unity in subroutine EQCON and execution is halted if the matrix containing the basis species appears to be algorithmically singular to subroutine LINVIF.

Subroutine ACTCOF calculates the equilibrium constants for each of the species and subroutine CALCQ calculates the equilibrium constants for each of the formation reactions from the current estimate to the equilibrium composition.

The test for convergence of the iteration scheme is performed in lines 360 through 393. The solution is considered to have converged when the maximum fractional disagreement between the equilibrium constants calculated from the free energy change and the composition estimate is less than CNVG.

If the convergence test fails subroutine ADJEXT is called to adjust the extents of the formation reactions in order to obtain a better estimate to the equilibrium composition. The convergence forcer is calculated in subroutine CNVFRG and the molar amounts of each specie are updated in subroutine CORMOL. Subroutine CALCQ is then called again so that the mole fractions sent to ACTCOF during the next iteration correctly reflect the composition. A message is written out at lines 423 through 428 if the iterative procedure terminates without converging.

Throughout the iterative procedure subroutines GIBBS, DEBUG, PMAT, DPMAT, PVEC and IPVEC are called, depending upon the value of IDEBUG, to provide intermediate information concerning the basis species and convergence of the numerical scheme.

#### B.2.5 Output of Results

Following the loop for determining the equilibrium compositions subroutine GIBBS is called to calculate the final system Gibbs Free Energy. Lines 439 through 454 then determine chemical potentials for each of the species. Subroutine ORDER is called to return the species to the original order of the problem statement. Subroutines TOTSI and RATIO then determine the total silicon concentration, the group III-V atom ratio in the vapor phase, the activities of Si, Ga, As, In and P in a solid phase and the III/V saturation ratio.

The results of the equilibrium calculation are written out at lines 463 through 520 if IWRAP<2. A wrap-up file is written at line 521 if IWRAP>0. If a temperature, pressure or composition loop option has been chosen (IOPT>0) the program jumps to the bottom of this loop at line 606. Otherwise the set of independent formation reaction equations are written out followed by a comparison of the equilibrium constants for these reactions as calculated by the free energy change and the equilibrium compositions.

The phrase "NOT BINDING" frequently appears to the right of the equilibrium constant comparisons and indicates that these particular reactions were not included in the convergence test due to the small concentration ( $N_i < 10^{-21}$  g-moles) of the reaction products. Thus the two calculated equilibrium constants for these species may not be in agreement.

The punctuation ? and ?? sometimes accompany specie mole numbers in the wrap-up file. A single question mark indicates that the equilibrium constant for this formation reaction did not converge but is within 10% of the desired value. Double question marks indicate that the discrepancy between the equilibrium constants as calculated from the free energy change and the final composition is greater than 10%. Occasionally, values which are accompanied by a single question mark may be useful.

If the iteration for equilibrium does not converge there are several options which may be used. First, the results reported are always the best results which were obtained during the iterative procedure. This is true even if the solution diverges because the set of mole numbers which most closely approximate equilibrium is stored in vector BESTN. Therefore, if the solution fails to converge but the BESTN values are found to have sufficient accuracy, simply use the result.

In other situations the value of RLXMIN may be adjusted. Typically RLXMIN is set to 0.05 to allow the iterative procedure to continue over unusually intricate contours on the Gibbs Free Energy surface. If the solution has not diverged, i.e. the last iteration is the best estimate to the equilibrium solution, then increasing the value of RLXMIN will usually allow the solution to converge. If the solution has diverged the value of RLXMIN should be decreased to allow smaller steps to be taken.

Finally, if all else fails, the temperature and pressure looping options may be used to approach the desired equilibrium conditions from above or below the parameters of interest.

Table B.2.6 Listing of the Main Program

```

1 C  MCMPEC.STOIC .... MULTICOMPONENT MULTIPHASE EQUILIBRIUM CALDE
2 C                               STOICICMETRIC FORMULATION
3 C
4 C
5     DIMENSION A(50,13),ACCEF(50),A0(50),A1(50),A2(50),A3(50),
6     &          B(13),BCALC(13),CHMPT(50),COEFF(6),
7     &          D(13,13),DINV(13,13),DD(13,13),DG(50),DH0(50),DS0(50),
8     &          DZETA(50),FRAC(50),FRACIN(50),GNU(50,13),
9     &          ICP(50),IDXBAS(13),INDEX(50),INERT(13),G(50),STDCP(50),
10    &          TOTMC(50),WKA(50)
11    INTEGER BSPCE(50,3),ISPCE(50,3),PHASE(50,3),SPECIE(50,3),
12    &          STRING(6,4),TITLE(20),V,S,C,E,VP1,VPS,VPSP1,VSC,VSCF,
13    &          BQUES(50),QUES(50),QUEST1/'?'  '?,QUEST2/'??'  '?,
14    &          ELMNT(13)/13*'  '?,VAPOR(3)/'  V', 'AFC', 'F'  '?,
15    &          SOLN(3)/'SCL', 'UTI', 'CN' '?,COND(3)/'CON', 'DN', 'SED'//,
16    &          RPSPS/'S' + '?,RPAS/'<=' '?,RPBL/'>'  '?,SSPS/'  ' + '?,
17    &          BLNKS/'  ' '?,LP/'('//
18    REAL KEQ(50),NV,NS,LAMBDA
19    REAL*8 DD,DINV,WKA,N(50),BESTN(50),NTEMP(50),DPRME(13,13),DZETA
20 C
21 C  A(I,J)   : ELEMENTAL ABUNDANCE MATRIX
22 C  B(J)     : TOTAL NUMBER OF GRAM-MOLES OF ELEMENT J
23 C  DH0(I)   : ENTHALPY OF FORMATION OF SPECIES I
24 C  DS0(I)   : ENTROPY OF FORMATION OF SPECIES I
25 C  STDCP(I) : STANDARD CHEMICAL POTENTIAL OF SPECIES I
26 C
27 C  ***** HEAT CAPACITY CORRELATIONS *****
28 C  ICP(I)=0 : CP(I) = A0(I) + A1(I)*T + A2(I)/T**2 + A3(I)*ALOG(T)
29 C  ICP(I)=1 : CP(I) = A0(I) + A1(I)*T + A2(I)*T**2 + A3(I)*T**3
30 C
31 C
32     IRD=5
33     IWRT=6
34     IFILE=2
35     IDIM1=50
36     IDIM2=13
37     FRCZIN=0.0
38     DH0Z=0.0
39     DS0Z=0.0
40     A0Z=0.0
41     A1Z=0.0
42     A2Z=0.0
43     A3Z=0.0
44     TOTMV=0.0
45 C
46 C  SUPPRESS PRINTING OF OVERFLOW, UNDERFLOW, DIVIDE BY ZERO
47 C  AND EXPONENTIAL ARGUMENT ERROR MESSAGES
48 C
49     CALL ERRSET(207,0,-1,0,0,209)
50     CALL ERRSET(252,0,-1,0,0,253)
51 C
52 C  READ TITLE
53 C
54     READ(IRD,5) (TITLE(K),K=1,20)

```

```

55      5 FORMAT(20A4)
56 C
57 C NUMBER OF ELEMENTS, VAPOR SPECIES, SOLUTION SPECIES,
58 C CONDENSED PURE PHASES, SYSTEM TEMPERATURE (K) AND PRESSURE (PA)
59 C
60      READ(IR0,10) E,V,S,C,T,P,T0,P0
61      10 FORMAT(4I5,4F10.0)
62      VP1=V+1
63      VPS=V+S
64      VPSP1=V+S+1
65      VSC=V+S+C
66      VSCC=V+S+C+Z
67 C
68 C READ ELEMENTS
69 C
70      READ(IR0,15) (ELMNT(J),J=1,E)
71      15 FORMAT(13(1X,A2))
72 C
73 C VAPOR SPECIES INFORMATION
74 C
75      IF(V.EQ.0) GO TO 118
76      DO 110 I=1,V
77      READ(IR0,20) (SPECIE(I,K),K=1,3),CHO(I),DS0(I)
78      READ(IR0,21) A0(I),A1(I),A2(I),A3(I),ICP(I)
79      READ(IR0,22) (A(I,J),J=1,13)
80      20 FORMAT(3A4,2E12.5)
81      21 FORMAT(4E12.5,12)
82      22 FORMAT(13(F5.0,1X))
83      DO 110 J=1,3
84      PHASE(I,J)=VAPOR(J)
85      110 CONTINUE
86 C
87 C INERT SPECIE
88 C
89      READ(IR0,20) (INERT(K),K=1,3),CHOZ,DS0Z
90      READ(IR0,21) A0Z,A1Z,A2Z,A3Z,ICPZ
91      READ(IR0,22) JUMMY
92      118 CONTINUE
93 C
94 C SOLUTION SPECIES INFORMATION
95 C
96      IF(S.EQ.0) GO TO 125
97      DO 120 I=VP1,VPS
98      READ(IR0,20) (SPECIE(I,K),K=1,3),CHO(I),DS0(I)
99      READ(IR0,21) A0(I),A1(I),A2(I),A3(I),ICP(I)
100     READ(IR0,22) (A(I,J),J=1,13)
101     DO 120 J=1,3
102     PHASE(I,J)=SOLN(J)
103     120 CONTINUE
104     125 CONTINUE
105 C
106 C CONDENSED PHASE DATA
107 C
108     IF(C.EQ.0) GO TO 135

```

```

109      DO 130 I=VPSP1,VSC
110      READ(IRD,20) (SPECIE(I,K),K=1,3),DHJ(I),DSJ(I)
111      READ(IRD,21) AJ(I),A1(I),A2(I),A3(I),ICP(I)
112      READ(IRD,22) (A(I,J),J=1,13)
113      FRAC(I)=1.0
114      FRACIN(I)=1.0
115      DO 130 J=1,3
116      PHASE(I,J)=COND(J)
117 130 CONTINUE
118 135 CCNTINUE
119 C
120 C   MAXIMUM NUMBER OF ITERATIONS, CONVERGENCE CRITERION AND OPTIONS
121 C
122      READ(IRD,136) IDEBUG,IOPT,ISS,IWRAP,MAXIT,NMAX,CHVS,TINC,PINC,
123      & RLXMIN
124 136 FORMAT(6I5,4F10.0)
125      IF(IWRAP.EQ.3) IFILE=IWRAP
126 C
127 C   SET THE LOOP LIMITS FOR THE TEMPERATURE, PRESSURE AND COMPOSITION
128 C   LOOPS. THE COMPOSITION LOOP STARTS HERE
129 C
130      NCMP=1
131      NTP=1
132      IF(ICPT.EQ.1.OR.IOPT.EQ.2) NTP=NMAX
133      IF(ICPT.EQ.3) NCMP=NMAX
134      DO 2000 ICMP=1,NCMP
135      IDATA=0
136 C
137 C   TOTAL NUMBER OF MOLES OF VAPOR AND MOLE FRACTIONS
138 C
139      IF(V.EQ.0) GO TO 138
140      READ(IRD,137) TOTMV
141      READ(IRD,137) (FRACIN(I),I=1,V),FRCZIN
142 137 FORMAT(6E12.5)
143 C
144 C   TOTAL NUMBER OF MOLES OF SOLUTION SPECIES, MOLE FRACTIONS
145 C   AND EXCESS FREE ENERGY CORRELATION PARAMETERS
146 C
147 138 CONTINUE
148      IF(S.EQ.0) GO TO 140
149      READ(IRD,137) TOTMS
150      READ(IRD,137) (FRACIN(I),I=VP1,VPS)
151      READ(IRD,139) IXSCOR,AXS,BXS
152 139 FORMAT(15,2E12.5)
153 140 CONTINUE
154 C
155 C   TOTAL NUMBER OF MOLES IN PURE CONDENSED PHASES
156 C
157      IF(C.EQ.0) GO TO 142
158      READ(IRD,137) (TOTMC(I),I=VPSP1,VSC)
159 142 CONTINUE
160 C
161 C   SAVE THE ORIGINAL SPECIE ORDER SO THE PROBLEM
162 C   CAN BE PLACED IN THIS ORDER AFTER THE ITERATIVE PROCEDURE

```

```

163 C
164     DO 165 I=1,V3C
165     DO 165 K=1,3
166     ISPCE(I,K)=SPECIE(I,K)
167 165 CONTINUE
168     IF(ICMP.GT.1.OR.IWRAP.EQ.3) GC TC 187
169 C
170 C  WRITE-OUT SOME OF THE INPUT DATA
171 C
172     IPAGE=1
173     WRITE(IWRT,400) (TITLE(K),K=1,20),IPAGE
174     WRITE(IWRT,410) T,P
175     IF(IWRAP.GT.1) GC TC 187
176     WRITE(IWRT,170)
177 170 FORMAT('0',/,1X,T55,'HEAT CAPACITY CORRELATION COEFFICIENTS',
178 &/,1X,T16,'ENTHALPY OF',T33,'ENTROPY OF',T58,'ICP=0: CP = A0',
179 &' + A1*T + A2/T**2 + A3*LN(T)',/,1X,T17,'FORMATION',T33,'FORMAT',
180 &'ION',T58,'ICP=1: CP = A0 + A1*T + A2*T**2 + A3*T**3',/,1X,T4,
181 &'SPECIE',T20,'DH0',T37,'DS0',T54,'A0',T73,'A1',T93,'A2',T113,
182 &'A3',T122,'ICP',/,1X,T4,'SYMBOL',T15,'(KCAL/G-MOLE)',T30,
183 &'(KCAL/G-MOLE-K)',T47,'(KCAL/G-MOLE-K)',T65,'(KCAL/G-MOLE-K**2)',
184 &T86,'(.....)',T106,'(.....)',T122,'(-)',
185 &/,'+',12(' '),T15,13(' '),T30,15(' '),T47,15(' '),
186 &T65,18(' '),T86,15(' '),T106,15(' '),T122,3(' '))
187     DO 180 I=1,V3C
188     WRITE(IWRT,175) (SPECIE(I,K),K=1,3),DH0(I),DS0(I),A0(I),A1(I),
189 &
190     A2(I),A3(I),ICP(I)
191     IF(I.EQ.V) WRITE(IWRT,175) (INERT(K),K=1,3),DH0Z,DS0Z,A0Z,A1Z,
192 &
193     A2Z,A3Z,ICPZ
194 175 FORMAT(1X,3A4,T17,F9.3,T33,F9.6,T50,F9.6,T68,E12.5,T88,E12.5,
195 &T108,E12.5,T123,I1)
196 180 CONTINUE
197     WRITE(IWRT,184) TO,PO,MAXIT,CNMG,ICDBG
198 184 FORMAT('0',/,'0',T10,'THE ENTHALPY AND ENTROPY OF FORMATION ',
199 &'REFERENCE TEMPERATURE AND PRESSURE ARE:',5X,'T0 = ',F6.1,' K',
200 &5X,'PO = ',F9.1,' PA',/,,'0',T35,'MAXIMUM NUMBER OF ITERATIONS ',
201 &'ALLOWED = ',15,/,,'0',T50,'CONVERGENCE CRITERION = ',E12.4,
202 &/,'0',T48,'OUTPUT PARAMETER ICDBG = ',12)
203     IF(S.GT.1) WRITE(IWRT,185) IXSCOR,AXS,8XS
204 185 FORMAT('0','EXCESS FREE ENERGY CORRELATION DATA :',
205 &
206     2X,'IXSCOR = ',15,5X,'AXS = ',E12.5,5X,'8XS = ',E12.5)
207     IF(ISS.GT.0) WRITE(IWRT,186) ISS
208 186 FORMAT('0',T24,'ISS= ',12,' THE III-V LIQUID SOLUTION IS ',
209 &
210     'AT EQUILIBRIUM WITH THE III-V STOICHIOMETRIC SOLID')
211 187 CONTINUE
212 C
213 C  THE TEMPERATURE AND PRESSURE LOOPS BEGIN HERE
214 C
215     DO 2000 ITP=1,NTP
216     IF(ICPT.EQ.1.AND.ITP.GT.1) T=T+TINC
217     IF(ICPT.EQ.2.AND.ITP.GT.1) P=P+PINC
218 C
219 C  CALCULATE THE STANDARD STATE CHEMICAL POTENTIALS
220 C  AND AN INITIAL ESTIMATE OF THE EQUILIBRIUM COMPOSITIONS

```

```

217 C
218 CALL STSTOP(A0,A1,A2,A3,A02,A12,A22,A32,DH0,DS0,DH0Z,DS0Z,STDCP,
219 & STDCPZ,ICP,ICPZ,TJ,T,IDI1,V,S,C)
220 IF(ITP.GT.1.AND.ISS.EQ.0) GO TO 195
221 DO 190 I=1,VPS
222 FRAC(I)=FRACIN(I)
223 190 CONTINUE
224 FRACZ=FRACZIN
225 CALL ESTMTE(TOTMV,TOTMS,TOTMC,FRAC,N,FRACZ,ZV,
226 & IDI1,V,S,C)
227 195 CONTINUE
228 C
229 C SOURCE ZONE STEADY-STATE LIQUID COMPOSITION MODEL
230 C
231 IF(ISS.GT.0) CALL STEADY(SPECIE,A,STDCP,ELMNT,XIII,T,TO,V,S,C,
232 & IDI1,IDI2,ISS,INRT)
233 C
234 C CALCULATE THE TOTAL GRAM-MOLES OF EACH ELEMENT
235 C BASED ON THE INITIAL COMPOSITION ESTIMATES IN THE PHASES
236 C
237 DO 200 J=1,E
238 BCALC(J)=0.
239 DO 200 I=1,VSC
240 BCALC(J)=A(I,J)*N(I)+BCALC(J)
241 B(J)=BCALC(J)
242 200 CONTINUE
243 IF(INRAP.GT.1) GO TO 476
244 IF(ITP.GT.1) GO TO 472
245 C
246 C WRITE-OUT THE INITIAL COMPOSITION ESTIMATES, STANDARD STATE
247 C CHEMICAL POTENTIALS AND THE ELEMENTAL ABUNDANCE MATRIX
248 C
249 IPAGE=IPAGE+1
250 WRITE(INRT,400) (TITLE(K),K=1,20),IPAGE
251 400 FORMAT('1',/, '0',T34,'STOICHIOMETRIC FORMULATION FOR DETERMINING',
252 & ' EQUILIBRIUM COMPOSITIONS',/, '0',T30,20A4,T120,
253 & 'PAGE ',I2)
254 WRITE(INRT,410) T,P
255 410 FORMAT('0',T43,'TEMPERATURE = ',F6.1,' K',5X,'PRESSURE = ',E12.5,
256 & ' PA')
257 WRITE(INRT,420) (ELMNT(K),K=1,13)
258 420 FORMAT('0',/,T48,'INPUT DATA AND INITIAL COMPOSITION ESTIMATES',
259 &/, '0',T29,'INITIAL',T43,'STANDARD',/,1X,T27,'COMPOSITION',
260 &T43,'CHEMICAL',/,1X,T4,'SPECIE',T29,'ESTIMATE',T42,'POTENTIAL',
261 &T72,'ELEMENTAL ABUNDANCE MATRIX',/,1X,T4,'SYMBOL',T17,'PHASE',
262 &T28,'(G-MOLES)',T40,'(KCAL/G-MOLE)',T55,13(A2,4X),/, '+',
263 &12(' '),T15,2(' '),T25,14(' '),T40,13(' '),T55,75(' '))
264 DO 440 I=1,VSC
265 WRITE(INRT,430) (SPECIE(I,K),K=1,3),(PHASE(I,K),K=1,3),N(I),
266 & STDCP(I),(A(I,J),J=1,E)
267 IF(I.EQ.V) WRITE(INRT,430) (INERT(K),K=1,3),(PHASE(I,K),K=1,3),
268 & ZV,STDCPZ
269 430 FORMAT(1X,3A4,T15,3A3,T25,C14.7,T42,F9.3,T55,13(F5.7,1X))
270 440 CONTINUE

```

```

271     IF(ISS.GT.0) WRITE(IWRT,445) XIII
272 445 FORMAT(4X,'X=',F6.4)
273     WRITE(IWRT,450)
274 450 FORMAT('J',/, '0',T44,'TOTAL GRAM-MOLES OF EACH ELEMENT FROM IN.',
275 &         'PUT DATA',/, '1X,T40,'AND AS CALCULATED FROM THE INITIAL',
276 &         'COMPOSITION ESTIMATES',/, '0',4(4X,'INPUT DATA',3X,
277 &         'CALCULATED',5X))
278     NPRT=E/4
279     NCHK=NPRT*4
280     IF(NCHK.NE.E) NPRT=NPRT+1
281     ISTRT=1
282     DO 470 K=1,NPRT
283     NEND=ISTRT+3
284     IF(NEND.GT.E) NEND=E
285     WRITE(IWRT,460) (ELMNT(J),Z(J),BCALC(J),J=ISTRT,NEND)
286 460 FORMAT(1X,4(A2,1X,E12.5,1X,E12.5,4X))
287     ISTRT=NEND+1
288 470 CONTINUE
289 472 CONTINUE
290     IPAGE=IPAGE+1
291     WRITE(IWRT,400) (TITLE(K),K=1,20),IPAGE
292     WRITE(IWRT,410) T,P
293     WRITE(IWRT,475)
294 475 FORMAT('J',T58,'EXECUTION DIAGNOSTICS',/, '+',T58,9(' '),1X,
295 &         '11(' ',/, '0')
296 476 CONTINUE
297 C
298 C DIVIDE THE STANDARD STATE CHEMICAL POTENTIALS BY RT
299 C
300     RT=0.0019872*T
301     DO 480 I=1,VSC
302     STDCP(I)=STDCP(I)/RT
303 480 CONTINUE
304     STDCPZ=STDCPZ/RT
305 C
306 C CALCULATE THE TOTAL SILICON AND THE III/V RATIO IN THE VAPOR PHASE
307 C AND WRITE-OUT THE INITIAL RESULTS TO THE WRAPUP FILE
308 C
309     IF(ITP.GT.1.OR.IWRAP.EQ.0) GO TO 485
310     CALL TCTS1(A,ELMNT,FRAC,N,SITCT,SINF,ACTSIS,T,P,IDIM1,IDIM2,V,E)
311     CALL RATIO(A,ELMNT,FRAC,N,STDCP,ACTGAS,ACTINS,ACTASS,ACTPS,
312 &         RIIIIV,RGAAS,RINP,T,P,TO,FO,IDIM1,IDIM2,V,E)
313     ITBST=1
314     BSTCVG=0
315     CALL WRAPUP(TITLE,SPECIE,INERT,N,FRAC,QUES,ZV,FRACZ,SITCT,SINF,
316 &         ACTSIS,ACTGAS,ACTINS,ACTPS,ACTASS,RIIIIV,RGAAS,RINP,
317 &         BSTCVG,ITBST,CNVC,CNMG,ISS,XIII,T,P,ICATA,IDIM1,IFILE,V,VSC)
318 485 CONTINUE
319 C
320 C ITERATIVE SOLUTION FOR THE EQUILIBRIUM COMPOSITIONS
321 C
322     RELMAX=1.0E10
323     IACFF=0
324     DO 600 ITER=1,MAXIT

```

```

325 C
326 C DETERMINE THE OPTIMUM SET OF BASIS SPECIES
327 C
328     CALL OPTBAS(N,BESTN,A,D,DPRME,STDRP,SPECIE,PHASE,AC,A1,A2,A3,
329     &BQUES,CHD,DSO,ICP,IDXBAS,ITER,IDIM1,IDIM2,V,S,C,E,ISTOP,ICHNG,
330     &IWRT)
331     IF(ISTOP.EQ.1) GO TO 504
332     IF(ITER.GT.1.AND.ICHNG.EQ.0) GO TO 500
333     IF(IDEBUG.LT.2) GO TO 490
334     CALL IPVEC(IDXBAS,IDIM2,E,6HIDXBAS,IWRT)
335     CALL PMAT(A,IDIM1,IDIM2,VSC,E,6FA      ,IWRT)
336     CALL PMAT(D,IDIM2,IDIM2,E,E,6FD      ,IWRT)
337     CALL DPMAT(DPRME,IDIM2,IDIM2,E,E,6HDPME ,IWRT)
338 490 CONTINUE
339 C
340 C CALCULATE THE STOICHIOMETRIC COEFFICIENTS AND THE EQUILIBRIUM CONSTANTS
341 C
342     CALL EQCON(A,D,DD,DINV,DG,GNU,STDRP,KEQ,IDXBAS,WKA,RT,
343     &      ITER,IDIM1,IDIM2,V,S,C,E,ISTOP,IWRT)
344     IF(ISTOP.EQ.1) GO TO 604
345     IF(IDEBUG.LT.2) GO TO 500
346     CALL DPMAT(DINV,IDIM2,IDIM2,E,E,6HDINV  ,IWRT)
347     CALL PMAT(GNU,IDIM1,IDIM2,VSC,E,6HGNU   ,IWRT)
348     CALL FVEC(KEQ,IDIM1,VSC,6HKEQ      ,IWRT)
349 500 CONTINUE
350 C
351 C CALCULATE THE ACTIVITY COEFFICIENTS
352 C
353     CALL ACTCOF(FRAC,ACDEF,ISPEC,SPECIE,INDEX,IDIM1,RELMAX,IXSUT,
354     &      AXS,BXS,T,IACFF,V,S,C,IWRT)
355 C
356 C CALCULATE THE EQUILIBRIUM CONSTANTS FROM THE CURRENT COMPOSITIONS
357 C
358     CALL CALCO(GNU,N,ACDEF,FRAC,PHASE,VAPOR,SOLN,IDXBAS,C,
359     &      ZV,FRACZ,P,P0,V,S,C,E,IDIM1,IDIM2,IWRT)
360 C
361 C CALCULATE THE ERROR BETWEEN THE EQUILIBRIUM CONSTANTS
362 C CALCULATED BY THE COMPOSITIONS AND THE EQUILIBRIUM CONSTANTS
363 C CALCULATED FROM THE GIBBS FREE ENERGY CHANGE
364 C
365     RELMAX=0.
366     DO 590 I=1,VSC
367     QUES(I)=BLNKS
368     DO 570 J=1,E
369     IF(I.EQ.IDXBAS(J)) GO TO 590
370 570 CONTINUE
371     RELERR=(KEQ(I)-Q(I))/KEQ(I)
372 C
373 C ASSIGN "?" TO QUES(I) IF THE CONVERGENCE CRITERION IS NOT MET
374 C AND "???" TO QUES(I) IF THERE IS LESS THAN ONE SIGNIFICANT FIGURE
375 C
376     IF(ABS(RELERR).GT.CNV3) QUES(I)=QUEST1
377     IF(ABS(RELERR).GT.0.1) QUES(I)=QUEST2
378     IF(ABS(RELERR).GT.RELMAX.AND.N(I).GT.1.00E-21)

```

```

379      &                                RELMAX=ABS(FELERF)
380      590 CONTINUE
381 C
382 C   KEEP THE BEST ESTIMATE TO THE EQUILIBRIUM SOLUTION
383 C   IN CASE THE NUMERICAL PROCEDURE DIVERGES
384 C
385      IF(ITER.GT.1.AND.RELMAX.GT.BSTCVG) GO TO 594
386      BSTCVG=RELMAX
387      ITHST=ITER
388      DO 593 IBEST=1,VSC
389      BQUES(IBEST)=QUES(IBEST)
390      BESTN(IBEST)=N(IBEST)
391      593 CONTINUE
392      594 CONTINUE
393      IF(RELMAX.LE.CNVC) GO TO 610
394      IF(IDEBUG.EQ.2) CALL PVFC(FRAC,IDIM1,VSC,6HFRAC ,IWRT)
395      IF(IDEBUG.GE.1) CALL PVFC(Q,IDIM1,VSC,6HQ ,IWRT)
396      IF(ITER.EQ.MAXIT) GO TO 595
397 C
398 C   MAKE ADJUSTMENTS TO THE EXTENTS OF REACTION
399 C
400      CALL ADJEXT(N,KEQ,Q,GNU,DZETA,IDXBAS,COND,PHASE,IDIM1,IDIM2,
401      &          V,S,C,E,IWRT)
402      CALL CNVFC(N,NTEMP,STDCP,ACDEF,DZETA,GNU,IDXBAS,VAPOR,COND,
403      &          SOLN,PHASE,ZV,RT,P,PO,RLXMIN,LAMBDA,IDIM1,IDIM2,V,S,C,E)
404      CALL CORVEL(N,DZETA,GNU,IDXBAS,IDIM1,IDIM2,LAMBDA,VSC,E)
405      595 IF(ITER.LT.MAXIT) GO TO 597
406 C
407 C   IF THE SOLUTION DID NOT CONVERGE TRANSFER THE BEST ESTIMATE
408 C   TO THE EQUILIBRIUM SOLUTION FROM VECTOR BESTN INTO N.
409 C
410      DO 596 IBEST=1,VSC
411      QUES(IBEST)=BQUES(IBEST)
412      N(IBEST)=BESTN(IBEST)
413      596 CONTINUE
414      597 CONTINUE
415      CALL CALCO(GNU,N,ACDEF,FRAC,PHASE,VAPOR,SOLN,IDXBAS,Q,
416      &          ZV,FRACZ,P,PO,V,S,C,E,IDIM1,IDIM2,IWRT)
417      IF(IDEBUG.EQ.0) GO TO 600
418      CALL GIBBS(N,STDCP,STDCPZ,ACDEF,FRAC,ZV,FRACZ,COND,SOLN,PHASE,
419      &          RT,P,PO,IDIM1,V,S,C,GFE)
420      CALL DEBUG(N,DZETA,VSC,IDIM1,ITER,LAMBDA,GFE,RELMAX,IWRT)
421      600 CONTINUE
422      604 CONTINUE
423      IF(IWRAP.LT.3) WRITE(IWRT,605)MAXIT,RELMAX,BSTCVG,ITHST
424      605 FORMAT('0','***** ITERATION FOR EQUILIBRIUM COMPOSITION ',
425      &          'DID NOT CONVERGE *****',
426      &          '(AFTER ',14,' ITERATIONS RELMAX =',E12.5,' )',
427      &          '&Z, '0',' BEST CONVERG. OCC',E12.5,' AT ITERATION ',14)
428      610 CONTINUE
429      CALL GIBBS(N,STDCP,STDCPZ,ACDEF,FRAC,ZV,FRACZ,COND,SOLN,PHASE,
430      &          RT,P,PO,IDIM1,V,S,C,GFE)
431 C
432 C   CALCULATE THE GRAM-MOLES OF EACH ELEMENT AFTER THE ITERATION

```

```

433 C
434     DO 700 J=1,5
435     BCALC(J)=J.0
436     DO 700 I=1,VSC
437     BCALC(J)=BCALC(J)+A(I,J)*N(I)
438 700 CONTINUE
439 C
440 C   CALCULATE THE CHEMICAL POTENTIAL OF EACH SPECIE
441 C
442     DO 800 I=1,VSC
443     PPJ=1.0
444     IF(PHASE(I,1).EQ.VAPOR(1)) PPJ=P/P0
445     ARG=FRAC(I)*ACDEF(I)*PPJ
446     CHMPT(I)=RT*(STDCP(I)+ALOG(ARG))
447 800 CONTINUE
448     ARG=1.0
449     IF(FRACZ.GT.0.0) ARG=F*FRACZ*P/P0
450     CHMPTZ=RT*(STDCPZ+ALOG(ARG))
451     DO 810 I=1,VSC
452     DO 810 K=1,3
453     BSPCE(I,K)=SPECIE(I,K)
454 810 CONTINUE
455 C
456 C   PUT THE MATRICIES AND VECTORS INTO THE ORIGINAL PROBLEM STATEMENT OF DE
457 C
458     CALL ORDER(TSPCE,SPECIE,PHASE,N,A,STDCP,P0,A1,A2,A3,DH0,C50,
459     EDZETA,CHMPT,ACDEF,FRAC,CUES,DG,G,KEQ,ICP,IDIM1,IDIM2,E,VSC,
460     EIWRT)
461 C
462 C   CALCULATE THE TOTAL SILICON AND THE III/V RATIO IN THE VAPOR PHASE
463 C
464     CALL TCTSI(A,ELMNT,FRAC,N,SITCT,SINF,ACTSIS,T,P,IDIM1,IDIM2,V,E)
465     CALL RATIO(A,ELMNT,FRAC,N,STDCP,ACTGAS,ACTINS,ACTADS,ACTPS,
466     & RIIIIV,EGAAS,SINF,T,P,T0,P0,IDIM1,IDIM2,V,E)
467     IF(IWRAP.GT.1) GO TO 971
468 C
469 C   WRITE-OUT THE RESULTS
470 C
471     IPAGE=IPAGE+1
472     WRITE(IWRT,400) (TITLE(K),K=1,20),IPAGE
473     WRITE(IWRT,410) T,P
474     WRITE(IWRT,900) ITBST,CFS,BSTCVG,CNMG,LAMBDA
475 900 FORMAT('0',/,1X,T45,'EQUILIBRIUM COMPOSITIONS AFTER ',I5,
476     & ' ITERATIONS',/, '0',T42,'SYSTEM GIBBS FREE ENERGY = ',E14.7,
477     & ' (KCAL)',
478     & /, '0', 'RELATIVE ERROR = ',E12.5,5X, 'CONVLENGCE CRITERION = ',
479     & E12.5,5X, 'RELAXATION PARAMETER AT LAST ITERATION = ',E12.5,
480     & /, '0',T57,'ESTIMATED',/,1X,T25,'EQUILIBRIUM',T35,'EQUILIBRIUM',
481     & T56,'COMPOSITION',T92,'CHEMICAL',
482     & /,1X,T4,'SPECIE',T29,'M.LE',T29,'COMPOSITION',T57,
483     & 'UNCERTAINTY',T91,'POTENTIAL',T109,'ACTIVITY',
484     & /,1X,T4,'BY MOLE',T17,'PHASE',T27,'FRACTION',T40,'(G-MOLE)',
485     & T57,'(G-MOLE)',T90,'(KCAL/G-MOLE)',T107,'COEFFICIENT',
486     & /, '+',12(' '),T15,9(' '),T25,12(' '),T37,14(' '),T54,

```

```

487      & 14(' '),T59,14(' '),T106,12(' ')
488      ZZETA=0.0
489      ZACT=1.0
490      DO 920 I=1,VSC
491      WRITE(IWRT,910) (SPECIE(I,K),K=1,3),(PHASE(I,K),K=1,3),FRAC(I),
492      & N(I),ZZETA(I),CHMPT(I),ACTFF(I)
493      IF(I.EQ.V) WRITE(IWRT,910) (INERT(K),K=1,3),(PHASE(I,K),K=1,3),
494      & FRACZ,ZV,ZZETA,CHMPTZ,ZACT
495 910 FORMAT(1X,3A4,T15,3A3,T24,E12.5,T37,E14.7,T54,E14.7,T92,F9.3,
496      & T106,E12.5)
497 920 CONTINUE
498      IF(ISS.GT.0) WRITE(IWRT,945) XIII
499      WRITE(IWRT,930) SIMF
500 930 FORMAT('0',T35,'MOLE FRACTION OF SILICON SPECIED IN ',
501      & ' VAPOR PHASE = ',E12.5)
502      WRITE(IWRT,940) RIIIIV
503 940 FORMAT('0',T50,'III/IV RATIO IN THE VAPOR PHASE = ',F9.4)
504      WRITE(IWRT,950)
505 950 FORMAT('0',/, '0',T44,'TOTAL GRAM-MOLES OF EACH ELEMENT FROM IN',
506      & 'PUT DATA',/,1X,T42,'AND AS CALCULATED FROM THE EQUILIBRIUM',
507      & ' COMPOSITIONS',/, '0',4(4X,'INPUT DATA',3X,
508      & 'CALCULATED',5X))
509      NPRT=E/4
510      NCHK=NPRT*4
511      IF(NCHK.NE.E) NPRT=NPRT*4
512      ISTART=1
513      DO 970 K=1,NPRT
514      NEND=ISTART+3
515      IF(NEND.GT.E) NEND=E
516      WRITE(IWRT,960) (CUMNT(J),E(J),BCALC(J),J=ISTART,NEND)
517 960 FORMAT(1X,4(A2,1X,E12.5,1X,E12.5,4X))
518      ISTART=NEND+1
519 970 CONTINUE
520 971 CONTINUE
521      IF(IWRAP.GT.3) CALL WRAPUP(TITLE,SPECIE,INERT,V,FRAC,QUEC,ZV,FRACZ
522      & ,SITCT,SIMF,ACTSIS,ACTCAS,ACTINS,ACTPS,ACTASS,RIIIIV,RGAAS,FINF,
523      & BSSTCVG,ITBST,RELMAX,CNVC,ISS,XIII,T,P,IDATA,IDMI,IFILE,V,MOI)
524      IF(IIP.GT.1.OR.ICMP.GT.1.OR.IWRAP.GT.1) GO TO 1900
525 C
526 C WRITE-OUT THE INDEPENDENT REACTION EQUATIONS
527 C
528 C IPAGE=IPAGE+1
529 C WRITE(IWRT,400) (TITLE(K),K=1,20), IPAGE
530 C WRITE(IWRT,410) T,P
531 C WRITE(IWRT,980)
532 980 FORMAT('0',T34,'A SET OF INDEPENDENT REACTION EQUATIONS FOR ',
533      & 'THIS SYSTEM IS AS FOLLOWS:',/, '0')
534      DO 1100 I=1,VSC
535 C
536 C DETERMINE THE NUMBER OF BASIS SPECIES IN EACH FORMATION REACTION
537 C
538      NSPEC=0
539      DO 990 K=1,E
540      IF(I.EQ.IDXBAS(K)) GO TO 1100

```

```

541     IF(ABS(GNU(I,K)).LT.1.0E-6) GO TO 990
542     NSPEC=NSPEC+1
543 990 CONTINUE
544 C
545 C  FILL THE CHARACTER ARRAY "STRING" WITH THE REACTION REACTANT SPECIES
546 C
547     NLCCP=1
548     IF(NSPEC.GT.4) NLCCP=FLCAT(NSPEC)/4.0+0.5
549     DO 1000 K=1,3
550     STRING(1,K)=BSPACE(I,K)
551 1000 CONTINUE
552     STRING(1,4)=RPAS
553     COEFF(1)=1.0
554     IST=1
555     ICNT=0
556     DO 1060 ILCCP=1,NLCCP
557     NCNT=NSPEC-ICNT+1
558     IF(NCNT.GT.5) NCNT=5
559     DO 1020 IDX=2,NCNT
560     ICNT=ICNT+1
561     DO 1015 IBASE=IST,E
562     IF(ABS(GNU(I,IBASE)).LT.1.0E-6) GO TO 1015
563     IDXB=IDXBAS(IBASE)
564     DO 1010 K=1,3
565     STRING(IDX,K)=BSPACE(IDXB,K)
566 1010 CONTINUE
567     COEFF(IDX)=GNU(I,IBASE)
568     STRING(IDX,4)=RPSPS
569     GO TO 1013
570 1015 CONTINUE
571 1012 IST=IBASE+1
572 1020 CONTINUE
573     STRING(NCNT,4)=RPBL
574     IF(ILCCP.EQ.1) WRITE(IWRT,1040)(LP,COEFF(IJK),
575     &                                     (STRING(IJK,K),K=1,4),IJK=1,NCNT)
576 1040 FORMAT('0',A1,F5.2,4A4,4(A1,E10.3,4A4))
577     IF(ILCCP.GT.1) WRITE(IWRT,1050) SSPS,(LP,COEFF(IJK),
578     &                                     (STRING(IJK,K),K=1,4),IJK=2,NCNT)
579 1050 FORMAT(1X,T20,4A,4(A1,E10.3,4A4))
580 1060 CONTINUE
581 1100 CONTINUE
582 C
583 C  WRITE-OUT A COMPARISON BETWEEN THE EQUILIBRIUM CONSTANTS
584 C  AS CALCULATED BY THE GIBBS FREE ENERGY CHANGE AND BY COMPOSITION
585 C
586     IPAGE=IPAGE+1
587     WRITE(IWRT,400) (TITLE(K),K=1,20), IPAGE
588     WRITE(IWRT,410) T,F
589     WRITE(IWRT,1110)
590 1110 FORMAT('0',/,1X,T40,'EQUILIBRIUM CONSTANTS FROM THE INDEPENDENT',
591     & ' REACTIONS',/, '0',T20,'GIBBS FREE ENERGY CHANGE',T47,
592     & 'EQUILIBRIUM CONSTANT',T73,'EQUILIBRIUM CONSTANT',/,1X,
593     & 'REACTION PRODUCT',T25,'(KCAL/G-MOLE)',T45,'FROM GIBBS FREE',
594     & 'ENERGY',T70,'FROM PREDICTED COMPOSITION',/, ' ',T20)

```

```
595      824('_' ),T45,22('_' ),T70,26('_' )
596      DL 1200 I=1,VSC
597      IF(N(I).GT.1.00E-21) WRITE(IWRT,1120) (SPECIE(I,K),K=1,3),DG(I),
598      &                                          KEG(I),G(I)
599      IF(N(I).LE.1.00E-21) WRITE(IWRT,1121) (SPECIE(I,K),K=1,3),DG(I),
600      &                                          KEG(I),G(I)
601 1120 FORMAT(1X,3A4,T28,F8.3,T51,E12.5,T77,E12.5)
602 1121 FORMAT(1X,3A4,T28,F8.3,T51,E12.5,T77,E12.5,2X,'(NOT BINDING)')
603 1200 CONTINUE
604      IF(ISS.GT.0) WRITE(IWRT,445) XIII
605 1900 IF(ISTOP.EQ.1) GO TO 3000
606 2000 CONTINUE
607 3000 WRITE(IWRT,3001)
608 3001 FORMAT('1', ' ')
609      STOP
610      END
```

### B.3 A Description of the Major Variables in MCMPEC.STOIC

Variables which are used in the IMSL subroutines LIWIF, LEQ1IF, LUDATF and LUELMF are not included in this list. FORTRAN default typing applies unless otherwise specified.

<u>Variable</u>	<u>Description</u>	<u>Units</u>
A (I,J)	elemental abundance matrix	$\frac{\text{atoms of element } j}{\text{molecule of specie } i}$
ACOE (I)	activity coefficient of specie i	-
AMAX	maximum value the convergence forcer may attain	-
AMIN	minimum value the convergence forcer may attain	-
AXS	activity coefficient correlation parameter	variable
A0 (I)	heat capacity correlation parameter	kcal/g-mole-K
A1 (I)	heat capacity correlation parameter	kcal/g-mole-K <sup>2</sup>
A2 (I)	heat capacity correlation parameter	variable
A3 (I)	heat capacity correlation parameter	variable
A0Z	inert specie heat capacity correlation parameter	kcal/g-mole-K
A1Z	inert specie heat capacity correlation parameter	kcal/g-mole-K <sup>2</sup>
A2Z	inert specie heat capacity correlation parameter	variable
A3Z	inert specie heat capacity correlation parameter	variable

<u>Variable</u>	<u>Description</u>	<u>Units</u>
B (J)	moles of element J specified in the system	g-moles
BCALC (J)	moles of element J as calculated by algorithm	g-moles
BESTN	The best estimate to the equilibrium mole numbers	g-moles
BXS	activity coefficient correlation parameter	variable
C	number of pure condensed phases (integer)	-
CHMPT (I)	chemical potential of specie i	kcal/g-mole
CHMPTZ	chemical potential of the inert	kcal/g-mole
CNVG	composition convergence criterion	-
COND (3)	vector containing the character string 'CONDENSED'	-
D (I, J)	matrix of basis species	$\frac{\text{atoms of } j}{\text{molecule of } i}$
DELH	total enthalpy change	kcal/g-mole
DELN (I)	change in moles of specie i	g-mole
DELS	total entropy change	kcal/g-mole-K
DG (I)	Gibbs Free Energy change of reaction i	kcal/g-mole
DGDL	change in system Gibbs Free Energy with respect to the convergence forcer	kcal/g-mole

<u>Variable</u>	<u>Description</u>	<u>Units</u>
DHO (I)	enthalpy of formation of specie i	kcal/g-mole
DHOZ	enthalpy of formation of the inert specie	kcal/g-mole
DINV (I, J)	inverse of matrix D	-
DPRME (I, J)	Gram-Schmidt orthogonalization of matrix D	-
DSO (I)	entropy of formation of specie i	kcal/g-mole-K
DSOZ	entropy of formation of the inert specie	kcal/g-mole-K
DZETA(I)	change in reaction extent for specie	-
E	number of elements in the system (integer)	-
ELIII (K)	vector containing character string of group III elements	-
ELMNT (J)	vector containing character strings of the elements present in the system	-
ELV (K)	vector containing character strings of group V element	-
EPCP2	$E + C + 2$ (integer)	-
EP3	$E + 3$ (integer)	-
EP3PC	$E + 3 + C$ (integer)	-
FRAC (I)	mole fraction of specie i in its phase	-
FRACZ	mole fraction of inert in the vapor	-

<u>Variable</u>	<u>Description</u>	<u>Units</u>
GNU (I, J)	formation reaction coefficient matrix	g-mole
GFE	Gibbs free energy of the system	kcal/g-mole
GSTAR	GFE divided by RT	-
IACFF	activity coefficient switch	-
IALG	convergence forcer algorithm switch	-
ICHNG	parameter which indicates whether or not the basis species have changed	-
ICMP	index for the composition loop	-
ICP (I)	heat capacity correlation parameter	-
IDATA	switch used with the wrap-up file	-
IDGT	number of significant figures in each matrix element	-
IDIM1	maximum number of species allowed in system	-
IDIM2	maximum number of elements allowed in system	-
IDEBUG	option to aid in trouble-shooting	-
IDXBAS (J)	vector containing the index of each basis specie	-
IFILE	logical unit designator of the wrap-up file	-
INERT (3)	vector containing the inert specie name	-

<u>Variable</u>	<u>Description</u>	<u>Units</u>
IOPT	parameter to allow various computational options	-
IOUT	number of pure condensed phases removed by subroutine ADDR MV	-
IRD	logical unit designator for data input	-
ISPCE (i, J)	array containing the original specie order	-
ISS	steady state option parameter	-
ISTOP	switch which halts the computation if problems develop	-
ITER	current iteration number in the equilibrium calculation	-
ITP	index for the temperature and pressure loop	-
ITST	parameter which indicates linear dependence in the basis specie matrix	-
IWRAP	switch used with the wrap-up file	-
IWRT	logical unit designator for data output	-
IXSCOR	parameter which chooses the solution phase activity coefficient model	-
KEQ (I)	equilibrium constant for formation reaction i as calculated from the Gibbs Free Energy change (real)	-
LAMBDA	convergence forcer (real)	-
MAXIT	maximum number of iterations to be used	-
N (I)	moles of specie i (real)	g-moles
NMAX	total number of loops to be made in the composition or temperature and pressure loops	-

<u>Variable</u>	<u>Description</u>	<u>Units</u>
NS	total moles in solution (real)	g-moles
NSPEC	number of species in the formation reaction	-
NV	total moles in the vapor (real)	g-moles
P	system pressure	Pa
PHASE (I, 3)	matrix containing a character string to denote the phase of each specie	-
PINC	pressure increment for each loop	Pa
PO	formation data reference pressure	Pa
Q (I)	equilibrium constant for formation reaction i as calculated from composition	-
RELERR	fractional change between KEQ(I) and Q(I)	-
RELMAX	maximum value of RELERR during an iteration	-
RLXMIN	The minimum allowable valve of the convergence forcer	-
RIIIIV	vapor phase III/V atomic ratio	-
RT	product of the ideal gas constant and the temperature	kcal/g-mole
S	total number of species in the solution phase	-
SIMF	mole fraction of silicon species in the vapor	-
SITOT	moles of silicon species in the vapor	g-moles
SOLN (3)	vector containing the character string 'SOLUTION'	-

<u>Variable</u>	<u>Description</u>	<u>Units</u>
SPECIE (I, 3)	matrix of character strings containing the names of each specie	-
STDCP (I)	standard chemical potential of specie i	kcal/g-mole
STDCPZ	standard chemical potential of the inert	kcal/g-mole
SUMIII	total moles of group III atoms in the vapor	g-mole
SUMV	total moles of group V atoms in the vapor	g-mole
T	system temperature	K
TITLE (K)	vector containing an 80 character title	-
TINC	temperature increment for each loop	K
TOTMC (I)	total moles of pure condensed phase i as input	g-moles
TOTMOL	total moles in a single phase	g-moles
TOTMS	total moles in the solution phase	g-moles
TOTMV	total moles in the vapor phase	g-moles
TO	formation data reference temperature	K
V	total number of species in the vapor (integer)	-
VAPOR (3)	vector containing the character string 'VAPOR'	-

<u>Variable</u>	<u>Description</u>	<u>Units</u>
WKA	work area for LEQTIF	
WKA1	work area for LINVIF	
XIII	group III specie fraction in the steady state liquid "pure" condensed phase	-
ZV	moles of inert in the system	g-moles
ZACT	activity coefficient of the inert	-

## B.4 Descriptions of the Subroutines

The subroutine structure of MCMPEC.STOIC is shown in Figure B2. Subroutine ERRSET is a system routine which is used to suppress the printing of various arithmetic error messages. This subroutine may not be available at all installations and therefore the two calls to ERRSET may have to be removed if this code is to be implemented on other systems.

The IMSL subroutine LINVIF is part of a package of routines which include LEQTIF, LIJELMF and LUDATF. A brief discussion of this IMSL package is located in section B.4.19. The remaining subroutines are discussed in the following sections.

### B.4.1 STSTCP

A listing of subroutine STSTCP is shown in Figure B3. STSTCP calculates the standard state chemical potential for each specie in the system. The reference state is the system temperature  $T$ , the formation pressure  $P_0$ , and pure component in the phase in which the specie is present.

The pure component Gibbs Free Energy (standard chemical potential) of specie  $i$  at temperature  $T_0$  and pressure  $P_0$  is:

$$\mu_i^0(T_0, P_0) = \underline{G}_i^0 = \Delta \underline{H}_f^0 - T_0 \Delta \underline{S}_f^0 \quad (1)$$

For a system temperature  $T$  the standard chemical potential of specie  $i$  is given by:

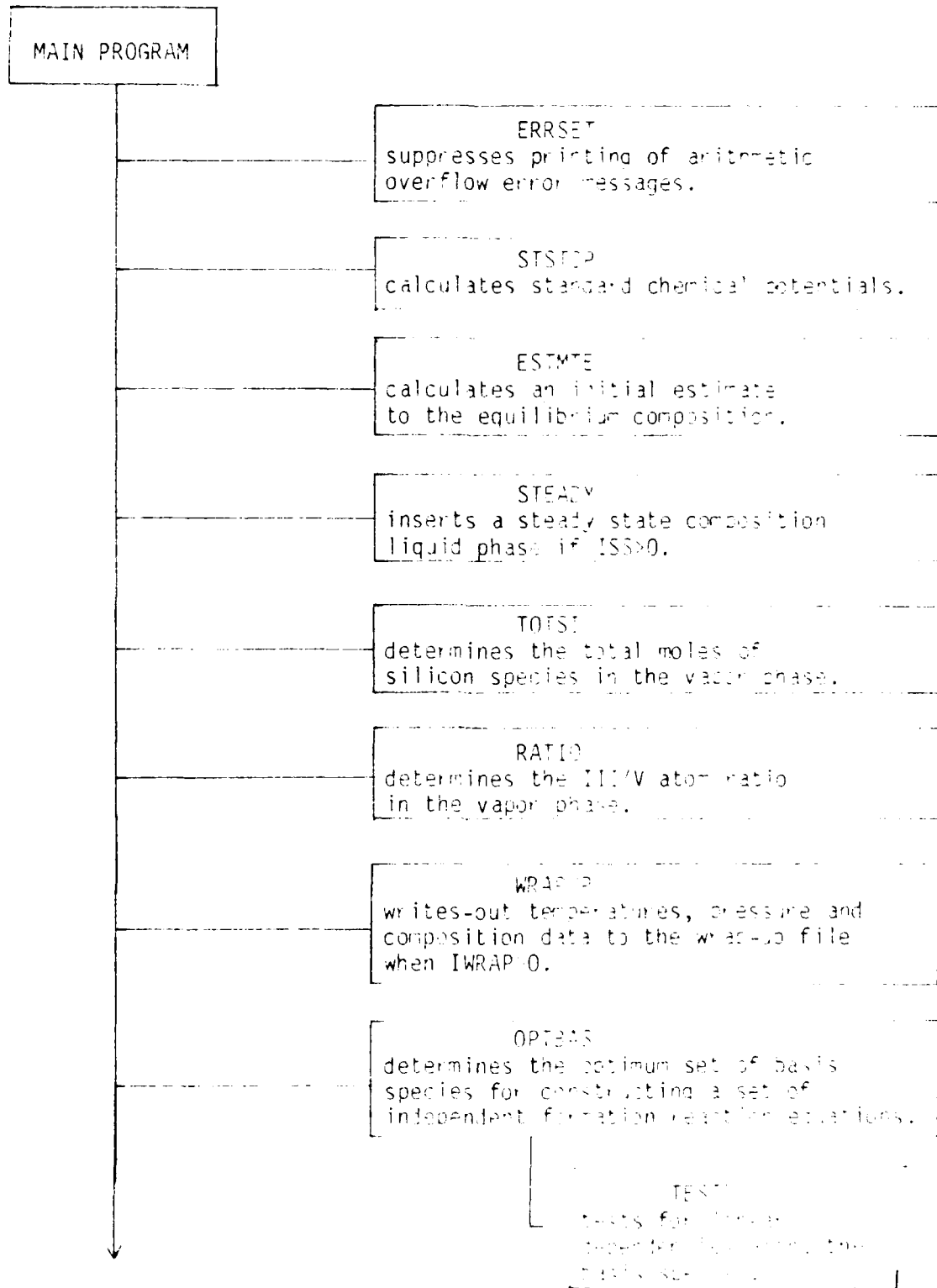
$$\begin{aligned} \mu_i^0(T, P_0) = & \Delta \underline{H}_f(T_0) + \int_{T_0}^T C_p^i dT \\ & - T \left[ \Delta \underline{S}_f(T_0) + \int_{T_0}^T \frac{C_p^i}{T} dT \right] \end{aligned} \quad (2)$$

Two heat capacity correlations are available and are chosen by the parameter ICP. These correlations are:

ICP	<u>Heat Capacity Correlation</u>	
0	$C_p(T) = a_0 + a_1 T + a_2 T^{-2} + a_3 \ln(T)$	(3)
1	$C_p(T) = a_0 + A_1 T + a_2 T^2 + a_3 T^3$	(4)

Figure B2

## Subprogram Structure of MCMPEC.ST010



IPVEC  
writes out integer vectors  
when IDEBUG>1.

PMAT  
writes out single precision  
matrices when IDEBUG>1.

PMAT

PMAT

EODCN  
calculates the stoichiometric  
coefficients for a set of  
independent formation reactions  
and the equilibrium constants  
for these reactions.

LINVF  
inverts the matrix  
of basis species.

DPMAT  
writes-out double precision  
matrices when IDEBUG>1.

PMAT

PVEC  
writes out real vectors  
when IDEBUG>1.

ACTCOF  
calculates the species  
activity coefficients.

QACON  
calculates the formation  
reaction equilibrium constants,  
 $K_f$ , from composition.

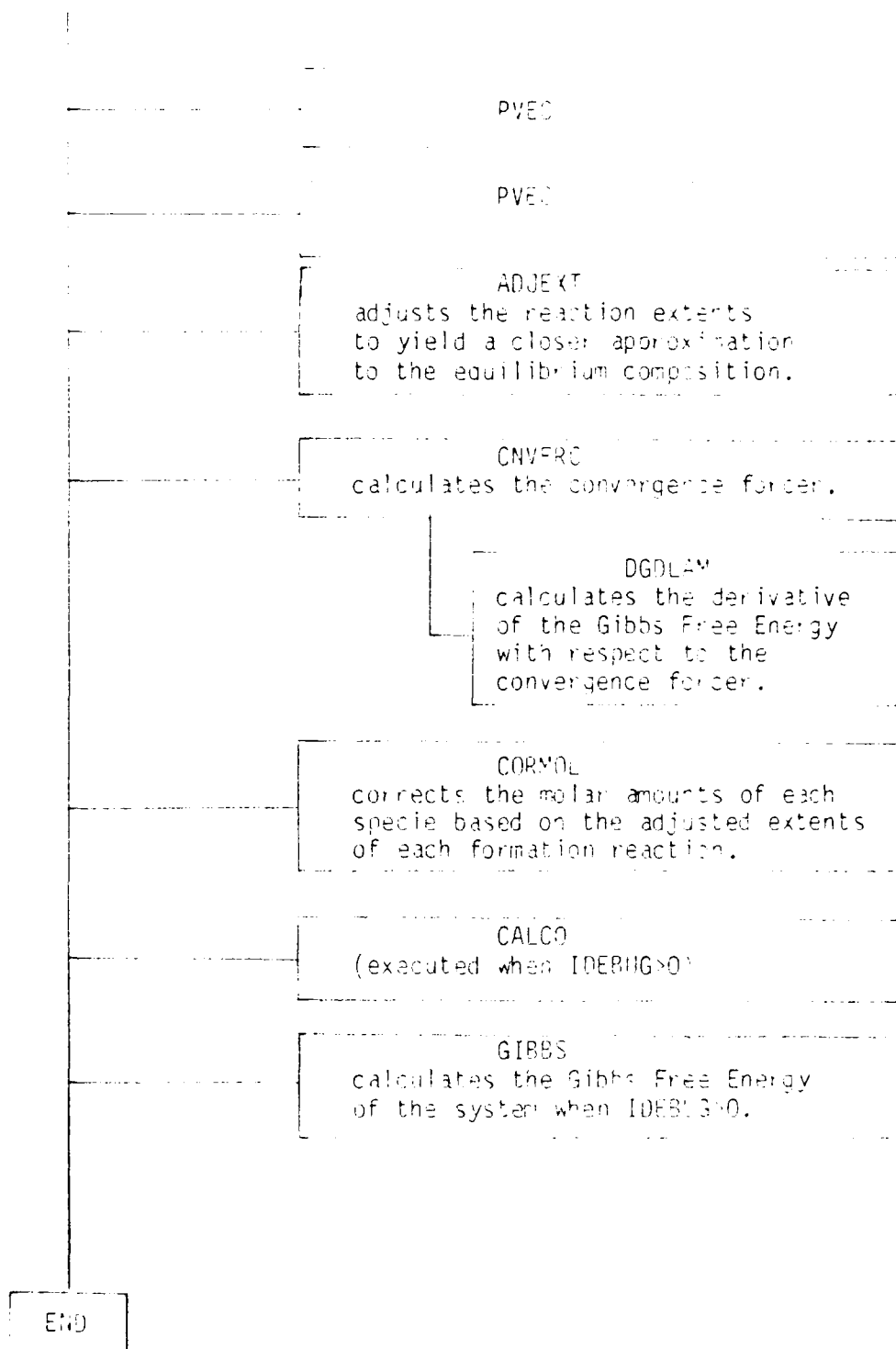


Figure B3. Subroutine STSTCP

```

1      SUBROUTINE STSTCP(A0,A1,A2,A3,A0Z,A1Z,A2Z,A3Z,DH0,DS0,DH0Z,DS0Z,
2      &                    STDCP,STDCPZ,ICP,ICPZ,T0,T,IDIM1,V,S,C)
3 C
4 C THIS SUBROUTINE CALCULATES THE STANDARD STATE CHEMICAL POTENTIALS
5 C REFERENCE STATE: PURE COMPONENT (APPROPRIATE PHASE)
6 C AT TEMPERATURE T.
7 C
8      DIMENSION A0(IDIM1),A1(IDIM1),A2(IDIM1),A3(IDIM1),DH0(IDIM1),
9      &                    DS0(IDIM1),STDCP(IDIM1),ICP(IDIM1))
10     INTEGER V,S,C,VSC
11     VSC=V+S+C
12     DT=T-T0
13     DT2=T**2-T0**2
14     DT3=T**3-T0**3
15     DT4=T**4-T0**4
16     DTM1=1.0/T-1.0/T0
17     DTM2=1.0/T/T-1.0/T0/T0
18     DLNT=ALOG(T)-ALOG(T0)
19     DLNT2=ALOG(T)**2-ALOG(T0)**2
20     DTLNT=1*ALOG(T)-T0*ALOG(T0)
21 C
22 C CHEMICAL POTENTIALS FOR THE VAPOR, SOLUTION AND CONDENSED PHASES
23 C
24     DO 100 I=1,VSC
25     DELH=A0(I)*DT+A1(I)*DT2/2.-A2(I)*DTM1+A3(I)*(DTLNT-DT)
26     DELS=A0(I)*DLNT+A1(I)*DT-A2(I)*DTM2/2.+A3(I)*DLNT2/2.
27     IF(ICP(I).EQ.1) DELH=A0(I)*DT+A1(I)*DT2/2.+A2(I)*DT3/3.
28     &                    +A3(I)*DT4/4.
29     IF(ICP(I).EQ.1) DELS=A0(I)*DLNT+A1(I)*DT+A2(I)*DT2/2.
30     &                    +A3(I)*DT3/3.
31     STDCP(I)=DH0(I)+DELH-T*(DS0(I)+DELS)
32 100 CONTINUE
33 C
34 C CHEMICAL POTENTIAL FOR THE INERT COMPONENT IN THE VAPOR PHASE
35 C
36     DELH=A0Z*DT+A1Z*DT2/2.-A2Z*DTM1+A3Z*(DTLNT-DT)
37     DELS=A0Z*DLNT+A1Z*DT-A2Z*DTM2/2.+A3Z*DLNT2/2.
38     IF(ICPZ.EQ.1) DELH=A0Z*DT+A1Z*DT2/2.+A2Z*DT3/3.
39     &                    +A3Z*DT4/4.
40     IF(ICPZ.EQ.1) DELS=A0Z*DLNT+A1Z*DT+A2Z*DT2/2.
41     &                    +A3Z*DT3/3.
42     STDCPZ=DH0Z+DELH-T*(DS0Z+DELS)
43     RETURN
44     END

```

Obviously various other correlations (constant, linear, quadratic, etc.) may be generated from these two functions by simply setting the appropriate coefficients to zero.

Lines 12 through 20 calculate the necessary limit differentials which result from performing the indicated integrations in equation 2 using the heat capacity correlations in equations 3 and 4. The integrals are evaluated as DELH and DELS and the standard chemical potential for each specie, STDCP(I), is then calculated.

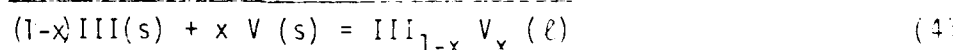
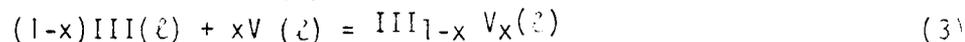
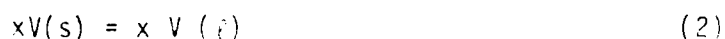
#### B.4.2 ESTMTE

A listing of subroutine ESTMTE is provided in Figure 34. ESTMTE simply calculates the number of moles of each specie from the specie mole fraction and the total number of moles in the phase. ESTMTE is provided as a subroutine to allow the inclusion of an algorithm which will yield an estimate to the equilibrium composition and therefore reduce the number of iterations required to obtain convergence. Currently the inlet composition is used as this initial estimate.

#### B.4.3 STEADY

Subroutine STEADY inserts a pure condensed phase into the system in order to model a III-V liquid solution with a steady state composition. The composition of this liquid is that which would exist at equilibrium with the stoichiometric III-V solid at the system temperature. This subroutine is invoked when ISS>0, a Ga/As liquid phase being inserted for ISS=1 and In/P liquid phase for ISS=2. This phase is inserted as the last pure condensed phase in the system (specie V+S+C).

A solid liquid equilibrium model for a binary liquid with the mole fraction of group V specie designated as x is obtained by writing the following reactions.



Reaction 4, which is the sum of the previous three reactions, represents the formation of a liquid solution having a composition  $(1-x)\text{III}$  and  $xV$ .

The Gibbs Free Energies of reactions 1 and 2 are simply those due to melting at  $T_m$  corrected for the temperature,  $T$ , of the solution.

$$G_1 = (1-x) \left[ S_m^{\text{III}}(T_m^{\text{III}} - T) + \Delta C_p^{\text{III}}(T - T_m^{\text{III}} - T \ln \frac{T_m^{\text{III}}}{T}) \right] \quad (5)$$

$$G_2 = x \left[ S_m^V(T_m^V - T) + \Delta C_p^V(T - T_m^V - T \ln \frac{T_m^V}{T}) \right] \quad (6)$$

Figure B4. Subroutine ESTMTE

```
1      SUBROUTINE ESTMTE(TCTMV,TCTMS,TCTMC,FRAC,N,FRACZ,ZV, IDIM1,  
2      &      V,S,C)  
3      C  
4      C THIS SUBROUTINE CALCULATES AN INITIAL ESTIMATE  
5      C TO THE SYSTEM EQUILIBRIUM COMPOSITIONS  
6      C  
7      DIMENSION TOTMC(IDIM1),FRAC(IDIM1)  
8      INTEGER V,S,C,VS,VS1,VSC  
9      REAL*8 N(IDIM1)  
10     VS=V+S  
11     VS1=VS+1  
12     VSC=V+S+C  
13     TCTMCL=TCTMV  
14     DO 50 I=1,VS  
15     IF(I.GT.V) TCTMCL=TCTMS  
16     N(I)=TCTMCL*FRAC(I)  
17     50 CONTINUE  
18     ZV=FRACZ*TCTMV  
19     IF(C.EQ.0) RETURN  
20     DO 60 I=VS1,VSC  
21     N(I)=TCTMC(I)  
22     60 CONTINUE  
23     RETURN  
24     END
```

Where it has been assumed that  $\Delta C_p$ , the difference between the liquid and solid heat capacities, may be approximated as a constant.

The Gibbs Free Energy of reaction 3 is that due to the mixing of the group III and V liquids. This free energy consists of an ideal free energy of mixing comprised of a configurational entropy term and an excess Gibbs Free Energy term due to nonidealities. Applying a simple solution theory model for the excess Gibbs Free Energy yields [5]:

$$G_3 = RT[x \ln x + (1-x) \ln(1-x)] + (A_{xs} + B_{xs}T)x(1-x) \quad (7)$$

The Gibbs Free Energy of the liquid solution represented by reaction 4 is therefore given by:

$$G_4 = G_1 + G_2 + G_3 \quad (8)$$

Determination of the mole fraction of group V atoms in the melt,  $x$ , is accomplished by solving the implicit equation developed by Vieland [6] modified to include a simple solution rather than a regular solution model.

$$T = \frac{T_m^{IIIIV} S_m^{IIIIV} - A_{xs} (2x - 2x^2 - 0.5)}{S_m^{IIIIV} - R \ln 4x(1-x) + B_{xs} (2x - 2x^2 - 0.5)} \quad (9)$$

The thermodynamic constants necessary for the evaluation of equations 8 and 9 are listed in Table B.3. Figures B5 and B6 demonstrate how well the theory predicts the liquidus temperatures in the Ga/As and In/P systems.

Table B.3

Thermodynamic Data for the Ga/As and In/P systems

	$\Delta S_m$ (Cal/g-mole-K)	$T_m$ (K)	$\Delta C_p$ (Cal/g-mole-K)	$A_{xs}$ (Cal/g-mole)	$B_{xs}$ (Cal/g-mole-K)
Ga	4.411	302.9	-0.05	4666	-8.741
As	4.7	1090	1.0		
GaAs	16.64	1511	0		
In	1.815	429.8	-0.2	32750	-23.95
P	0.5011	313.3	0.47		
InP	10.81	1332.2	0		

Figure 85  
The Ga/As System Liquidus Line  
(Data refs. 7, 12, 13)

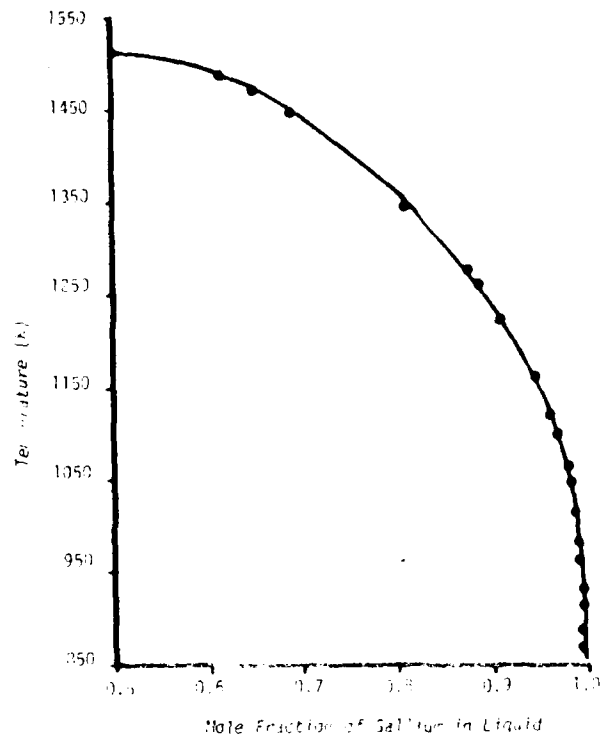
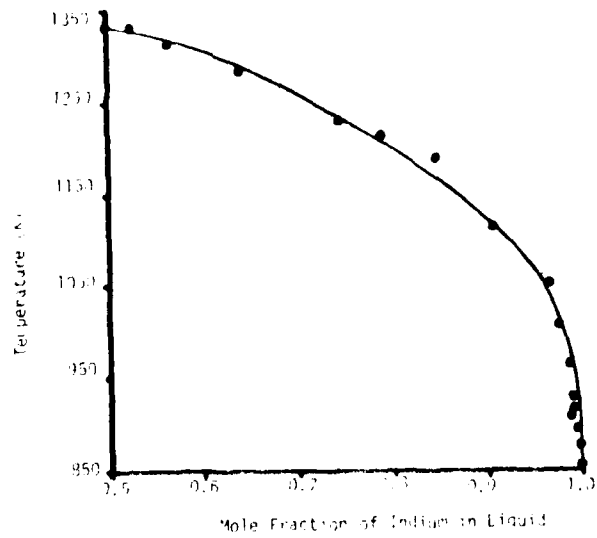


Figure 86  
The In/P System Liquidus Line  
(Data refs. 8, 9, 10, 11)



A listing of subroutine STEADY is shown in Figure 87. Lines 16 and 17 define a statement function which corresponds to the right hand side of equation 9. Hollerith strings are assigned to the specie identifier matrix in lines 19 through 21. The standard state chemical potentials and excess Gibbs Free Energy correlation parameters for the Ga/As and In/P systems are assigned in lines 29 through 54.

An "interval halving" root finding algorithm for solving the implicit equations is located at lines 57 through 80. The iteration is considered to have converged when the two sides of the equation differ by less than 0.01%.

The standard state chemical potential of the liquid solution is calculated in lines 86 and 91. Finally, the elemental abundance matrix is assigned the appropriate values which reflect the elemental composition of the liquid solution in lines 93 through 107.

Figure B7. Subroutine STEADY

```

1      SUBROUTINE STEADY(SPECIE,A,STOCP,ELMNT,AXS,T,DT,DT2,DTM1,DTM2,
2      & IDIM2,ISS,IAST)
3 C
4 C      SUBROUTINE TO CALCULATE THE SOLID-LIQUID EQUILIBRIUM CONSTANTS
5 C      FOR USE IN THE STEADY-STATE APPROXIMATION IN THE SLURRY ZONE
6 C
7 C      ISS      SYSTEM
8 C      1      GA(L)-AS(L)/GA-AS (S)
9 C      2      IN(L)-P(L)/IN-P (S)
10 C
11      DIMENSION A(IDIM1,IDIM2),STOCP(IDIM1)
12      INTEGER SPECIE(IDIM1,3),ELMNT(IDIM2),IIIL(2),VLC(2),V,S,C,VSC,
13      & LAST/'1-X)'/,GA/'GA'/,AS/'AS'/,IN/'IN'/,P/'P'/'/'
14      DATA IIIL(1)/' GAX'/,IIIL(2)/' INAX'/,
15      & VLC(1)/' -AS('/,VLC(2)/' - P('/
16      THETA2(XV)=(T*IIIV*DSIIIV-AXS*(0.5-XV**2-(1.-XV)**2))/
17      & (DSIIIV-R*ALOG(4.*XV*(1.-XV))+XS*(0.5-XV**2-(1.-XV)**2))
18      VSC=V+S+C
19      SPECIE(VSC,1)=IIIL(ISS)
20      SPECIE(VSC,2)=VLC(ISS)
21      SPECIE(VSC,3)=LAST
22      DT=T-TJ
23      DT2=T**2-TJ**2
24      DTM1=1.0/T-1.0/TJ
25      DTM2=1.0/T**2-1.0/TJ**2
26      DLNT=ALOG(T/TJ)
27      IF(ISS.EQ.2) GO TO 50
28 C
29 C      GA-AS SYSTEM
30 C
31      TMIIV=302.9
32      TMV=1090.
33      TMIIV=1511.
34      DSIIIV=0.004411
35      DSIV=0.0047
36      DSIIIV=0.01604
37      DSIII=-0.00005
38      DCV=0.001
39      AXS=4.066
40      BXS=-0.000741
41      GO TO 60
42 C
43 C      IN-P SYSTEM
44 C
45      50 TMIIV=429.5
46      TMV=313.3
47      TMIIV=1337.2
48      DSIIIV=0.001315
49      DSIV=0.000011
50      DSIIIV=0.01041
51      DSIII=-0.00007
52      DCV=0.000472
53      AXS=02.75
54      BXS=-0.02045

```

```

55      6J CONTINUE
56 C
57 C BINARY FURT FIDING ROUTINE FOR THE GROUP III AND V ELEMENTS
58 C
59      XV=0.5
60      XMIN=0.0
61      XMAX=1.0
62      R=0.0019872
63      THETA1=T
64      XCLD=0.4
65      THTCLO=THETA2(XCLD)
66      DO 100 I=1,50
67      THET2=THET-R(XV)
68      ERR=(THET2-THETA1)/THETA1
69      IF(ABS(ERR).LT.0.0001) GO TO 200
70      SWITCH=(THET2-THTCLO)/(XV-XCLD)
71      THTCLO=THET2
72      XCLD=XV
73      IF(SWITCH.GT.0. AND.THET2.LT.THETA1) GO TO 80
74      IF(SWITCH.LT.0. AND.THET2.GT.THETA1) GO TO 80
75      XMAX=XV
76      XV=0.5*(XMIN+XV)
77      GO TO 100
78      8J XMIN=XV
79      XV=0.5*(XMAX+XV)
80      10J CONTINUE
81      WRITE(I*,T,120)
82      120 FORMAT('0',I*,*'*'*'*' SUBJECTING STEADY STATE ACTION FOR SOURCE ',
83      & 'COMPOSITION DID NOT CONVERGE')
84      200 CONTINUE
85 C
86 C CALCULATE THE STANDARD CHEMICAL POTENTIAL OF THE SOURCE SOLUTION
87 C
88      DGA=(1.0-XV)*(DBIII*(TM11-T)+DCIII*(T-TM11-T*ALOG(T/TM11)))
89      DGB=XV*(DBV*(TMV-T)+DCV*(T-TMV-T*ALOG(T/TMV)))
90      DGC=(AXS+XV*1)*XV+(1.-XV)*R*T*(XV*ALOG(XV)+(1.-XV)*ALOG(1.-XV))
91      STGCP(VEC)=DGA+DGB+DGC
92 C
93 C LOCATE THE GROUP III AND V ELEMENTS IN THE ELEMENTAL ABUNDANCE ARRAY
94 C AND INSERT THE CALCULATED ABUNDANCES INTO THIS ARRAY
95 C
96      IX3=0
97      IX5=0
98      DO 300 I=1,101M2
99      IF(IGS.FG.2) GO TO 250
100     IF(ELMNT(I).EQ.5A) IX3=I
101     IF(ELMNT(I).EQ.5D) IX5=I
102     GO TO 300
103     250 IF(ELMNT(I).EQ.1A) IX3=I
104     IF(ELMNT(I).EQ.2) IX5=I
105     300 CONTINUE
106     A(VEC,IX3)=1.0-XV
107     A(VEC,IX5)=XV
108     X11=1.0-XV
109     RETURN
110     END

```

## B.4.4 TOTSI

Subroutine TOTSI, shown in Figure B8, calculates the total moles of silicon species in the vapor phase, the mole fraction of silicon species in the vapor phase and the activity of elemental silicon in a solid solution.

A character string comparison is made to determine which member of vector ELMNT is assigned the string "SI" and the moles of all vapor species with a nonzero value in their elemental abundance vectors corresponding to this position are summed. The mole fraction of silicon species in the vapor phase is then calculated from the total moles of all species in the vapor phase.

The activity of silicon in a solid solution which is in equilibrium with the vapor phase is calculated based on the silicon monomer concentration in the vapor via the reaction,



The activity of silicon in a solid solution is therefore given by,

$$a_{\text{Si}} = \frac{P_{\text{Si}}}{K P_0} \quad (2)$$

where:  $P_{\text{Si}}$  = partial pressure of Si(v)  
 $P_0$  = reference state pressure  
 $a_{\text{Si}}$  = solid solution silicon activity

The equilibrium constant K is calculated from the Gibbs Free Energy change of reaction 1 and is shown at lines 41 through 43.

## B.4.5 RATIO

Subroutine RATIO, shown in Figure B9, calculates the group III/V atom ratio in the vapor phase, the activities of Ga, In, As and P in a solid solution which is in equilibrium with the vapor phase, and the saturation ratios of GaAs and InP.

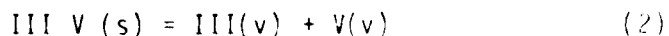
The III/V atom ratio is determined at lines 20 through 45 using all of the group III and V elements in the periodic table. This results in a total III/V ratio which does not distinguish between the individual elements in each group.

Solid solution activities for Ga, In, As and P in equilibrium with the vapor phase are calculated using the same method which was applied in subroutine TOTSI for silicon. First the vapor phase monomers of each element are identified and then the activities are calculated. The thermodynamics data for each system is provided at lines 58 through 105.

Finally, the saturation ratios for GaAs and InP are calculated in order to provide a measure of the vapor phase supersaturation. The saturation ratio is defined by

$$R_{\text{SAT}} = \frac{P_{\text{III}} P_{\text{V}}}{K_{\text{III V}} P_0^2} \quad (1)$$

where the equilibrium constant,  $K_{\text{III V}}$  is calculated from the Gibbs Free Energy change of the reaction



Thus the saturation ratio is a comparison between the equilibrium constant for reaction 2 as calculated from the free energy change and from the vapor phase composition. A supersaturated vapor phase exists when  $RSAT > 1$ .

#### B.4.6 OPTBAS

Subroutine OPTBAS, shown in Figure B10, determines the optimum set of basis species to be used in the formation reaction equations. A bubble sort is performed at lines 18 through 74 which orders arrays STDCP, A, DHO, DSO, AO, AI, A2, A3, SPECIE, PHASE, ICP and N in descending order of N. This places the species which are present in the greatest molar amounts in the first positions of the array indices. Thus, when the basis specie set is chosen using the algorithm outlined in section B.5 the optimum set of basis species will result.

Line 79 tests parameter ICHNG to determine whether the specie order has changed since the last iteration. If not (ICHNG=0) then the optimum set of basis species will not change and the remainder of this subroutine is skipped.

The set of basis species is constructed at lines 80 through 97. Subroutine TESTD checks the D matrix for linear dependencies between the rows. If a complete set of basis species cannot be found a message is written out at lines 99 and 100 and parameter ISTOP is set to unity. The iterative procedure is then halted at the next line in the main program.

#### B.4.7 TESTD

Subroutine TESTD tests the rows of the D matrix for linear independence by building a Gram-Schmidt orthogonalized matrix  $D'$  from D. The Gram-Schmidt orthogonalization procedure essentially subtracts away the projection of all the rows in the matrix which are above the row being orthogonalized. If the resulting orthogonalized row is composed of all zeros then this row was linearly dependent upon at least one of the above rows in the matrix. The equations used to construct matrix  $D'$  from D are presented in section B.5.

A listing of TESTD is provided in Figure B11.

## Figure B8. Subroutine TOTSI

```

1      SUBROUTINE TOTSI(I,ELMNT,FRAC,N,SITOT,ACTSIS,T,V,ICDIM1,ICDIM2,
2      &      V,E)
3 C
4 C      SUBROUTINE TO CALCULATE THE TOTAL SI IN THE VAPOR PHASE
5 C      AND THE ACTIVITY OF SI IN A SOLID SOLUTION
6 C
7      DIMENSION A(ICDIM1,ICDIM2),FRAC(ICDIM1)
8      INTEGER ELMNT(ICDIM2),V,E,SIVPR/'SI'/
9      REAL*8 N(ICDIM1)
10     T0=298.15
11     P0=101325.0
12     RT=J.0019372*T
13 C
14 C      DETERMINE THE TOTAL AMOUNT OF SILICON IN THE VAPOR
15 C
16     SITOT=J.0
17     SIMF=J.0
18     ACTSIS=0.
19     DO 100 J=1,E
20     KSI=J
21     IF(ELMNT(J).EQ.SIVPR) GO TO 130
22 100 CONTINUE
23     GO TO 300
24 130 CONTINUE
25     DO 140 I=1,V
26     IF(A(I,KSI).LT.0.001) GO TO 140
27     SITOT=SITOT+N(I)
28     SIMF=SIMF+FRAC(I)
29 140 CONTINUE
30 C
31 C      FIND SI(V) AND CALCULATE THE ACTIVITY OF SOLID SI IN SOLUTION
32 C
33     DO 200 I=1,V
34     ICNT=0
35     IF(A(I,KSI).LT.0.001) GO TO 300
36     DO 150 J=1,E
37     IF(A(I,J).LT.0.001) GO TO 150
38     ICNT=ICNT+1
39 150 CONTINUE
40     IF(ICNT.GT.1) GO TO 200
41     DG=108.-0.00091*(T-T0)-5.011E-7/2.*(T**2-T0**2)-147.6*(1/T-1/T0)
42     &      -T*(J.035637-0.00091*ALOG(T/T0)-5.011E-7*(T-T0)
43     &      -147.6/2.*(1/T**2-1/T0**2))
44     ACTSIS=FRAC(I)*P0*EXP(DG/RT)
45     IF(N(I).LT.1.00E-1) ACTSIS=0.
46     GO TO 300
47 200 CONTINUE
48 300 CONTINUE
49     RETURN
50     END

```

Figure B9. Subroutine RATIO

```

1      SUBROUTINE RATIO(I,ELMNT,FRAC,N,STOCP,ACTAS,ACTIN,ACTASB,
2      &      ACTINB,PIIIIV,FCOAS,FCOINB,T,P,T0,-0.1D+21,1D+12,V,0)
3 C
4 C THIS SUBROUTINE CALCULATES THE VAPOR PIII/V RATIO,
5 C THE GA, IN, AS AND P SOLID SOLUTION ACTIVITIES,
6 C AND THE SATURATION RATIOS OF GA-AS AND IN-P.
7 C
8      DIMENSION A(IDIM1,IDIM2),FRAC(IDIM1),STOCP(IDIM1),KIII(5),KV(5)
9      REAL*8 N(IDIM1)
10     INTEGER ELMNT(IDIM2),ELT(1(5),ELV(5),V,E
11     DATA ELIII(1)/'B'/,ELIII(2)/'AL'/,ELIII(3)/'GA'/,ELIII(4)/'IN'/,
12     &      ELIII(5)/'TL'/,ELV(1)/'N'/,ELV(2)/'P'/,ELV(3)/'AS'/,
13     &      ELV(4)/'SB'/,ELV(5)/'BT'/'
14     FNCOG(T)=EH+P1*(T-T0)+A2/2.*(T+T2-T0+T2)-A3*(1/T-1/T0)
15     &      +A4*(T*ALOG(T)-T-T0+ALOG(T0)+T0)+A5/3.*(T+T3-T0+T3)
16     &      -T*(A6+A1*ALOG(T/T0)+A2*(T-T0)-A3/2.*(1/T+2-1/T0+2)
17     &      +-4/2.*(ALOG(T)**2-ALOG(T0)**2)+A5/2.*(T+T2-T0+T2))
18     RT=0.0019572*T
19 C
20 C DETERMINE WHICH INDICES CORRESPOND TO COLUMN III AND V ELEMENTS
21 C
22     DO 100 K=1,5
23     KIII(K)=0
24     KV(K)=0
25     DO 100 J=1,E
26     IF(ELMNT(J).EQ.ELIII(K)) KIII(K)=J
27     IF(ELMNT(J).EQ.ELV(K)) KV(K)=J
28 100 CONTINUE
29 C
30 C SUM-UP THE GROUP III AND V SPECIES AND CALCULATE THE RATIO
31 C
32     SUMIII=0.0
33     SUMV=0.0
34     DO 200 I=1,V
35     DO 200 K=1,5
36     IDXIII=KIII(K)
37     IDXV=KV(K)
38     IF(IDXIII.EQ.0) GO TO 120
39     SUMIII=SUMIII+A(I,IDXIII)*FRAC(I)
40 120 CONTINUE
41     IF(IDXV.EQ.0) GO TO 200
42     SUMV=SUMV+A(I,IDXV)*FRAC(I)
43 200 CONTINUE
44     PIIIIV=1.0/10
45     IF(SUMV.GT.0.0) PIIIIV=SUMIII/SUMV
46 C
47 C FIND THE SPECIES: GA(V), IN(V), P(V) AND AS(V)
48 C AND CALCULATE THE ACTIVITIES FOR GA, IN, AS AND P IN SOLID SOLUTION.
49 C
50     ACTASB=0.
51     ACTINB=0.
52     ACTAS=0.
53     ACTP=0.
54     KGA=0

```

```

55      KAS=0
56      KIN=0
57      KP=0
58 C
59 C   GA DATA
60 C
61      KSPC=KIII(3)
62      A1=0.023733
63      A2=2.09E-6
64      A3=-266.2
65      A4=-0.003612
66      A5=0.
67      DH=65.0
68      DS=0.030617
69      DC 400 IJK=1,4
70      GC TC(245,220,230,240),IJK
71 C
72 C   INDIUM DATA
73 C
74      220 KSPC=KIII(4)
75      A1=-0.001015
76      A2=-1.614E-6
77      A3=0.
78      A4=0.
79      A5=-1.689E-9
80      DH=67.3
81      DS=0.027637
82      GC TC 245
83 C
84 C   PROSEMERGUS (P) DATA
85 C
86      230 KSPC=KV(2)
87      A1=-0.000732
88      A2=0.
89      A3=0.
90      A4=0.
91      A5=0.
92      DH=73.62
93      DS=0.00915
94      GC TC 245
95 C
96 C   ARSENIC (AS) DATA
97 C
98      240 KSPC=KV(3)
99      A1=-0.001768
100     A2=-1.5E-6
101     A3=15.04
102     A4=0.0001967
103     A5=0.
104     DH=68.7
105     DS=0.023041
106     245 IF(KSPC,19.0) GC TC 100
107     DC 300 I=1,4
108     ICN=0

```

```

109      IF(A(I,K5PC).LT.0.001) GO TO 200
110      DG=200-141.2
111      IF(A(I,0).LT.0.001) GO TO 250
112      ICNT=ICNT+1
113      200 CONTINUE
114      IF(ICNT.GT.1) GO TO 300
115      IF(A(I,K5PC).GT.1.001) GO TO 300
116      DG=FNODG(T)
117      ACTIV=PA*AC(1)*P/P0*EXP(DG/RT)
118      IF(IJK.EQ.1) ACTGAS=ACTIV
119      IF(IJK.EQ.1) KGA=I
120      IF(IJK.EQ.2) ACTIND=ACTIV
121      IF(IJK.EQ.2) KIN=I
122      IF(IJK.EQ.3) ACTPS=ACTIV
123      IF(IJK.EQ.3) KPI=I
124      IF(IJK.EQ.4) ACTASS=ACTIV
125      IF(IJK.EQ.4) KAS=I
126      GO TO 400
127      300 CONTINUE
128      400 CONTINUE
129      C
130      C CALCULATE THE SATURATION RATIOS FOR GA-AS AND IN-P.
131      C
132      RGAAS=0.
133      RINP=0.
134      C
135      C GA-AS SYSTEM SATURATION RATIO
136      C
137      A1=0.01040
138      A2=2.8E-6
139      A3=0.
140      A4=0.
141      A5=0.
142      DH=-19.52
143      DS=-0.002948
144      K3=KGA
145      K5=KAS
146      DG=500-141.2
147      IF(K3.EQ.0.OR.K5.EQ.0) GO TO 470
148      IF(N(K3).LT.1.00E-50.OR.N(K5).LT.1.00E-50) GO TO 470
149      DG=STDCP(K3)+STDCP(K5)-FNODG(T)/RT
150      RSAT=FRAC(K3)*FRAC(K5)*P**2*EXP(DG)/P0**2
151      IF(I.EQ.1) RGAAS=RSAT
152      IF(I.EQ.2) RINP=RSAT
153      C
154      C IN-P SYSTEM SATURATION RATIO
155      C
156      470 A1=0.01227
157      A2=0.
158      A3=-114.0
159      DH=-14.0
160      DS=-0.00946
161      K3=KIN
162      K5=KPI
163      ) CONTINUE
164      ) CONTINUE

```

Figure B10. Subroutine OPTBAS

```

1      SUBROUTINE OPTBAS(N,BESTN,A,D,OPRME,STDCP,PHASE,PHAS,ICP,
2      &A3,BGUBS,DH0,DS0,ICP,ICXAS,ITER,ICIM1,ICIM2,V,S,C,E,VSC,
3      &IWR7)
4      C
5      C THIS SUBROUTINE DETERMINES THE OPTIMUM SET OF BASIS SPECIES
6      C
7      DIMENSION A(ICIM1,ICIM2),D(ICIM2,ICIM2),ICXAS(ICIM2),
8      &          STDCP(ICIM1),A0(ICIM1),A1(ICIM1),A2(ICIM1),A3(ICIM1),
9      &          DH0(ICIM1),DS0(ICIM1),ICP(ICIM1)
10     REAL*8 N(ICIM1),BESTN(ICIM1),OPRME(ICIM2,ICIM2),TEMP
11     INTEGER SPECIE(ICIM1,3),PHASE(ICIM1,3),BGUBS(ICIM1),V,S,C,E,VSC,
12     &          VSCM1
13     ISTEP=0
14     ICHNG=0
15     VSC=V+S+C
16     VSCM1=VSC-1
17     C
18     C BUBBLE SORT THE N VECTOR INTO DESCENDING ORDER
19     C AND ORDER STDCP, A, DH0, DS0, A0, A1, A2, A3, SPECIE, PHASE
20     C AND ICP CORRESPONDINGLY
21     C
22     DO 300 I=1,VSCM1
23     IP1=I+1
24     DO 200 II=IP1,VSC
25     IF(N(II).LE.N(I)) GO TO 200
26     ICHNG=1
27     TEMP=N(I)
28     N(I)=N(II)
29     N(II)=TEMP
30     TEMP=BESTN(I)
31     BESTN(I)=BESTN(II)
32     BESTN(II)=TEMP
33     TEMP=STDCP(I)
34     STDCP(I)=STDCP(II)
35     STDCP(II)=TEMP
36     TEMP=A0(I)
37     A0(I)=A0(II)
38     A0(II)=TEMP
39     TEMP=A1(I)
40     A1(I)=A1(II)
41     A1(II)=TEMP
42     TEMP=A2(I)
43     A2(I)=A2(II)
44     A2(II)=TEMP
45     TEMP=A3(I)
46     A3(I)=A3(II)
47     A3(II)=TEMP
48     TEMP=DH0(I)
49     DH0(I)=DH0(II)
50     DH0(II)=TEMP
51     TEMP=DS0(I)
52     DS0(I)=DS0(II)
53     DS0(II)=TEMP
54     ITEMP=ICXAS(I)

```

```

55     BQUES(I)=BQUES(II)
56     BQUES(II)=ITEMP
57     ITEMP=ICP(I)
58     ICP(I)=ICP(II)
59     ICP(II)=ITEMP
60     DO 50 J=1,3
61     ITEMP=SPECIE(I,J)
62     SPECIE(I,J)=SPECIE(II,J)
63     SPECIE(II,J)=ITEMP
64     ITEMP=PHASE(I,J)
65     PHASE(I,J)=PHASE(II,J)
66     PHASE(II,J)=ITEMP
67     50 CONTINUE
68     DO 100 J=1,E
69     TEMP=A(I,J)
70     A(I,J)=A(II,J)
71     A(II,J)=TEMP
72     100 CONTINUE
73     200 CONTINUE
74     300 CONTINUE
75 C
76 C IF THE PREVIOUSLY USED BASIS IS STILL THE OPTIMUM BASIS
77 C SKIP THE REST OF THIS SUBROUTINE AND CONTINUE WITH THE CALCULATIONS
78 C
79 C     IF(ITER.GT.1.AND.ICHNG.EQ.0) GO TO 480
80 C
81 C BUILD THE D MATRIX WHICH WILL CONTAIN THE OPTIMUM BASIS
82 C
83     DO 320 J=1,E
84     DPRME(I,J)=A(I,J)
85     320 CONTINUE
86     MA=0
87     DO 400 MD=1,E
88     340 MA=MA+1
89     IF(MA.GT.VSC) GO TO 450
90     DO 350 J=1,E
91     D(MD,J)=-(MA,J)
92     350 CONTINUE
93     IDXBAS(70)=MA
94     IF(MD.EQ.1) GO TO 400
95     CALL TESTD(D,DPRME,MD,E,ICIM2,.TST)
96     IF(ITST.EQ.0) GO TO 340
97     400 CONTINUE
98     GO TO 480
99     450 WRITE(IWRT,460) ITER
100     460 FORMAT('G',***** ITERATION ',E,' AN OPTIMUM SET OF BASIS ',
101     'E' SPECIES COULD NOT BE FOUND FOR THIS SYSTEM IN COMPUTING OPTBAS')
102     ISTOP=1
103     480 RETURN
104     END

```

Figure B11. Subroutine TESTD

```

1      SUBROUTINE TESTD(D,DPRME,MD,E,IDIM2,ITST)
2 C
3 C THIS SUBROUTINE TESTS THE D MATRIX FOR LINEAR DEPENDENCE
4 C USING A GRAM-SCHMIDT ORTHOGONALIZATION ALGORITHM
5 C
6      DIMENSION D(IDIM2,IDIM2)
7      REAL*8 DPRME(IDIM2,IDIM2),ANUM,DENCM
8      INTEGER E
9      ITST=0
10     DC 100 J=1,E
11     DPRME(MD,J)=D(MD,J)
12 100 CONTINUE
13     MDM1=MD-1
14     DC 400 L=1,MDM1
15     ANUM=0.0
16     DENCM=0.0
17     DC 200 K=1,E
18     ANUM=ANUM+D(MD,K)*DPRME(L,K)
19     DENCM=DENCM+DPRME(L,K)**2
20 200 CONTINUE
21     DC 300 J=1,E
22     DPRME(MD,J)=DPRME(MD,J)-DPRME(L,J)*ANUM/DENCM
23 300 CONTINUE
24 400 CONTINUE
25 C
26 C TEST FOR "ZEROS" ON THE NEW ROW
27 C
28     DC 500 J=1,E
29     IF(DABS(DPRME(MD,J)).GT.1.00-5) ITST=ITST+1
30 500 CONTINUE
31     RETURN
32     END

```

## B.4.8 EQCON

Subroutine EQCON, shown in Figure B12, calculates the equilibrium constants for each of the formation reactions from the Gibbs Free Energy change of the reaction. Array D, which contains the optimum set of basis species, is inverted at line 26 using IMSL subroutine LINVIF. A message is written out at lines 27, 28 and 29 if the inverted matrix has less than four significant figures. If array D appears to be algorithmically singular to LINVIF a message is written out at lines 30 through 32, parameter ISTOP is set to unity and the iterative process is halted in the main program.

Lines 35 through 45 calculate the stoichiometric coefficients for the formation reactions using equation 4 from section B.5. The equilibrium constants for these reactions are then calculated at lines 46 through 57.

## B.4.9 ACTCOF

A listing of subroutine ACTCOF, which calculates the activity coefficients for each specie, is shown in Figure B13. Initially all of the activity coefficients are set to unity. The iteration process for the equilibrium composition proceeds under this assumption of an ideal system until REIMAX, the convergence test parameter, becomes less than 0.1. At this point three options become available for the solution phase. The first option (IXSCOR=0) simply assumes an ideal solution phase. The second option (IXSCOR=1) treats the solution phase using simple solution theory and is applicable to binary solutions only. The activity coefficient for specie  $i$  is given by:

$$\gamma_i = \exp [(A_{xs} + B_{xs} T)(1-X_i)^2/RT] \quad (1)$$

The third option (IXSCOR2=2) allows the first specie in the solution phase to have an activity coefficient described by Henry's constant, H.

$$\gamma_{v+1} = H = A_{xs} \exp[B_{xs}/T] \quad (2)$$

The vapor phase is always assumed to be ideal.

## B.4.10 CALCO

A listing of CALCO is shown in Figure B14. This subroutine calculates the "equilibrium constants" for each of the formation reactions based on the current estimate to the equilibrium composition. These equilibrium constants are calculated by the following relationship.

$$Q_i = \gamma_i X_i P_{pi} / \prod_{k=1}^E (\gamma_k X_k P_{pk})^{\nu_{ik}} \quad (1)$$

where:  $\gamma_i$  = activity coefficient

$X_i$  = mole fraction

$\nu_{ik}$  = stoichiometric coefficient

$P_{pi} = \begin{cases} P/P_0 & \text{vapor species} \\ 1 & \text{condensed phases} \end{cases}$

Figure B12. Subroutine EQCON

```

1      SUBROUTINE EQCON(A,D,DC,DINV,DC,GNU,STDCP,KEG,IDXBAS,WKA,
2      &
3      &
4      &
5      &
6      &
7      &
8      &
9      &
10     DCUBLE PRECISION DC,DINV,WKA
11     INTEGER V,S,C,E,VSC
12     REAL KEG(IDIM1)
13     VSC=V+S+C
14     ISTCP=0
15 C
16 C   STORE ARRAY D IN ARRAY DC AND USE ARRAY DC IN THE CALL TO LINVIF
17 C
18     DC 100 I=1,E
19     DC 100 J=1,E
20     DO(I,J)=D(I,J)
21 100 CONTINUE
22 C
23 C   INVERT MATRIX DC USING IMSL SUBROUTINE LINVIF
24 C
25     IDGT=4
26     CALL LINVIF(DC,E,ICIM2,DINV,IDGT,WKA,IER)
27     IF(IER.EQ.34) WRITE(IWRT,110) ITER,IDGT
28 110 FORMAT('0','***** ITERATION ',IS,' ACCURACY TEST FAILED IN ',
29     &'SUBROUTINE LINVIF DURING MATRIX INVERSION..... IDGT=',I2)
30     IF(IER.EQ.129) WRITE(IWRT,120) ITER
31 120 FORMAT('0','***** ITERATION ',IS,' MATRIX D IS SINGULAR',
32     &' IN SUBROUTINE EQCON')
33     IF(IER.EQ.129) ISTCP=1
34     IF(ISTCP.EQ.1) GO TO 600
35 C
36 C   CALCULATE THE REACTION COEFFICIENT MATRIX
37 C
38     DC 300 I=1,VSC
39     DC 300 J=1,E
40     TEMP=0.0
41     DC 200 JJ=1,E
42     TEMP=TEMP+A(I,JJ)*DINV(JJ,J)
43 200 CONTINUE
44     GNU(I,J)=TEMP
45 300 CONTINUE
46 C
47 C   CALCULATE THE EQUILIBRIUM CONSTANTS FOR THE FORMATION REACTIONS
48 C
49     DC 500 I=1,VSC
50     ARG=(-1.0)*STDCP(I)
51     DC 400 K=1,E
52     IDXE=ICXBAS(K)
53     ARG=ARG+GNU(I,K)*STDCP(IDXE)
54 400 CONTINUE

```

```
55      DG(I)=(-1.0)*ARG*RT
56      KEG(I)=EXP(ARG)
57      500 CONTINUE
58      600 RETURN
59      END
```

Figure B13. Subroutine ACTCOF

```

1      SUBROUTINE ACTCOF(FRAC,ACCEF,ISPCE,SPECIE,INDEX,IDIM1,RELMAX,
2      &
3      & IXSCCR,AXS,EXS,T,IACFF,V,S,C,IWRT)
4      C SUBROUTINE TO CALCULATE ACTIVITY COEFFICIENTS FOR THE SOLUTION PHASE
5      C
6      C IXSCCR ALGORITHM
7      C 1 BINARY SIMPLE SOLUTION THEORY  $GE=(AXS+EXS*T)**X1*X2$ 
8      C 2 HENRY'S CONSTANT FOR THE FIRST SOLUTION SPECIE  $H=AXS+EXP(BXS/T)$ 
9      C
10     DIMENSION ACCEF(IDIM1),FRAC(IDIM1),INDEX(IDIM1)
11     INTEGER ISPCE(IDIM1,3),SPECIE(IDIM1,3),V,S,C,VSC
12     VSC=V+S+C
13     DO 100 I=1,VSC
14     ACCEF(I)=1.0
15 100 CONTINUE
16     IF(AES(RELMAX).LT.0.1) IACFF=1
17     IF(IXSCCR.EQ.2) IACFF=1
18     IF(IXSCCR.LT.1.OR.IXSCCR.GT.2.OR.S.LE.1) IACFF=0
19     IF(IACFF.EQ.0) GO TO 500
20     RT=0.0015872*T
21     C
22     C IDENTIFY THE SOLUTION SPECIES
23     C
24     DO 150 J=1,S
25     K=V+J
26     DO 150 I=1,VSC
27     IF(SPECIE(I,1).EQ.ISPCE(K,1).AND.
28     & SPECIE(I,2).EQ.ISPCE(K,2).AND.
29     & SPECIE(I,3).EQ.ISPCE(K,3)) INDEX(J)=I
30 150 CONTINUE
31     ITEST=1
32     DO 155 J=1,S
33     IF(INDEX(J).LT.1.OR.INDEX(J).GT.VSC) ITEST=0
34 155 CONTINUE
35     IF(ITEST.EQ.0) WRITE(IWRT,160)
36 160 FORMAT('0','***** THE SOLUTION SPECIES COULD NOT BE IDENTIFIED',
37     & ' IN SUBROUTINE ACTCOF')
38     IF(IXSCCR.EQ.2) GO TO 200
39     C
40     C BINARY SIMPLE SOLUTION THEORY
41     C
42     IDX1=INDEX(1)
43     IDX2=INDEX(2)
44     X1=FRAC(IDX1)
45     X2=1.0-X1
46     ARG1=(AXS+BXS*T)**X2**2/RT
47     ARG2=(AXS+BXS*T)**X1**2/RT
48     ACCEF(IDX1)=EXP(ARG1)
49     ACCEF(IDX2)=EXP(ARG2)
50     GO TO 500
51     C
52     C HENRY'S CONSTANT FOR THE FIRST SOLUTION SPECIE
53     C
54 200 IDX1=INDEX(1)
55     ACCEF(IDX1)=AXS*EXP(BXS/T)
56 500 RETURN
57     END

```



The product in the denominator is taken over the basis species in the system.

#### B.4.11 ADJEXT

Subroutine ADJEXT, shown in Figure B15, adjusts the extents of each formation reaction using equation 8 from section B.5. The predicted change in each reaction extent is calculated in lines 11 through 31. The  $\Delta g_i$  values are set to zero in lines 28 and 29 for species which are present in only very small amounts. Nonnegativity of the basis species molar amounts is assured by application of equations 10 and 11 in section B.5 in lines 32 through 51.

#### B.4.12 CNVFERC and DGDGLAM

Listings of subroutine CNVFERC and function subprogram DGDGLAM are shown in Figure B16. Subroutine CNVFERC calculates a convergence factor,  $\lambda$ , using equation 14 from section B.5.

At line 20 subroutine CORMOL is called to determine the molar amounts which would be present if  $\lambda=1$  and the derivative is evaluated in line 21. The derivative is evaluated for  $\lambda=0$  at line 27 and line 30. Lines 31 and 32 limit the maximum and minimum values of the convergence factor to 1.0 and  $RLXMIN$  respectively.

Function subroutine DGDGLAM calculates the derivative of the system Gibbs Free Energy with respect to the convergence factor using the following relation from Smith and Missen [2].

$$\frac{dG}{d\lambda} = RT \sum_{i=1}^{VSC} (n_i^1 - n_i^0) \left[ -\frac{0}{n_i^0} + \ln \left( \frac{n_i^1 n_i^0 p_{pi}}{n_T} \right) \right] \quad (1)$$

where:  $n_T$  = total moles in the phase

$n_i$  = equations 9 and 10 section B.5

$p_{pi} = \begin{cases} P/P_0 & \text{vapor phase} \\ 1 & \text{condensed phases} \end{cases}$

#### B.4.13 CORMOL

Subroutine CORMOL, shown in Figure B17, corrects the molar amounts of each specie to reflect the adjusted extents of the formation reactions using equations 9 and 10 in section B.5. The minimum molar amount any specie may attain is set to  $1.65 \times 10^{-24}$  moles (one molecule).

Figure B15. Subroutine ADJEXT

```

1      SUBROUTINE ADJEXT(N,KEG,G,CNU,DZETA,IDXBAS,CCND,PHASE,ICIM1,ICIM2,
2      &
3      &
4      &
5      &
6      &
7      &
8      &
9      &
10     &
11     &
12     &
13     &
14     DC 200 I=1,VSC
15     DELI=1.0
16     IF(PHASE(I,1).EQ.CCND(1)) DELI=0.0
17     DENCM=DELI/N(I)
18     DZETA(I)=0.0
19     DC 100 J=1,E
20     K=IDXBAS(J)
21     IF(I.EQ.K) GO TO 200
22     DELK=1.0
23     IF(PHASE(K,1).EQ.CCND(1)) DELK=0.0
24     DENCM=DENCM-DELK*GNC(I,J)**2/N(K)
25     100 CONTINUE
26     IF(DENCM.EQ.0.0) DENCM=ALCG(KEG(I))-ALCG(G(I))
27     DZETA(I)=(ALCG(KEG(I))-ALCG(G(I)))/DAES(DENCM)
28     IF(N(I).LT.1.66E-24.AND.DZETA(I).LT.0.0) DZETA(I)=0.0
29     IF(DZETA(I).LT.0.0.AND.DAES(DZETA(I)).GT.N(I))
30     &
31     200 CONTINUE
32     &
33     &
34     &
35     &
36     AKAPA=1.0
37     DC 400 J=1,E
38     K=IDXBAS(J)
39     TCTDN=0.0
40     DC 300 I=1,VSC
41     TCTDN=TCTDN-GNC(I,J)*DZETA(I)
42     300 CONTINUE
43     TEST=N(K)+TCTDN*AKAPA
44     IF(TEST.LT.0.0.AND.N(K).GT.1.66E-24) AKAPA=(-1.0)*N(K)/TCTDN
45     400 CONTINUE
46     DC 500 I=1,VSC
47     DC 450 J=1,E
48     IF(I.EQ.IDXBAS(J)) GO TO 500
49     450 CONTINUE
50     DZETA(I)=DZETA(I)*AKAPA
51     500 CONTINUE
52     RETURN
53     END

```

Figure B16. Subroutine CNVFRC

```

1      SUBROUTINE CNVFRC(N, NTEMP, STDCP, ACCEF, DZETA, GNO, I, XH40, VAPCH,
2      &                CCNO, SOLN, PHASE, ZV, RT, P, Q, FLXMIN, LAMBDA, IDIM1,
3      &                IDIM2, V, S, T, U)
4      C
5      C SUBROUTINE TO CALCULATE THE CONVERGENCE FUNCTION LAMBDA
6      C
7      DIMENSION IXHAS(IDIM2), GNO(IDIM1, IDIM2),
8      &          STDCP(IDIM1), ACCEF(IDIM1)
9      INTEGER VAPCH(3), CCNO(3), SOLN(3), PHASE(IDIM1, 3), V, S, T, U, VSC
10     REAL LAMBDA
11     REAL*8 N(IDIM1), NTEMP(IDIM1), DZETA(IDIM1)
12     VSC=V+S+U
13     C
14     C CALCULATE DG/DLAMBDA AT LAMBDA=1.0
15     C
16     LAMBDA=1.0
17     DO 100 I=1, VSC
18     NTEMP(I)=N(I)
19     100 CONTINUE
20     CALL CORMOL(NTEMP, DZETA, GNO, IXHAS, IDIM1, IDIM2, LAMBDA, VSC, T)
21     DGDL1=DGDLAM(N, NTEMP, STDCP, ACCEF, PHASE, VAPCH, SOLN, ZV, RT, P, Q,
22     &          IDIM1, VSC)
23     IF(DGDL1.LE.0.0) GO TO 500
24     C
25     C CALCULATE DG/DLAMBDA AT LAMBDA=0.0
26     C
27     DGDL3=(-1.0)*DGDLAM(NTEMP, N, STDCP, ACCEF, PHASE, VAPCH, SOLN, ZV,
28     &          RT, P, Q, IDIM1, VSC)
29     IF(DGDL3.EQ.DGDL1) DGDL1=0.0
30     LAMBDA=DGDL3/(DGDL3-DGDL1)
31     IF(LAMBDA.GT.1.0) LAMBDA=1.0
32     IF(LAMBDA.LT.0.0) LAMBDA=FLXMIN
33     500 CONTINUE
34     RETURN
35     END
36     FUNCTION DGDLAM(M1, N2, STDCP, ACCEF, PHASE, VAPCH, SOLN, ZV, RT, P, Q,
37     &          IDIM1, VSC)
38     C
39     C SUBPROGRAM TO CALCULATE DG/DLAMBDA
40     C
41     DIMENSION ACCEF(IDIM1), STDCP(IDIM1)
42     INTEGER PHASE(IDIM1, 3), VAPCH(3), SOLN(3), VSC
43     REAL*8 N1(IDIM1), N2(IDIM1), NV, NS
44     C
45     C CALCULATE THE TOTAL NUMBER OF MOLES IN THE SOLUTION AND VAPOR PHASE
46     C
47     NS=0.0
48     NV=ZV
49     DO 100 I=1, VSC
50     IF(PHASE(I, 1).EQ.VAPCH(1)) NV=NV+N2(I)
51     IF(PHASE(I, 1).EQ.SOLN(1)) NS=NS+N2(I)
52     100 CONTINUE
53     C
54     C CALCULATE DG/DLAMBDA

```

```
55 C
56     DGDL=0.0
57     DO 200 I=1,VBC
58     AFG=1.0
59     IF(PHASE(I,1).EQ.VAPOR(I)) AFG=ALCOF(I)*N2(I)+R/R0/AV
60     IF(PHASE(I,1).EQ.SOLN(I)) AFG=ALCOF(I)*N2(I)/NS
61     DGDL=DGDL+(N2(I)-N1(I))*(STDCP(I)+ALCO(AFG))
62 200 CONTINUE
63     DGDLAM=DGDL*FT
64     RETURN
65     END
```

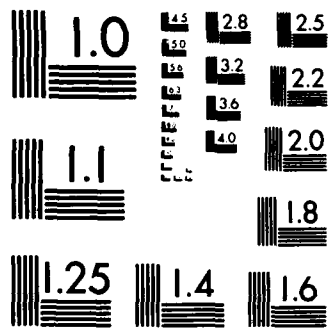
Figure B17. Subroutine CORMOL

```

1      SUBROUTINE CORMOL(N,DZETA,CNU,IDXBAS,IDIM1,IDIM2,LAMBDA,VSC,E)
2 C
3 C  SUBROUTINE TO CORRECT THE MOLAR AMOUNTS OF EACH SPECIE
4 C
5      DIMENSION GNU(IDIM1,IDIM2),IDXEAS(IDIM2)
6      REAL LAMBDA
7      REAL*8 N(IDIM1),DZETA(IDIM1)
8      INTEGER VSC,E
9 C
10 C  CORRECT EACH NONBASIS SPECIE
11 C
12      DO 200 I=1,VSC
13      DO 100 J=1,E
14      IF(I.EQ.IDXBAS(J)) GO TO 200
15      100 CONTINUE
16      N(I)=N(I)+DZETA(I)*LAMBDA
17      IF(N(I).LT.1.65E-24) N(I)=1.65E-24
18      200 CONTINUE
19 C
20 C  CORRECT EACH BASIS SPECIE
21 C
22      DO 400 J=1,E
23      K=IDXEAS(J)
24      DO 300 I=1,VSC
25      N(K)=N(K)-GNU(I,J)*DZETA(I)*LAMBDA
26      300 CONTINUE
27      IF(N(K).LT.1.65E-24) N(K)=1.65E-24
28      400 CONTINUE
29      RETURN
30      END

```





MICROCOPY RESOLUTION TEST CHART  
NATIONAL BUREAU OF STANDARDS-1963-A

## B.4.14 ORDER

A listing of subroutine ORDER is shown in Figure B18. Subroutine ORDER places arrays N, STDCP, AO, A1, A2, A3, DHO, DSO, ICP, DZETA, CHMPT, ACOEF, FRAC, DG, Q, KEQ, SPECIE, PHASE and A into the specie order of the original problem statement. This makes the output readily accessible and also is necessary for the correct operation of the composition looping option (IOPT=3).

## B.4.15 WRAPUP

Subroutine WRAPUP, shown in Figure B19 writes a wrap-up file to logical unit designator IFILE. This subroutine is accessed when parameter IWRAP>0. For IWRAP=1 or 2 the value of IFILE is set at 2. For IWRAP=3 IFILE is set equal to IWRT which is the line printer logical unit designator. This subroutine provides concise data output and is quite useful when the input data set has been verified to be correct and parametric studies are desired.

## B.4.16 DEBUG

Subroutine DEBUG is accessed when parameter IDEBUG>1. This subroutine provides an output of the convergence forcer, system Gibbs Free Energy, the relative state of convergence, specie molar amounts and changes in the reaction extents. A listing of DEBUG is shown in Figure B20.

## B.4.17 GIBBS

Subroutine GIBBS, shown in Figure B21, calculates the total system Gibbs Free Energy using the relation

$$G = RT \sum_{i=1}^{VSC} n_i [\mu_i^0 + \ln (\gamma_i X_i P_{pi})] \quad (1)$$

where:  $\gamma_i$  = activity coefficient

$X_i$  = mole fraction of  $i$

$P_{pi} = \begin{cases} P/P_0 & \text{vapor phase} \\ 1 & \text{condensed phases} \end{cases}$

## B.4.18 PMAT, DPMAT, PVEC, and IPVEC

Subroutines PMAT, DPMAT, PVEC and IPVEC are used to write out single precision, double precision matrices, and single precision and integer vectors when the debugging option is active. Listings of these subroutines are shown in Figure B22 through B25.

Figure B18. Subroutine ORDER

```

1      SUBROUTINE ORDER(ISPCE, SPECIE, PHASE, N, A, STDCP, A0, A1, A2, A3, DH0,
2      &DS0, DZETA, CHMPT, ACCEF, FRAC, DG, Q, KEQ, ICP, IDIM1, IDIM2, E, VSC,
3      &IWRT)
4 C
5 C  SUBROUTINE TO ORDER THE ARRAYS BACK TO THE ORIGINAL ORDER
6 C  OF THE PROBLEM STATEMENT
7 C
8      DIMENSION A(IDIM1, IDIM2), STDCP(IDIM1), A0(IDIM1), A1(IDIM1),
9      &A2(IDIM1), A3(IDIM1), CHMPT(IDIM1), ACCEF(IDIM1), DH0(IDIM1),
10     &DS0(IDIM1), FRAC(IDIM1), DG(IDIM1), Q(IDIM1), ICP(IDIM1)
11     INTEGER QUES(IDIM1), ISPCE(IDIM1, 3), SPECIE(IDIM1, 3),
12     & PHASE(IDIM1, 3), E, VSC, VSCM1
13     REAL KEQ(IDIM1)
14     REAL*8 N(IDIM1), DZETA(IDIM1), TEMP
15     VSCM1=VSC-1
16     DO 300 I=1, VSCM1
17     IP1=I+1
18     DO 200 II=IP1, VSC
19     IF((ISPCE(I, 1).EQ.SPECIE(II, 1)).AND.
20     & ISPCE(I, 2).EQ.SPECIE(II, 2)).AND.
21     & ISPCE(I, 3).EQ.SPECIE(II, 3)) GO TO 50
22     GO TO 200
23     50 TEMP=N(I)
24     N(I)=N(II)
25     N(II)=TEMP
26     TEMP=STDCP(I)
27     STDCP(I)=STDCP(II)
28     STDCP(II)=TEMP
29     TEMP=A0(I)
30     A0(I)=A0(II)
31     A0(II)=TEMP
32     TEMP=A1(I)
33     A1(I)=A1(II)
34     A1(II)=TEMP
35     TEMP=A2(I)
36     A2(I)=A2(II)
37     A2(II)=TEMP
38     TEMP=A3(I)
39     A3(I)=A3(II)
40     A3(II)=TEMP
41     TEMP=DH0(I)
42     DH0(I)=DH0(II)
43     DH0(II)=TEMP
44     TEMP=DS0(I)
45     DS0(I)=DS0(II)
46     DS0(II)=TEMP
47     ITEMP=ICP(I)
48     ICP(I)=ICP(II)
49     ICP(II)=ITEMP
50     TEMP=DZETA(I)
51     DZETA(I)=DZETA(II)
52     DZETA(II)=TEMP
53     TEMP=CHMPT(I)
54     CHMPT(I)=CHMPT(II)

```

```
55     CHMPT(II)=TEMP
56     TEMP=ACDEF(I)
57     ACDEF(I)=ACDEF(II)
58     ACDEF(II)=TEMP
59     TEMP=FRAC(I)
60     FRAC(I)=FRAC(II)
61     FRAC(II)=TEMP
62     ITEMP=GUES(I)
63     GUES(I)=GUES(II)
64     GUES(II)=ITEMP
65     TEMP=DG(I)
66     DG(I)=DG(II)
67     DG(II)=TEMP
68     TEMP=C(I)
69     Q(I)=Q(II)
70     Q(II)=TEMP
71     TEMP=KEQ(I)
72     KEQ(I)=KEQ(II)
73     KEQ(II)=TEMP
74     DO 60 J=1,3
75         ITEMP=SPECIE(I,J)
76         SPECIE(I,J)=SPECIE(II,J)
77         SPECIE(II,J)=ITEMP
78         ITEMP=PHASE(I,J)
79         PHASE(I,J)=PHASE(II,J)
80         PHASE(II,J)=ITEMP
81     60 CONTINUE
82     DO 100 J=1,E
83         TEMP=A(I,J)
84         A(I,J)=A(II,J)
85         A(II,J)=TEMP
86     100 CONTINUE
87     200 CGNTINUE
88     300 CONTINUE
89     RETURN
90     END
```

Figure B19. Subroutine WRAPUP

```

1     SUBROUTINE WRAPUP(TITLE, SPECIE, INERT, N, FRAC, GUES, ZV, P, ACTZ, SITCT,
2     & SIMF, ACTSIS, ACTGAS, ACTINS, ACTPS, ACTASS, RIIIV, V, RGAAS, RINP,
3     & ESTCVG, ITBST, RELMAX, CNVG, ISS, XIII, T, P, IDATA, IDIM1, IFILE, V, VSC)
4 C
5 C SUBROUTINE TO WRITE-OUT A SUMMARY OF THE RESULTS TO A FILE
6 C
7     DIMENSION INERT(3), FRAC(IDIM1)
8     INTEGER TITLE(20), SPECIE(IDIM1,3), GUES(IDIM1), V, VSC,
9     & EL(5) / 'SI', 'GA', 'IN', 'F', 'AS' /
10    REAL*8 N(IDIM1)
11    IF(IDATA.EQ.0) WRITE(IFILE,50) (TITLE(K), K=1,20)
12    50 FORMAT(20A4)
13    WRITE(IFILE,55) T, P
14    55 FORMAT('TEMPERATURE = ', F7.1, ' K', /, 'PRESSURE = ', E12.5, ' PA')
15    IF(AES(RELMAX).GT.CNVG.AND.IDATA.NE.0) WRITE(IFILE,58) RELMAX,
16    & CNVG, ESTCVG, ITBST
17    58 FORMAT(66(' '), /, '* ', 5X, 'ITERATION FOR EQUILIBRIUM COMPOSITION ',
18    & 'DID NOT CONVERGE', 5X, '* ', /, '* ', 1X, 'MAXIMUM DIFFER=',
19    & E12.5, 2X, 'CONVERGENCE CRITERION=', E12.5, 1X, '* ',
20    & /, '* ', 9X, 'BEST CONVERGENCE=', E12.5, ' AT ITERATION ', 14, 8X, '* ',
21    & /, '* ', 12X, 'THE BEST OBTAINED RESULTS ARE SHOWN BELOW', 11X, '* ',
22    & /, 66(' '))
23    IF(IDATA.EQ.0) WRITE(IFILE,60)
24    60 FORMAT(13X, 'INITIAL COMPOSITIONS')
25    IF(IDATA.EQ.1) WRITE(IFILE,70)
26    70 FORMAT(13X, 'EQUILIBRIUM COMPOSITIONS')
27    IF(IDATA.EQ.0) WRITE(IFILE,80)
28    80 FORMAT('SPECIE', 7X, 'MOLE FFACTION', 4X, 'GRAM MOLES')
29    DO 200 I=1, VSC
30    WRITE(IFILE,100) (SPECIE(I,K), K=1,3), FRAC(I), N(I), GUES(I)
31    IF(I.NE.V) GO TO 200
32    WRITE(IFILE,100) (INERT(K), K=1,3), FRACZ, ZV
33    100 FORMAT(3A4, 2X, E12.5, 2X, E12.5, 1X, A4)
34    IF(RIIIV.GT.0.AND.RIIIV.LT.1.0E6) WRITE(IFILE,105) RIIIV
35    105 FORMAT('VAPOR RIIIV ', 10X, F9.4)
36    IF(SITCT.GT.0) WRITE(IFILE,110) SIMF, SITCT
37    110 FORMAT('SI IN VAPOR ', 2X, E12.5, 2X, E12.5)
38    IF(ACTSIS.GT.0) WRITE(IFILE,120) EL(1), ACTSIS
39    120 FORMAT(1A2, ' ACTIVITY', 13X, E12.5)
40    IF(ACTGAS.GT.0) WRITE(IFILE,120) EL(2), ACTGAS
41    IF(ACTINS.GT.0) WRITE(IFILE,120) EL(3), ACTINS
42    IF(ACTPS.GT.0) WRITE(IFILE,120) EL(4), ACTPS
43    IF(ACTASS.GT.0) WRITE(IFILE,120) EL(5), ACTASS
44    IF(RGAAS.GT.0) WRITE(IFILE,130) RGAAS
45    130 FORMAT('GA-AS SATURATION RATIO ', E12.5)
46    IF(RINP.GT.0) WRITE(IFILE,135) RINP
47    135 FORMAT(' IN-P SATURATION RATIO ', E12.5)
48    200 CONTINUE
49    IF(ISS.GT.0) WRITE(IFILE,205) XIII
50    205 FORMAT(3X, 'X=', F6.4)
51    WRITE(IFILE,210)
52    210 FORMAT(' ')
53    IDATA=1
54    RETURN
55    END

```

Figure B20. Subroutine DEBUG

```
1      SUBROUTINE DEBUG(N,DZETA,VSC,ICIM1,ITER,ALMEDA,GFE,  
2      &  
3      &  
4      & ROUTINE TO WRITE-OUT N, DZETA, ALMEDA DURING THE ITERATION PROCESS  
5      &  
6      REAL*8 N(ICIM1),DZETA(ICIM1)  
7      INTEGER VSC  
8      WRITE(IWRT,10) ITER,ALMEDA,GFE,FMX  
9      1) FORMAT('J', 'ITERATION = ',I5, 'SX', 'LAMEDA = ',E14.7,  
10     & 'SX', 'GIBBS FREE ENERGY = ',E14.7, 'KCAL',  
11     & 'SX', 'RELATIVE ERROR = ',E12.5, '/',I3,  
12     & 'N-VALUES',T20, 'DELTA-ZETA VALUES')  
13     DO 50 I=1,VSC  
14     WRITE(IWRT,20) N(I),DZETA(I)  
15     2) FORMAT(1X,E14.7,T20,E14.7)  
16     50 CONTINUE  
17     RETURN  
18     END
```

Figure B21. Subroutine GIBBS

```

1      SUBROUTINE GIBBS(N,STDCP,STDCPZ,ACCEF,FRAC,ZV,FRACZ,CCND,SCLN,
2      &
3      &
4      &
5      &
6      &
7      &
8      &
9      &
10     &
11     &
12     &
13     &
14     &
15     &
16     &
17     &
18     &
19     &
20     &
21     &
22     &
23     &
24     &

```

SUBROUTINE TO CALCULATE THE GIBBS FREE ENERGY OF THE SYSTEM

```

DIMENSION STDCP(IDIM1),FRAC(IDIM1),ACCEF(IDIM1)
REAL*8 N(IDIM1)
INTEGER COND(3),SCLN(3),PHASE(IDIM1,3),V,S,C,VSC
VSC=V+S+C
GAS CONSTANT IS IN UNITS OF: KCAL/G-MOLE-K
ARG=1.0
IF(FRACZ.GT.0.0) ARG=FRACZ*P/P0
GSTAR=ZV*(STDCPZ+ALCG(ARG))
DO 150 I=1,VSC
ARG=ACCEF(I)*FRAC(I)*P/P0
IF(PHASE(I,1).EQ.CCND(1)) ARG=1
IF(PHASE(I,1).EQ.SCLN(1)) ARG=ACCEF(I)*FRAC(I)
GSTAR=GSTAR+N(I)*(STDCP(I)+ALCG(ARG))
150 CONTINUE
GFE=GSTAR*RT
RETURN
END

```

Figure B22. Subroutine PMAT

```

1      SUBROUTINE PMAT(MATRIX,NDIM1,NDIM2,L1,L2,NAME,IWRT)
2 C
3 C      SUBROUTINE TO WRITE-CUT REAL MATRICIES
4 C
5      INTEGER*2 NAME(3)
6      REAL MATRIX(NDIM1,NDIM2)
7      WRITE(IWRT,10) (NAME(J),J=1,3)
8      10 FORMAT('0','MATRIX ',3A2)
9      DO 100 I=1,L1
10     WRITE(IWRT,20) (MATRIX(I,J),J=1,L2)
11     20 FORMAT(1X,10(E11.4,2X))
12 100 CONTINUE
13     RETURN
14     END

```

Figure B23 Subroutine DPMAT

```

1      SUBROUTINE DPMAT(DMTRIX,NDIM1,NDIM2,L1,L2,NAME,IWRT)
2 C
3 C      SUBROUTINE TO WRITE-CUT DOUBLE PRECISION REAL MATRICIES
4 C
5      DOUBLE PRECISION DMTRIX(NDIM1,NDIM2)
6      INTEGER*2 NAME(3)
7      WRITE(IWRT,10) (NAME(J),J=1,3)
8      10 FORMAT('0','MATRIX ',3A2)
9      DO 100 I=1,L1
10     WRITE(IWRT,20) (DMTRIX(I,J),J=1,L2)
11     20 FORMAT(1X,10(D11.4,2X))
12 100 CONTINUE
13     RETURN
14     END

```

Figure B24. Subroutine PVEC

```

1      SUBROUTINE PVEC(VECTOR,NDIM,L,NAME,IWRT)
2 C
3 C      SUBROUTINE TO WRITE-OUT REAL VECTORS
4 C
5      DIMENSION VECTOR(NDIM)
6      INTEGER*2 NAME(3)
7      WRITE(IWRT,10) (NAME(J),J=1,3)
8      10 FORMAT('0','THE TRANPOSED ',3A2,' VECTOR IS:')
9      WRITE(IWRT,20) (VECTOR(J),J=1,L)
10     20 FORMAT(1X,10(E11.4,2X))
11     RETURN
12     END

```

Figure B25. Subroutine IPVEC

```

1      SUBROUTINE IPVEC(IVECTOR,NDIM,L,NAME,IWRT)
2 C
3 C      SUBROUTINE TO WRITE-OUT INTEGER VECTORS
4 C
5      DIMENSION IVECTOR(NDIM)
6      INTEGER*2 NAME(3)
7      WRITE(IWRT,10) (NAME(J),J=1,3)
8      10 FORMAT('0','THE TRANPOSED ',3A2,' VECTOR IS:')
9      WRITE(IWRT,20) (IVECTOR(J),J=1,L)
10     20 FORMAT(1X,10(I11,2X))
11     RETURN
12     END

```

## B.4.19 IMSL Subroutines LINVIF, LEQTIF, LUELMF, and LUDATF.

The calling sequence of the IMSL subroutines is shown in Figure B26 and listings of these subroutines are provided in Figure B27. Subroutine LINVIF inverts matrices by placing ones on the diagonal of matrix B and then calling LEQTIF to solve the matrix problem

$$A X = B \quad (1)$$

for matrix X, the inverse of A.

Double precision arithmetic is used and the routines test to see that IDGT significant figures are present in the result. If less than IDGT significant figures are present parameter IER is set to 34. Parameter IER is set to 129 if matrix A is found to be algorithmically singular.

Figure 326

IMSL Subroutine Calling Sequence

LINVIF: Driver program to invert matrix A. This subroutine puts ones on the diagonal of matrix B for LEOTIF

LEOTIF: driver program to solve the matrix problem  $A \cdot X = S$  for matrix X

LUDATE: Performs an LU decomposition of matrix A with partial pivoting.

LUELMF: Performs appropriate substitutions to obtain the X matrix and writes the X matrix into B.

Figure B27 IMSL Subroutines LINVIF, LEQTIF, LUDATF and LUELMF

```

1      SUBROUTINE LINVIF (A,N,IA,AINV,IDGT,WKAREA,IER)
2 C
3 C  IMSL SUBROUTINE FOR INVERTING REAL MATRICIES
4 C
5      DOUBLE PRECISION A(IA,N),AINV(IA,N),WKAREA(1),ZEROC,CNE
6      DATA          ZEROC/0.000/,CNE/1.000/
7      IER=0
8      DC 10 I=1,N
9          DC 5 J=1,N
10         AINV(I,J) = ZEROC
11     5    CONTINUE
12         AINV(I,I) = CNE
13     10  CONTINUE
14     CALL LEQTIF (A,N,N,IA,AINV,IDGT,WKAREA,IER)
15     IF (IER .EQ. 0) GC TC 9005
16     9000 CONTINUE
17     9005 RETURN
18     END

```

```

1      SUBROUTINE LEQTIF (A,M,N,IA,B,IDGT,WKAREA,IER)
2 C
3 C  IMSL SUBROUTINE LEQTIF FOR SOLVING THE MATRIX PROBLEM A*X=B
4 C
5      DIMENSION      A(IA,1),B(IA,1),WKAREA(1)
6      DOUBLE PRECISION A,B,WKAREA,D1,D2,WA
7 C                    INITIALIZE IER
8 C                    FIRST EXECUTABLE STATEMENT
9      IER=0
10 C                    DECOMPOSE A
11     CALL LUDATF (A,A,N,IA,IDGT,D1,D2,WKAREA,WKAREA,WA,IER)
12     IF (IER .GT. 128) GC TC 9005
13 C                    CALL ROUTINE LUELMF (FORWARD AND
14 C                    BACKWARD SUBSTITUTIONS)
15     DC 10 J=1,M
16         CALL LUELMF (A,B(1,J),WKAREA,N,IA,B(1,J))
17     10  CONTINUE
18     9005 RETURN
19     END

```

```

1      SUBROUTINE LUCATF (A,LU,N,IA,IDGT,D1,D2,IPVT,EQUIL,WA,IER)
2 C
3 C      THIS SUBROUTINE IS USED WITH SUBROUTINE LEGTIF
4 C
5      DIMENSION      A(IA,1),LU(IA,1),IPVT(1),EQUIL(1)
6      DOUBLE PRECISION A,LU,D1,D2,EQUIL,WA,ZERO,CNE,FOUR,SIXTN,SIXTH,
7      *              RN,WREL,BIGA,EIG,P,SUM,AI,WI,T,TEST,G
8      DATA          ZERC,CNE,FOUR,SIXTN,SIXTH/(0.0),1.0,4.0,
9      *              16.0,0.062500/
10 C
11 C              FIRST EXECUTABLE STATEMENT
12 C              INITIALIZATION
13
12      IER = 0
13      RN = N
14      WREL = ZERC
15      D1 = CNE
16      D2 = ZERC
17      BIGA = ZERC
18      DO 10 I=1,N
19          BIG = ZERC
20          DO 5 J=1,N
21              P = A(I,J)
22              LU(I,J) = P
23              F = DABS(P)
24              IF (P .GT. BIG) BIG = F
25          5 CONTINUE
26              IF (EIG .GT. BIGA) BIGA = EIG
27              IF (EIG .EQ. ZERC) GO TO 110
28              EQUIL(I) = CNE/EIG
29      10 CONTINUE
30      DO 105 J=1,N
31          JMI = J-1
32          IF (JMI .LT. 1) GO TO 40
33 C              COMPUTE U(I,J), I=1,.....,J-1
34          DO 35 I=1,JMI
35              SUM = LU(I,J)
36              IMI = I-1
37              IF (IDGT .EQ. 0) GO TO 25
38 C              WITH ACCURACY TEST
39              AI = DABS(SUM)
40              WI = ZERC
41              IF (IMI .LT. 1) GO TO 20
42              DO 15 K=1,IMI
43                  T = LU(I,K)*LU(K,J)
44                  SUM = SUM-T
45                  WI = WI+DABS(T)
46          15 CONTINUE
47              LU(I,J) = SUM
48          20 WI = WI+DABS(SUM)
49              IF (AI .EQ. ZERC) AI = BIGA
50              TEST = WI/AI
51              IF (TEST .GT. WREL) WREL = TEST
52              GO TO 35
53 C              WITHOUT ACCURACY
54          25 IF (IMI .LT. 1) GO TO 35

```

```

55          DC 30 K=1,IM1
56          SUM = SUM-LU(I,K)*LU(K,J)
57 30      CCNTINUE
58          LU(I,J) = SUM
59 35      CCNTINUE
60 40      P = ZERC
61 C
62          DC 70 I=J,N
63          SUM = LU(I,J)
64          IF (IDGT .EG. 0) GC TC 55
65 C
66          AI = DABS(SUM)
67          WI = ZERC
68          IF (JMI .LT. 1) GC TC 50
69          DC 45 K=1,JMI
70          T = LU(I,K)*LU(K,J)
71          SUM = SUM-T
72          WI = WI+DABS(T)
73 45      CCNTINUE
74          LU(I,J) = SUM
75 50      WI = WI+DABS(SUM)
76          IF (AI .EG. ZERC) AI = EIGA
77          TEST = WI/AI
78          IF (TEST .GT. WFEL) WREL = TEST
79          GC TC 65
80 C
81          IF (JMI .LT. 1) GC TC 65
82          DC 60 K=1,JMI
83          SUM = SUM-LU(I,K)*LU(K,J)
84 60      CCNTINUE
85          LU(I,J) = SUM
86 65      Q = EQUIL(I)*DABS(SUM)
87          IF (P .GE. Q) GC TC 70
88          P = Q
89          IMAX = I
90 70      CCNTINUE
91 C
92          IF (RN+P .EG. RN) GC TC 110
93          IF (J .EQ. IMAX) GC TC 80
94 C
95          D1 = -D1
96          DC 75 K=1,N
97          P = LU(IMAX,K)
98          LU(IMAX,K) = LU(J,K)
99          LU(J,K) = P
100 75      CCNTINUE
101          EQUIL(IMAX) = EQUIL(J)
102 80      IPVT(J) = IMAX
103          D1 = D1*LU(J,J)
104 85      IF (DABS(D1) .LE. ONE) GC TC 90
105          D1 = D1*SIXTH
106          D2 = D2+FCUR
107          GC TC 85
108 90      IF (DABS(D1) .GE. SIXTH) GC TC 55

```

```

109         D1 = D1*SIXTN
110         D2 = D2-FCUR
111         GC TC 90
112     95     CCNTINUE
113         JF1 = J+1
114         IF (JF1 .GT. N) GC TC 105
115 C         DIVIDE BY FIVCT ELEMENT U(J,J)
116         P = LU(J,J)
117         DC 100 I=JF1,N
118             LU(I,J) = LU(I,J)/P
119     100     CCNTINUE
120     105     CCNTINUE
121 C         PERFORM ACCURACY TEST
122         IF (IDGT .EQ. 0) GC TC 9005
123         P = 3*N+3
124         WA = F*WFEL
125         IF (WA+10.00**(-IDGT) .NE. WA) GC TC 9005
126         IER = 34
127         GC TC 9005
128 C         ALGORITHMIC SINGULARITY
129     110     IER = 125
130         D1 = ZERC
131         D2 = ZERC
132     9005     RETURN
133         END

```

```

1      SUBROUTINE LUELMF (A,B,IPVT,N,IA,X)
2 C
3 C      THIS SUBROUTINE IS USED WITH SUBROUTINE LECTIF
4 C
5      DIMENSION      A(IA,1),B(1),IPVT(1),X(1)
6      DOUBLE PRECISION A,B,X,SUM
7 C
8 C
9      DC 5 I=1,N
10     S X(I) = B(I)
11     IW = 0
12     DC 20 I=1,N
13     IP = IPVT(I)
14     SUM = X(IP)
15     X(IP) = X(I)
16     IF (IW .EQ. 0) GC TC 15
17     IW1 = I-1
18     DC 10 J=IW,IW1
19     SUM = SUM-A(I,J)*X(J)
20     10    CONTINUE
21     GC TC 20
22     15    IF (SUM .NE. 0.D0) IW = I
23     20    X(I) = SUM
24 C
25 C
26     DC 30 IB=1,N
27     I = N+1-IB
28     IP1 = I+1
29     SUM = X(I)
30     IF (IP1 .GT. N) GC TC 30
31     DC 25 J=IP1,N
32     SUM = SUM-A(I,J)*X(J)
33     25    CONTINUE
34     30    X(I) = SUM/A(I,I)
35     RETURN
36     END

```

SOLVE LY = E FOR Y

SOLVE UX = Y FOR X

### B.5 Theoretical Development of the Stoichiometric Algorithm

The stoichiometric algorithms employed by Cruise [1] and Smith and Missen [2] may be extended to include a solution phase in addition to vapor and pure condensed phases. A stoichiometric algorithm is one in which a set of formation reaction equations are used to provide a driving force in the numerical solution of the equilibrium problem. The formation reaction for any specie  $i$  in a system containing  $E$  elements is written as

$$S_i = \sum_{k=1}^E v_{ik} S_k^b \quad (1)$$

The reactants in equation 1 are called the basis species (thus the superscript "b") and form a linearly independent set of species from within the system which represent all of the elements present in the system. The stoichiometric coefficient  $v_{ik}$  describes the number of molecules of basis specie  $k$  which are required in the formation of specie  $i$ .

The technique used in this stoichiometric algorithm to calculate the equilibrium composition of the system is as follows. First, the equilibrium constants for the formation reactions in equation 1 are calculated from the Gibbs Free Energy change of the reactions. Next, the current compositions for each of the species present are used to calculate another "equilibrium constant". The values of the two constants are then used in finite difference equations which approximate derivatives of the equilibrium constants with respect to the reaction extents. These equations predict changes in the reaction extents which will yield an improved approximation to the equilibrium composition of the system.

The discrete formulation of this algorithm, applied to a system consisting of a vapor phase have  $V$  species, a solution phase have  $S$  species and  $C$  pure condensed phases, starts with the definitions of the elemental abundance matrix, a vector representing the molar amount of each specie and a vector containing the total moles of each element present in the system.

$$\underline{A} = \begin{pmatrix} a_{11} & \cdots & a_{1E} \\ a_{VSC,1} & \cdots & a_{VSC,E} \end{pmatrix}$$

$$\underline{N}^T = (n_1 \dots n_{VSC})$$

$$\underline{B}^T = (b_1 \dots b_E)$$

where:  $a_{ij}$  = number of atoms of element  $j$  in specie  $i$

$n_i$  = moles of specie  $i$  in the system

$b_j$  = moles of element  $j$  in the system

VSC = V+S+C

$E$  = number of elements in the system

These definitions result in the following relationship which describes the system mass balance.

$$\underline{A}^T \underline{N} = \underline{B} \quad (2)$$

In order to construct a set of formation reactions, as in equation 1, a set of basis species which are linearly independent from each other yet represent all of the elements present in the system must be found. A further restriction is placed upon the set of basis species when the convergence rate of the algorithm is considered. Obviously, the molar amounts of each specie must be nonnegative for a physically realistic situation to exist. If a basis specie which has a very small initial composition is chosen, and the formation of another specie requires the consumption of this basis specie, then the rate of convergence will be slow in order to prevent the molar amount of the basis specie from becoming negative. Thus, a rapidly converging algorithm will employ an optimum set of basis species which, in addition to the two previously mentioned requirements, are present in the greatest molar amounts available. Also, since the molar amounts of each specie change after each iteration, this optimum set of basis species may need to be rechosen at each iteration.

The optimum set of basis species is chosen by first sorting vector  $N$  into descending order ( $n_1 > n_2 > \dots > n_{VSC}$ ) and ordering the rows of  $A$  correspondingly. The first row of  $A$  is then transferred into the first row of a new matrix  $D$ . The second row of  $A$  is then transferred into the next row of  $D$  and tested for linear independence. If it is linearly independent the row is kept and the process continues. If not the next row in  $A$  is tried. This process is continued until  $D$  is filled. For a system comprised of  $E$  elements there will be  $E$  basis species, therefore matrix  $D$  will always be square.

An efficient method of testing for linear independence between the rows of the  $D$  matrix is to build the Gram-Schmidt orthogonalized matrix  $D'$  using the formulation [4]

$$d'_{ij} = d_{ij}$$

$$d'_{ij} = d_{ij} - \sum_{\ell=1}^{i-1} d'_{\ell j} \frac{\sum_{k=1}^E d_{ik} d'_{\ell k}}{\sum_{k=1}^E (d'_{\ell k})^2} \quad (3)$$

where:  $i = 2, 3, \dots, md$

$j = 1, 2, \dots, E$

$md =$  current row in matrix  $D$

A linear dependence between row  $md$  of  $D$  and the remaining rows in  $D$  exists if row  $md$  of  $D'$  contains all zeros.

The matrix containing the stoichiometric coefficients for all of the formation reactions is given by:

$$N = \begin{pmatrix} v_{i1} & \dots & v_{iE} \\ \vdots & & \\ v_{sc,1} & \dots & v_{sc,E} \end{pmatrix} = A D^{-1} \quad (4)$$

Equilibrium constants may now be calculated for each of the formation reaction equations using the Gibbs Free Energy change of each reaction.

$$\ln K_{eqi} = \frac{1}{RT} \left( \sum_{k=1}^E v_{ik} \mu_k^\circ - \mu_i^\circ \right) \quad (5)$$

where:  $\mu_i^\circ =$  standard chemical potential of specie  $i$

$\mu_k^\circ =$  standard chemical potential of basis specie  $k$

An "equilibrium constant" for each formation reaction may also be calculated from the current estimate to the equilibrium composition.

$$\ln Q_i = \ln a_i - \sum_{k=1}^E v_{ik} \ln a_k \quad (6)$$

where:  $a_i = \gamma_i n_i P_{pi} / n_T$  (activity of specie  $i$ )

$\gamma_i =$  activity coefficient

$n_T =$  total moles of species in the same phase as specie  $i$

$P_{pi} = \begin{cases} P/P_0 & \text{vapor species} \\ 1 & \text{nonvapor species} \end{cases}$

Defining the extent of reaction,  $\xi_i$ , as

$$\xi_i = (n_j' - n_j) / \nu_{ij}$$

where:  $n_j'$  = composition of specie  $j$  at reaction extent  $\xi_i$

the "equilibrium constant" as calculated from the current composition may be written as

$$\ln Q_i = \ln [\beta_i (n_i + \xi_i)] - \sum_{k=1}^E \gamma_{ik} \ln [\beta_i (n_k + \nu_{ik} \xi_i)] \quad (7)$$

$$\text{where: } \beta_i = \gamma_i P_{pi} / n_T$$

As an approximation assume that  $\beta_i$  and  $\xi_k$  are constant for small changes in  $\xi_i$ . Introducing a function  $\delta_i$  to account for nonvapor phases, a finite difference approximation which relates changes in the extent of reaction to the difference between the actual equilibrium constant and the "equilibrium constant" calculated from the current composition is obtained by differentiation of equation 7.

$$\frac{\ln K_{eqi} - \ln Q_i}{\Delta \xi_i} \approx \frac{d \ln Q_i}{d \xi_i} \approx \frac{\xi_i}{n_i} - \sum_{k=1}^E \frac{\delta_k \nu_{ik}^2}{n_k} \quad (8)$$

$$\text{where: } \delta_j, \delta_k = \begin{cases} 1 & \text{vapor phase} \\ 0 & \text{nonvapor phases} \end{cases}$$

Thus the difference between the equilibrium constant for formation reaction  $i$  as calculated from the Gibbs Free Energy ( $K_{eqi}$ ) and as calculated from the current approximation to the equilibrium composition ( $Q_i$ ) results in a prediction of  $\Delta \xi_i$  which will yield a better approximation to the system equilibrium composition.

In order to prevent the occurrence of negative molar amounts the effect of  $\Delta \xi_i$  on the new composition must be tested. Thus, for the nonbasis species:

$$n_i' = n_i \Delta \xi_i' \quad (9)$$

and for the basis species

$$n_k' = n_k - \sum_{i=1}^{VSC} \nu_{ik} \Delta \xi_i \quad (10)$$

$$\text{where: } \Delta \xi_i' = \begin{cases} \Delta \xi_i & \text{if } \Delta \xi_i > 0 \\ -n_i & \text{if } \Delta \xi_i < 0 \text{ and } |\Delta \xi_i| > n_i \end{cases} \quad (11)$$

In order to assure that nonbasis species remain positive  $\Delta \xi_i'$  is set equal to  $-n_i$  if  $\Delta \xi_i < 0$  and  $|\Delta \xi_i| > n_i$ . Nonnegativity of the basis species is assured by applying the relation

$$K = -n_k / \sum_{i=1}^{VSC} (-\nu_{ik} \Delta \xi_i) \quad (12)$$

to each of the basis species in the system and choosing the smallest positive value of  $\kappa$  which results while  $\kappa$  is constrained to be no greater than unity.

In order to assure convergence of the numerical scheme it is necessary to apply a convergence forcer. The Gibbs Free Energy of the system is given by

$$G = \sum_{i=1}^{VSC} n_i [\mu_i^\circ + RT \ln a_i] \quad (11)$$

The procedure used for determining the value of the convergence forcer,  $\lambda$ , is as follows.

1) Evaluate the derivative:

$$\left(\frac{dG}{d\lambda}\right)_{\lambda=1} = \sum_{i=1}^{VSC} \Delta n_i [\mu_i^\circ + \ln a_i'] \quad (12)$$

$$\text{where: } a_i' = \beta_i n_i'$$

$$\Delta n_i = n_i' - n_i$$

If  $\left(\frac{dG}{d\lambda}\right)_{\lambda=1} \leq 0$  then set  $\lambda=1$ .

2) If  $\left(\frac{dG}{d\lambda}\right)_{\lambda=1} > 0$  then evaluate:

$$\left(\frac{dG}{d\lambda}\right)_{\lambda=0} = \sum_{i=1}^{VSC} \Delta n_i [\mu_i^\circ + \ln a_i] \quad (13)$$

The optimum value of  $\lambda$  is then approximated by:

$$\lambda = \frac{\left(\frac{dG}{d\lambda}\right)_{\lambda=0}}{\left(\frac{dG}{d\lambda}\right)_{\lambda=0} - \left(\frac{dG}{d\lambda}\right)_{\lambda=1}} \quad (14)$$

Equation 14 represents a single step of a Regula-Falsi root finding algorithm which yields a sufficiently accurate estimate to the optimum value of the convergence forcer. Infrequently, equation 14 will predict a negative value for  $\lambda$  and in this case  $\lambda$  is set to 0.00 in order to allow the iterative solution to continue.

### 8.6 Example Calculation: The GaAs Chloride System Source Zone

The results of an equilibrium calculation for the GaAs chloride system source zone are shown in Figure B28. The wrap-up file of these results and the data file which yielded them are shown in Figures B29 and B30 respectively. This calculation determines the gas phase composition leaving the source zone of a chloride system CVD reactor at a temperature of 700C and 1 atm pressure. The inlet gas composition was 1%  $\text{AsCl}_3$  and 99%  $\text{H}_2$ . The steady state liquid option (ISS=1) was active and excess solid  $\text{SiO}_2$  was assumed present in order to determine the amount of silicon which would be present in the vapor.

Figure B28. The GaAs Chloride System Source Zone

STOICHIOMETRIC FORMULATION FOR DETERMINING EQUILIBRIUM COMPOSITIONS  
THE GaAs CHLORIDE SYSTEM SOURCE ZONE - A TEST OF MCMPEC STDIC

TEMPERATURE = 973.0 K PRESSURE = 0.101325 06 PA

PAGE 1

SPECIE AT NUMBER	ENTHALPY OF FORMATION		ENTROPY OF FORMATION		HEAT CAPACITY CORRELATION COEFFICIENTS		ICP	
	(KCAL/MOLE)	(KJ/MOLE)	(KCAL/MOLE-K)	(KJ/MOLE-K)	(KCAL/MOLE-K**2)	(KJ/MOLE-K**2)	AI	ICP
GA (V)	0	0	0	0	0	0	0	0
AS (V)	0	0	0	0	0	0	0	0
CL (V)	0	0	0	0	0	0	0	0
CL2 (V)	0	0	0	0	0	0	0	0
CL3 (V)	0	0	0	0	0	0	0	0
CL4 (V)	0	0	0	0	0	0	0	0
CL5 (V)	0	0	0	0	0	0	0	0
CL6 (V)	0	0	0	0	0	0	0	0
CL7 (V)	0	0	0	0	0	0	0	0
CL8 (V)	0	0	0	0	0	0	0	0
CL9 (V)	0	0	0	0	0	0	0	0
CL10 (V)	0	0	0	0	0	0	0	0
CL11 (V)	0	0	0	0	0	0	0	0
CL12 (V)	0	0	0	0	0	0	0	0
CL13 (V)	0	0	0	0	0	0	0	0
CL14 (V)	0	0	0	0	0	0	0	0
CL15 (V)	0	0	0	0	0	0	0	0
CL16 (V)	0	0	0	0	0	0	0	0
CL17 (V)	0	0	0	0	0	0	0	0
CL18 (V)	0	0	0	0	0	0	0	0
CL19 (V)	0	0	0	0	0	0	0	0
CL20 (V)	0	0	0	0	0	0	0	0
CL21 (V)	0	0	0	0	0	0	0	0
CL22 (V)	0	0	0	0	0	0	0	0
CL23 (V)	0	0	0	0	0	0	0	0
CL24 (V)	0	0	0	0	0	0	0	0
CL25 (V)	0	0	0	0	0	0	0	0
CL26 (V)	0	0	0	0	0	0	0	0
CL27 (V)	0	0	0	0	0	0	0	0
CL28 (V)	0	0	0	0	0	0	0	0
CL29 (V)	0	0	0	0	0	0	0	0
CL30 (V)	0	0	0	0	0	0	0	0
CL31 (V)	0	0	0	0	0	0	0	0
CL32 (V)	0	0	0	0	0	0	0	0
CL33 (V)	0	0	0	0	0	0	0	0
CL34 (V)	0	0	0	0	0	0	0	0
CL35 (V)	0	0	0	0	0	0	0	0
CL36 (V)	0	0	0	0	0	0	0	0
CL37 (V)	0	0	0	0	0	0	0	0
CL38 (V)	0	0	0	0	0	0	0	0
CL39 (V)	0	0	0	0	0	0	0	0
CL40 (V)	0	0	0	0	0	0	0	0
CL41 (V)	0	0	0	0	0	0	0	0
CL42 (V)	0	0	0	0	0	0	0	0
CL43 (V)	0	0	0	0	0	0	0	0
CL44 (V)	0	0	0	0	0	0	0	0
CL45 (V)	0	0	0	0	0	0	0	0
CL46 (V)	0	0	0	0	0	0	0	0
CL47 (V)	0	0	0	0	0	0	0	0
CL48 (V)	0	0	0	0	0	0	0	0
CL49 (V)	0	0	0	0	0	0	0	0
CL50 (V)	0	0	0	0	0	0	0	0
CL51 (V)	0	0	0	0	0	0	0	0
CL52 (V)	0	0	0	0	0	0	0	0
CL53 (V)	0	0	0	0	0	0	0	0
CL54 (V)	0	0	0	0	0	0	0	0
CL55 (V)	0	0	0	0	0	0	0	0
CL56 (V)	0	0	0	0	0	0	0	0
CL57 (V)	0	0	0	0	0	0	0	0
CL58 (V)	0	0	0	0	0	0	0	0
CL59 (V)	0	0	0	0	0	0	0	0
CL60 (V)	0	0	0	0	0	0	0	0
CL61 (V)	0	0	0	0	0	0	0	0
CL62 (V)	0	0	0	0	0	0	0	0
CL63 (V)	0	0	0	0	0	0	0	0
CL64 (V)	0	0	0	0	0	0	0	0
CL65 (V)	0	0	0	0	0	0	0	0
CL66 (V)	0	0	0	0	0	0	0	0
CL67 (V)	0	0	0	0	0	0	0	0
CL68 (V)	0	0	0	0	0	0	0	0
CL69 (V)	0	0	0	0	0	0	0	0
CL70 (V)	0	0	0	0	0	0	0	0
CL71 (V)	0	0	0	0	0	0	0	0
CL72 (V)	0	0	0	0	0	0	0	0
CL73 (V)	0	0	0	0	0	0	0	0
CL74 (V)	0	0	0	0	0	0	0	0
CL75 (V)	0	0	0	0	0	0	0	0
CL76 (V)	0	0	0	0	0	0	0	0
CL77 (V)	0	0	0	0	0	0	0	0
CL78 (V)	0	0	0	0	0	0	0	0
CL79 (V)	0	0	0	0	0	0	0	0
CL80 (V)	0	0	0	0	0	0	0	0
CL81 (V)	0	0	0	0	0	0	0	0
CL82 (V)	0	0	0	0	0	0	0	0
CL83 (V)	0	0	0	0	0	0	0	0
CL84 (V)	0	0	0	0	0	0	0	0
CL85 (V)	0	0	0	0	0	0	0	0
CL86 (V)	0	0	0	0	0	0	0	0
CL87 (V)	0	0	0	0	0	0	0	0
CL88 (V)	0	0	0	0	0	0	0	0
CL89 (V)	0	0	0	0	0	0	0	0
CL90 (V)	0	0	0	0	0	0	0	0
CL91 (V)	0	0	0	0	0	0	0	0
CL92 (V)	0	0	0	0	0	0	0	0
CL93 (V)	0	0	0	0	0	0	0	0
CL94 (V)	0	0	0	0	0	0	0	0
CL95 (V)	0	0	0	0	0	0	0	0
CL96 (V)	0	0	0	0	0	0	0	0
CL97 (V)	0	0	0	0	0	0	0	0
CL98 (V)	0	0	0	0	0	0	0	0
CL99 (V)	0	0	0	0	0	0	0	0
CL100 (V)	0	0	0	0	0	0	0	0

THE ENTHALPY AND ENTROPY OF FORMATION REFERENCE TEMPERATURE AND PRESSURE ARE T0 = 298.2 K P0 = 101325.0 PA  
MAXIMUM NUMBER OF ITERATIONS ALLOWED = 1000  
CONVERGENCE CRITERION = 0.1000E-03  
OUTPUT PARAMETER IDEBUR = 0

1000 = THE III-V LIQUID SOLUTION IS AT EQUILIBRIUM WITH THE III-V STOICHIOMETRIC SOLID

STOICHIOMETRIC FORMULATION FOR DETERMINING EQUILIBRIUM COMPOSITIONS  
THE GA/AS CHLORIDE SYSTEM SOURCE ZONE. A TEST OF MCMPEC. STOIC  
TEMPERATURE = 973.2 K PRESSURE = 0.10130E 06 PA

INPUT DATA AND INITIAL COMPOSITION ESTIMATES

SPECIE	PHASE	INITIAL COMPOSITION ESTIMATE (G MOLES)	STANDARD CHEMICAL POTENTIAL (KCAL/MOLE)	H	CL	GA	AS	ELEMENTAL ABUNDANCE MATRIX
AS (V)	VAPOR	0.10000000-19	31.129	0.0	0.0	0.0	1.000	
AS2 (V)	VAPOR	0.10000000-19	-14.549	0.0	0.0	0.0	2.000	
AS-CL (V)	VAPOR	0.10000000-19	-6.659	0.0	1.000	0.0	1.000	
AS-CL2 (V)	VAPOR	0.10000000-19	-1.807	0.0	2.000	0.0	1.000	
AS-TH (V)	VAPOR	0.99999999-02	-61.494	1.000	0.0	0.0	1.000	
AS-TH3 (V)	VAPOR	0.10000000-19	12.913	3.000	0.0	0.0	1.000	
CL (V)	VAPOR	0.10000000-19	13.770	0.0	0.0	0.0	0.0	1.000
CL2 (V)	VAPOR	0.10000000-19	-4.061	0.0	0.0	0.0	0.0	1.000
GA (V)	VAPOR	0.10000000-19	32.200	0.0	0.0	0.0	0.0	1.000
GA-CL (V)	VAPOR	0.10000000-19	-41.543	0.0	1.000	0.0	1.000	
GA-CL2 (V)	VAPOR	0.10000000-19	-74.373	0.0	2.000	0.0	1.000	
GA-CL3 (V)	VAPOR	0.10000000-19	-106.769	0.0	3.000	0.0	1.000	
GA2-CL6 (V)	VAPOR	0.10000000-19	-204.777	0.0	6.000	0.0	2.000	
H (V)	VAPOR	0.99999999-02	31.264	1.000	0.0	0.0	0.0	
H2 (V)	VAPOR	0.99999999-02	-31.264	2.000	0.0	0.0	0.0	
H-CL (V)	VAPOR	0.10000000-19	-51.474	1.000	1.000	0.0	0.0	
H-CL2 (V)	VAPOR	0.10000000-19	-43.521	2.000	1.000	0.0	0.0	
O2 (V)	VAPOR	0.10000000-19	3.343	0.0	0.0	0.0	0.0	
U-H (V)	VAPOR	0.10000000-19	70.171	0.0	0.0	0.0	0.0	
SI-CL (V)	VAPOR	0.10000000-19	10.751	0.0	0.0	1.000	0.0	
SI-CL2 (V)	VAPOR	0.10000000-19	-55.020	0.0	0.0	2.000	0.0	
SI-CL3 (V)	VAPOR	0.10000000-19	-93.773	0.0	0.0	3.000	0.0	
SI-CL4 (V)	VAPOR	0.10000000-19	-138.448	0.0	0.0	4.000	0.0	
SI-H (V)	VAPOR	0.10000000-19	60.058	1.000	0.0	0.0	0.0	
SI-H4 (V)	VAPOR	0.10000000-19	17.145	4.000	0.0	0.0	0.0	
SI-H-CL (V)	VAPOR	0.10000000-19	-94.142	1.000	0.0	1.000	0.0	
SI-H-CL2 (V)	VAPOR	0.10000000-19	-22.548	2.000	0.0	1.000	0.0	
SI-H-CL3 (V)	VAPOR	0.10000000-19	-70.611	3.000	0.0	1.000	0.0	
SI-H-CL4 (V)	VAPOR	0.10000000-19	-107.040	4.000	0.0	1.000	0.0	
SI-CL6 (V)	VAPOR	0.10000000-19	30.164	5.000	0.0	2.000	0.0	
SI-CL7 (V)	VAPOR	0.10000000-19	0.0	0.0	0.0	0.0	0.0	
SI-CL8 (V)	VAPOR	0.10000000-19	-81.605	0.0	0.0	1.000	0.0	
SI-CL9 (V)	VAPOR	0.10000000-19	-3.011	0.0	0.0	0.0	0.0	
DATA5 (V)	CONDENSED	0.10000000 01		0.0	0.0	0.0	0.0	
DATA6 (V)	CONDENSED	0.10000000 01		0.0	0.0	0.0	0.0	

TOTAL GRAM-MOLES OF EACH ELEMENT FROM INPUT DATA  
AND AS CALCULATED FROM THE INITIAL COMPOSITION ESTIMATES

	INPUT DATA	CALCULATED	AS	CL	GA	AS	SI	INPUT DATA	CALCULATED	AS
H	0.10000E 01	0.10000E 01	0	0.00000E-01	0.00000E-01	0.00000E-01	0.00000E-01	0.10000E 01	0.10000E 01	0.10000E 01
GA	0.10000E 00	0.10000E 00	0	0.30000E-01	0.30000E-01	0.30000E-01	0.30000E-01	0.10000E 01	0.10000E 01	0.10000E 01

STOICHIOMETRIC FORMULATION FOR DETERMINING EQUILIBRIUM COMPOSITIONS  
THE GAS/AS CHLORIDE SYSTEM SOURCE ZONE. A TEST OF MCMPEC. STOIC.

PAGE 3

TEMPERATURE = 973.2 K PRESSURE = 0.101325E+05 PA

-----  
EXECUTION DIAGNOSTICS

THE Na/AS CHLORINE SYSTEM SOURCE ZONE. A TEST OF MEMPEC-STOIC.

TEMPERATURE = 973.2 K PRESSURE = 0.10133E+05 PA

EQUILIBRIUM COMPOSITIONS AFTER 101 ITERATIONS

SYSTEM RISKS FREE ENERGY = -0.189593E+01 (KCAL)

RELATIVE ERROR = 0.24542E-04 CONVERGENCE CRITERION = 0.10000E-03 RELAXATION PARAMETER AT LAST ITERATION = 0.50000E-01

SPECIE SYMBOL	PHASE	EQUILIBRIUM MOLE FRACTION	EQUILIBRIUM COMPOSITION (G-MOLES)	ESTIMATED COMPOSITION UNCERTAINTY (G-MOLES)	CHEMICAL POTENTIAL (KCAL/G-MOLE)	ACTIVITY COEFFICIENT
AS (V)	VAPOR	0.71622E-09	0.73249020-09	0.0	-4.583	0.10000E+01
AS2 (V)	VAPOR	0.31360E-03	0.32071220-03	0.0	-13.166	0.10000E+01
AS3 (V)	VAPOR	0.99355E-04	0.10212870-04	0.0	-19.749	0.10000E+01
AS4 (V)	VAPOR	0.25945E-02	0.23108330-02	0.0	-24.331	0.10000E+01
AS-CL (V)	VAPOR	0.57099E-10	0.68619720-10	0.0	-51.972	0.10000E+01
AS-CL2 (V)	VAPOR	0.34819E-21	0.35529700-21	0.0	-97.361	0.10000E+01
AS-CL3 (V)	VAPOR	0.54670E-18	0.57551650-18	0.0	-142.749	0.10000E+01
AS-H (V)	VAPOR	0.54510E-09	0.57790300-09	0.0	-8.277	0.10000E+01
AS-H3 (V)	VAPOR	0.35294E-05	0.36095810-05	0.0	-11.666	0.10000E+01
CL (V)	VAPOR	0.45795E-13	0.47955420-13	0.0	-45.389	0.10000E+01
CL2 (V)	VAPOR	0.33612E-19	0.34374010-19	0.0	-90.778	0.10000E+01
CL3 (V)	VAPOR	0.12531E-07	0.12815350-07	0.0	-11.988	0.10000E+01
AS-CL (V)	VAPOR	0.29201E-01	0.29853230-01	0.0	-48.377	0.10000E+01
AS-CL2 (V)	VAPOR	0.44176E-04	0.45175900-04	0.0	-93.766	0.10000E+01
AS-CL3 (V)	VAPOR	0.53788E-07	0.54597860-07	0.0	-139.155	0.10000E+01
AS-CL6 (V)	VAPOR	0.31041E-16	0.31744310-16	0.0	-279.309	0.10000E+01
AS-CL6 (V)	VAPOR	0.10628E-08	0.10868760-08	0.0	-1.694	0.10000E+01
AS-CL6 (V)	VAPOR	0.94903E+00	0.95977150+00	0.0	-3.389	0.10000E+01
AS-CL6 (V)	VAPOR	0.45221E-04	0.46246170-04	0.0	-47.083	0.10000E+01
AS-CL6 (V)	VAPOR	0.53505E-08	0.54944830-08	0.0	-87.974	0.10000E+01
AS-CL6 (V)	VAPOR	0.14134E-23	0.16506000-23	0.0	-62.421	0.10000E+01
AS-CL6 (V)	VAPOR	0.18134E-23	0.18500000-23	0.0	-109.452	0.10000E+01
AS-CL6 (V)	VAPOR	0.11915E-19	0.12182540-19	0.0	-86.200	0.10000E+01
AS-CL6 (V)	VAPOR	0.17775E-13	0.18179100-13	0.0	-12.624	0.10000E+01
AS-CL6 (V)	VAPOR	0.45562E-17	0.47274080-17	0.0	-58.013	0.10000E+01
AS-CL6 (V)	VAPOR	0.29754E-10	0.31233920-10	0.0	-103.102	0.10000E+01
AS-CL6 (V)	VAPOR	0.43993E-12	0.45006830-12	0.0	-148.791	0.10000E+01
AS-CL6 (V)	VAPOR	0.31197E-12	0.31197350-12	0.0	-174.180	0.10000E+01
AS-CL6 (V)	VAPOR	0.19951E-15	0.20200000-15	0.0	-19.402	0.10000E+01
AS-CL6 (V)	VAPOR	0.20422E-08	0.20834650-08	0.0	-150.485	0.10000E+01
AS-CL6 (V)	VAPOR	0.57641E-10	0.59947790-10	0.0	-196.791	0.10000E+01
AS-CL6 (V)	VAPOR	0.26166E-09	0.27065070-09	0.0	-33.094	0.10000E+01
AS-CL6 (V)	VAPOR	0.78151E-09	0.80089510-09	0.0	-127.210	0.10000E+01
AS-CL6 (V)	VAPOR	0.14291E-10	0.14477100-10	0.0	-131.795	0.10000E+01
AS-CL6 (V)	VAPOR	0.13275E-12	0.13615170-12	0.0	-274.001	0.10000E+01
AS-CL6 (V)	VAPOR	0.38134E-23	0.35500000-23	0.0	-35.415	0.10000E+01
AS-CL6 (V)	VAPOR	0.96132E-17	0.99510230-17	0.0	0.0	0.10000E+01
AS-CL6 (V)	VAPOR	0.0	0.0	0.0	0.0	0.10000E+01
AS-CL6 (V)	VAPOR	0.10000E+01	0.10000000+01	0.0	-2.605	0.10000E+01
AS-CL6 (V)	VAPOR	0.10000E+01	0.10000000+01	0.0	-131.795	0.10000E+01
AS-CL6 (V)	VAPOR	0.10000E+01	0.10000000+01	0.0	-3.011	0.10000E+01

MOLE FRACTION OF SILICON SPECIES IN VAPOR PHASE = 0.31814E-09

RELAXATION PARAMETER AT LAST ITERATION = 0.50000E-01

TOTAL GRAM-MOLES OF EACH ELEMENT FROM INPUT DATA AND AS CALCULATED FROM THE EQUILIBRIUM COMPOSITIONS

INPUT DATA	CALCULATED	INPUT DATA	CALCULATED	INPUT DATA	CALCULATED
AS	0.00000E+01	AS	0.00000E+01	AS	0.00000E+01
CL	0.00000E+01	CL	0.00000E+01	CL	0.00000E+01
H	0.00000E+01	H	0.00000E+01	H	0.00000E+01

STOICHIOMETRIC FORMULATION FOR DETERMINING EQUILIBRIUM COMPOSITIONS

THE GAS/AS CHLORIDE SYSTEM SOURCE ZONE. A TEST OF NONPEC-STOIC.

PAGE 5

TEMPERATURE = 273.2 N PRESSURE = 0.10132E+06 PA

A SET OF INDEPENDENT REACTION EQUATIONS FOR THIS SYSTEM IS AS FOLLOWS:

- ( 1.00 AS2 (V) ) = ( 0.500E+00 AS4 (V) )
- ( 1.00 AS3 (V) ) = ( 0.750E+00 AS4 (V) )
- ( 1.00 H-CL (V) ) = ( 0.500E+00 H2 (V) ) + (-0.101E+01 GAX-AS(1-X)) + ( 0.100E+01 GA-CL (V) ) + ( 0.153E-02 AS4 (V) )
- ( 1.00 GA-CL2 (V) ) = (-0.101E+01 GAX-AS(1-X)) + ( 0.200E+01 GA-CL (V) ) + ( 0.153E-02 AS4 (V) )
- ( 1.00 AS-H3 (V) ) = ( 0.153E+01 H2 (V) ) + ( 0.250E+00 AS4 (V) )
- ( 1.00 GA-CL3 (V) ) = (-0.201E+01 GAX-AS(1-X)) + ( 0.300E+01 GA-CL (V) ) + ( 0.353E-02 AS4 (V) )
- ( 1.00 GA (V) ) = ( 0.101E+01 GAX-AS(1-X)) + (-0.153E-02 AS4 (V) )
- ( 1.00 AS-H (V) ) = ( 0.500E+00 H2 (V) ) + ( 0.250E+00 AS4 (V) )
- ( 1.00 SI-H4 (V) ) = ( 0.100E+01 SI-O2 (S) ) + ( 0.400E+01 H2 (V) ) + (-0.200E+01 H2-O (V) )
- ( 1.00 H (V) ) = ( 0.500E+00 H2 (V) )
- ( 1.00 SI-H3-CL (V) ) = ( 0.100E+01 SI-O2 (S) ) + ( 0.350E+01 H2 (V) ) + (-0.101E+01 GAX-AS(1-X)) + ( 0.100E+01 GA-CL (V) ) + ( 0.153E-02 AS4 (V) ) + (-0.200E+01 H2-O (V) )
- ( 1.00 AS (V) ) = ( 0.250E+00 AS4 (V) )
- ( 1.00 SI-H2-CL2 (V) ) = ( 0.100E+01 SI-O2 (S) ) + ( 0.300E+01 H2 (V) ) + ( 0.201E+01 GAX-AS(1-X)) + ( 0.200E+01 GA-CL (V) ) + ( 0.353E-02 AS4 (V) ) + (-0.200E+01 H2-O (V) )
- ( 1.00 SI-H-CL3 (V) ) = ( 0.100E+01 SI-O2 (S) ) + ( 0.100E+01 GA-CL (V) ) + ( 0.252E+00 AS4 (V) )
- ( 1.00 SI-H-CL3 (V) ) = ( 0.100E+01 SI-O2 (S) ) + ( 0.350E+01 H2 (V) ) + ( 0.101E+01 GAX-AS(1-X)) + ( 0.101E+01 GA-CL (V) ) + ( 0.400E+01 H2-O (V) )
- ( 1.00 SI-CL2 (V) ) = ( 0.100E+01 SI-O2 (S) ) + ( 0.200E+01 H2 (V) ) + (-0.201E+01 GAX-AS(1-X)) + ( 0.200E+01 GA-CL (V) ) + ( 0.322E-02 AS4 (V) ) + (-0.200E+01 H2-O (V) )
- ( 1.00 SI-O (V) ) = ( 0.100E+01 SI-O2 (S) ) + ( 0.100E+01 H2 (V) ) + (-0.100E+01 H2-O (V) )
- ( 1.00 SI-CL3 (V) ) = ( 0.100E+01 SI-O2 (S) ) + ( 0.200E+01 H2 (V) ) + (-0.100E+01 GAX-AS(1-X)) + ( 0.100E+01 GA-CL (V) ) + ( 0.100E+01 H2-O (V) )
- ( 1.00 SI-CL4 (V) ) = ( 0.100E+01 SI-O2 (S) ) + ( 0.200E+01 H2 (V) ) + ( 0.100E+01 GAX-AS(1-X)) + ( 0.100E+01 GA-CL (V) ) + ( 0.153E-02 AS4 (V) ) + (-0.100E+01 H2-O (V) )
- ( 1.00 SI-H (V) ) = ( 0.100E+01 SI-O2 (S) ) + ( 0.100E+01 H2 (V) ) + (-0.100E+01 GAX-AS(1-X)) + ( 0.100E+01 GA-CL (V) ) + ( 0.100E+01 H2-O (V) )
- ( 1.00 SI-H (V) ) = ( 0.100E+01 SI-O2 (S) ) + ( 0.100E+01 H2 (V) ) + ( 0.100E+01 GAX-AS(1-X)) + ( 0.100E+01 GA-CL (V) ) + ( 0.100E+01 H2-O (V) )

1.00 AS-CL3 (V) ) + (-0.101E+01 GAX-AS(1-X)) + ( 0.100E+01 GA-CL (V) ) + ( 0.255E+00 ASA (V) )  
 1.00 SI (V) ) + ( 0.100E+01 SI-02 (S) ) + ( 0.200E+01 H2 (V) ) + (-0.200E+01 H2-0 (V) )  
 1.00 CL2 (V) ) + (-0.201E+01 GAX-AS(1-X)) + ( 0.200E+01 GA-CL (V) ) + ( 0.225E-02 ASA (V) )  
 1.00 0-H (V) ) + (-0.500E+00 H2 (V) ) + ( 0.100E+01 H2-0 (V) )  
 1.00 0-1 CL2 (V) ) + (-0.201E+01 GAX-AS(1-X)) + ( 0.200E+01 GA-CL (V) ) + ( 0.255E+00 ASA (V) )  
 1.00 SI-02 (S) ) + ( 0.100E+01 SI-02 (S) )  
 1.00 SI (S) ) + ( 0.100E+01 SI-02 (S) ) + ( 0.200E+01 H2 (V) ) + (-0.200E+01 H2-0 (V) )  
 1.00 SI2-CL3 (V) ) + ( 0.200E+01 SI-02 (S) ) + ( 0.400E+01 H2 (V) ) + (-0.600E+01 GA-CL (V) )  
 + ( 0.225E-02 ASA (V) ) + (-0.400E+01 H2-0 (V) )  
 1.00 0 (V) ) + (-0.100E+01 H2 (V) ) + ( 0.100E+01 H2-0 (V) )  
 1.00 02 (V) ) + (-0.200E+01 H2 (V) ) + ( 0.200E+01 H2-0 (V) )

EQUILIBRIUM CONSTANTS FOR THE IMPERMENT REACTIONS

REACTION PRODUCT	SISSS FREE ENERGY CHANGE (KCAL/G-MOLE)	EQUILIBRIUM CONSTANT FROM SISSS FREE ENERGY	EQUILIBRIUM CONSTANT FROM PREDICTED COMPOSITION
3S (V)	37.777	0.12952E-09	0.12952E-09
3S2 (V)	9.711	0.65973E-02	0.65973E-02
3S3 (V)	8.978	0.96359E-02	0.76359E-02
3S4 (V)	0.0	0.10000E+01	0.10000E+01
3S-CL (V)	35.504	0.16544E-07	0.16544E-07
3S-CL2 (V)	78.902	0.19115E-17	0.17115E-17
3S-CL3 (V)	57.749	0.10754E-12	0.10754E-12
3S-H (V)	33.751	0.23343E-07	0.23343E-07
3S-H3 (V)	21.239	0.16997E-04	0.16997E-04
L (V)	52.505	0.15135E-11	0.15135E-11
LC2 (V)	73.011	0.40207E-16	0.40207E-16
JA (V)	35.237	0.12409E-07	0.12409E-07
JA-CL (V)	-0.000	0.10000E+01	0.10000E+01
JA-CL2 (V)	5.705	0.52222E-01	0.52222E-01
JA-CL3 (V)	11.845	0.21870E-02	0.21870E-02
JA2-CL5 (V)	32.433	0.52084E-07	0.52084E-07
4 (V)	39.928	0.10802E-08	0.10802E-08
42 (V)	0.0	0.10000E+01	0.10000E+01
4-CL (V)	12.463	0.17076E-02	0.15394E-02
42-0 (V)	0.0	0.10000E+01	0.29997E+00
5 (V)	91.673	0.25912E-20	0.24594E-15
52 (V)	92.778	0.14838E-20	0.37438E-07
5H (V)	52.251	0.13460E-11	0.18460E-11
5I (V)	156.175	0.75021E-35	0.75021E-35
5I-CL (V)	142.271	0.11248E-21	0.11129E-21
5I-CL2 (V)	108.748	0.10026E-21	0.10026E-21
5I-CL3 (V)	107.142	0.87058E-24	0.87058E-24
5I-CL4 (V)	101.202	0.18780E-22	0.18780E-22
5I-4 (V)	147.224	0.96834E-33	0.96834E-33
5I-44 (V)	131.451	0.93993E-25	0.93993E-25
5I-4-CL3	97.696	0.10431E-21	0.10431E-21
5I-4-CL3	101.959	0.14075E-22	0.14075E-22
5I-4-CL	106.912	0.12240E-23	0.12240E-23
5I-0 (V)	55.017	0.30042E-19	0.30042E-19
5I-02 (V)	101.905	0.12245E-22	0.12245E-22
5I-02-CL6 (V)	244.171	0.00055E-48	0.00055E-48
5I-02 (V)	201.197	0.12247E-22	0.12247E-22
5I-02 (V)	82.373	0.23409E-18	0.23409E-18
5I-02 (V)	0.0	0.10000E+01	0.10000E+01
5I-02 (S)	-0.000	0.10000E+01	0.10000E+01
JAA-ASCL(X)			
101.9935			

(NOT BINDING)

(NOT BINDING)

(NOT BINDING)

(NOT BINDING)

(NOT BINDING)

(NOT BINDING)





References

1. Cruise, D.R., J. Phys. Chem., 8, 18, 1964.
2. Smith, W.R. and Missen R.W., Canad. J. of Chem. Eng., 45, 1968.
3. Shaw D.W., J. Crystal Growth, 8, 1971.
4. Clark M. and Mansen K., Numerical Methods of Reactor Analysis, Academic Press, 1964.
5. Prausnitz J.M., Molecular Thermodynamics of Fluid-Phase Equilibrium, Prentice Hall, 1969.
6. Vieland L.J., Acta Metallurgica, 11, 1963.
7. Thurmond C.D., J. Phys. Chem. Solids, 26, 1965.
8. Shafer M. and Weiser K., J. Phys. Chem. 61, 1957.
9. Perea and Fonstad, J. Electrochem. Soc. 127, 2, 1980.
10. Boomgard and Schol, Philips Res. Rep., 12, 127, 1957.
11. Sol, Claviou, Linh, Moulin, J. Cryst. Growth, 127, 325.
12. Hall, J. Electrochem. Soc., 110, 385, 1963.
13. Koster and Thoma, Z. Metall. 46, 291, 1955.

**END**

**FILMED**

**1-84**

**DTIC**